

**Characterizing the Gut Microbiota of Obese Cats and Exploring the Association Between
Gut Microbiota and Memory in Dogs Using Metagenomic Sequencing**

by

Xiaolei Ma

A dissertation submitted to the Graduate Faculty of
Auburn University
in partial fulfillment of the
requirements for the Degree of
Doctor of Philosophy

Auburn, Alabama
December 14, 2024

Keywords: Gut microbiome, Metagenomic sequencing, Whole-Genome Shotgun Sequencing,
Animal Health, Cat Obesity, Canine Memory performance

Copyright 2024 by Xiaolei Ma

Approved by

Dr. Xu Wang, Chair, Associate Professor, Department of Pathobiology

Dr. Frank F. Bartol, Professor, Department of Anatomy, Physiology and Pharmacology

Dr. Emily C. Graff, Associate Professor, Department of Pathobiology

Dr. Mark Liles, Professor, Department of Biological Sciences

Abstract

The gut microbiota plays a crucial role in the health and physiology of animals, significantly affecting various biological processes and disease mechanisms. However, there are limited studies on the gut microbiota in cats and dogs, especially regarding the specific characteristics of the gut microbiota in obese cats and its relationship to memory performance in dogs. This dissertation aims to address these shortcomings by characterizing the gut microbiota of obese cats and exploring the association between gut microbiota and memory in dogs using metagenomic sequencing.

The first part of this study focuses on the importance of employing appropriate fecal sample collection methods to ensure accurate characterization of the gut microbiota in cats. For domestic cats, lubricants are often necessary to obtain an adequate number of samples. We evaluated the impact of mineral oil lubrication during the collection of cat stool samples on subsequent gut microbiome analysis. We also compared the two primary methods of collecting cat fecal samples using a fecal ring versus using a litter box. This study aims to provide valuable insights into the impact of different fecal collection methods and to assist in the development of standardized protocols for collecting fecal samples in feline microbiome studies.

In addition, metagenomic analysis of the gut microbiota in obese cats was performed to identify key microbial species and their potential roles in obesity-related metabolic dysregulation. We observed a significant reduction in microbial diversity in obese cat gut microbiota, suggesting potential dysbiosis. A panel of seven significantly altered, highly abundant species can serve as a microbiome indicator of obesity. Our findings in the obese cat microbiome composition, abundance, and functional capacities provide new insights into feline obesity.

Finally, this dissertation also explored the potential links between gut microbiota composition and memory performance in dogs. A single bacterial species, *Bifidobacterium pseudolongum*, was identified and confirmed to be correlated with memory performance in dogs. Using a random forest regression model, we found that the abundance of 17 bacterial taxa in the microbiome exhibited a stronger predictive capacity for memory performance. Our findings offer valuable insights into microbiome underpinnings of mammalian cognitive functions and suggest avenues for developing psychobiotics to enhance canine memory and learning.

Overall, this dissertation contributes to a deeper understanding of the gut microbiota in both cats and dogs, highlighting its relevance in veterinary medicine and its potential implications for improving health and treatment strategies in these companion animals.

Acknowledgments

I would like to express my deepest gratitude to the many individuals whose support and guidance were instrumental in the success of my dissertation at Auburn University.

First of all, I would like to express my heartfelt gratitude to my advisor, Dr. Xu Wang, who has given me firm support and profound guidance during my doctoral career. I have really appreciated the opportunity to work with such an outstanding researcher over the past five years. His patience and encouragement helped me through challenging times, and his vast knowledge and commitment to scientific rigor significantly enhanced my research skills.

I am also deeply grateful to my committee members: Dr. Frank F. Bartol, Associate Dean for Research and Graduate Studies; Associate Professor Dr. Emily C. Graff; Dr Mark Likes, Acting Associate Dean for Research and Graduate Studies. I sincerely appreciate you taking the time to review my work and providing your invaluable feedback. I am truly grateful for your guidance throughout this process.

My sincere gratitude extends to Wenqi Cao, Xiao Xiong, Haolong Wang, Ying Zhang, Yue Zhang, and Abbi Lynn, my lab mates, for their constant support and companionship. Your assistance is very important to my research, and your friendship makes me have a very pleasant time in the laboratory. I also wish to thank Dr. Zheng, Dr. Zhang, and Dr. Zhu for their insightful guidance, stimulating discussions, and continuous engagement in our projects.

Additionally, I want to express my appreciation to my friends and peers for their unwavering support. Each of you has contributed to my journey in meaningful ways.

Finally, I would like to express my deepest thanks to my family, especially my parents. Your faith in me has always been my motivation and inspiration. This significant achievement

would not have been possible without your steadfast support and encouragement. Thank you all from the bottom of my heart, and War Eagle!

Table of Contents

Abstract	2
Acknowledgments.....	4
Table of Contents.....	6
List of Tables	10
List of Figures.....	12
List of Abbreviations	16
CHAPTER 1	17
Introduction.....	17
1.1 Background.....	17
1.1.1 Functional anatomy of the mammalian gastrointestinal tract	17
1.1.2 Establishment of the gut microbiome	21
1.1.3 The role of gut microbiota	27
1.1.4 Therapeutic approaches	29
1.1.5 Animal models.....	33
1.2 Dissertation Structure.....	38
CHAPTER 2	40
Analysis of the Impact of Different Sampling Methods on Reconstructing the Gut Microbiome Profiles in Cats Based on Metagenomic Sequencing Technology	40
CHAPTER 2.1	40
Effect of mineral oil as a lubricant to collect feces from cats for microbiome studies.....	40
2.1.1 Introduction.....	40
2.1.2 Materials and methods	41
2.1.3 Results.....	45
2.1.4 Discussion and conclusion.....	52
CHAPTER 2.2	55
Evaluation of fecal sample collection methods for feline gut microbiome profiling: fecal loop vs. litter box	55
2.2.1 Introduction.....	55

2.2.2 Materials and methods	58
2.2.3 Results.....	66
2.2.4 Discussion and conclusion.....	77
CHAPTER 3	81
Whole-genome shotgun metagenomic sequencing reveals distinct gut microbiome signatures of obese cats.....	81
3.1 Introduction.....	81
3.2 Materials and methods	83
3.2.1 Animal selection and maintenance	83
3.2.2 Morphometrics, blood glucose, and insulin measurements in obese cats.....	85
3.2.3 Fecal sample collection and microbial DNA extraction	85
3.2.4 Metagenomic sequencing, quality control, and preprocessing of metagenomic reads	86
3.2.5 Feline gut metagenome assembly and microbial gene annotation.....	87
3.2.6 Taxonomy assignment and taxonomy abundance analysis	88
3.2.7 Microbial diversity analysis in normal and obese cats	89
3.2.8 Analysis of age and sex effects in the normal cat group.....	89
3.2.9 Identification of significantly altered genera or species in normal and obese cats.....	90
3.2.10 Linear discriminant analysis in normal and obese cat gut microbiota.....	93
3.2.11 Metagenomic assembly, genome completeness, and synteny analysis of a previously uncharacterized species <i>Erysipelotrichaceae bacterium AU001MAG</i>	93
3.2.12 qPCR validation of microbial abundance changes	94
3.2.13 Enrichment of functional categories and pathways	95
3.2.14 Data availability	95
3.3 Results.....	95
3.3.1 A comprehensive characterization of feline gut microbiota using deep WGS metagenomic data	95
3.3.2 High blood glucose levels and insulin resistance were associated with feline obesity	97
3.3.3 Lack of significant sex or age effects on gut microbiome within the normal cat group	98
3.3.4 Significant reduction in microbial diversity in obese cat gut microbiota	101
3.3.5 Phylum-level characterization of feline gut microbiota revealed a significantly lower Firmicutes-to-Bacteroidetes ratio in obese cats	101

3.3.6 The top 20 most abundant bacterial genera distinguish the normal and obese cat gut microbiota.	103
3.3.7 Linear discriminant analysis revealed the most featured bacterial families, genera, and species in normal vs. obese cat gut microbiota.	104
3.3.8 Metagenomic-assembled genome (MAG) of the most featured species in LDA analysis - a previously uncharacterized Erysipelotrichaceae bacterium AU001MAG.....	107
3.3.9 Hallmark of the obese cat gut microbiome - dramatic increases in abundance of Bifidobacterium sp., Dialister sp., Olsenella provencensis, and Campylobacter upsaliensis	109
3.3.10 Hallmark of the obese cat gut microbiome – depletion of two highly abundant species in the normal gut microbiome, Erysipelotrichaceae bacterium AU001MAG and Phascolarctobacterium succinatutens.....	113
3.3.11 Distinct metabolic pathways and CAZy families in normal and obese cat gut microbiota	114
3.4 Discussion and conclusion.....	118
CHAPTER 4	129
Metagenomic analysis reveals associations between memory performance and Bifidobacterium pseudolongum abundance in canine gut microbiome.....	130
4.1 Introduction.....	130
4.2 Materials and methods	131
4.2.1 Study subject and ethics statement	131
4.2.2 Phenotypic measurement and analysis.....	132
4.2.3 Statistical analysis.....	137
4.2.4 Fecal sample collection, microbial DNA extraction, and quality control.....	138
4.2.5 Whole-genome shotgun (WGS) metagenomic library preparation and sequencing .	139
4.2.6 Metagenome data processing, alignment, and taxonomy annotation	140
4.2.7 Microbial diversity analysis.....	142
4.2.8 Identification of the most featured bacterial taxa between high and low memory performance groups	142
4.2.9 Correlation between bacterial taxa and overall memory score.....	143
4.2.10 Random forest regression analysis.....	143
4.2.11 Reconstruction of MAGs and qPCR validation of abundance differences for Bifidobacterium pseudolongum.....	143

4.2.12 Data availability	145
4.2.13 Code availability	Error! Bookmark not defined.
4.3 Results	145
4.3.1 Substantial variability was identified in canine memory performance at puppy, juvenile, and young adult stages	145
4.3.2 Microbial diversity in canine gut microbiome was not affected by sex or litter, and was only slightly lower in 3-month puppies	146
4.3.3 Linear discriminant analysis revealed a single most featured bacterial species, <i>Bifidobacterium pseudolongum</i> , is associated with memory performance	148
4.3.4 Other bacterial taxa differ in abundance between high-OMS and low-OMS groups in addition to <i>B. pseudolongum</i>	150
4.3.5 Confirmation of memory performance associated microbial taxa using the 80 metagenomes as a validation set.....	150
4.3.6 Quantitative polymerase chain reaction validation confirmed that changes in <i>Bifidobacterium pseudolongum</i> abundance is associated with differences in working memory performance in the same dogs	156
4.3.7 Predictability of microbiome composition for working memory performance using random forest regression.....	158
4.4 Discussion and conclusion.....	160
CHAPTER 5	164
Overall Conclusion and Future Direction	164
Reference	167

List of Tables

Table 2.1 Characteristics of study participants and fecal sample collection date/time.	59
Table 2.2 Amount of fecal material collected and DNA yield from fecal samples.....	62
Table 2.3 Whole-genome shotgun metagenomic sequencing yield, quality control, and alignment statistics.....	63
Table 2.4 Correlation of taxonomic abundance at phylum, class, order, family, genus, and species level between fecal loop (FL) and litter box (LB) groups.....	65
Table 3.1 Bodyweight and body condition score measurements in normal and obese cats.	84
Table 3.2 Whole genome shotgun metagenomic sequencing yield, control statistics, and mapping rate.....	87
Table 3.3 Top 20 most abundant bacterial genera in the cat rectum microbiota.	88
Table 3.4 Top 20 most abundant bacterial species in the cat rectum microbiota.	89
Table 3.5 Significantly altered genera in obese cat rectum microbiota.	91
Table 3.6 Significantly decreased species in obese cat rectum microbiota.	91
Table 3.7 Significantly increased species in obese cat rectum microbiota compared to normal cat	93
Table 3.8 Blood glucose and HOMA-IR measurements in obese cats at the time of fecal sample collection.....	98
Table 4.1 Information of 27 dogs enrolled in this study.....	132
Table 4.2 Short-term memory test scores for 27 dogs at the puppy stage (3.0~3.5 month), juvenile stage (5.2~6.2 month), and young adult stage (12.8~16.0 month).	133
Table 4.3 Whole-genome shotgun metagenomic sequencing yield and mapping percentages to the canine microbiome contigs.	141

Table 4.4 Bacterial taxa with significant abundance differences between high performers and low performers in short-term memory tests..... 151

Table 4.5 Bacterial taxa with significant positive or negative correlation between relative abundance and memory performance. 153

List of Figures

Figure 1.1 Gross anatomy of the mammalian gastrointestinal tract	18
Figure 2.1 Metagenomic sequencing statistics from fecal samples in two groups.....	46
Figure 2.2 Microbial diversity analyses at different taxonomic levels from fecal samples collected with mineral oil (miOil) or without lubrication (noLub).....	48
Figure 2.3 Phylum level taxonomy composition and relative abundance and correlation plots of microbes with high abundance (>1%) at family and genus levels.	50
Figure 2.4 The number, alpha diversity and beta diversity of the microbial genes identified in the miOil and noLub groups.	52
Figure 2.5 Rarefaction analyses to assess species and gene richness from the results of sampling	60
Figure 2.6 Metagenomic sequencing statistics from fecal samples collected by fecal loop (FL) and litter box (LB) approaches.	66
Figure 2.7 Microbial diversity analyses at different taxonomic levels from fecal samples collected by fecal loop (FL) and litter box (LB) approaches.....	69
Figure 2.8 Microbial diversity analyses using long-read reference assembly at different taxonomic levels from fecal samples collected by fecal loop (FL) and litter box (LB) approaches	70
Figure 2.9 Relative abundance of major phyla and microbiome abundance (> 0.1%) correlation at class and order levels in the feline microbiome from samples collected by fecal loop (FL) and litter box (LB) approaches	73

Figure 2.10 Relative abundance of major phyla and microbiome abundance correlation at class and order levels in the feline microbiome from samples collected by fecal loop (FL) and litter box (LB) approaches from the alignment results against long-read reference assembly	74
Figure 2.11 Number of non-redundant microbial genes and gene level diversity in the feline fecal microbiome from samples collected by fecal loop (FL) and litter box (LB) approaches.....	76
Figure 2.12 Number of non-redundant microbial genes and gene level diversity in the feline fecal microbiome from samples collected by fecal loop (FL) and litter box (LB) approaches from the alignment results against long-read reference assembly.....	77
Figure 3.1 Graphic illustration of the experimental design	84
Figure 3.2 Body weight, body condition score, serum glucose level, and insulin resistance parameters for obese cats	96
Figure 3.3 Rarefaction analyses to assess species and gene richness from the results of sampling	97
Figure 3.4 Principal Coordinates Analysis (PCoA) plots of beta diversity between rectum microbiota of cats of different sex or age using Bray-Curtis distance.....	99
Figure 3.5 Significant changes of microbial diversity and phylum-level composition in cat gut microbiota	100
Figure 3.6 Bacterial relative abundance correlations between between WGS metagenomic data in this research and 16S rDNA ampliconic sequencing data in Fisher et al. 2017 at phylum and genus levels.....	102
Figure 3.7 Top 20 abundant bacterial genera and species in cat gut microbiota, and their relationship to cat obesity	104

Figure 3.8 Significant differences in taxonomic abundance that discriminate normal and obese cat gut microbiome at the family, genus, and species levels	106
Figure 3.9 MAG genome quality assessment, normal and obese microbiota coverage, and syntenic analysis of the most featured species in obese cat gut microbiome, <i>Erysipelotrichaceae bacterium AU001MAG</i>	109
Figure 3.10 Krona plots reflecting the phylogenetic relationship and composition changes in Firmicutes, Actinobacteria, and Proteobacteria	111
Figure 3.11 Heatmap of species abundance from the Bifidobacterium genus in normal vs. obese cat rectum microbiome.	113
Figure 3.12 Significantly altered metabolic pathways and CAZy families in obese and normal cat gut microbiota	115
Figure 3.13 Numbers of CAZyme (Carbohydrate-Active Enzymes) genes identified in normal and obese cat gut microbiomes	117
Figure 4.1 Memory performance in detection dogs at three developmental timepoints	136
Figure 4.2 Distribution of overall memory score and effect of growth stage, sex, litter, and breed on the canine memory performance.....	138
Figure 4.3 Effect of developmental stage, sex, litter, and breed.....	147
Figure 4.4 Microbial composition differences in the canine gut microbiome between the high and low memory performance groups	149
Figure 4.5 Correlation between memory performance and bacterial taxa abundance in 80 metagenomes.....	155
Figure 4.6 Correlation between memory performance and bacterial species abundance in the canine gut microbiome.....	156

Figure 4.7 Quantitative PCR validation of *Bifidobacterium pseudolongum* across all 80
microbiome samples 157

Figure 4.8 Variable importance and predictability modeled by random forest regression using 31
bacterial taxa with significant correlation with memory performance 159

List of Abbreviations

BCS	Body Condition Score
bp	base pair
BW	body weight
BWA	Burrows-Wheeler Aligner
CAZy	Carbohydrate-Active enZYme
CPM	counts per million mapped reads
DNA	deoxyribonucleic acid
FL	Fecal loop
GI	Gastrointestinal
HAHFC	high-abundance, high-fold change microbial species
HGT	horizontal gene transfer
IACUC	Institutional Animal Care and Use Committee
KEGG	Kyoto Encyclopedia of Genes and Genomes
LB	Litter box
LefSe	linear discriminant analysis Effect Size
miOil	lubrication using mineral oil
NCBI	National Center for Biotechnology Information
NIH	National Institutes of Health
noLub	no lubricant applied
OMS	Overall Memory Score
PCoA	principal coordinates analysis
PE	paired-end
PERMANOVA	permutational multivariate analysis of variance
qPCR	quantitative polymerase chain reaction
rDNA	ribosomal DNA
SCFA	short-chain fatty acid
SHAP	SHapley Additive exPlanations
WGS	whole-genome shotgun

CHAPTER 1

Introduction

1.1 Background

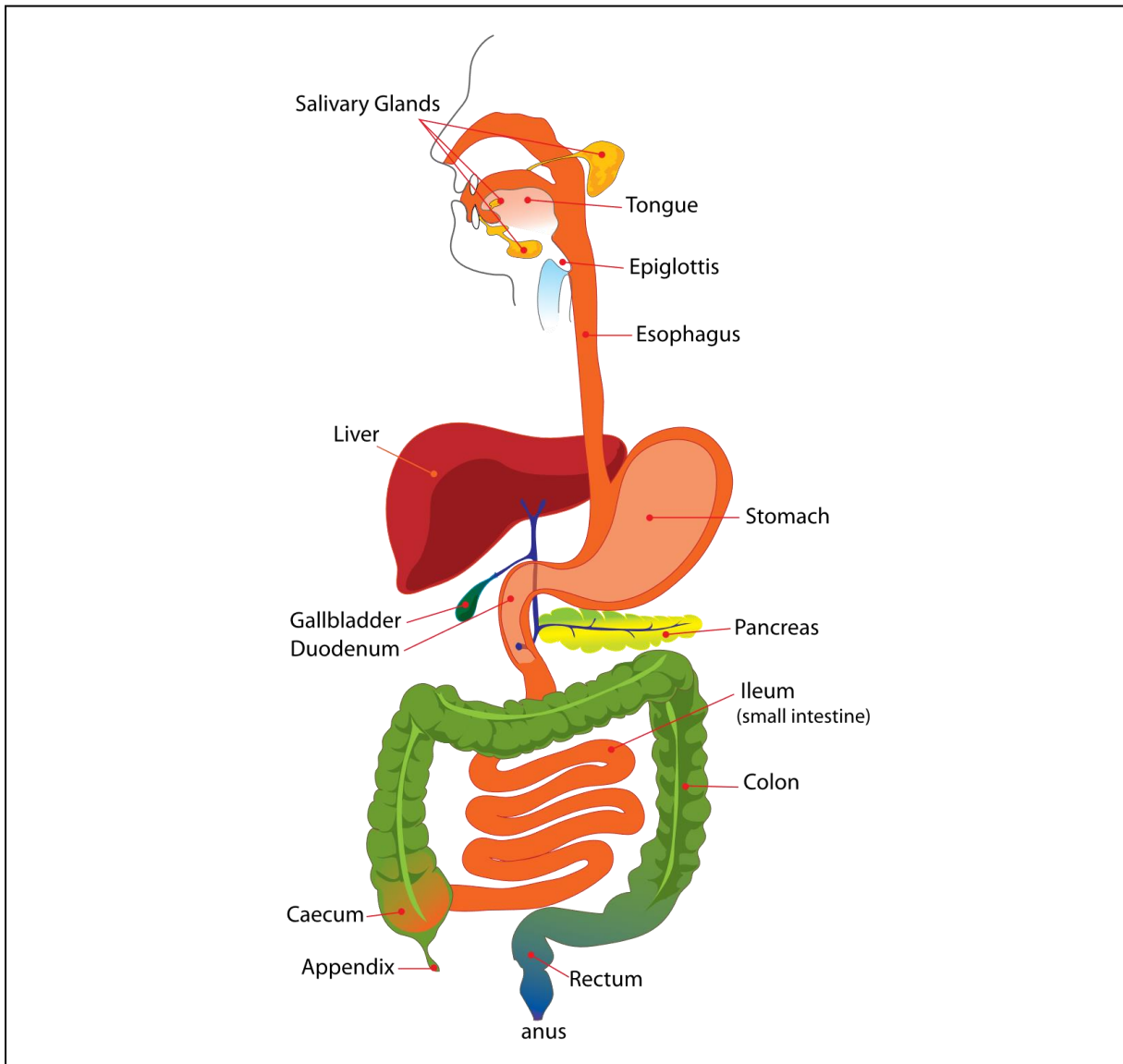
1.1.1 Functional anatomy of the mammalian gastrointestinal tract

The mammalian gastrointestinal (GI) tract is a complex network of organs. It plays a fundamental role in maintaining physiological processes essential for survival. It is responsible for digesting food, absorbing nutrients, and eliminating waste [1]. It is specifically designed to convert ingested food into essential nutrients and energy required for survival. Subsequently, it efficiently processes and prepares solid waste, or stool, for excretion during bowel movements.

1.1.1.1 Gross anatomy

The gross anatomy of the mammalian gastrointestinal (GI) tract includes the mouth, esophagus, stomach, small intestine (consisting of the duodenum, jejunum, and ileum), large intestine (comprising the caecum, colon, and rectum), and the anus [2]. The GI tract also includes vital accessory organs such as the liver, pancreas, gallbladder, and salivary glands [3]. The form and location of these organs are shown in Figure 1.1.

Figure 1.1 Gross anatomy of the mammalian gastrointestinal tract (From Wikimedia Commons, the free media repository).



1.1.1.2 Microanatomy and histophysiology

The microanatomy of the digestive tract starts with the mouth, which is constituted by oral mucosa, tongue, teeth, periodontium, and salivary glands. The oral mucosa is lined with stratified squamous epithelium, providing a protective barrier against mechanical forces, pathogens, and toxins. It also assists in food processing and aids in the secretion of mucus, which lubricates food

for easier swallowing [4]. Tongue, teeth, and periodontium play an important role in chewing and swallowing food, preparing food for further digestion in the gastrointestinal tract. The salivary glands serve several key functions in the digestive system. They contain acinar cells for enzyme secretion and ductal cells for saliva transport. Saliva provides essential lubrication for both eating and speaking. It contains the enzyme amylase, which begins the breakdown of carbohydrates into simpler sugars, initiating digestion in the mouth [5]. Additionally, saliva plays some important roles in taste facilitation, oral health protection, and pH buffering to maintain the balance required for oral hygiene [6].

The esophagus is a muscular tube that connects the pharynx (throat) to the stomach. Its primary function is to transport food and liquid from the mouth to the stomach through coordinated muscle contractions [7]. The epiglottis is a leaf-like cartilage flap at the base of the tongue. It closes over the trachea when swallowing, ensuring that food and liquid are directed into the esophagus and not into the respiratory tract [8]. The esophagus is lined with stratified squamous epithelium to protect against abrasion from food particles [9].

The stomach in mammals is transversely arranged and takes a saclike form [10]. It is divided into distinct regions: 1) The cardiac region, which is adjacent to the esophagus. It primarily secretes mucus through its specialized glands called cardiac glands, to protect the stomach lining and the pyloric region [11]; 2) The pyloric region, which is regulated by the pyloric sphincter. It serves as a valve that controls the release of chyme (partially digested food) into the duodenum (the first part of the small intestine) [12].

The small intestine is an important organ of the digestive system, consisting of the duodenum, jejunum and ileum. The small intestine is located in the lower part of the abdominal cavity, below the stomach [13]. Its wall comprises four main layers: the mucosa, submucosa, muscularis externa, and serosa. The mucosa features absorptive cells with microvilli. They help absorb nutrients. Goblet cells produce mucus to protect the lining [14]. The submucosa contains connective tissue for support, blood vessels for nutrient supply, and glands that help neutralize stomach acid [15]. The muscularis externa has a smooth muscle layer that promotes peristalsis and segmentation, aiding the movement and mixing of intestinal contents [16]. The serosa is the outermost layer of the small intestine and plays a key role in reducing friction between the intestine and surrounding organs. It secretes serous fluid, which is a lubricating fluid that allows the intestines to move smoothly within the abdominal cavity. It prevents irritation and damage caused by friction [17].

The large intestine comprises the caecum, colon, and rectum. It is characterized by a wider diameter compared to the small intestine. It has unique structural features, such as taenia coli, anus, and appendix. The large intestine is located in the lower abdominal cavity and surrounds the small intestine in a square or question mark shape [18]. Compared to small intestine, the large intestine lacks microvilli structures and has a smoother inner surface. Its wall is lined with simple columnar epithelium and abundant goblet cells that secrete mucus to facilitate the passage of feces [19]. The submucosa contains connective tissue, blood vessels, and lymphatics, supporting nutrient supply and immune function [20]. Different from the smooth muscle layer of small intestine, the muscularis externa of large intestine has three distinct longitudinal muscle bands called taeniae coli. It aids in peristalsis and segmentation, promoting the elimination of

feces [21]. The main function of the small intestine is to digest and absorb nutrients. In contrast, the large intestine mainly absorbs water and electrolytes, forming and storing feces.

The liver, pancreas, and gallbladder each have accessory but vital roles in the gastrointestinal tract. The liver produces bile, which is essential for the digestion of fat. The liver also processes nutrients absorbed from the small intestine [22]. At the same time, it can detoxify harmful substances and store important vitamins and minerals [23]. The pancreas secretes digestive enzymes (amylase, lipase, and protease) and bicarbonate [24]. These enzymes help break down carbohydrates into simple sugars, fats into fatty acids and glycerol, and proteins into amino acids. The bicarbonate can neutralize the chyme (partially digested food) that comes from the stomach into the small intestine [25]. In addition, the pancreas can regulate blood sugar by releasing insulin and glucagon [26]. The gallbladder stores and concentrates bile from the liver and releases it into the small intestine to aid fat digestion [27]. These organs work together to ensure efficient digestion and nutrient absorption, but dysfunction in any one organ can disrupt the health of the overall digestive system.

1.1.2 Establishment of the gut microbiome

1.1.2.1 Origins of the gut microbiome

The gut microbiota refers to the diverse community of microorganisms inhabiting the intestines of humans and animals. Its primary members are various bacterial species, alongside smaller populations of fungi, archaea, viruses, and protozoa, collectively constituting the gut micro-ecosystem [28, 29]. The development of the gut microbiome begins at birth, when a newborn is first exposed to bacteria from the mother and the environment. Some research suggested that

some microbial colonization may occur in utero through the placenta [30, 31]. DNA from a variety of bacteria was detected in the placenta, umbilical cord blood, amniotic fluid and fetal stool, suggesting that the gut was not sterile at birth [30, 32, 33]. However, due to the lack of direct evidence of active bacterial colonization before birth, this theory remains unproven. Further research is needed to confirm these findings. The initial microbial colonization of the intestine can be influenced by factors such as the mode of delivery (vaginal birth or cesarean section), early feeding practices (breastfeeding or formula feeding), environment exposure and host genetics.

Mode of delivery: Within the first few days after birth, the newborn intestine is rapidly colonized by maternal and environmental bacteria. One of the most important influencing factors is the mode of delivery. Infants delivered vaginally (i.e., born through the birth canal) acquire a microbiome similar to their mothers' vaginal flora, which is dominated by *Lactobacillus*, *Prevotella*, and *Sneathia* [34, 35]. However, C-section infants develop a microbiota more similar to the skin microbiome, including *Staphylococcus*, *Corynebacterium*, and *Propionibacterium* [36]. C-section infants also experience delayed colonization of beneficial bacteria such as *Bifidobacterium* and *Bacteroides* [37-39]. C-section infants also have increased rates of *Clostridium difficile*, which is particularly widespread in hospital settings [40]. The risk of colonization of this bacterium increases with the number of days staying in hospital [40]. These microbiota differences in C-section infants can persist for up to a year, and some minor changes can persist even for up to seven years, although the mechanisms of the long-term effects on development and health remain uncertain [41].

The C-section rates are increasing in many parts of the world, including Europe, the United States, large cities in China, Australia, and Brazil [42]. These rates far exceed the 10 to 15% recommended by the World Health Organization (WHO) [43]. Studies have shown that infants born via C-section face an increased risk of obesity, allergies, and asthma in childhood [44-47]. These findings emphasized the critical role of the first exposure to microbiome.

Early feeding practices: Breastfeeding shapes a baby's gut microbiome in several ways. Beneficial bacteria are transmitted directly from breast milk and the mother's skin. Prebiotic nutrients and bioactive compounds further support this process. Breast milk is rich in human milk oligosaccharides (HMOs), which promote the growth of beneficial bacteria such as bifidobacteria. HMOs are scarce in formula-milk. Exclusively breastfed infants typically have microbiota dominated by *Bifidobacterium*, which is able to protect the infant against a number of enteropathogenic microorganisms [48]. Breastmilk also contains immunological compounds like IgA, lactoferrin, and lysozyme [49]. They support the expansion of commensal bacteria by inhibiting harmful pathogens from attaching to the intestinal mucosal surface [50]. In addition, vitamin D is mainly contained in formula, which is recommended for breastfed babies, and it may affect microbiome development [51]. Vitamin D plays a role in the development of regulatory T-cells and dendritic cells [52]. Although direct evidence is lacking, one study suggests that lower vitamin D intake in adult African Americans is associated with a different microbiome composition compared to Caucasian Americans [53]. Larger, long-term studies are needed to confirm these findings.

Environmental exposure: Environmental exposure has been shown to affect the gut microbiome development. A recent longitudinal study by the Home Microbiome Consortium demonstrates significant interactions among the microbiomes of humans, home, and pets [54]. Singletons exhibit distinct colonization patterns compared to infants with older siblings. Infants who live with older sisters or brothers have lower levels of *Clostridium* species and higher levels of microbial diversity [38, 55, 56]. Infants without older siblings are reported to have lower levels of bifidobacteria in the gut microbiome [40]. Studies indicate that firstborns have less mature microbiota, compared to infants with older siblings. The less mature gut microbiome may increase the risk of allergy [46]. Pets and house dust have also been reported to play a role in affecting infant microbial colonization [40, 57, 58]. However, due to limited available data and further research, there are contradictions in current findings.

Host genetics: Several studies have reported that host genetics have effects on the microbiota composition [59, 60, 61]. An interesting study analyzed the microbiome development of three dichorionic triplets by next-generation sequencing. The results showed that at one month of age, monozygotic twins had more similar microbiomes than their siblings [62]. By the 12th month, the characteristics of the three babies became more consistent [62]. This suggests that host genes initially play an important role. However, after 12 months, environmental factors became more dominant. Another comprehensive research of fecal samples from 416 adult twins showed greater microbiota similarity between twin pairs, especially monozygotic twins [63].

Individual genes also play a role. For example, individuals with a functional fucosyltransferase 2 (*FUT2*) gene, have different microbial communities compared to individuals without *FUT2* gene

[64]. This gene plays a role in affecting glycosylation of mucus and breastmilk oligosaccharides [65, 66]. It also can regulate the presence of mucosal ABH and Lewis blood group antigen [67]. Consistent with this, a recent study found that bifidobacterium colonizes earlier and at higher levels in breastfed infants whose mothers have *FUT2* gene [68]. Other candidate genes, like NOD2 and MEFV, also have the potential to impact the gut microbiota composition of infants and are linked to conditions such as inflammatory bowel disease and lower bacterial diversity [69-71].

1.1.2.2 Development of the gut microbiome with age from birth to adulthood

The development of the gut microbiome from birth to adulthood in mammalian animals is a dynamic and complex process. The gut microbiome begins to form at birth and undergoes significant changes throughout the whole lifespan. Early life is a critical period for the establishment of the gut microbiota [72, 73]. Initial microbial colonization is critical for the physiological and immune development of infants, which may have long-term effects later in life [74]. The initial colonization is influenced by many factors such as mode of delivery, breastfeeding, environmental exposure, and host genetics. The influence of the difference in gut microbial composition during early life continues into early childhood, with the microbiome gradually developing a composition similar to that of adults [75, 76].

At birth, a baby's gut is almost sterile, but soon becomes colonized with microorganisms. The first bacteria to dominate the gut are facultative anaerobic bacteria such as *Escherichia*, *Streptococcus* and *Enterococcus* [77, 78]. This is because newborns have more oxygen in their intestines. Some studies showed steady changes in the species and diversity of bacteria, while

others reported unpredictable changes, including a temporary drop in diversity in the first week [77, 79, 80]. With less competition, newborns have more bacteria than adults [81]. Facultative anaerobic bacteria consume oxygen and create a better environment for strict anaerobic bacteria to grow. Over the next few weeks, these anaerobic bacteria multiply, feeding on the lactic acid in the breast milk. Breast milk contains beneficial bacteria and prebiotics like human milk oligosaccharides (HMOs) and IgA, that promote the growth of beneficial bacteria such as *Bifidobacteria* and *Lactobacilli* [48]. Formula-fed infants tend to have a more diverse microbiome but with fewer beneficial bacteria compared to breastfed infants. Recent studies show that breast milk has its own microbiota. Exclusively breastfed infants ingest 10^5 to 10^7 bacteria each day [82]. Early milk, or colostrum, contains bacteria from the ducts and skin, including *Staphylococci*, *Streptococci*, and *Lactobacilli* [83]. However, by six months, bacteria from the oral cavity, like *Veillonella* and *Prevotella*, become more common in the breast milk [83]. Some research suggests that gut bacteria from the mother may travel to the mammary gland and pass to the baby through breastfeeding [84]. *Bifidobacterium*, *Bacteroides*, and *Clostridia* have been found in the mother's feces, breastmilk, and the baby's feces, suggesting this transfer [85]. Breast milk provides immune components, like IgA, that are important for the growth and development of the infant's immune system. This is why WHO recommends exclusive breastfeeding for the first 6 months of life, followed by complementary breastfeeding up to two years of age as solid foods are introduced.

Usually, around 4 to 6 months following childbirth, solid foods are introduced into the child's feeding. The introduction of solid food alters both the composition and function of gut bacteria. As solid foods are introduced, genes responsible for digesting breast milk sugars become less

active, while genes for breaking down complex sugars and starch become more abundant [78]. The impact of solid food varies by region and dietary habits. In Western countries, a complex diet for children can increase *Bacteroides* and *Clostridium* in the gut microbiome, with altered *Lactobacilli* communities, and reduced *Bifidobacterium* [77, 78, 80, 86]. By the age of three, the gut microbiota resembles that of an adult [80, 86]. One study showed that the cessation of the breastfeeding pushed the microbiome into an adult state more than the introduction of solid foods [78]. These findings highlight the important role of both breast milk and diet in shaping the early microbiota.

Studies have shown that the microbiome of adults is relatively stable and resilient [87, 88].

Although the microbiome can be influenced by extreme external stressors, such as diet changes or antibiotic treatment, the significant resilience enables the gut microbiome to return to its original state once the alteration stops [89, 90]. This ability to bounce back is crucial for maintaining a balanced microbial community. A balanced microbial community is crucial for overall health and functionality.

1.1.3 The role of gut microbiota

The human gut harbors thousands of bacterial species, with an estimated bacterial population of approximately 38 trillion, exceeding the number of human cells, which is around 30 trillion. The dry weight of these bacteria is roughly 200 grams [91]. The gut microbiome contains over 3 million bacterial genes, which is 150 times the number of genes in the human genome [92].

These microorganisms play a vital role in various physiological processes, including digestion, nutrient absorption, immune modulation, metabolism and Gut-Brain Communication:

Nutrient Absorption and Metabolism: Gut microbiota plays critical roles in the digestion and metabolism of dietary nutrients [93]. They can break down complex carbohydrates such as cellulose, resistant starch, pectin, and oligosaccharides, converting them into short-chain fatty acids (SCFAs) like acetate, propionate, and butyrate. These SCFAs not only provide energy for intestinal cells but also help maintain intestinal mucosal integrity [94]. Additionally, gut microbiota participates in protein breakdown, producing amino acids and other metabolic products crucial for host nitrogen balance and intestinal health [95, 96]. They can also influence lipid metabolism, including cholesterol metabolism and fatty acid synthesis, which are important for cardiovascular health and energy balance [97]. Furthermore, microbes can aid in synthesizing vitamins such as B and K vitamins [98, 99].

Immune System Support and Regulation: Intestinal microbes adhere, settle, and proliferate within the intestinal tract, forming a 'barrier' with potent antimicrobial effects against pathogens [100]. Competition exists among the gut microbiota: beneficial species occupy intestinal space and nutritional resources, outcompeting harmful microbes and preventing their growth and proliferation [101]. Additionally, certain gut microbes produce antimicrobial substances like bacteriocins, which directly kill or inhibit the growth of harmful microorganisms [102, 103]. Moreover, some gut microbes can produce SCFAs or lactic acid, regulating intestinal pH to create an environment unfavorable for pathogen growth [104-106]. Furthermore, the gut microbiota plays a pivotal role in enhancing host immune function. For instance, Lactobacilli and Bifidobacteria can effectively boost host immune responses [107].

Gut-Brain Communication: Gut microbiota influences host physiological and psychological functions via the gut-brain axis [108]. The gut-brain axis constitutes a bidirectional communication system between the gut and the brain, involving gut microbiota, the immune system, the neuroendocrine system, and the nervous system [109]. Through the gut-brain axis, gut microbiota exerts significant effects on host immunity, metabolism, anxiety, depression, and cognitive function [110-113].

The gut environment and microbiota maintain a complex dynamic equilibrium in humans and animals. Balanced gut microbiota promotes both physical and mental health, whereas dysbiosis may lead to gut-brain axis dysregulation, resulting in gastrointestinal disorders (e.g., IBS [114, 115], IBD [116, 117]), liver diseases (e.g., hepatic encephalopathy [118, 119]), CNS diseases (e.g., multiple sclerosis [120], Alzheimer's disease [121], and autism [122]). Dysbiosis can also affect mental health, contributing to conditions such as anxiety and depression [123, 124]. Furthermore, alterations in gut microbiota can lead to metabolic diseases (e.g., obesity [125], diabetes [126]), cardiovascular diseases (e.g., coronary artery disease [127], hypertension [128]), and immune-related diseases (e.g., rheumatoid arthritis [128]).

1.1.4 Therapeutic approaches

The gut microbiota plays a crucial role in maintaining health. Imbalances in the gut flora, known as dysbiosis, have been linked to various diseases. Therapeutic approaches that target the microbiome aim to restore balance or enhance its beneficial functions. These therapies range from promoting the growth of beneficial microorganisms to directly modifying bacterial

genomes. Each treatment has a specific mechanism of action. Each targets different aspects of microbiome function and brings different outcomes. Here are the main approaches:

Prebiotics: Prebiotics are non-digestible food components that promote the growth and activity of beneficial bacteria in the gut, such as *Bifidobacterium* and *Lactobacillus* [129, 130]. There are several types of prebiotics, primarily oligosaccharide carbohydrates (OSCs), but some non-carbohydrate compounds also meet prebiotic criteria [131, 132]. Prebiotics are naturally present in a range of foods, including vegetables like asparagus, sugar beet, garlic, chicory, onion, and Jerusalem artichoke; grains such as wheat, barley, and rye; fruits like bananas and tomatoes; legumes such as peas and beans; as well as in human and cow's milk [133]. Recently, they have also been identified in seaweeds and microalgae [133]. Some prebiotics are produced using lactose, sucrose and starch as raw materials [134].

Prebiotics remain undigested as they travel through the upper GI tract to the colon, where they are fermented by gut microbes [135]. This fermentation produces short-chain fatty acids (SCFAs), such as acetate, propionate, and butyrate [136]. These SCFAs support gut health by providing energy to colon cells and strengthening the gut barrier [137]. They also have systemic benefits, such as immune system modulation and anti-inflammatory effects [138]. Prebiotics selectively promote the growth of beneficial bacteria such as *Bifidobacteria* and *Lactobacillus*, improving the balance of gut microbiota and outcompeting harmful pathogens [139]. Prebiotics can also impact metabolism by enhancing lipid profiles and improving the absorption of minerals like calcium and magnesium, which contribute to bone health [140].

Ongoing studies have explored the potential of prebiotics to treat various conditions, including irritable bowel syndrome (IBS), inflammatory bowel disease (IBD), and mental health problems, through the gut-brain axis [141-143].

Probiotics: Probiotics are live microorganisms that provide health benefits when taken in adequate amounts [144]. To be effective, they must be safe for consumption, survive the gastrointestinal tract, and adhere to the intestinal mucosa. Probiotics can enhance gut health, boost immune function, and lower the risk of specific infections and diseases [145, 146]. They work by balancing gut microbiota, inhibiting harmful pathogens, and modulating the immune response [147, 148]. Probiotics are commonly found in dietary supplements and functional foods and are also used for the treatment of various gastrointestinal disorders [149, 150].

Fecal microbiota transplant (FMT): Fecal microbiota transplantation (FMT) is a medical procedure in which stool from a healthy donor is transplanted into the gastrointestinal tract of a patient to restore a balanced gut microbiota and help treat various gastrointestinal and systemic diseases [151]. The practice dates back to 4th century China, where it was used to treat severe diarrhea and food poisoning [152]. This practice has evolved over centuries, and in modern medicine, it gained significant attention in the 20th century, particularly for its effectiveness in treating recurrent *Clostridium difficile* infection (CDI) [153]. Initially, FMT was primarily used to treat recurrent and refractory CDI, enteric infections with bacteria that cause severe diarrhea and colitis [154]. However, research has expanded its potential applications to inflammatory bowel diseases (IBD) such as Crohn's disease and ulcerative colitis, irritable bowel syndrome

(IBS), metabolic syndrome (including obesity and type 2 diabetes), neurological disorders such as autism spectrum disorder and multiple sclerosis, and other infections, including infections with antibiotic-resistant bacteria [155-157].

The FMT process involves several steps to ensure safety and efficacy: the potential donor is rigorously screened for infectious and GI diseases, and the donor's stool is processed to isolate the microbiota [158-161]. This preparation involves homogenizing the feces, filtering, and sometimes adding a cryoprotectant if the sample is to be stored [162]. The prepared fecal microbiota can then be delivered to the recipient by various methods, including colonoscopy (direct access to the colon), enema (a less invasive method), nasogastric or nasoduodenal tubes (access to the stomach or small intestine through the nose), and oral capsules containing freeze-dried fecal microbiota [163, 164].

FMT is generally considered safe, with few reports of adverse effects. They are usually mild gastrointestinal symptoms such as colic, bloating and diarrhea [165, 166]. However, long-term safety and efficacy are still being investigated, and ongoing studies are aimed at better understanding potential risks and benefits.

Gene editing: Recent advances in genetic manipulation techniques, particularly CRISPR-Cas and transposon-based systems, have revolutionized the ability to modify both model and non-model gut bacteria [167, 168]. CRISPR-Cas technology allows precise editing of bacterial genomes, allowing researchers to knock out or insert specific genes that affect microbial behavior and function [169]. On the other hand, transposon systems facilitate the random

insertion of genetic material, helping to identify essential genes associated with specific traits or functions of gut bacteria [170]. Several challenges remain in the genetic manipulation of gut bacteria. A major challenge is the efficient delivery of DNA into bacterial cells, since many gut bacteria have defense mechanisms that degrade foreign DNA [171, 172]. Researchers are exploring innovative solutions, such as targeted integration using CRISPR-Cas9, which could bypass some of these barriers [173, 174]. In addition, transposon-based integration approaches are being developed to improve the efficiency of gene delivery and expression in bacterial populations [175].

Gene editing offers unique advantages over prebiotics and fecal microbiota transplantation (FMT) for manipulating the gut microbiome. Its precision allows for the targeted modification of specific genes in bacteria, leading to the development of customized strains that are effective in addressing specific health problems. Unlike complex mixtures introduced through FMT, gene editing simplifies intervention by focusing on specific strains, resulting in more stable and predictable outcomes. In addition, engineered strains can induce long-lasting changes in the microbiome. In contrast, prebiotics and FMT usually require continuous administration.

These approaches to manipulate gut microbiome have advanced our understanding of host-microbiome interactions, paving the way for more effective microbiome-based therapies. As the field grows, more research needs to be carried out and more ethical and safety factors must be carefully considered.

1.1.5 Animal models

Animal models play a crucial role in gut microbiome studies, providing insights into the complex interactions between the host and its microbiota. They allow researchers to manipulate variables such as diet, environment, and microbiota composition to observe physiological and pathological outcomes. Animal studies can help assess the effects of specific bacteria on health and disease, and evaluate potential therapeutic interventions. Moreover, they allow us to investigate the underlying mechanisms of host-microbiome interactions, which can be challenging to conduct in human subjects due to ethical constraints. Animal models for studying the gut microbiome include rodents, large animals like cats, dogs, and minipigs, as well as invertebrate models like fruit flies and worms.

It is essential to understand the characteristics of different animal models and how they differ from humans. First, it helps researchers determine which models best mimic human gut physiology and microbiome interactions, leading to more reliable experimental results. Second, recognition of anatomical and physiological differences facilitates the interpretation of findings, ensuring that conclusions drawn from animal studies can be appropriately translated into the human context. Such knowledge facilitates the development of effective therapies and interventions for gut-related diseases, ultimately improving the efficacy and safety of treatment in humans.

Traditional rodent models: Rodent models, especially mice and rats, are widely used for gut microbiome studies due to their genetic similarity to humans (mice: ~70%; rats: ~90%) and the convenience of researchers to control environmental variables [176, 177]. Rodents have a simpler GI tract than humans, with a shorter colon, which is proportional to their body size [178,

179]. Rodents have similar organ systems compared to humans, including heart, brain, lungs, kidneys, and liver [180]. For example, the circulatory, reproductive, digestive, hormonal, and nervous systems of rodents function similarly to those of humans [177]. This similarity extends to hormonal regulation of body functions and susceptibility to many of the same diseases, such as cardiovascular disease, diabetes, and neurological diseases [181-183]. These genetic and physiological similarities allow researchers to study disease mechanisms, test new treatments, and understand complex biological processes in ways that are generally applicable to human health.

Germ-free mice are experimental animals that are completely free of any microbes, including bacteria, viruses, fungi, and parasites [184]. They are kept in a sterile environment ensuring that they are not exposed to microorganisms throughout their lives [185]. These mice are valuable tools in microbiome studies because they allow scientists to study the effects of individual or groups of microbes on host physiology, immune function, and metabolism in a highly controlled environment. By colonizing germ-free mice with specific microbial communities, researchers can analyze the contribution of these microbes to various health conditions or disease mechanisms [186]. Currently, germ-free mice have been particularly useful in microbiome studies to study the relationship between gut microbiota and diseases such as obesity, inflammatory bowel disease, and even neurodevelopmental disorders [187-189].

Large animal research models: Cats share both differences and similarities with humans in their gut anatomy and physiology. This makes them valuable models in certain areas of research, but there are limitations. Cats share a great deal of genetic similarity with humans, with domestic

cats sharing approximately 90% of their genes with humans [190]. In addition, the genome structure and organization of cats are more similar to those of humans compared to mice and dogs, which further enhances their utility in genetic studies [191].

However, cats are obligate carnivores, whereas humans are omnivores [192]. This means that their digestive systems are highly specialized in processing animal-derived proteins and fats rather than carbohydrates [193]. They have shorter guts compared to humans, which is typical of carnivorous species [194]. Because they do not rely heavily on plant materials that require prolonged fermentation [195]. They are also limited in their ability to metabolize carbohydrates compared to humans due to their low levels of enzymes such as amylase [196]. These differences in genetic, dietary, and digestive functions mean that while cats are useful in genetic disease studies and those related to carnivorous diets and protein metabolism, they are less suitable for studies focusing on omnivorous diets and carbohydrate handling.

To date, there have been over 20 studies on the feline gut microbiota, demonstrating that factors such as diet, prebiotics or probiotics, age, diarrhea, or other health conditions can influence its composition [197-220]. Similar to cats, dogs have both differences and similarities to humans in terms of gut anatomy and physiology, making them valuable models for some gastrointestinal studies but less applicable in other areas. First of all, dogs share a significant amount of genetic similarity with humans, approximately 84% of the DNA in dogs is shared with humans [221]. Like humans, dogs are monogastric and have a single-chamber stomach that allows for similar digestive processes, including the breakdown of food through gastric acids and enzymes [222]. The structure of the small and large intestine in dogs is also similar to that in humans and plays a

comparable role in nutrient absorption and water reabsorption [222]. These similarities make the dog an appropriate model to study various aspects of the human digestive system, including the gut microbiome and GI diseases. However, compared to humans, dogs are omnivores and have a stronger carnivorous tendency, which affects their digestive physiology [223]. Their digestive tract is shorter than that of humans, digests proteins and fats more efficiently, and has limited capacity to process carbohydrates [223, 224]. In addition, dogs have shorter intestinal transit times than humans, which may affect nutrient absorption and gut microbiota development [225, 226]. These differences highlight the limitations of using dogs as direct models for studies related to carbohydrate metabolism and intestinal transport.

Pigs, especially minipigs, share significant anatomical and physiological similarities with humans, making them valuable models for gut microbiome studies. What's more, pigs share a great degree of genetic similarity with humans, with about 98% of the pig genome being similar to the human genome [227]. This genetic similarity makes the pig a valuable model for studying human diseases and for biomedical research, including organ transplantation (xenotransplantation) [228, 229]. The structure of the porcine digestive system, including similar large bowel length and surface area, is very similar to that of humans [230]. Both species exhibit an omnivorous diet and similar GI transit times [231, 232]. In addition, the microbial composition of the pig gut, especially the large intestine, has significant similarities to the human microbiome [233]. However, there are differences such as the relative size of the pig stomach and the larger cecum, which may affect microbial fermentation and nutrient absorption differently from humans. Despite these differences, the pig remains one of the most relevant large animal models for the study of human gut health and microbiome-related diseases.

Some simple invertebrates, such as flies, worms, and bees, are also valuable animal models for gut microbiome studies. They have relatively simple and well-characterized gut microbiota, which makes it easier to study specific microbial interactions and their impact on host physiology [234]. In addition, these models are cost-effective, have short generation times, and are easy to genetically manipulate, allowing high-throughput and detailed mechanistic studies [234].

1.2 Dissertation Structure

The gut microbiota is essential for the health and physiology of animals, influencing a wide range of biological processes and disease mechanisms. However, research on the gut microbiota in cats and dogs is limited, particularly concerning the unique characteristics of the gut microbiota in obese cats and its relationship with memory performance in dogs. This dissertation seeks to fill these gaps by characterizing the gut microbiota of obese cats and investigating its association with memory in dogs through metagenomic sequencing. The work focuses on three key aspects: (1) standardized fecal sample collection methods for accurately characterizing the gut microbiota in cats; (2) the metagenomic analysis of gut microbiota in obese cats to identify microbial species associated with feline obesity; and (3) the exploration of the relationship between gut microbiota composition and memory performance in dogs.

In Chapter 1, we introduced the background of the study, highlighting the crucial role of gut microbiota in animal health and physiology. We discussed the current understanding of the establishment of gut microbiome and how gut microbiota influences various biological processes, including metabolism, immune function, and behavioral outcomes.

In Chapter 2, the research focuses on the methodologies for collecting fecal samples from domestic cats. It evaluates the impact of the use of lubrication during sample collection and compares two primary fecal collection techniques: using a fecal ring versus a litter box. This chapter aims to provide insights into how these methods can affect the analysis of gut microbiota and seeks to develop standardized protocols for fecal sample collection in feline microbiome studies.

In Chapter 3, the study presents the metagenomic analysis of the gut microbiota in obese cats. The study identifies key microbial species associated with obesity and reveals a significant reduction in microbial diversity, suggesting potential dysbiosis. The findings indicate a panel of seven specific microbial species that could serve as indicators of obesity in cats. This chapter contributes new insights into the composition, abundance, and functional capacities of the gut microbiome in obese cats, emphasizing its role in metabolic dysregulation.

In Chapter 4, this part explores the relationship between gut microbiota composition and memory performance in dogs. It identifies *Bifidobacterium pseudolongum* as a bacterial species correlated with memory performance. Utilizing a random forest regression model, the study reveals that the abundance of 17 bacterial taxa in the microbiome has a strong predictive capacity for memory performance. The findings shed light on the microbiome's influence on cognitive functions in mammals and suggest potential strategies for enhancing canine memory and learning.

In Chapter 5, we concluded the whole work and outlined the future direction of the research regarding animal health.

CHAPTER 2

Analysis of the Impact of Different Sampling Methods on Reconstructing the Gut Microbiome Profiles in Cats Based on Metagenomic Sequencing Technology

CHAPTER 2.1

Effect of mineral oil as a lubricant to collect feces from cats for microbiome studies

2.1.1 Introduction

The gut microbiota is the collection of microorganisms that inhabit the host's gastrointestinal tract. There is clinical and physiological importance to understanding the gut microbiome based on its interactions with the host in healthy states and its involvement in the etiology of many diseases, including rheumatoid arthritis [235], colorectal cancer [236, 237], cardiovascular disease [238], and inflammatory bowel disease [239, 240].

Low-stress handling and fear reduction techniques are the new standard of care for veterinary patients [241, 242]. Using a lubricant can minimize stress, discomfort, and pain and prevent escalating fear in cats. An additional challenge of the dry collection (nonlubricated) approach using a fecal loop is that, in many cases, little to no fecal material is obtained, resulting in variable and insufficient amounts of material for metagenomic analysis, which leads to missing data and an imbalanced experimental design. During sample collection with a fecal loop, lubrication can consistently guarantee sufficient specimens for analysis. In addition to the previously mentioned welfare benefits, the lubrication approach will reduce potential host contamination. Fecal loop use could cause abrasion to the intestinal wall, leading to the shedding of host cells and bleeding, which increases host DNA contamination. Therefore, using lubricant will allow sufficient fecal sample collection with reduced incidence of bleeding, pain, discomfort, and potential infection and less chance for host contamination in the fecal samples. However, using lubricant might alter the microbial composition and abundance in the gut microbiome. Currently, no research has addressed this issue.

Reproducibility and stability of microbial profiles recovered from fecal samples are vital to the reliability of the analytical results. In this study, we evaluated the WGS metagenomic data consistency from cat fecal samples collected using mineral oil lubrication vs no lubrication, to provide information for veterinarians and researchers regarding appropriate methods to evaluate the cat gut microbiome.

2.1.2 Materials and methods

2.1.2.1 Animals

The study was approved by the Auburn University Institutional Animal Care and Use Committee (IACUC) with protocol number PRN 2019-3482. Eight obese, 6-year-old, neutered male cats were enrolled. All the animals were maintained at the Scott-Ritchey Research Center, College of Veterinary Medicine, Auburn University (Auburn, Alabama), and cared for according to the principles outlined in the NIH Guide for the Care and Use of Laboratory Animals.

2.1.2.2 Study design

The sample size of 8 was determined based on the rarefaction plots in our published research on the feline microbiome [243], to ensure at least 90% of bacterial species and microbial genes in the reference assembly (NCBI Assembly ID JAIZPE000000000) were covered. Two fecal samples were collected from each of the 8 enrolled cats under sedation. The first batch of collections was performed without any lubrication (noLub sample group), and the second batch of collections was performed on the same day with mineral oil lubricant (miOil sample group). All fecal specimens were placed into 1.5 mL sterile Eppendorf tubes, flash-frozen, and stored immediately in a -80°C freezer (CryoCube F570, Eppendorf North America, Enfield, Connecticut).

2.1.2.3 Sedation and rectum fecal sample collection procedure

Adopting low-stress handling methods [242], cats were sedated to effect using a cocktail of intramuscularly administered medetomidine, ketamine, and butorphanol. For each participant, the small end of a plastic fecal loop (cat. no. 7500, Covetrus, Dublin, Ohio) was inserted into the rectum and descending colon to obtain an adequate amount (>200 mg) of feces. For the miOil samples, the fecal loop was coated with mineral oil (Equate, Bentonville, Arkansas), and the

same sampling procedure was repeated.

2.1.2.4 Microbial DNA extraction and quality control

Genomic DNA samples were extracted from 200 mg fecal samples using the Allprep PowerFecal DNA/RNA kit (Qiagen, Redwood City, California) according to the manufacturer's protocols. To reduce technical variability, the homogenization step was performed for all fecal samples in the same batch using a PowerLyzer24 instrument (Qiagen, Redwood City, California). DNA concentrations were measured by a Qubit 3.0 Fluorometer (Thermo Fisher Scientific, Waltham, Massachusetts), and the A260/A280 absorption ratios were assessed by a NanoDrop One C Microvolume Spectrophotometer (Thermo Scientific, Waltham, Massachusetts).

2.1.2.5 Whole-genome shotgun metagenomic library construction and sequencing

For each sample, 1 µg of DNA was sheared into fragments of 500 bp by an M220 Focused-ultrasonicator (Covaris, Woburn, Massachusetts). Whole-genome shotgun metagenomic sequencing libraries were constructed using NEBNext Ultra II DNA Library Prep Kit for Illumina (New England BioLabs, Ipswich, Massachusetts). LabChip GX Touch HT Nucleic Acid Analyzer (PerkinElmer, Hopkinton, Massachusetts) was used to determine the library concentrations and size distributions, which were 600 bp on average, including sequencing adapters. The final libraries were measured by qPCR before being sequenced on an Illumina NovaSeq6000 sequencing machine in 150-bp paired-end mode at Novogene (Novogene Corporation Inc., Sacramento, California).

2.1.2.6 Processing and bioinformatic analysis of metagenomic data

The 16 metagenomes yielded a total of 1.28 billion raw sequencing reads (192 Gbp). After trimming the adapter sequences and low-quality bases using Trimmomatic (version 0.36) [244], the high-quality reads were aligned to the feline reference genome *Felis_catus_9.0* [245] using Burrows-Wheeler Aligner (BWA) (version 0.7.17-r1188) [246] to detect host contaminations. The feline reads were extracted using SAMtools (version 1.6) [247] and BEDTools (version 2.30.0) [248]. The remaining microbial reads were aligned to the feline gut metagenomic reference contigs (GCA_022675345.1) [249] with comprehensive taxonomy assignments and microbial gene annotations. Taxonomic abundances were determined in the form of read counts, which were normalized by the total amount of sequences to obtain counts per million mapped reads (CPM) for subsequent metagenomic analyses.

2.1.2.7 Microbial diversity analyses

Alpha- and beta-diversity analyses were performed with the R package *vegan* (version 2.5.7) [250]. The alpha diversity measures of microbial profiles at different taxonomic levels and the microbial gene level were calculated using the Shannon index [251]. Beta diversity was calculated based on the Bray-Curtis dissimilarity matrices [252] generated from the composition of the microbial profiles. Visualization of the beta diversity was in the format of PCoA (Principal Coordinates Analysis) plot using the R software [253].

2.1.2.8 Statistical analysis

The statistical analyses were performed using the statistical software package R, version 4.0.2 [253]. Differences in DNA yield (ng/mg fecal specimen), library yield (Gbp), percentage of host contamination, number of microbial genes, relative abundance of specific taxa, and Shannon

index from α -diversity analyses of microbial profiles at each taxonomic levels between groups, were analyzed using the Wilcoxon signed-rank test in the R software [254, 255]. Permutational multivariate analysis of variance (PERMANOVA) test was performed using Adonis function in the R package vegan [256-260], to estimate the percentage of variability (R^2) explained by different fecal sample collection methods based on Bray-Curtis distance matrices. When P -value was less than 0.05, the null hypothesis was rejected. To estimate the correlation of taxonomy composition of fecal samples collected using mineral oil lubrication or without lubrication, Spearman's rank-order correlation coefficients were calculated using the R software. The P -value was determined using Spearman's correlation test (a permutation test). To determine the differences in the variance, non-parametric Levene's test of equality of variances was performed using the R software.

2.1.2.9 Data availability

The whole-genome shotgun metagenomic sequencing data is available at NCBI SRA under accession number PRJNA821230.

2.1.3 Results

2.1.3.1 Fecal sample collection using mineral oil lubrication does not alter microbial DNA yield

No significant differences were observed in DNA yield per mg fecal specimen between miOil and noLub groups (75.75 ng [25.80-125.70] vs 60.72 ng [33.49-87.95], $P = 0.95$, Wilcoxon signed-rank test; Figure 2.1A), suggesting a lack of effect on microbial DNA yield using mineral oil lubricant.

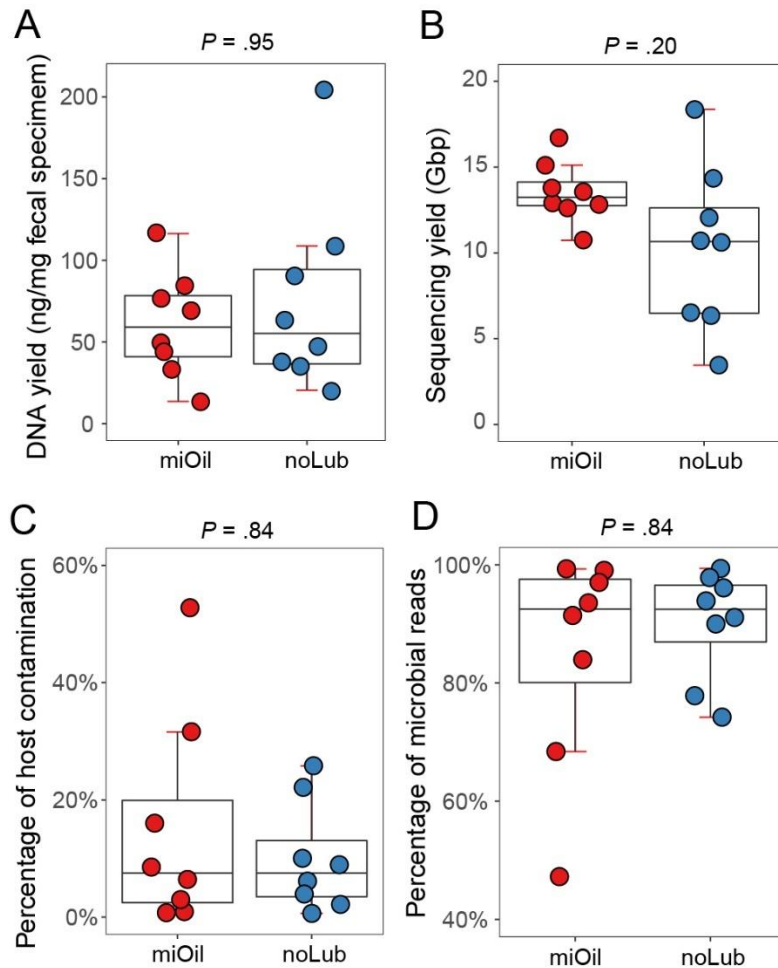


Figure 2.1 Metagenomic sequencing statistics from fecal samples in miOil and noLub groups. (A) Boxplot of DNA yield (ng) per mg fecal specimens in miOil (red) and noLub (blue) groups. (B) Boxplot of metagenomic library yield (Gbp) of each sample in miOil (red) and noLub (blue) groups. (C) Boxplot of percentage of host contamination in miOil (red) and noLub (blue) groups. (D) Boxplot of percentage of microbial reads in miOil (red) and noLub (blue) groups.

2.1.3.2 WGS metagenomics sequencing yield and levels of host contamination are not significantly affected by mineral oil lubrication

In total, 1.28 billion 150-bp reads (or 192 Gbp reads) were generated in the WGS metagenomic sequencing of 16 fecal DNA samples. Of these, 1.2% were adapter sequences or low-quality bases, and 12.5% were cat sequences. The yield from the miOil group (13.5 Gbp on average) was not

statistically different from the noLub group (10.3 Gbp; $P = 0.2$, Wilcoxon signed-rank test; Figure 2.1B). We did observe an increased variation in sequencing yield in the noLub group (23.1) compared to the miOil group (3.2), which is statistically significant ($P = 0.04$, Levene's test of homogeneity of variance). The percentage of host contamination was not significantly different between the miOil group and the noLub group ($P = 0.84$, Wilcoxon signed-rank test; Figure 2.1C,D).

2.1.3.3 Fecal sample collection using mineral oil lubrication does not change the number of microbial taxa discovered in the WGS metagenomic sequencing data

In the WGS metagenomic data from the noLub group, on average, we discovered 84.5 phyla [75.1-93.9], 73.8 classes [69.1-78.4], 157.8 orders [146.4-169.1], 330.5 families [303.7-357.3], 1141.6 genera [1002.5-1280.7], and 4985.9 species [4300.3-5671.5]. Under mineral oil lubrication, there was no significant change in the number of phyla (86.6, [77.2-96]; $P = 0.96$), classes (75.1, [71-79.2]; $P = 0.96$), orders (162.4, [153-171.8]; $P = 0.83$), families (342.8, [323.1-362.4]; $P = 0.83$), genera (1196.6, [1076.2-1317]; $P = 0.67$), and species (5300.6, [4679.3-5921.9]; $P = 0.67$) detected in the rectum microbiome (Figure 2.2).

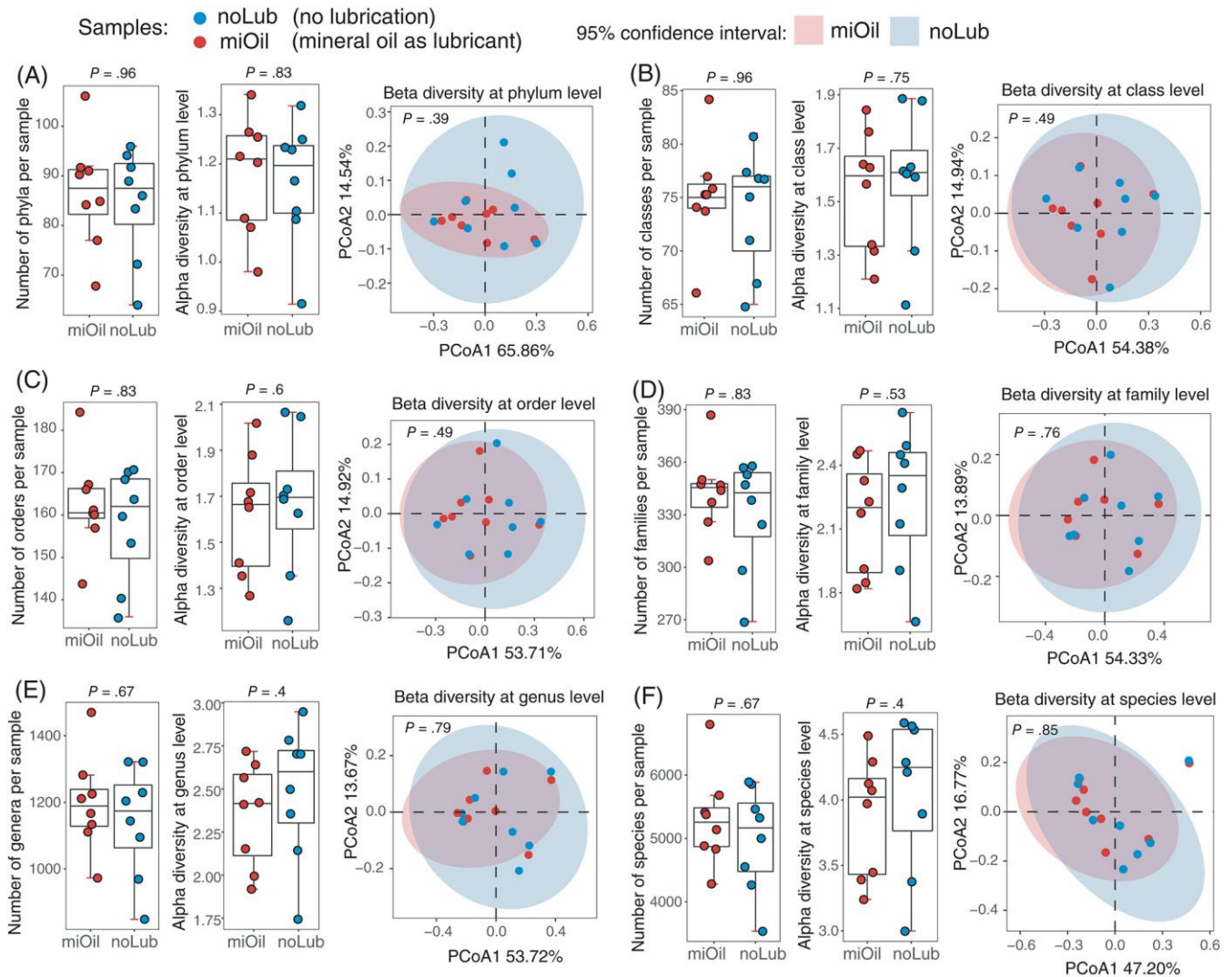


Figure 2.2 Microbial diversity analyses at different taxonomic levels from fecal samples collected with mineral oil (miOil) or without lubrication (noLub). Boxplots of number of categories of nonredundant taxonomic units and Shannon index of alpha diversity for each sample and principal coordinates analysis (PCoA) plot of beta diversity using Bray-Curtis dissimilarity for microbial profiles from the miOil (red) and noLub (blue) groups at (A) phylum, (B) class, (C) order, (D) family, (E) genus, and (F) species levels.

2.1.3.4 Fecal sample collection using mineral oil lubrication does not change the microbial diversity measured by WGS metagenomic sequencing at all taxonomic levels

Alpha-diversity was measured for the noLub and miOil metagenomes using the Shannon index (Figure 2.2). No significant differences in α -diversity were detected between the noLub and

miOil samples at phylum (1.16 vs 1.18, [1.06-1.27] vs [1.08-1.28]; $P = 0.83$), class (1.59 vs 1.54, [1.37-1.82] vs [1.35-1.73]; $P = 0.75$), order (1.67 vs 1.62, [1.41-1.93] vs [1.4-1.84]; $P = 0.6$), family (2.25 vs 2.15, [1.97-2.52] vs [1.93-2.37]; $P = 0.53$), genus (2.48 vs 2.35, [2.16-2.81] vs [2.1-2.6]; $P = 0.4$), and species level (4.06 vs 3.88, [3.56-4.55] vs [3.49-4.26]; $P = 0.4$; Figure 2.2). When β -diversity was examined using Bray-Curtis dissimilarity in PCoA analyses, no significant changes were detected either ($P > 0.39$ for comparisons at all 6 taxonomical levels; PERMANOVA test; Figure 2.2). The overlapping confidence intervals indicated the microbial compositions could not be distinguished between the 2 fecal sample collection methods.

2.1.3.5 Use of mineral oil lubrication did not alter the relative abundance of major microbial phyla in the cat rectal microbiome

The top five most abundant phyla in the cat gut microbiota are Bacteroidetes, Firmicutes, Actinobacteria, Proteobacteria, and Fusobacteria [198, 249]. In our WGS metagenomic data, none of the 5 major phyla (Bacteroidetes, Firmicutes, Actinobacteria, Proteobacteria, and Fusobacteria) had significant differences in their relative abundance between miOil and noLub groups ($P > 0.05$, adjusted $P > 0.85$; Wilcoxon signed-rank tests; Figure 2.3A).

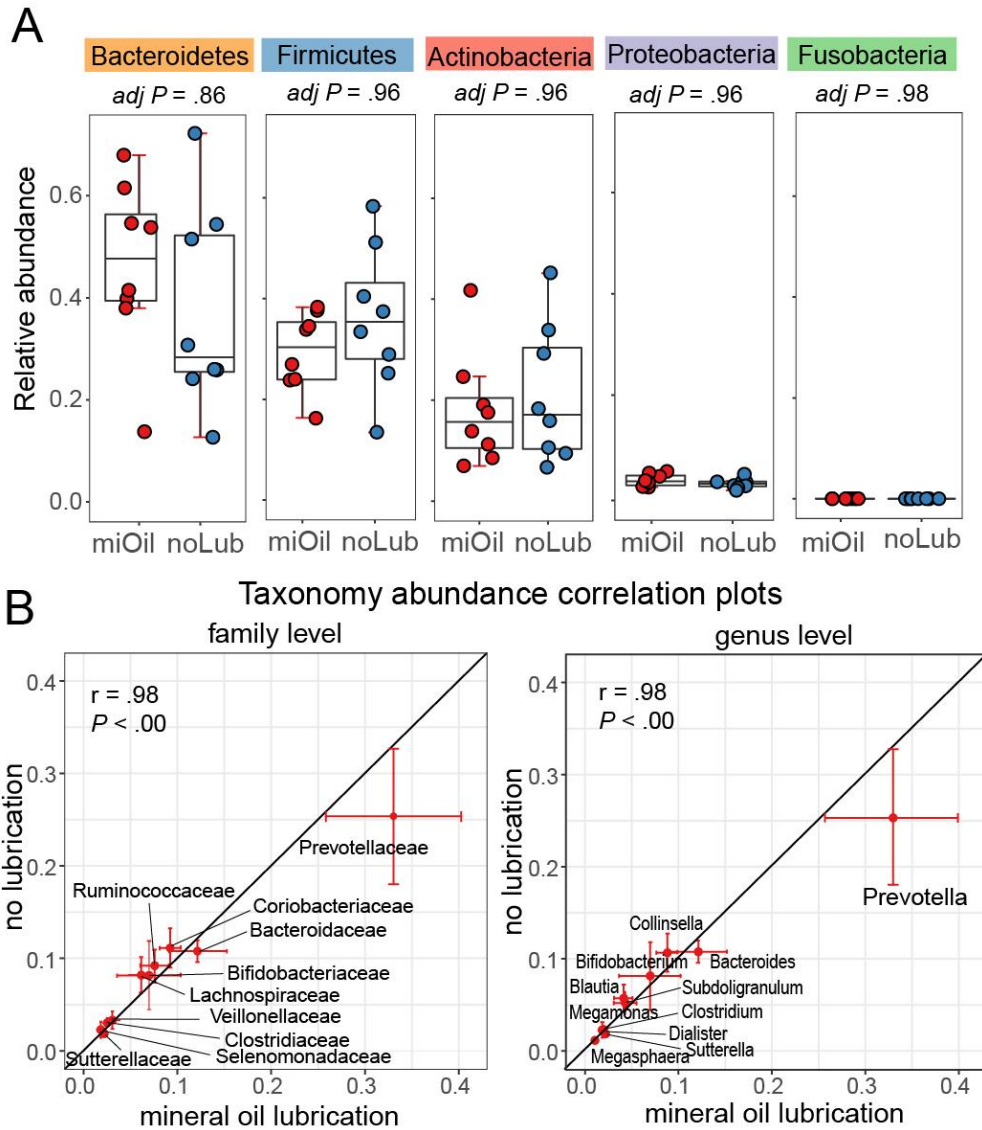


Figure 2.3 Phylum level taxonomy composition and relative abundance and correlation plots of microbes with high abundance (>1%) at family and genus levels. (A) Boxplots of top 4 high-abundance phyla (relative abundance >0.01%) in miOil (red) and noLub (blue) groups. (B) Correlation plots of microbes with high abundance (>1%) at family and genus levels.

2.1.3.6 Correlation of taxonomy composition inferred from fecal samples collected using mineral oil lubrication vs. no lubrication

In both the miOil and noLub groups, 99.72% of the metagenomic sequences belonged to bacteria reads, 0.11% were viral reads, 0.01% were archaeal reads, and the rest (0.16%) remained unknown. Considering the biological importance, we examined the microbial taxa with high

relative abundance (>1.00%) at different taxonomical levels, which included 7 classes, 7 orders, 10 families, 11 genera, and 14 species. No significant changes were detected between miOil and noLub groups in the relative abundance at any taxonomic level (adjusted $P > 0.8$, Wilcoxon signed-rank test). The Spearman's rank-order correlation coefficients were extremely high between the noLub and miOil groups at the family ($\rho = 0.99$, $P < 0.000001$) and the genus levels ($\rho = 0.98$, $P < 0.0000001$; Spearman's rank-order correlation test; Figure 2.3B).

2.1.3.7 Number of microbial genes annotated from fecal samples collected using mineral oil lubrication vs. no lubrication

A total of 834,014 nonredundant microbial genes were identified in the 16 metagenomes. Of these, 798,430 genes were identified in 8 miOil metagenomes, and 769,476 genes were identified in 8 noLub metagenomes (Figure 2.4A). There was no significant difference in the number of observed genes between fecal samples collected with mineral oil and samples collected without lubrication ($P = 0.31$, Wilcoxon signed-rank test; Figure 2.4A). The alpha diversity based on the Shannon index of the observed genes from the 2 groups showed no significant difference either ($P = 0.38$, Wilcoxon signed-rank test; Figure 2.4B). Based on the Bray-Curtis distance matrix, no significant dissimilarity was detected between miOil and noLub groups in the PCoA analysis, and 95% confidence interval ellipses were overlapped ($P = 0.94$, PERMANOVA test; Figure 2.4C).

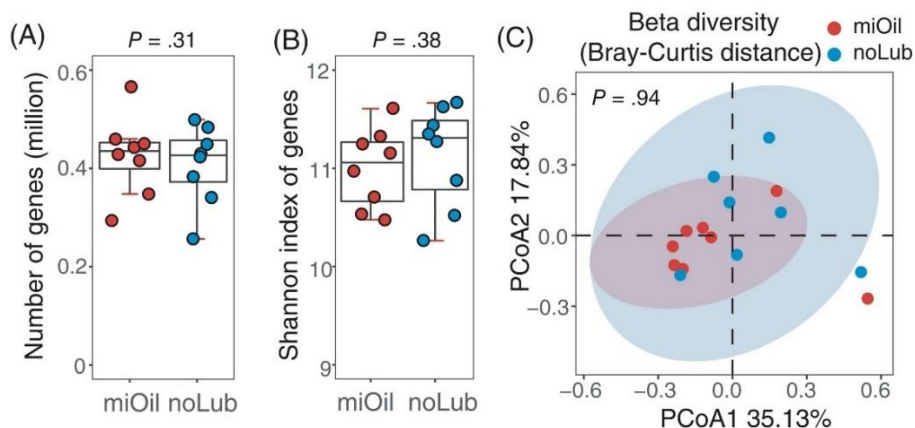


Figure 2.4 The number, alpha diversity and beta diversity of the microbial genes identified in the miOil and noLub groups. (A) Boxplot of the number of observed genes in the miOil (red) and noLub (blue) groups. (B) Boxplot of Shannon index of genes identified in the miOil (red) and noLub (blue) groups. (C) PCoA plot of beta diversity based on Bray-Curtis distance of the genes identified in the miOil (red) and noLub (blue) groups.

2.1.4 Discussion and conclusion

Fecal specimen collection is a commonly used approach in veterinary clinics and research to detect zoonotic parasites and diagnose pathogenic infections. Common methods for fecal sample collection in veterinary medicine include collection from the litter box and collection from the rectum using a fecal loop. Studies using cat fecal samples from litter boxes have 2 potential shortcomings. First, it is difficult to determine the freshness of the specimen, and excessive time at room temperature will shift the microbial composition. Second, it is likely the sample is contaminated by the environment. For projects designed to accurately represent the gut microbiome, fecal samples are collected from the rectum using a fecal loop, which can cause increased distress compared to litterbox collections. Lubrication is necessary to increase sample quality and to improve animal welfare during sample collection. In this group of cats, our results suggest that if adequately lubricated, the mineral oil applied will not affect the fecal microbial

DNA extraction or gut microbiome analysis. The benefits of collection with lubrication include improved animal welfare and reduced variability in sequencing yield.

Fecal sample collection using a fecal loop in cats is challenging. It can cause discomfort, pain, and bleeding in the cat and result in little to no samples if it is done incorrectly. In an earlier attempt to collect fecal samples from the 8 cats enrolled in this research using a dry collection approach, we were only able to obtain a sufficient quantity of feces from 6/8 cats, and bleeding was observed in 5/8 cats. This failure led us to explore modifications to the fecal sample collection methods. Lubrication can ease the fecal sample collection process and ensure a sufficient amount of samples, but the lubricant could introduce materials that could prevent DNA extraction and sequencing or alter the microbiome composition. To determine if using lubricants during fecal sample collection has potential effects on the gut microbiome, we performed fecal collections with lubrication and without lubrication on the same 8 cats. The sample size was determined from the rarefaction plots from a previous study, in which a sample size of $n = 6$ will detect >90% of the bacterial species and microbial genes in the cat reference microbiome [243]. In our metagenomic data analyses, we did not observe any significant changes in alpha-diversity, beta-diversity, the number of taxa discovered at each taxonomy level, and the relative abundances of taxonomic units are also highly correlated, indicating that the microbial composition was not affected by the use of lubricant.

We expected to see less host sequence contamination in the samples collected with mineral oil lubrication because the use of the fecal loop without lubrication is more likely to damage the intestinal wall, resulting in a higher proportion of host contamination. However, we did not

observe any significant differences in host contamination, which could be because we sampled the same cat on the same day, and the more readily sloughed host cells had already exfoliated after the fecal loop collection without lubrication. The level of host DNA contamination (12.5%) is acceptable in both groups, given that intestinal cells are constantly sloughed off into the gut lumen.

Lubrication did not cause any issues in microbial DNA extraction, and a similar yield was observed in both groups, which is sufficient for subsequent research purposes. Interestingly, we observed a lower variability of the metagenomic sequencing yield, and this homogenous yield across the samples is beneficial for achieving an even level of metagenome coverage.

Whole-genome shotgun (WGS) metagenomic sequencing was performed in this study to assess the feline microbiome, as this method is rapidly becoming the new standard for assessing microbiomes across all species. We anticipate that the results will be applicable to 16S rDNA ampliconic sequencing, because a high correlation in taxonomic composition was observed in the feline microbiome using these 2 approaches [243].

One limitation of this study is that our results only applied to fecal samples stored immediately in an ultracold freezer after collection. The same results might not hold in other storage conditions (room temperature, 4°C refrigeration, DNA stabilizing solution, etc.).

CHAPTER 2.2

Evaluation of fecal sample collection methods for feline gut microbiome profiling: fecal loop vs. litter box

2.2.1 Introduction

Understanding the feline microbiome is essential in veterinary medicine, informing the diagnosis and treatment of conditions such as gastrointestinal disorders, obesity, and immune-mediated diseases [243, 261, 262]. Additionally, research on the feline microbiome offers insights into zoonotic disease transmission and the transfer of beneficial microorganisms between cats and their owners [263, 264]. Thus, investigating the feline microbiome is crucial for advancing veterinary medicine and enhancing our understanding of human-animal interactions. The method of collecting fecal samples is crucial for obtaining accurate microbial profiles in microbiome studies [265-268], providing insights into microbial population structures and their correlations with health or disease. The two most commonly used methods for collecting feline fecal samples are: (1) the fecal loop method, which involves using a small plastic instrument with a looped end to collect a sample of the cat's stool from the rectum, and (2) the litter box approach, which involves collecting the cat's stool directly from the litter box. For the latter approach, it is vital to collect the sample immediately after the animal defecates to minimize the risk of environmental contamination of the microbiome. The fecal loop method provides a precise and sanitary collection technique, which minimizes the risk of cross-contamination and exposure of anaerobes to oxygen. However, this approach is often invasive and potentially uncomfortable or painful for

cats. It should only be performed by veterinarians or experienced personnel who can insert the loop into the rectum and gently scoop out a small amount of feces. Moreover, sedation may be required prior to fecal loop collection, which can increase the time and cost involved in the process, particularly when dealing with multiple cats. The litter box method involves regularly monitoring the litter box, and promptly collecting the fresh stool with a clean and sterile container or scoop when the cat defecates. This approach is a non-invasive and cost-effective method commonly used in large-scale population studies, involving sample collection by cat owners. However, there is a greater risk of introducing environmental contaminations, which may affect the accuracy and completeness of the microbial community representation in the sample [269-271]. Collecting fecal samples directly from the litter box may limit the information available to the clinician and researcher regarding fecal consistency [272]. The choice of method depends on factors such as the specific research goals, the need for precision and sanitation, the invasiveness and discomfort for the cat, and the potential for environmental contamination.

Researchers should be mindful of the potential limitations and take steps to minimize environmental contamination and ensure timely sample collection. In addition to the conditions of the fecal sample, the stability of the microbial community within fecal samples is a critical aspect of microbiome research. This is particularly important when considering the method of sample collection, as gut microbial profiles are often linked to health status and have the potential to indicate the development of metabolic diseases, gastrointestinal disorders, and even cancer [273-281]. Using a fecal loop may reduce environmental contamination, but it also poses the risk of contaminating the sample with cells from the host's bowel wall or blood due to improper technique. Furthermore, it is important to note that using a fecal loop for sample

collection may result in insufficient amounts of fecal material, which in turn could lead to an incomplete representation of the microbial community [282-284]. Conversely, collecting fecal samples directly from the litter box may eliminate the risk of inadequate sample collection; however, it may also increase the likelihood of environmental contamination and the introduction of extraneous bacterial taxa into the samples. It is essential to note that fecal samples collected directly from litter boxes may not be collected promptly, which can lead to prolonged exposure to ambient conditions. Room temperature and oxygen levels are crucial environmental factors that influence the growth and survival of bacteria, potentially leading to changes in the composition of the gut microbiome. Research studies have shown that long-term storage at room temperature may alter the microbial diversity and community [270, 285-287], leading to an inaccurate representation of the fecal microbiome. Oxygen levels significantly affect the growth and metabolic processes of both aerobic and anaerobic bacteria [284]. This emphasizes consideration of environmental conditions when determining the optimal method for collecting cat fecal samples.

More than 10 previous studies have explored fecal collection and storage methods, examining variables such as temperature, storage duration at different temperatures, and the application of stabilizers like the OMNI-gene GUT kit, 95% ethanol, RNAlater, and other preservative solutions [271, 288-301]. While these studies have identified various methods to achieve stable microbial composition results, a universally accepted standard protocol has yet to emerge. This standard is crucial to the consistency, reliability, and comparability of results across studies. The majority of such studies concentrated on the methods of collecting and storing human fecal samples, while research on handling animal fecal samples is relatively limited. In the case of

cats, the only prior study was our own research, which focused on the fecal loop collection method, specifically examining the use of lubricant versus no lubricant [302]. This research is the first investigation into two fecal sample collection methods in cats, specifically examining the potential variances in gut microbiome composition resulting from the use of a fecal loop for collection compared to direct retrieval from a litter box. This research addresses a previously unexplored area by systematically comparing microbiome profiles derived from fecal samples collected via these two distinct methods. To assess the potential impact of various collection methods on the composition of the microbial community, we collected two sets of fecal samples from a group of cats housed in a controlled research environment. One set was collected using fecal loops, while the other was collected directly from the litter box. The collected samples underwent whole-genome shotgun metagenomic sequencing, followed by comprehensive analyses of microbial diversity, composition, and abundance at all taxonomic and gene levels. Our study aimed to provide valuable insights into the impact of different fecal collection methods and to contribute to the development of standardized protocols for collecting fecal samples in feline microbiome research.

2.2.2 Materials and methods

2.2.2.1 Animals

The Auburn University Institutional Animal Care and Use Committee (IACUC) approved the study. Four intact female and six intact male cats, raised and maintained at the Scott-Ritchey Research Center, Auburn University College of Veterinary Medicine (Auburn, AL, USA), were enrolled in this study (Table 2.1). The age range of the 10 adult cats is 2.7–7.0 years old, with a mean age of 4.4 years. All cats are housed in USDA and AAALAC accredited facilities in indoor

wards with heating and air conditioning that allow compliance with federally mandated climate control parameters including an ambient temperature of ~72 degrees Fahrenheit, ranging from 64 to 84 degrees, with humidity between 30 and 70%. Cats were allowed *ad libitum* access to food and water. They were fed a Hill’s Science Diet maintenance-formula dry food mixed with an equal amount of Friskies canned food. There was a rotation of the canned food protein sources (tuna, salmon, chicken, beef, and turkey) to increase enrichment. All cats were provided access to the same rotating protein source and there was no changes in diet throughout the study. The cats are born, raised, and housed in the colony and are maintained in these conditions throughout adulthood or until adoption. They were all cared for according to the principles outlined in the NIH Guide to the Care and Use of Laboratory Animals.

Table 2.1 Characteristics of study participants and fecal sample collection date/time.

Cat ID	Sex	Date of birth	Date of litterbox collection	Time of litterbox collection	Date of fecal loop collection	Time of fecal loop collection
9-1866	F	10/20/2015	10/4/2022	6:00	10/4/2022	13:00
944	F	3/17/2019	10/5/2022	14:00	10/10/2022	13:30
924	F	9/20/2018	9/27/2022	22:00	9/28/2022	8:20
960	F	1/25/2020	10/12/2022	12:00	10/13/2022	11:15
926	M	9/20/2018	9/28/2022	6:00	9/28/2022	12:00
936	M	1/21/2019	9/27/2022	18:00	9/28/2022	8:20
9-2033	M	5/5/2018	9/27/2022	6:00	9/28/2022	8:30
921	M	2/25/2018	10/4/2022	14:00	10/5/2022	14:00
9-2060	M	8/6/2018	9/28/2022	6:00	9/28/2022	12:00
9-1952	M	3/23/2017	9/28/2022	12:00	9/29/2022	15:00

F: Intact female; M: Intact male.

2.2.2.2 Sample size determination

To perform a systematic comparison of microbiome profiles generated from fecal samples collected using these two methods, we collected two sets of fecal samples from these cats. One

set was obtained using fecal loops, while the other was collected directly from the litter box. In total, 20 fecal samples were collected from 10 cats. Our previous work has discovered that more than 90% of microbial genes and species are covered in a feline microbiome study when the sample size reaches eight [302]. In this study, we performed rarefaction analyses on the 20 samples in this study at both the gene level (Figure 2.5A) and the species levels (Figure 2.5B), through random subsampling from 20 samples multiple times and plotting the average gene and species richness against different numbers of included samples using a customized R script.

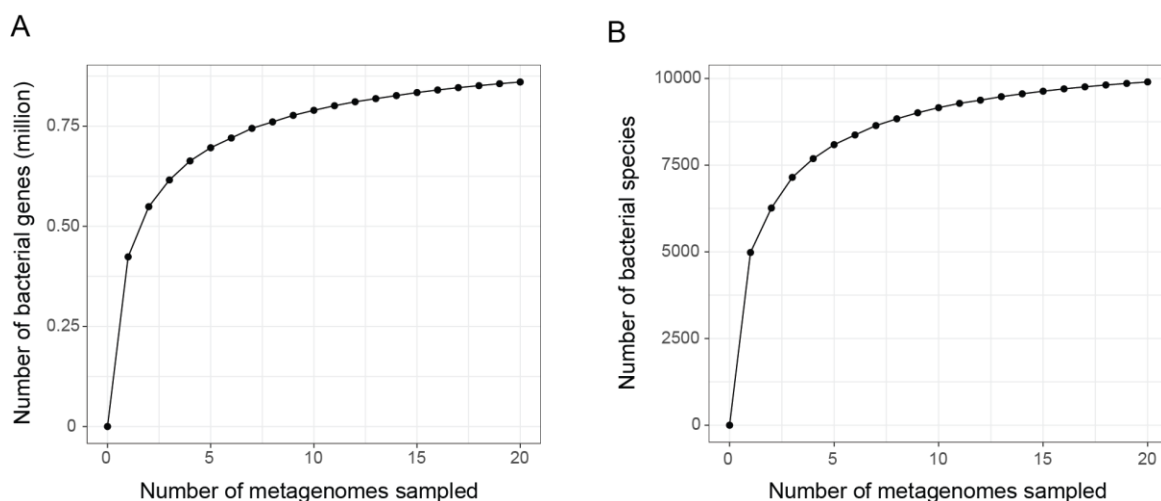


Figure 2.5 Rarefaction analyses to assess species and gene richness from the results of sampling. (A) Rarefaction curve based on bacterial gene profiles of 20 samples. (B) Rarefaction curve based on taxonomy profiles at the species level of 20 samples.

2.2.2.3 Fecal sample collection and storage

Each cat was given 24 h to acclimate to a single housing environment. Afterward, each cat was provided with a fresh litter box and monitored every 2–6 h. After the cat defecated, the sample was immediately collected in a sterile 1.5 mL Eppendorf tube and stored at -80°C . The following morning, after collecting the fecal sample from the litterbox, the cat was sedated with intramuscular administration of medetomidine, ketamine, and butorphanol. A plastic fecal loop (Catalog number 7500, Covetrus, Dublin, OH, USA) was inserted into the rectum and

descending colon to collect the fecal sample. The fecal loop was coated with mineral oil (Equate, Bentonville, AR, USA) as a lubricant, as described in our previous study [302]. The samples were collected using 1.5 mL sterile Eppendorf tubes (Eppendorf, Hamburg, Germany) and immediately stored at -80°C (CryoCube F570, Eppendorf North America, Enfield, CT, USA) until analysis.

2.2.2.4 Whole-genome shotgun metagenomic sequencing

The Qiagen Allprep PowerFecal DNA/RNA kit (Qiagen, Redwood City, CA, USA) was used for microbial DNA extraction. For each cat, the weight of fecal specimens was measured (Table 2.2) before being placed into a Microbial Lysis Tube for homogenization using a PowerLyzer24 instrument (Qiagen, Redwood City, CA, USA). DNA extraction procedures were conducted for all fecal samples in the same batch to minimize technical variability. The DNA concentrations were measured using a Qubit 3.0 Fluorometer (Thermo Fisher Scientific, Waltham, MA, USA), and the A260/A280 absorption ratios were determined with a NanoDrop One C Microvolume Spectrophotometer (Thermo Fisher Scientific, Waltham, MA, USA). 500 ng of DNA from each sample was fragmented into 500-bp fragments using an M220 Focused-ultrasonicator (Covaris, Woburn, MA, USA). The WGS metagenomic libraries were prepared using the NEBNext Ultra II DNA Library Prep Kit for Illumina (New England BioLabs, Ipswich, MA, USA). TapeStation 4,200 (Agilent Technologies, Santa Clara, CA, USA) was utilized to evaluate the library size distributions. Subsequently, the final libraries were quantified using qPCR before being sequenced on an Illumina NovaSeq6000 sequencing platform in 150-bp paired-end mode by Novogene Corporation Inc. in Sacramento, CA, USA.

Table 2.2 Amount of fecal material collected and DNA yield from fecal samples.

Cat ID	Group	Weight of feces collected (mg)	DNA yield (µg)	Group	Weight of feces collected (mg)	DNA yield (µg)
9-1866	LB	205	238	FL	112	181
944	LB	208	165	FL	165	113
924	LB	212	121	FL	192	134
960	LB	201	156	FL	190	39.4
926	LB	198	138	FL	160	89.2
936	LB	215	202	FL	100	179
9-2033	LB	219	150	FL	201	79.4
921	LB	202	193	FL	165	65.4
9-2060	LB	216	290	FL	212	226
9-1952	LB	212	286	FL	176	144

LB: fecal collection by picking from litterbox; FL: fecal collection by using fecal loop.

2.2.2.5 Bioinformatic processing of metagenomic data

A total of 1.02 billion raw metagenomic reads, or 153 Gigabases (Gbp) of sequences, were generated from the 20 metagenomes (Table 2.3). The sequencing depth of coverage was 9.59 ± 2.04 per sample. Trimmomatic (version 0.36) [244] was utilized to remove adapter sequences and low-quality bases. Host and viral sequences were eliminated by aligning the high-quality reads to the feline reference genome *Felis_catus_9.0* [303] and the viral genome downloaded from National Center for Biotechnology Information (NCBI) using Burrows-Wheeler Aligner (BWA) (v0.7.17-r1188) [246]. The virus reference consists of 5,540 high-quality complete viral genomes curated by NCBI, with a total genome length of 166.4 megabases (Mb). The remaining microbial reads were extracted using SAMtools (version 1.17) [304] and aligned to the feline gut microbiome reference contigs assembled from 16 Illumina short-read metagenomics data (GCA_022675345.1; short-read reference assembly) [302]. To investigate whether different microbiome references will affect our analysis and conclusion, we also aligned metagenomic reads to the feline gut microbiome contigs assembled from Pacific Biosciences

HiFi long-read using N = 8 fecal samples (accession number: PRJNA1062788; long-read reference assembly). The read mapping percentages against both short-read and long-read assemblies are summarized in Table 2.3.

Table 2.3 Whole-genome shotgun metagenomic sequencing yield, quality control, and alignment statistics.

Cat ID	Group	Total number of reads	% adapters & low-quality reads	% host sequences	% read alignment (reference 1)	% read alignment (reference 2)
9-1866	LB	42,054,216	2.23%	0.49%	96.82%	89.25%
944	LB	48,132,278	1.24%	0.08%	98.01%	92.79%
924	LB	46,459,964	0.72%	0.14%	97.81%	90.50%
960	LB	49,593,768	1.00%	0.30%	96.09%	87.73%
926	LB	55,893,016	0.95%	0.11%	98.41%	93.59%
936	LB	23,861,570	0.69%	2.48%	96.87%	86.83%
9-2033	LB	30,247,308	0.62%	2.49%	96.88%	86.84%
921	LB	47,944,568	0.75%	0.07%	97.84%	92.86%
9-2060	LB	68,800,896	0.63%	0.09%	98.41%	92.18%
9-1952	LB	49,365,474	0.61%	0.07%	98.52%	91.07%
9-1866	FL	42,659,160	0.75%	0.13%	93.65%	84.40%
944	FL	59,450,856	0.55%	0.66%	97.64%	88.93%
924	FL	58,907,188	0.53%	6.65%	97.83%	88.40%
960	FL	52,903,612	0.53%	3.48%	97.47%	90.17%
926	FL	61,076,576	0.62%	1.10%	97.90%	91.02%
936	FL	52,452,186	0.51%	1.31%	98.14%	87.30%
9-2033	FL	59,764,500	0.70%	38.98%	96.42%	85.48%
921	FL	53,357,488	0.49%	0.08%	97.09%	91.40%
9-2060	FL	63,409,540	0.51%	0.27%	98.41%	93.33%
9-1952	FL	56,489,430	0.51%	0.24%	98.28%	91.47%

LB: fecal collection by picking from litterbox; FL: fecal collection using fecal loop.

Reference 1: feline gut reference contigs from Illumina short-read metagenomic assembly (GCA_022675345.1)

Reference 2: feline gut reference contigs from Pacific Biosciences long-read metagenomic assembly (PRJNA1062788)

2.2.2.6 Taxonomy assignment and quantification of taxonomy abundance

Taxonomy assignments were performed on reference contigs [292] against the NCBI-NR database using Kaiju (v1.7.3) [305] to determine taxonomy annotations at the phylum, class, order, family, genus, and species levels. More than 90% of the reference contigs were annotated with the NCBI (National Center for Biotechnology Information) taxonomy ID. Based on the

BWA alignments, read counts were obtained using BEDTools (version 2.30.0) [290] with the command ‘bedtools coverage -f 0.9 -a region.bed -b reads.bam - counts’[248]. The taxonomy counts table was generated by aggregating the read counts of all contigs with the same taxonomy annotation using a custom Perl script. The taxonomy counts were then normalized by the total number of mapped reads in a sample to quantify the relative abundance of each taxonomic unit.

2.2.2.7 Microbial diversity analyses

Alpha- and beta-diversity analyses were conducted on the microbial profiles at all taxonomic levels using the R package vegan (version 2.6–4) [306]. The alpha diversity was assessed using the Shannon index [307]. The beta diversity was calculated based on the Bray-Curtis distance [308] and visualized in the PCoA (Principal Coordinates Analysis) plot format. A permutational multivariate analysis of variance (PERMANOVA) test [309] was performed to assess the centroids and dispersion of the LB (litter box) and FL (fecal loop) groups, based on the dissimilarity matrix.

2.2.2.8 Microbial gene abundance analysis

Microbial gene predictions were performed on reference metagenomic contigs using MetaGeneMark (v3.38) [310]. The redundant genes were identified and combined using CD-HIT-est (v4.7) [311, 312] with the criterion of global sequence identity exceeding 95%. To determine the gene abundance, per-gene read counts were extracted using “BEDtools coverage,” and gene abundance was normalized by RPKM (Reads Per Kilobase gene model per Million reads).

2.2.2.9 Statistical analysis

The comparison of DNA yield, levels of host and viral contaminations, number of taxonomic units and microbial genes, alpha diversities, and relative abundance of each taxon between the LB and FL groups was conducted using the Wilcoxon signed-rank test [254, 313] in the R software [314]. For the multiple comparisons of the microbial profiles, we utilized the R package *qvalue* [315] to determine the false discovery rate. When the *p*-value was less than 0.05 or the *q*-value was less than 0.1, the null hypothesis was rejected. In addition to the pairwise nonparametric test, we also performed differential abundance testing using Analysis of Compositions of Microbiomes with Bias Correction (ANCOM-BC), which was implemented in the R package ANCOMBC [316]. To determine the differences in the variance, Levene’s test of equality of variances [317, 318] and the Brown–Forsythe test [319] were performed. To estimate the correlation of taxonomy composition in fecal samples between the LB and FL groups, Spearman’s rank correlation tests were conducted on the average relative abundance of taxa between the LB and FL groups using the “cor.test()” function from the stats R package (Table 2.4).

Table 2.4 Correlation of taxonomic abundance at phylum, class, order, family, genus, and species level between fecal loop (FL) and litter box (LB) groups.

Taxonomy level	% of FL taxa identified in LB (short-read assembly)	FL-LB abundance correlation (short-read assembly)	% of FL taxa identified in LB (long-read assembly)	FL-LB abundance correlation (long-read assembly)
Phylum	95.83%	0.9573	100.0%	0.9912
Class	97.80%	0.9804	100.0%	0.9915
Order	98.97%	0.9789	100.0%	0.9914
Family	96.97%	0.9698	100.0%	0.9912
Genus	94.07%	0.9373	99.21%	0.9876
Species	89.83%	0.8974	99.65%	0.9794

2.2.2.10 Data availability

The whole-genome shotgun metagenomic sequencing data is available at NCBI SRA under accession number PRJNA821230.

2.2.3 Results

2.2.3.1 Fecal sample collection using a fecal loop resulted in a lower DNA extraction yield compared to the litterbox method

The amount of fecal material per sample collected using a fecal loop (FL group) was significantly lower than that collected from the litter box approach ($P = 0.002$, Wilcoxon signed-rank test; Table 2.2). As a result, the DNA yield of the FL group ($4.376 \mu\text{g}$ [$2.905 \mu\text{g} - 5.848 \mu\text{g}$, 95% CI]) was significantly lower than that of the LB group ($6.787 \mu\text{g}$ [$5.285 \mu\text{g} - 8.288 \mu\text{g}$, 95% CI]) ($P = 0.004$, Wilcoxon signed-rank test; Figure 2.6A). This suggests that the fecal collection method using a fecal loop might result in a reduced amount of DNA for subsequent research.

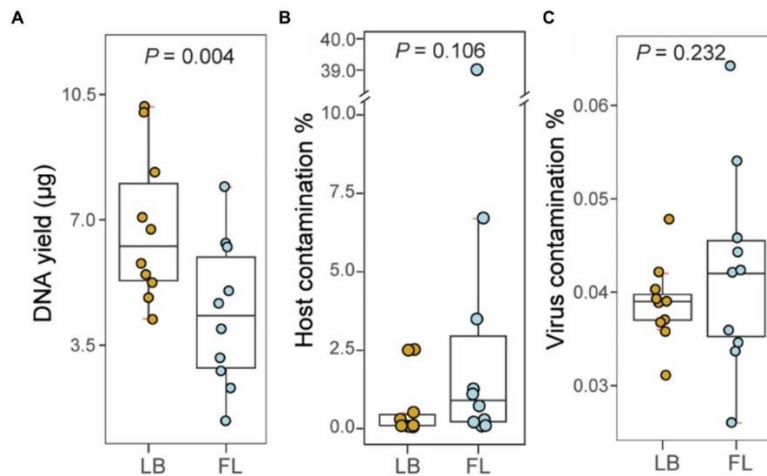


Figure 2.6 Metagenomic sequencing statistics from fecal samples collected by fecal loop (FL) and litter box (LB) approaches. (A) Boxplot of DNA yield (μg) extracted from fecal specimens in LB (brown) and FL (blue) groups. (B) Boxplot of percentage of host contamination in LB (brown) and FL (blue) groups. (C) Boxplot of percentage of viral contamination in LB (brown) and FL (blue) groups.

2.2.3.2 No significant difference was observed in the levels of contaminants in the WGS metagenomic sequencing data between the LB and FL groups

A total of 1.02 billion 150-bp reads (153.4 Gbp of sequences) were generated in total through whole-genome shotgun (WGS) metagenomic sequencing of 20 fecal DNA samples (51.1 million reads per sample; Table 2.3). On average, 0.76% of the adapter sequences and low-quality bases were trimmed and excluded from subsequent analysis. The level of feline sequence contamination was 8-fold higher in the FL group (5.290% [-3.306–13.886%, 95% CI]) than in the LB groups (0.631% [-0.073–1.337% 95%, CI]), but the difference did not reach statistical significance ($P = 0.11$, Wilcoxon signed-rank test; Figure 2.6B). The levels of viral contamination did not show a significant difference between the LB group (0.039% [0.036–0.042%, 95% CI]) and the FL group (0.042% [0.035–0.050%, 95% CI]) ($P = 0.232$, Wilcoxon signed-rank test; Figure 2.6C). However, there were higher variations in host and viral sequence contamination detected in FL samples, with marginal significance ($P = 0.05$, Levene's test of homogeneity of variance). When the Brown–Forsythe test was used, homogeneity of variances between the two groups cannot be rejected ($P = 0.25$).

2.2.3.3 No significant differences were found in the number of microbial taxa discovered in the fecal specimens from the LB and FL groups

From the WGS metagenomic data, a total of 127 phyla, 93 classes, 196 orders, 435 families, 1,892 genera, and 8,467 species were identified in 20 samples based on the short-read reference assembly. No significant difference was observed in the number of microbial taxa between the LB (79.8 taxa [73.0–86.6, 95% CI]) and FL groups (82.7 [77.5–87.9, 95% CI]) at the phylum ($P = 0.441$,

Wilcoxon signed-rank test), class (LB: 73.0 [67.7–78.3, 95% CI], FL: 72.1 [67.9–76.3, 95% CI], $P = 0.682$), order (LB: 151.5 [144.0–159.0, 95% CI], FL: 153.2 [146.5–159.9, 95% CI], $P = 0.959$), family (LB: 317.2 [300.2–334.2, 95% CI], FL: 327.7 [312.0–343.4, 95% CI], $P = 0.275$), genus (LB: 1093.9 [1007.2–1180.6, 95% CI], FL: 1146.2 [1069.5–1222.9, 95% CI], $P = 0.160$) and species levels (LB: 4074.3 [3709.4–4439.2, 95% CI], FL: 4288.0 [3985.3–4590.7, 95% CI], $P = 0.106$; Figure 2.7).

The short-read assembly contains a large number of rare taxa, which greatly inflates the number of identified taxa due to ambiguity and false positives in taxonomic assignments. To address this issue, we aligned the metagenomic reads to an improved long-read feline gut microbiome assembly with enhanced metagenomic contig size and completeness. A total of 19 phyla, 35 classes, 63 orders, 104 families, 298 genera, and 936 species were identified using the long-read reference. When we repeated the analyses, we did not discover any significant differences in the number of microbial taxa between the groups either (Figure 2.8).

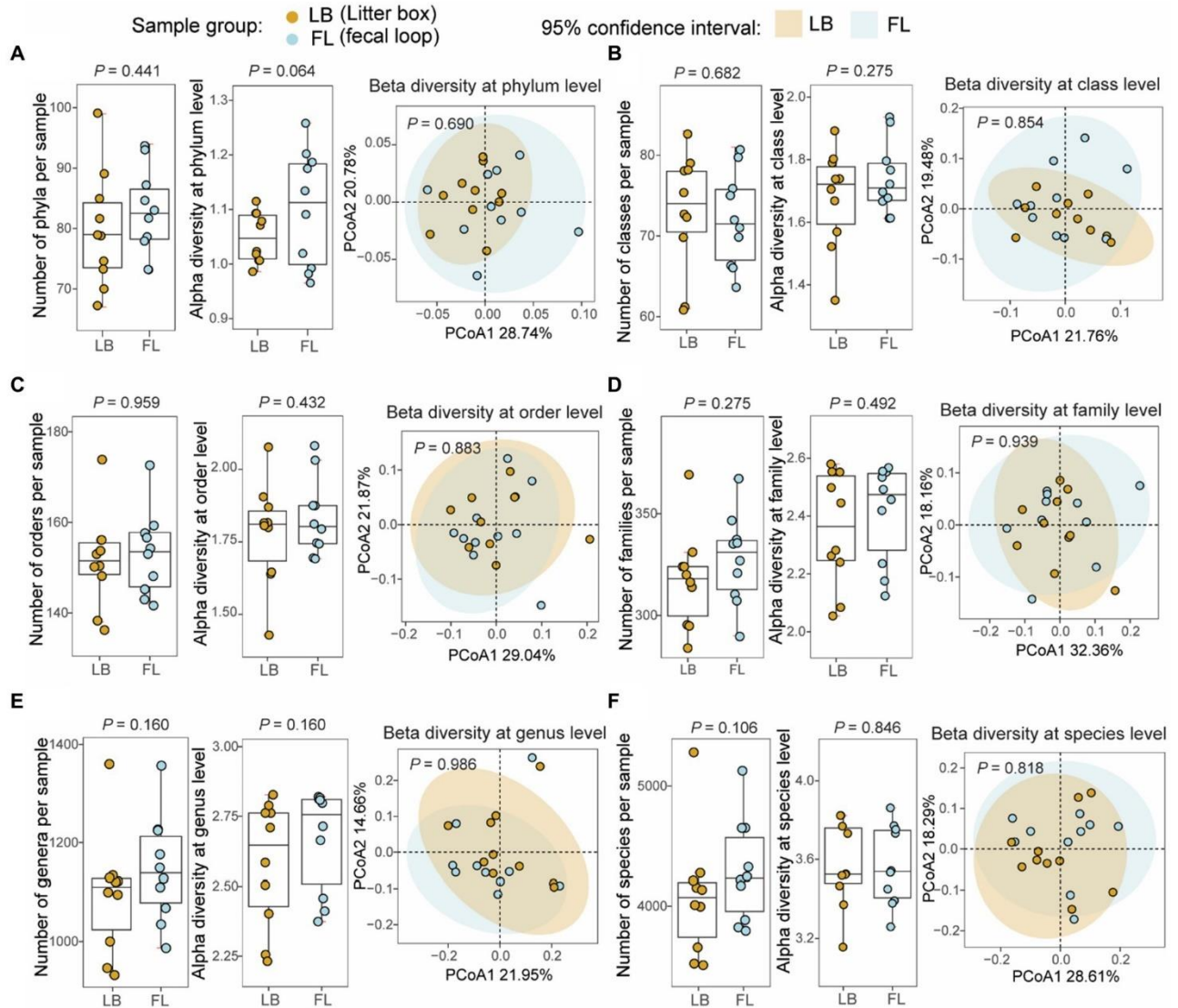


Figure 2.7 Microbial diversity analyses at different taxonomic levels from fecal samples collected by fecal loop (FL) and litter box (LB) approaches. Boxplots of non-redundant microbial taxa and alpha diversity (Shannon index) for each sample and principal coordinates analysis (PCoA) plot of beta diversity (Bray–Curtis dissimilarity) for microbial profiles from the LB (brown) and FL (blue) groups at (A) phylum, (B) class, (C) order, (D) family, (E) genus, and (F) species levels.

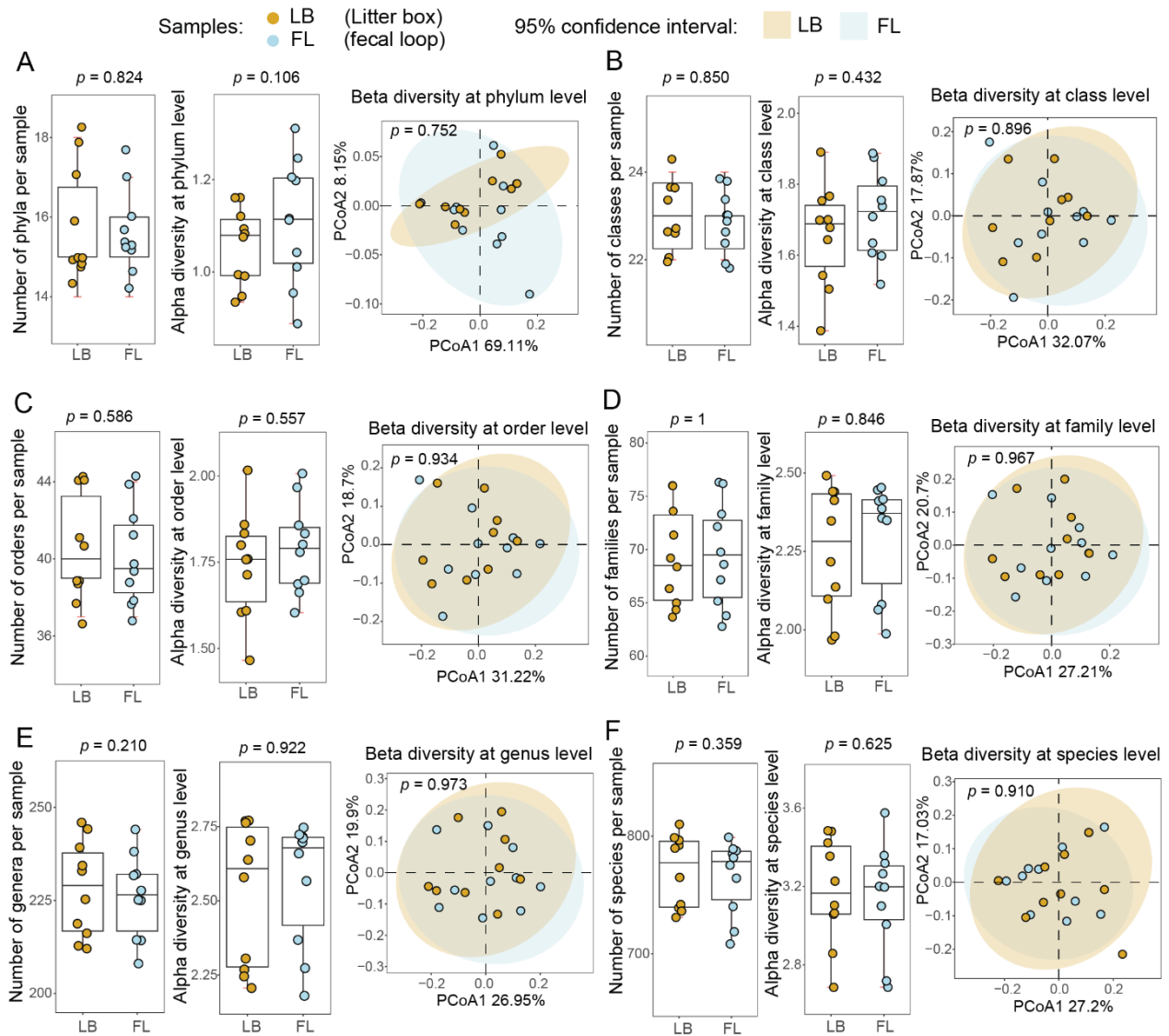


Figure 2.8 Microbial diversity analyses using long-read reference assembly at different taxonomic levels from fecal samples collected by fecal loop (FL) and litter box (LB) approaches. Boxplots of non-redundant microbial taxa and alpha diversity (Shannon index) for each sample and principal coordinates analysis (PCoA) plot of beta diversity (Bray-Curtis dissimilarity) for microbial profiles from the LB (brown) and FL (blue) groups at (A) phylum, (B) class, (C) order, (D) family, (E) genus, and (F) species levels.

2.2.3.4 No significant variation in microbial diversities was observed at all taxonomic levels between the LB and FL groups

Alpha-diversity, as measured by the Shannon index, and beta-diversity, assessed using the Bray-Curtis distance, were determined for microbial profiles in both the LB and FL groups ([Figure 2](#)).

For alpha-diversity, no significant differences were detected between the LB and FL groups at the phylum (LB: 1.05 [1.02–1.08, 95% CI], FL: 1.10 [1.03–1.18, 95% CI]; $P = 0.064$), class (LB: 1.68 [1.56–1.79, 95% CI], FL: 1.74 [1.66–1.82, 95% CI]; $P = 0.275$), order (LB: 1.78 [1.65–1.91, 95% CI], FL: 1.83 [1.74–1.93, 95% CI]; $P = 0.432$), family (LB: 2.36 [2.21–2.50, 95% CI], FL: 2.41 [2.29–2.53, 95% CI]; $P = 0.492$), genus (LB: 2.58 [2.42–2.74, 95% CI], FL: 2.67 [2.54–2.80, 95% CI]; $P = 0.160$), and species levels (LB: 3.57 [3.42–3.73, 95% CI], FL: 3.57 [3.42–3.71, 95% CI]; $P = 0.846$; Figure 2.7). When additional alpha diversity metrics were examined, we failed to discover any significant differences in Simpson diversity index, richness, or Chao1 index between FL and LB ($p > 0.05$). Similarly, no significant changes were detected in beta-diversity analysis either ($p > 0.689$ for all taxonomic levels, PERMANOVA test; Figure 2.7) using both Bray-Curtis and Jaccard distance measures. When we use the long-read assembled reference contigs as the mapping reference, the results remain consistent (Figure 2.8).

2.2.3.5 Consistent relative taxonomic abundance in the microbiome quantified from fecal samples collected by LB and FL

Through Wilcoxon signed-rank tests on all taxonomic categories at the phylum level in the LB and FL groups, no significant difference was detected in the relative abundance of the top five most abundant phyla: Firmicutes (LB: 48.6% [42.6–54.6%, 95% CI] vs. FL: 47.5% [43.1–51.9%, 95% CI]; $P_{adj} = 1$), Actinobacteria (LB: 39.4% [30.8–47.9%, 95% CI] vs. FL: 37.7% [29.4–46.0%, 95% CI]; $P_{adj} = 1$), Bacteroidetes (LB: 8.1% [6.1–10.1%, 95% CI] vs. FL: 9.6% [5.3–14.0%, 95% CI]; $P_{adj} = 0.880$), Proteobacteria (LB: 0.9% [0.4–1.4%, 95% CI] vs. FL: 1.9% [0.6–3.3%, 95% CI]; $P_{adj} = 0.639$), and Fusobacteria (LB: 0% [0–0%, 95% CI] vs. FL: 0% [0–0%, 95% CI]; $P_{adj} = 0.639$; Figure 2.9A). Collectively, these five predominant phyla represented

more than 97% of all phyla observed in both the LB and FL groups (97.6% [97.2–97.9%, 95% CI] vs. 97.5% [97.2–97.8%, 95% CI]; $P = 1$). When utilizing the long-read assembled feline gut microbiome contigs as the reference, the top five most abundant phyla remained consistent and maintained the same ranking order (Figure 2.10A). Upon examining lower taxonomic units, there were no significant differences in the relative abundance between the LB and FL groups at the class, order, family, genus, or species levels ($P_{adj} > 0.909$ for short-read assembly, and $P_{adj} > 0.379$ for long-read assembly). Furthermore, in addition to pairwise nonparametric tests, we employed the ANCOM approach for detecting differential abundance as outlined in the Methods section. Our analysis did not reveal any taxa with a statistically significant difference in abundance between the LB and FL groups ($FDR > 0.05$), and 99.5% of the tested taxa exhibited an $FDR = 1$, suggesting remarkable concordance in microbial abundance between the two fecal sample collection methods.

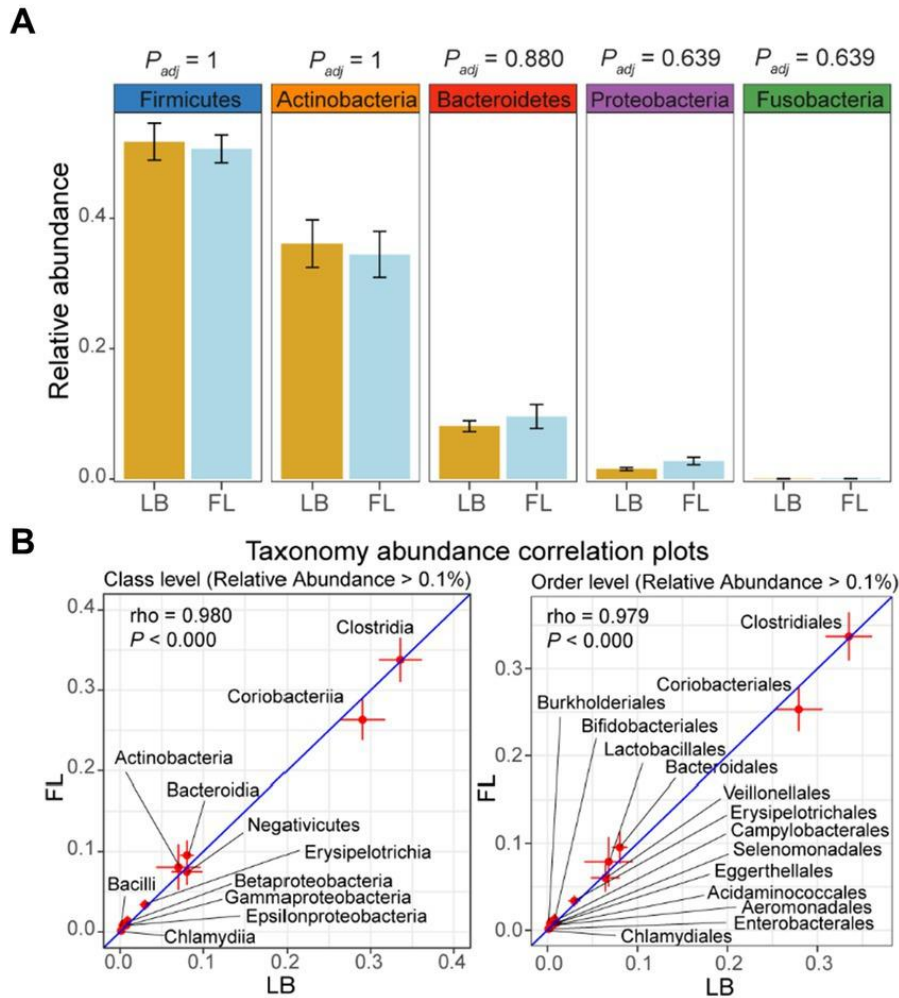


Figure 2.9 Relative abundance of major phyla and microbiome abundance (> 0.1%) correlation at class and order levels in the feline microbiome from samples collected by fecal loop (FL) and litter box (LB) approaches. (A) Boxplots of major phyla in LB (brown) and FL (blue) groups. (B) Correlation plots of microbes with high abundance (> 0.1%) at class and order levels. Each data point on the plot represents the averaged relative abundance of a particular taxon across samples within each group (FL on the y-axis and LB on the x-axis), and error bars indicate the standard error intervals around the mean for FL (vertical lines) and LB (horizontal lines) groups.

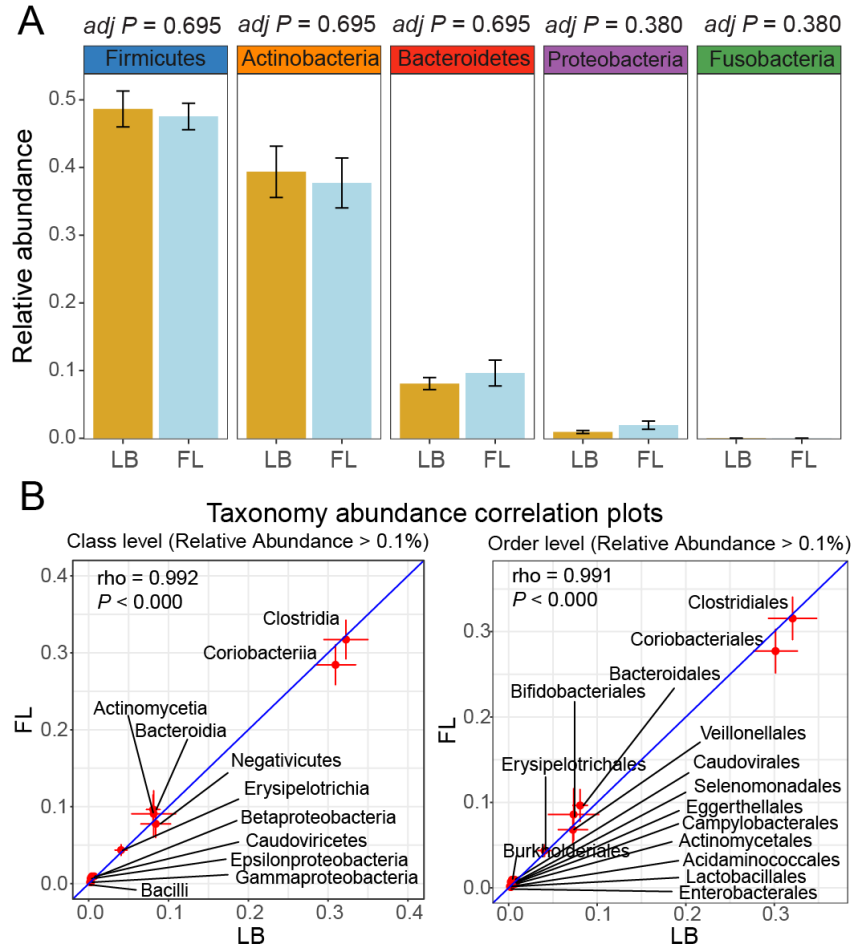


Figure 2.10 Relative abundance of major phyla and microbiome abundance correlation at class and order levels in the feline microbiome from samples collected by fecal loop (FL) and litter box (LB) approaches from the alignment results against long-read reference assembly. (A) Boxplots of major phyla in LB (brown) and FL (blue) groups. These five predominant phyla collectively represented more than 96% of all phyla observed in both the LB and FL groups (97.0% [96.2%-97.8% 95% CI] vs 96.8% [96.0%-96.7% 95% CI]; $P = 0.922$). (B) Correlation plots of microbes with high abundance (> 0.1%) at class and order levels.

2.2.3.6 A strong correlation in taxonomic composition was observed among fecal samples in the LB and FL groups

When using the long-read assembled feline gut microbiome reference contigs, the LB and FL groups showed nearly perfect abundance correlation at phylum, class, order, and family levels, with Spearman's rank-order correlation coefficients greater than 0.99 (Table 2.4 and Figure

2.10B; $P = 0.000$; Spearman's Rank-Order Correlation test). All taxa identified in the FL samples were also detected in the LB data (Table 2.4). At phylum, class, order, and family levels, results from short-read assembly demonstrated strong abundance correlations with lightly lower correlation coefficients, ranging from 0.957 and 0.980, with >95% taxa shared among FL and LB groups (Table 2.4 and Figure 2.9B). For the genus and species levels, the Spearman's correlation coefficients are 0.937 and 0.897, respectively (Table 2.4), which is presumably due to potential misannotations of shorter contigs in the short-read reference assembly at lower taxonomic units. For the long-read assembly with much greater contig completeness, abundance correlation coefficients remain remarkably high even at the genus ($\rho = 0.988$) and the species levels ($\rho = 0.979$; Table 2.4), with >99% of FL taxa also identified in LB samples, indicating excellent consistency in taxonomic abundance between the two fecal sample collection approaches.

2.2.3.7 The number, alpha diversity, and beta diversity of microbial genes are similar between the LB and FL groups

A total of 860,169 unique microbial genes were identified in the 20 metagenomes. Among these, 10 metagenomes from the LB group contained 796,138 nonredundant genes, while 10 metagenomes from the FL group contained 797,990 nonredundant genes (Figure 2.11A). Statistical analysis revealed no significant difference in the number of observed genes between fecal samples obtained from the fecal loop and litter box approaches ($P = 0.770$, Wilcoxon signed-rank test; Figure 2.11A). Additionally, the alpha diversity, as assessed by the Shannon index of observed genes, did not exhibit any significant difference between the two groups ($P = 1$, Wilcoxon signed-rank test; Figure 2.11B). Furthermore, the PCoA plot based on the Bray-Curtis distance matrix did not reveal any significant dissimilarities between the LB and FL

groups, as indicated by the overlapping 95% confidence interval ellipses ($P = 0.964$, PERMANOVA test; Figure 2.11C).

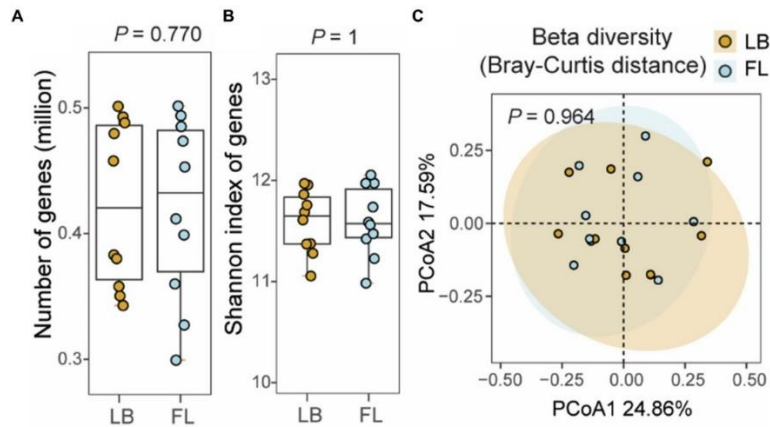


Figure 2.11 Number of non-redundant microbial genes and gene level diversity in the feline fecal microbiome from samples collected by fecal loop (FL) and litter box (LB) approaches. (A) Boxplot of the number of observed genes in the LB (brown) and FL (blue) groups. (B) Boxplot of Shannon index of genes identified in the LB (brown) and FL (blue) groups. (C) PCoA plot of beta diversity based on Bray-Curtis distance of the genes identified in the LB (brown) and FL (blue) groups.

No significant differences were observed in the number, alpha diversity, and beta diversity of the microbial genes identified in the LB and FL groups when long-read assembled feline gut microbiome reference contigs were used as the references (Figure 2.12). A total of 693,003 unique microbial genes were annotated across the 20 metagenomes. Among these, ten metagenomes from the LB group contained 678,212 nonredundant genes, while ten metagenomes from the FL group contained 678,524 nonredundant genes. Statistical analysis revealed no significant difference in the number of observed genes between fecal samples obtained from the fecal loop and litter box approaches ($P = 0.770$, Wilcoxon signed-rank test). There was no significant difference in alpha diversity between the two groups ($P = 0.432$, Wilcoxon signed-rank test). There was no significant dissimilarities between the LB and FL

groups, as indicated by the overlapping 95% confidence interval ellipses ($P = 0.961$, PERMANOVA test).

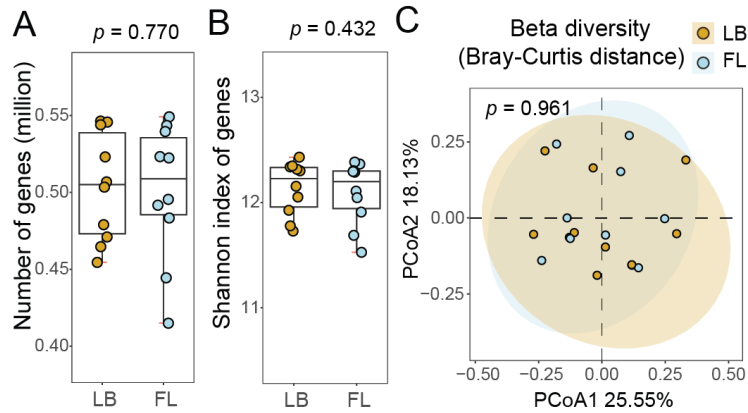


Figure 2.12 Number of non-redundant microbial genes and gene level diversity in the feline fecal microbiome from samples collected by fecal loop (FL) and litter box (LB) approaches from the alignment results against long-read reference assembly. (A) Boxplot of the number of observed genes in the LB (brown) and FL (blue) groups. (B) Boxplot of Shannon index of genes identified in the LB (brown) and FL (blue) groups. (C) PCoA plot of beta diversity based on Bray-Curtis distance of the genes identified in the LB (brown) and FL (blue) groups.

2.2.4 Discussion and conclusion

Fecal sample collection plays a crucial role in veterinary medicine for routinely diagnosing various health conditions, including parasitism [320], enteropathogenic bacteria [321] and viruses [322] in research for studying the gut microbiome. Establishing a gold standard for fecal sample collection is crucial for acquiring accurate, reliable, and reproducible microbiome data in a feasible manner. Such a standard safeguards the validity and consistency of microbiome research, facilitating the smooth transition of discoveries into clinical and therapeutic practices. Studies to optimize fecal sample collection techniques were mainly performed for humans, with no specific emphasis on investigating methods tailored for cats. Typically, there are two common methods of collecting feline fecal samples: from the litter box or from the rectum using a fecal

loop. Each method possesses its own unique advantages and disadvantages. The fecal loop method is generally considered a more accurate approach for faithfully representing the gut microbiome, as it minimizes the risks of potential cross-contamination and exposure to the environment. However, inserting a fecal loop into the cat rectum requires experienced veterinary professionals to administer sedation, which may not be practical for all situations, particularly in cases where the cat is uncooperative, aggressive, or unable to tolerate sedation due to health concerns. In contrast, fecal samples collected from the litterbox are noninvasive, but more susceptible to environmental contamination, and the duration after defecation may cause bacterial growth to shift the microbiome composition [323]. Our aim was to conduct a thorough comparison of their impact on microbiome studies to assess whether the two collection methods could be interchangeable under certain circumstances. In this study, we demonstrated that there was no significant difference in the microbial profiles of fecal samples collected from the litter box compared to those collected using a fecal loop. No significant changes were observed in terms of alpha-diversity, beta-diversity, the number of taxa identified at each taxonomic level, and the relative abundances of taxonomic units. Collectively, these findings suggest that the microbiome composition of fecal samples collected using a fecal loop is the same as those collected directly from the litterbox within 6 h post-defecation. This indicates that collecting fecal samples directly from a clean litterbox in a timely manner can be considered a reliable method for feline microbiome studies.

The fecal loop collection approach resulted in a significantly lower DNA yield than the litterbox approach. Due to the uncertainty regarding whether sufficient feces can be collected from the colon in a single trial, the fecal loop method may cause missing data in the research or require

multiple collections at different time points, which are not ideal for the experimental design. Consequently, the DNA yield was lower from fecal specimens collected using a fecal loop in this study. If consistent microbial DNA yield is a concern, the litter box approach will guarantee a superior DNA yield compared to the fecal loop approach.

Another disadvantage of using the fecal loop is the possibility of introducing host contaminations to the sample. Our results demonstrated that fecal samples collected using a fecal loop exhibited greater variability in the proportion of host contaminations compared to samples collected from the litter box, although this difference did not reach statistical significance. Notably, one of the fecal samples collected using a fecal loop in this study had a host contamination level of 39%, making it difficult to estimate the necessary sequencing data to achieve the desired depth. However, using a fecal loop to collect fecal samples remains indispensable for veterinary diagnosis. When fresh feces are needed for medical diagnosis, it is more appropriate to collect fresh fecal samples using a fecal loop in a clinical setting with trained personnel. This method enables the direct assessment of a presenting enteric complaint and the localization to the small, large, or mixed bowel based on fecal features [272], which may be challenging when relying on litter box samples exposed to unknown factors.

For citizen science projects or owner-participated research projects, the fecal loop collection approach is likely not feasible due to the requirement for access to sedation. In such cases, the litter box method is amenable to the participants as it only involves regularly monitoring the litter box. It supports the possibility of applying this feline fecal sample collection method in large-scale population microbiome studies when access to a veterinarian and medical facility is

not feasible. One limitation of our study is that we did not investigate the potential impact of extended room temperature exposure on the microbiome of the fecal samples. In our study, we monitored the litter box every 2 to 6 h to detect fecal deposits. The potential impact of prolonged exposure to room temperature on the composition of the microbiome in fecal samples is an area that requires further exploration.

CHAPTER 3

Whole-genome shotgun metagenomic sequencing reveals distinct gut microbiome signatures of obese cats

3.1 Introduction

A combination of excessive food intake and lack of physical exercise leads to an expansion of adipose tissue in the body, resulting in metabolic dysregulation. When excess body adipose tissue has accumulated to the extent that it has adverse effects on health, it is termed obesity. Feline obesity is a major epidemic with a current prevalence of around 45% [324-326] and is considered the second most common health problem in domestic cats in developed countries [327]. It is linked to many systemic health conditions, including altered lipid profiles [328], insulin resistance [329], neoplasia, urinary diseases [326], cardiovascular diseases [330], and reduced lifespan. There are no available licensed drugs for treating feline obesity, and classic interventions for weight loss such as calorie restrictions and physical exercise are often challenging and are ultimately ineffective [331]. Understanding the obese cat gut microbiota is necessary to facilitate the development of treatment strategies through dietary probiotics and gut microbiota manipulations.

The gut microbiome is the entire collection of microorganisms in the gastrointestinal tract. In humans, microorganisms are about 38 trillion in total, exceeding the number of human cells [332]. The gut microbiota is an integral part of the body, affecting many aspects of disease

physiology, including rheumatoid arthritis [235], colorectal cancer [236, 237], cardiovascular disease [238], and inflammatory bowel disease [239, 240]. Gut microbiome composition and function are directly related to digestion, nutrient metabolism, and assimilation, which play important modulative roles in total body adiposity. The gut microbiota modulates obesity through food absorption and low-grade inflammation [333, 334]. In mice, changes in intestinal bacterial compositions and microbial metabolites can cause increases in endotoxemia and further exacerbate obesity and insulin resistance [335, 336]. Studies in both humans and mice have shown that influencing the gut microbiota, such as with fecal transplantation, or external chemicals or drugs, can have favorable or unfavorable effects on fat gain [337-343]. Conversely, being overweight or obese can cause dysbiosis, often associated with low microbial diversity and richness in gut microbiota [344-346]. Many studies reported that the relative proportions of microbes in the gut microbiota correspond to body weight in humans [347]. Obesity can alter the microbial composition in the gut, and reduced levels of Bacteroidetes have been reported in obese versus lean members of twin pairs [346]. The reduction of Bacteroidetes in obese animals could be reversed through a calorie-restricted diet [348].

To date, there are over twenty studies on the feline gut microbiota [198-200, 202, 206, 214, 349-365], all of which used the 16S rDNA sequencing approach. Factors such as diets, pre-/probiotics, age, diarrhea, and other diseased states have been shown to influence gut microbiota composition [199, 200, 202, 220]. One study examined the effect of obesity on the gut microbiome and found that the gut microbiome of lean cats was significantly different ($P < 0.05$) from that of overweight and obese cats [349]. Lean and obese cat gut microbiota were also reported to respond differentially to dietary protein and carbohydrate ratio [360]. These previous

studies identified phylum and genus level changes in the obese cat microbiome, but failed to discover bacterial species-level changes in the feline gut microbiota. Another limitation is that these studies often performed using client-owned cats from diverse household environments, which diminished the statistical power to detect microbiome differences. Last but not least, fecal sample collection methods also affect the results of microbiome analysis. Many previous studies collected feces from litterbox, which could be contaminated, and the microbiota composition can shift after the fecal sample left the intestine. To address these issues and obtain comprehensive genome coverage for bacteria composition at the species level [366], whole-genome shotgun (WGS) metagenomic sequencing was performed in normal vs. obese cats, using fecal samples collected from the rectum and descending colon by a fecal loop. We assembled the first cat reference microbial contigs, predicted and annotated taxonomy identity and microbial genes, and discovered and validated significant changes in species abundance in obese vs. normal cat gut microbiota. Our results provide a deeper understanding of the feline gut microbiota and its link to body conditions, which shed light on the microbiome basis of feline obesity and will inform the development of weight loss therapy using probiotics and fecal transplantation.

3.2 Materials and methods

3.2.1 Animal selection and maintenance

All procedures were approved by the Auburn University Institutional Animal Care and Use Committee (IACUC) with protocol number PRN 2019-3482. Animals were provided and/or maintained by the Scott-Ritchey Research Center, College of Veterinary Medicine, Auburn University. The obese group consists of animals who participated in a study of the effects of obesity on feline health, which are obese, neutered male cats at 6 years of age ($n=8$). The normal

group includes eight lean and reproductively intact cats from the Scott-Ritchey breeding colony, ranging in age from 4 months to 6 years old (Figure 3.1 and Table 3.1).

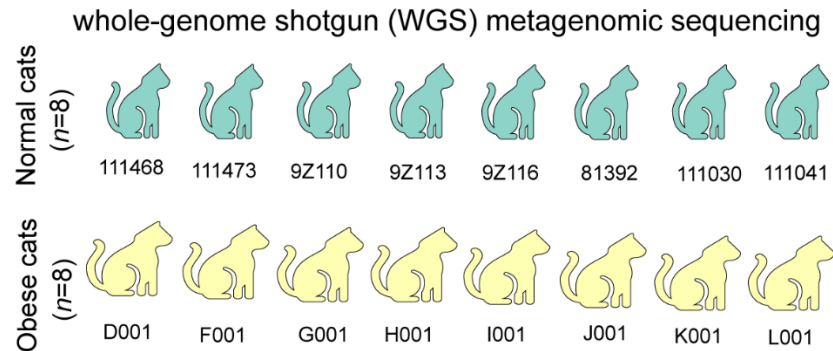


Figure 3.1 Graphic illustration of the experimental design.

Table 3.1 Bodyweight and body condition score measurements in normal and obese cats.

Cat ID	Group	Sex	Female sample collection date	Age at collection	BW at collection (kg)	lean BW (kg)*	% increase in BW	Body Condition Score
D001	obese	male	5/15/2019	6y	7.00	4.08	71.57	9
F001	obese	male	5/15/2019	6y	5.55	3.77	47.21	8
G001	obese	male	5/10/2019	6y	5.35	3.78	41.53	8
H001	obese	male	5/15/2019	6y	6.25	3.20	95.31	9
I001	obese	male	6/28/2019	6y	5.70	4.10	39.02	7
J001	obese	male	5/10/2019	6y	7.00	3.97	76.32	9
K001	obese	male	6/28/2019	6y	6.60	3.70	78.38	9
L001	obese	male	5/10/2019	6y	6.50	3.87	67.96	9
Mean ± s.d.					6.2 ± 0.65		64.7 ± 20.1	
Fc111468	normal	male	8/31/2020	4m	2.20	n/a	n/a	5
Fc111473	normal	male	9/10/2020	4m	2.60	n/a	n/a	5
Fc09Z110	normal	female	8/28/2020	8m	2.41	n/a	n/a	5
Fc09Z113	normal	female	8/28/2020	8m	2.54	n/a	n/a	5
Fc09Z116	normal	male	8/28/2020	8m	3.38	n/a	n/a	5
Fc081392	normal	female	7/12/2018	6y	2.64	n/a	n/a	5
Fc111030	normal	female	10/15/2019	6y	3.26	n/a	n/a	5
Fc111041	normal	male	1/9/2020	6y	4.08	n/a	n/a	5
Mean ± s.d.					2.9 ± 0.63		n/a	

* body weight measurement of obese cats when they were lean.

The normal cats were fed with Hill's Science Diet Adult Chicken Recipe Dry Cat Food with the following nutritional ingredients determined by the manufacturer (Hill's): 35.0% protein, 21.4% fat, 35.2% carbohydrate (nitrogen-free extract), and 1.6% crude fiber. The obese cats were on the LabDiet laboratory feline diet 5003 with the following ingredients provided by the manufacturer (LabDiet): 30.5% protein, 24.5% fat, 38.1% carbohydrate (nitrogen-free extract), and 2.3% crude fiber. Both diets were standard adult cat food with very similar nutritional ingredients. No probiotics were provided to any of these cats. No antibiotic treatments were applied to any of these cats within two months prior to the study. The cats were not experiencing any stress prior to the fecal sample collection either.

3.2.2 Morphometrics, blood glucose, and insulin measurements in obese cats

Cats were sedated to effect using medetomidine, ketamine, and butorphanol administered intramuscularly. Body condition score was evaluated using the World Small Animal Veterinary Association criteria for cats [367, 368]. Whole blood glucose was evaluated immediately using the AphaTrak 2 monitoring system (Zoetis, MI). Serum was separated from clotted whole blood by centrifugation at 800g for at least 15 minutes and was frozen at -80 C until needed. Serum insulin was determined using a commercially available ELISA kit specific to cats (Merckodia Inc., NC) [369]. The homeostatic model assessment for insulin resistance (HOMA-IR) was calculated as the basal glucose and insulin concentration product, divided by 22.5 [329].

3.2.3 Fecal sample collection and microbial DNA extraction

Fecal samples were collected under sedation immediately after blood collection to prevent interference of epinephrine-mediated hyperglycemia (Table 3.1). Plastic fecal loops were coated

with mineral oil and inserted into the rectum and descending colon of the cats until an adequate amount of feces was collected. The samples in this study reflect the fecal composition of the rectum and descending colon, which is representative of the lower gut. We referred to the microbiota characterized in the fecal samples in this research as cat gut microbiota.

Genomic DNA samples were extracted from 200 mg fecal samples using the Qiagen Allprep PowerFecal DNA/RNA kit (QIAGEN, MD) following the manufacturer's protocols. To achieve homogeneous results, the homogenization step was performed by the Qiagen PowerLyzer24 instrument (QIAGEN, MD) in the same batch. DNA and total RNA concentrations were measured by a Qubit 3 Fluorometer (Invitrogen, CA), and the A260/A280 absorption ratios were assessed using a NanoDrop One C Microvolume Spectrophotometer (Thermo Scientific, MA).

3.2.4 Metagenomic sequencing, quality control, and preprocessing of metagenomic reads

For each sample, 1.5~2 µg of DNA was fragmented by M220 Focused-ultrasonicator (Covaris, MA) to achieve a target insert size of 500 bp. Whole-genome shotgun metagenomic sequencing libraries were constructed using NEBNext Ultra II DNA Library Prep Kit for Illumina (New England Biolabs, MA), according to the manufacturer's protocols. Final library concentrations and size distributions were determined by LabChip GX Touch HT Nucleic Acid Analyzer (PerkinElmer, MA). The libraries were measured by qPCR before being sequenced on an Illumina NovaSeq6000 sequencing machine with 150-bp paired-end reads at the Genomics Service Laboratory at the HudsonAlpha Institute for Biotechnology (Huntsville, AL).

A total of 1.8 billion sequencing reads (or 271 Gbp reads) were obtained from 16 metagenomes (Table 3.2). Paired-end reads were merged to increase read length with PEAR (v0.9.11) [370].

Adapter sequences and low-quality sequences were cleaned from subsequent reads using Trimmomatic (v0.36) [244]. High-quality filtered reads were then mapped to the feline reference genome (GCF_000181335.3) using Burrows-Wheeler Aligner (BWA) (v0.7.17-r1188) [246] and SAMtools (v1.6) [247]. The retained reads were mapped to the viral genome database downloaded from National Center for Biotechnology Information (NCBI) to remove the viral sequences [371]. The remaining reads were extracted for subsequent analysis using BEDTools (v2.30.0) [248].

Table 3.2 Whole genome shotgun metagenomic sequencing yield, control statistics, and mapping rate.

Animal ID	total number of reads	total yield (Gbp)	% adapters & low quality reads	% host sequences	% viral sequences	% read alignment
111468	224,309,608	33.65	1.26%	1.75%	0.06%	96.54%
111473	252,204,562	37.83	0.78%	0.85%	0.05%	97.76%
81392	68,992,950	10.35	1.65%	19.62%	0.04%	78.82%
111030	67,304,938	10.10	1.05%	3.26%	0.05%	95.31%
111041	62,165,458	9.32	1.49%	3.14%	0.05%	95.31%
9Z110	177,167,802	26.58	1.68%	5.54%	0.04%	92.28%
9Z113	187,101,498	28.07	1.23%	3.43%	0.06%	94.74%
9Z116	71,831,380	10.77	1.84%	9.91%	0.05%	88.36%
D001	114,565,502	17.18	2.74%	16.53%	0.03%	81.42%
F001	88,239,704	13.24	3.37%	69.19%	0.01%	27.67%
G001	96,951,866	14.54	3.81%	35.50%	0.02%	61.68%
H001	81,550,038	12.23	2.44%	0.21%	0.04%	98.16%
I001	88,388,090	13.26	2.67%	2.09%	0.03%	95.74%
J001	93,732,658	14.06	3.11%	21.16%	0.02%	76.28%
K001	54,533,852	8.18	2.30%	2.66%	0.03%	95.46%
L001	77,921,032	11.69	3.89%	48.57%	0.02%	48.22%

3.2.5 Feline gut metagenome assembly and microbial gene annotation

The filtered reads were assembled into metagenomic contigs with MEGAHIT v1.1.2 with default parameters [372]. Contigs shorter than 400 bp were filtered out, and redundant contigs were removed using cd-hit-est (v4.7) [311, 312] with the criteria of global sequence identity more than 95%. Microbial genes were predicted from the assembled cat reference metagenomic contigs using MetaGeneMark (v3.38) [310].

3.2.6 Taxonomy assignment and taxonomy abundance analysis

Taxonomy assignments for these non-redundant metagenomic contigs were performed using Kaiju (v1.7.3) [373] against NCBI-NR database at superkingdom, phylum, class, order, family, genus, and species levels. 92.6% of the contigs were annotated and assigned an NCBI taxonomy ID (National Center for Biotechnology Information). Among these contigs, 54.6% are annotated to the species level. The filtered PE reads from each metagenome were aligned to the assembled cat reference metagenomic contigs (Table 3.2). For each sample, the relative taxonomic frequencies were calculated as the number of reads mapped to the contigs in a specific taxon normalized by the total number of aligned reads. The top 20 most abundant bacterial genera and species were listed in Table 3.3 and Table 3.4.

Table 3.3 Top 20 most abundant bacterial genera in the cat rectum microbiota.

Genus name	Phylum	Average relative abundance	STDEV	NCBI taxonomy ID
<i>Prevotella</i>	Bacteroidetes	24.31%	0.177	838
<i>Collinsella</i>	Actinobacteria	12.70%	0.085	102106
<i>Bacteroides</i>	Bacteroidetes	8.17%	0.057	816
<i>Blautia</i>	Firmicutes	4.04%	0.023	572511
<i>Clostridium</i>	Firmicutes	3.24%	0.022	1485
<i>Megasphaera</i>	Firmicutes	2.26%	0.035	906
<i>Sutterella</i>	Proteobacteria	1.76%	0.012	40544
<i>Faecalibacterium</i>	Firmicutes	1.65%	0.02	216851
<i>Megamonas</i>	Firmicutes	1.50%	0.013	158846
<i>Eubacterium</i>	Firmicutes	0.92%	0.01	1730
<i>Roseburia</i>	Firmicutes	0.75%	0.009	841
<i>Flavonifractor</i>	Firmicutes	0.75%	0.007	946234
<i>Ruminococcus</i>	Firmicutes	0.55%	0.004	1263
<i>Lactimicrobium</i>	Firmicutes	0.43%	0.005	2563777
<i>Dorea</i>	Firmicutes	0.42%	0.003	189330
<i>Lachnoclostridium</i>	Firmicutes	0.39%	0.002	1506553
<i>Phascolarctobacterium</i>	Firmicutes	0.38%	0.005	33024
<i>Agathobaculum</i>	Firmicutes	0.37%	0.003	2048137
<i>Parabacteroides</i>	Bacteroidetes	0.27%	0.002	375288
<i>Drancourtella</i>	Firmicutes	0.16%	0.002	1903506

STDEV: standard deviation; NCBI ID: National Center for Biotechnology Information, taxonomy ID

Table 3.4 Top 20 most abundant bacterial species in the cat rectum microbiota.

species name	normal average RA	normal STDEV	normal rank	obese average RA	obese STDEV	obese rank	NCBI ID
<i>Prevotella copri</i>	12.863%	0.074	1	19.646%	0.163	1	165179
<i>Erysipelotrichaceae bacterium AU001MAG</i>	3.066%	0.012	2	0.002%	0.000	847	-
<i>Collinsella tanakaei</i>	2.418%	0.016	3	2.399%	0.022	10	626935
<i>Megasphaera elsdenii</i>	1.940%	0.029	4	0.580%	0.007	29	907
<i>Collinsella stercoris</i>	1.833%	0.016	5	4.566%	0.033	2	147206
<i>Clostridium sp. CAG:169</i>	1.700%	0.011	6	0.625%	0.006	28	1262778
<i>Succinatimonas sp. CAG:777</i>	1.568%	0.014	7	0.332%	0.007	46	1262974
<i>Subdoligranulum variabile</i>	1.274%	0.009	8	2.691%	0.023	3	214851
<i>Acidaminococcus sp. CAG:542</i>	1.207%	0.018	9	0.053%	0.000	143	1262687
<i>Blautia sp. CAG:257</i>	1.170%	0.006	10	2.446%	0.019	9	1262756
<i>Prevotella sp. CAG:891</i>	1.157%	0.018	11	2.335%	0.027	11	1262937
<i>Collinsella intestinalis</i>	1.100%	0.015	12	0.677%	0.005	24	147207
<i>Clostridium sp. CAG:299</i>	0.898%	0.006	13	0.429%	0.003	36	1262792
<i>Faecalibacterium prausnitzii</i>	0.851%	0.007	14	0.228%	0.002	57	853
<i>Bacteroides plebeius</i>	0.771%	0.004	15	2.456%	0.021	5	310297
<i>Firmicutes bacterium CAG:424</i>	0.760%	0.004	16	0.379%	0.003	39	1263022
<i>Eubacterium sp. TM06-47</i>	0.683%	0.006	17	0.087%	0.001	111	2292354
<i>Bifidobacterium gallinarum</i>	0.681%	0.013	18	2.503%	0.037	4	78344
<i>Collinsella phocaensis</i>	0.677%	0.005	19	0.566%	0.004	30	1871016
<i>Bacteroides stercoris</i>	0.633%	0.004	20	2.010%	0.028	289	46506

RA: relative abundance; NCBI ID: taxonomy ID from National Center for Biotechnology Information.

3.2.7 Microbial diversity analysis in normal and obese cats

The alpha- and beta-diversity of taxonomy profiles were performed using R package vegan v2.5.7 [250]. Alpha-diversity was analyzed using the Shannon index [251] at the genus level and the species level. Beta-diversity was analyzed based on the Bray-Curtis dissimilarity [252] at the species level and visualized in the format of PCoA (Principal Coordinates Analysis) plot using R software [253].

3.2.8 Analysis of age and sex effects in the normal cat group

Given that age and sex may potentially affect the gut microbiome composition, we performed PCoA analysis at the species level in the control group and used permutational multivariate analysis of variance (PERMANOVA) to determine significant differences between different males and females, as well as between different age groups.

3.2.9 Identification of significantly altered genera or species in normal and obese cats

To assess the statistical significance of the differential abundance of genera or species in normal cats and obese cats, Mann-Whitney U tests [254] were performed in R. The heatmap plots were generated using R package pheatmap (v1.0.12), and the adjusted *P* values (*P*-adj) were calculated using R package qvalue (v2.22.0) [374]. Genera with an average frequency of at least 0.1% and a minimum absolute value of \log_2 fold change of 2 were listed in Table 3.5. Species with an average frequency of at least 0.01% and a minimum absolute value of \log_2 fold change of 2 were listed in Table 3.6 and Table 3.7.

Table 3.5 Significantly altered genera in obese cat rectum microbiota compared to normal cat.

Genus name*	obese average RA	normal average RA	adjusted P-value	log ₂ (fold change)	NCBI ID
<i>Anaerolactibacter</i>	0.00%	0.23%	0.006	-11.773	2563783
<i>Solobacterium</i>	0.00%	0.23%	0.006	-11.379	123375
<i>Lactimicrobium</i>	0.00%	0.87%	0.006	-11.125	2563777
<i>Galactobacillus</i>	0.00%	0.18%	0.006	-6.61	2060871
<i>Phascolarctobacterium</i>	0.02%	0.75%	0.006	-5.397	33024
<i>Butyricicoccus</i>	0.07%	0.33%	0.006	-2.188	580596
<i>Holdemanella</i>	0.01%	0.11%	0.008	-3.013	1573535
<i>Butyrivibrio</i>	0.03%	0.13%	0.008	-2.252	830
<i>Fusobacterium</i>	0.00%	0.12%	0.012	-4.743	848
<i>Escherichia</i>	0.01%	0.24%	0.012	-4.157	561
<i>Eubacterium</i>	0.27%	1.57%	0.012	-2.552	1730
<i>Lactobacillus</i>	0.04%	0.48%	0.017	-3.528	1578
<i>Faecalibacterium</i>	0.44%	2.86%	0.017	-2.705	216851
<i>Helicobacter</i>	0.07%	0.70%	0.023	-3.279	209
<i>Succinatimonas</i>	0.37%	1.60%	0.09	-2.099	674963
<i>Bifidobacterium</i>	8.02%	1.61%	0.049	2.32	1678
<i>Dialister</i>	1.94%	0.01%	0.059	7.897	39948

*Genera with an average frequency of at least 0.1% in normal or obese cats and a minimum absolute value of log₂ fold change of 2 were included.

RA: relative abundance; NCBI ID: taxonomy ID from National Center for Biotechnology Information.

Table 3.6 Significantly decreased species in obese cat rectum microbiota compared to normal cat.

Species name*	obese average RA	normal average RA	adjusted P-value	log ₂ (fold change)	NCBI ID	Phylum
<i>Erysipelotrichaceae bacterium AU001MAG</i>	0.002%	3.066%	0.012	-10.786	-	Firmicutes
<i>Anaerolactibacter massiliensis</i>	0.000%	0.060%	0.012	-9.926	2044573	Firmicutes
<i>Phascolarctobacterium succinatutens</i>	0.002%	0.623%	0.012	-8.572	626940	Firmicutes
<i>Clostridium ventriculi</i>	0.001%	0.176%	0.019	-8.399	1267	Firmicutes
<i>Clostridium colicanis</i>	0.000%	0.050%	0.019	-7.819	179628	Firmicutes
<i>Helicobacter sp. 48519</i>	0.001%	0.149%	0.021	-7.623	2315333	Proteobacteria
<i>Prevotella sp. CAG:755</i>	0.003%	0.069%	0.043	-4.511	1262935	Bacteroidetes
<i>Lactobacillus reuteri</i>	0.007%	0.149%	0.037	-4.413	1598	Firmicutes
<i>Lactobacillus sp.</i>	0.002%	0.051%	0.063	-4.412	1591	Firmicutes

Table 3.6 Continued.

Species name*	obese average RA	normal average RA	adjusted <i>P</i> -value	log ₂ (fold change)	NCBI ID	Phylum
<i>Escherichia coli</i>	0.011%	0.237%	0.016	-4.406	562	Proteobacteria
<i>Faecalibacterium prausnitzii</i>	0.009%	0.129%	0.028	-3.775	718252	Firmicutes
<i>Campylobacter helveticus</i>	0.018%	0.215%	0.026	-3.589	28898	Proteobacteria
<i>Eubacterium sp. AM28-29</i>	0.013%	0.128%	0.026	-3.285	2292349	Firmicutes
<i>Eubacterium sp. TM05-53</i>	0.008%	0.072%	0.021	-3.250	2292353	Firmicutes
<i>Clostridium perfringens</i>	0.023%	0.204%	0.087	-3.138	1502	Firmicutes
<i>Collinsella sp. AM42-18AC</i>	0.006%	0.052%	0.021	-3.058	2292321	Actinobacteria
<i>Allisonella histaminiformans</i>	0.011%	0.088%	0.017	-3.009	209880	Firmicutes
<i>Eubacterium sp. TM06-47</i>	0.087%	0.683%	0.028	-2.966	2292354	Firmicutes
<i>Prevotellamassilia timonensis</i>	0.008%	0.058%	0.028	-2.893	1852370	Bacteroidetes
<i>Helicobacter canis</i>	0.063%	0.453%	0.026	-2.849	29419	Proteobacteria
<i>Blautia wexlerae</i>	0.096%	0.576%	0.028	-2.588	418240	Firmicutes
<i>Collinsella sp. AM18-10</i>	0.018%	0.107%	0.046	-2.565	2292028	Actinobacteria
<i>Roseburia inulinivorans</i>	0.010%	0.054%	0.026	-2.468	360807	Firmicutes
<i>Blautia schinkii</i>	0.046%	0.248%	0.021	-2.419	180164	Firmicutes
<i>Dorea sp. Marseille-P4003</i>	0.024%	0.126%	0.043	-2.404	2040291	Firmicutes
<i>Faecalimonas umblicata</i>	0.013%	0.068%	0.016	-2.373	1912855	Firmicutes
<i>Succinatimonas sp. CAG:777</i>	0.332%	1.568%	0.043	-2.238	1262974	Proteobacteria
<i>Roseburia hominis</i>	0.092%	0.420%	0.028	-2.188	301301	Firmicutes
<i>Coprococcus sp. AF21-14LB</i>	0.024%	0.108%	0.021	-2.168	2292231	Firmicutes
<i>Lachnospiraceae bacterium</i>	0.013%	0.059%	0.026	-2.164	1898203	Firmicutes
<i>Butyrivococcus pullicaecorum</i>	0.056%	0.250%	0.012	-2.150	501571	Firmicutes
<i>Dorea formicigenerans</i>	0.014%	0.057%	0.046	-2.085	39486	Firmicutes
<i>uncultured Eubacterium sp.</i>	0.019%	0.081%	0.037	-2.084	165185	Firmicutes

*Species with an average frequency of at least 0.05% and a minimum of log₂ fold change of 2 or less were included. RA: relative abundance; NCBI ID: taxonomy ID from National Center for Biotechnology Information.

Table 3.7 Significantly increased species in obese cat rectum microbiota compared to normal cat.

Species name	obese average RA	normal average RA	adjusted <i>P</i> -value	log ₂ (fold change)	NCBI ID	Phylum
<i>Dialister sp. CAG:486</i>	1.935%	0.001%	0.043	10.598	1262870	Firmicutes
<i>Bifidobacterium adolescentis</i>	2.113%	0.036%	0.017	5.879	1680	Actinobacteria
<i>Megasphaera sp. An286</i>	0.073%	0.002%	0.046	5.261	1965622	Firmicutes
<i>Campylobacter upsaliensis</i>	0.497%	0.020%	0.043	4.640	28080	Proteobacteria
<i>Olsenella provencensis</i>	2.268%	0.115%	0.071	4.300	1852386	Actinobacteria
<i>Bacteroides coprophilus CAG:333</i>	0.099%	0.005%	0.026	4.226	1263041	Bacteroidetes
<i>Bacteroides xylanisolvens</i>	0.122%	0.007%	0.026	4.102	371601	Bacteroidetes
<i>Bifidobacterium longum</i>	0.633%	0.040%	0.019	3.975	216816	Actinobacteria
<i>Phocaecicola coprophilus</i>	0.529%	0.037%	0.037	3.831	387090	Bacteroidetes
<i>Megasphaera stantonii</i>	0.118%	0.011%	0.028	3.456	2144175	Firmicutes
<i>Olsenella sp. An290</i>	0.053%	0.005%	0.037	3.441	1965625	Actinobacteria
<i>Bifidobacterium pseudolongum</i>	0.187%	0.023%	0.071	3.044	1694	Actinobacteria
<i>Bacteroides ovatus</i>	0.101%	0.013%	0.071	2.901	28116	Bacteroidetes
<i>Collinsella sp. An268</i>	0.367%	0.058%	0.028	2.665	1965612	Actinobacteria
<i>Flavonifractor sp. An306</i>	0.119%	0.020%	0.100	2.566	1965629	Firmicutes
<i>Olsenella sp. Marseille-P2300</i>	0.067%	0.016%	0.071	2.083	1805478	Actinobacteria
<i>Olsenella mediterranea</i>	0.071%	0.017%	0.059	2.034	1871031	Actinobacteria
<i>Slackia equolifaciens</i>	0.133%	0.033%	0.028	2.002	498718	Actinobacteria

*Species with an average frequency of at least 0.05% and a minimum of log₂ fold change of 2 or more were included. RA: relative abundance; NCBI ID: taxonomy ID from National Center for Biotechnology Information.

3.2.10 Linear discriminant analysis in normal and obese cat gut microbiota

Linear discriminant analysis Effect Size (LEfSe v1.1.1) analysis was performed via Galaxy web application (<http://huttenhower.org/galaxy>) with default options to determine the most featured families, genera, and species that explain the differences between normal and obese cat gut microbiota. The relative taxonomic frequencies were used as the input of LEfSe pipeline.

3.2.11 Metagenomic assembly, genome completeness, and synteny analysis of a previously uncharacterized species *Erysipelotrichaceae bacterium AU001MAG*

The genome of the uncharacterized *Erysipelotrichaceae bacterium* species was assembled from the metagenomic reads using MEGAHIT [372], and this species is named *Erysipelotrichaceae bacterium AU001MAG*. CheckM [375] was used to assess the quality of this microbial genome and the two most related species in the family of Erysipelotrichaceae, *Lactimicrobium massiliense* (NCBI assembly accession number GCA_900343155) and *Bulleidia sp. zg-1006* (NCBI assembly accession number GCA_016812035). The synteny analysis of these species was performed with MCscan (Python version) [376].

3.2.12 qPCR validation of microbial abundance changes

A total of eight bacterial species were selected for qPCR (quantitative Polymerase Chain Reaction) validation, including *Prevotella copri*, the most abundant species with no significant changes between normal and obese microbiota, four highly abundant species enriched in obese cat gut microbiota (*Bifidobacterium adolescentis*, *Olsenella provencensis*, *Dialister sp. CAG:486*, and *Campylobacter upsaliensis*), and three species enriched in normal gut microbiota (*Erysipelotrichaceae bacterium AU001MAG*, *Phascolarcobacterium succinatutens*, and *Campylobacter helveticus*). The qPCR primers were designed in Oligo 7 software [377] and synthesized by Eurofins (Eurofins Genomics Inc., KY). For each qPCR reaction, 30 ng fecal DNA sample was mixed with PerfeCTa SYBR Green FastMix, Low ROX (Quantabio, Cat No. 95072-012) in 96-well plates, and the qPCR was performed on a Bio-Rad C1000 Touch Thermal Cycler with CFX96 Real-Time PCR Detection Systems (Bio-Rad Laboratories, CA). Non-parametric Wilcoxon Rank Sum test was performed on log₁₀ scale of expression values to assess the statistical significance.

3.2.13 Enrichment of functional categories and pathways

The HMP Unified Metabolic Analysis Network, HUMAnN 3.0 [378] was used to profile the abundance of microbial metabolic pathways from metagenomic sequencing data based on MetaCyc database [379]. Functional annotation was performed with eggNOG-mapper [380] based on eggNOG 5.0 database [381]. CAZymes (Carbohydrate-active Enzymes) were predicted using and automated carbohydrate-active enzyme annotation tool dbCAN [382]. Wilcoxon Rank Sum tests were performed to assess the statistical significance of the differential pathways in normal cats and obese cats.

3.2.14 Data availability

The whole-genome shotgun metagenomic sequencing data is available at NCBI SRA under accession number PRJNA758898. This whole-genome shotgun metagenomic assembly has been deposited at DDBJ/ENA/GenBank under the accession GCA_022675345.1.

3.3 Results

3.3.1 A comprehensive characterization of feline gut microbiota using deep WGS

metagenomic data

The body condition score (BCS) and body weight were measured for cats in this study (Table 3.1). We collected 16 fecal samples from eight overweight/obese cats (BCS \geq 7) and eight normal cats (BCS = 5) maintained in the same research environment (Figure 3.2A and Figure 3.1).

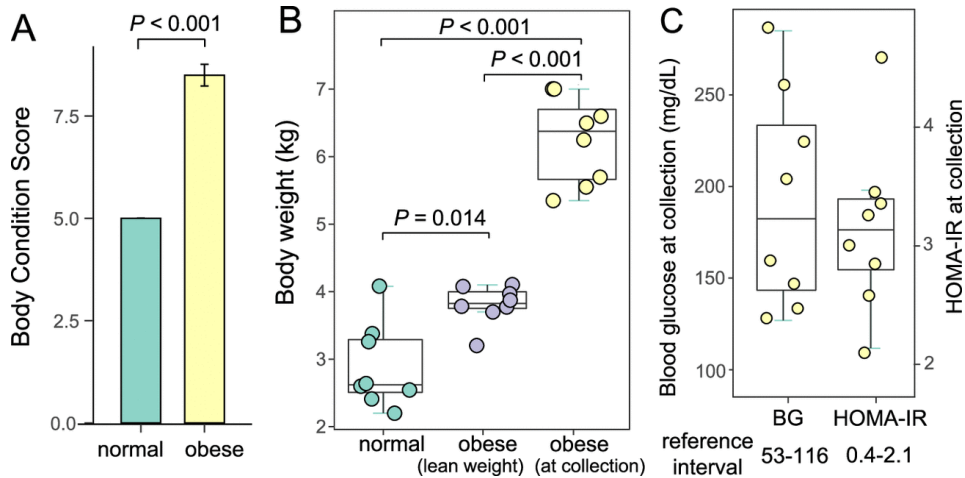


Figure 3.2 Body weight, body condition score, serum glucose level, and insulin resistance parameters for obese cats. (A) Bar plot of the body condition scores of normal and obese cats in this study. (B) Box plot of the body weight of normal cats, obese cats when they were lean, and obese cats at the time of fecal and blood sample collection. (C) Box plot of the blood glucose scores (left) and homeostatic model assessment for insulin resistance (HOMA-IR) scores (right) of obese cats at collection.

WGS (whole-genome shotgun) metagenomic sequencing of the fecal DNA generated 1.8 billion 150-bp reads (or 271 Gbp reads). Of these, 2.21% are adapter sequences or low-quality bases, 15.21% are host sequences from the feline genome, and 0.04% are viral reads (Table 3.2). After removing these non-microbial reads, we performed *de novo* metagenomic assembly using 16 samples combined for a feline reference gut microbiome. The non-redundant assembly contains 355,573 microbial contigs, with a total length of 961,105,174 bp (N50 = 11,097 bp). When filtered metagenomic sequences were aligned to this feline gut microbial reference assembly for each sample, the average mapping percentage was 82.7% (Table 3.2) with a mean coverage depth of 282 \times . A total of 1.14 million non-redundant microbial genes were identified from the reference contigs. Rarefaction analysis of non-redundant genes revealed a curve approaching saturation (Figure 3.3A). The number of bacterial species discovered in these metagenomes was also saturated, suggesting sufficient sequencing coverage and samples size (Figure 3.3B).

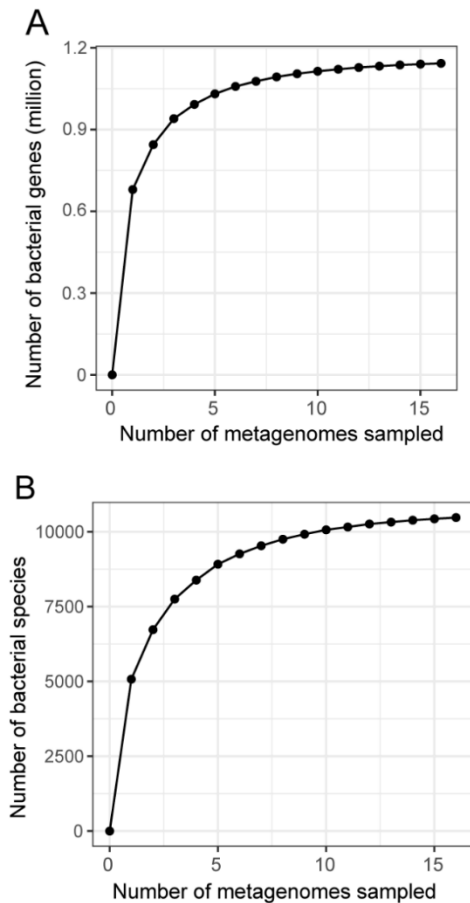


Figure 3.3 Rarefaction analyses to assess species and gene richness from the results of sampling. (A) Rarefaction curve based on bacterial gene profiles of 16 samples. (B) Rarefaction curve based on taxonomy profiles at the species level of 16 samples.

3.3.2 High blood glucose levels and insulin resistance were associated with feline obesity

The eight obese cats in this study were on a similar diet to lean cats, based on major nutrients and fiber content (see Materials and Methods). Before they became obese, their body weight ranged from 3.20 to 4.10 kg (Table 3.1). After *ad libitum* feeding, these animals had a mean body weight of 6.20 kg at the time of fecal sample collection (Table 3.1), which was significantly heavier (Figure 3.2B; $P < 0.001$, Mann-Whitney U test). Cats in the normal body weight group were from the Scott-Ritchey Research Center breeding colony housed in the same facility, and they were significantly lighter than the obese cats at the time of fecal sample collection (Figure

3.2B; $P < 0.001$, Mann-Whitney U test). Blood glucose levels of these obese cats were 192.4 ± 59.3 mg/dL (ranging from 127 to 285 mg/dL), which were all above the reference interval for cat blood glucose levels determined by Auburn University College of Veterinary Medicine Clinical Pathology Laboratory (Table 3.8 and Figure 3.2C). Serum insulin levels were also measured, and the homeostasis model assessment of insulin resistance (HOMA-IR) was 3.16 ± 0.72 (ranging from 2.44 to 3.89; Figure 3.2C), which were also higher than the population-based reference interval of HOMA-IR in healthy lean cats (0.4~2.1) [329]. Therefore, the eight obese cats had significantly elevated blood glucose levels with demonstratable insulin resistance at the time of fecal sample collection.

Table 3.8 Blood glucose and HOMA-IR measurements in obese cats at the time of fecal sample collection.

Cat ID	Group	Sex	Blood glucose at collection (mg/dL)	Blood glucose reference range	HOMA-IR at collection	HOMA-IR for normal cats
D001	obese	male	127	58~116	2.86	1.3+/-0.9
F001	obese	male	256	58~116	4.60	1.3+/-0.9
G001	obese	male	226	58~116	2.62	1.3+/-0.9
H001	obese	male	203	58~116	3.27	1.3+/-0.9
I001	obese	male	133	58~116	2.14	1.3+/-0.9
J001	obese	male	147	58~116	3.00	1.3+/-0.9
K001	obese	male	285	58~116	3.47	1.3+/-0.9
L001	obese	male	162	58~116	3.37	1.3+/-0.9
Mean \pm s.d.			192.4 ± 59.3		3.16 ± 0.72	

3.3.3 Lack of significant sex or age effects on gut microbiome within the normal cat group

In the normal cat group in this research, four male and four female participants were included, with ages ranging from 4 months to 6 years (Table 3.2). To determine whether there were significant differences in the microbiome composition between sex and age groups, we

performed Principal Coordinates Analysis (PCoA) analyses and discovered no significant effect of sex (Figure 3.4A; $P = 0.473$, PERMANOVA test) or age (Figure 3.4B, $P = 0.468$, PERMANOVA test) on the cat gut microbiome composition. Compared to the obese cat microbiota from 6-year males, the normal cats formed a cluster, which was well separated from the obese cat microbiota (Figure 3.5C; $P = 0.001$, PERMANOVA test). These results justified the inclusion of these eight cats in the normal body weight group.

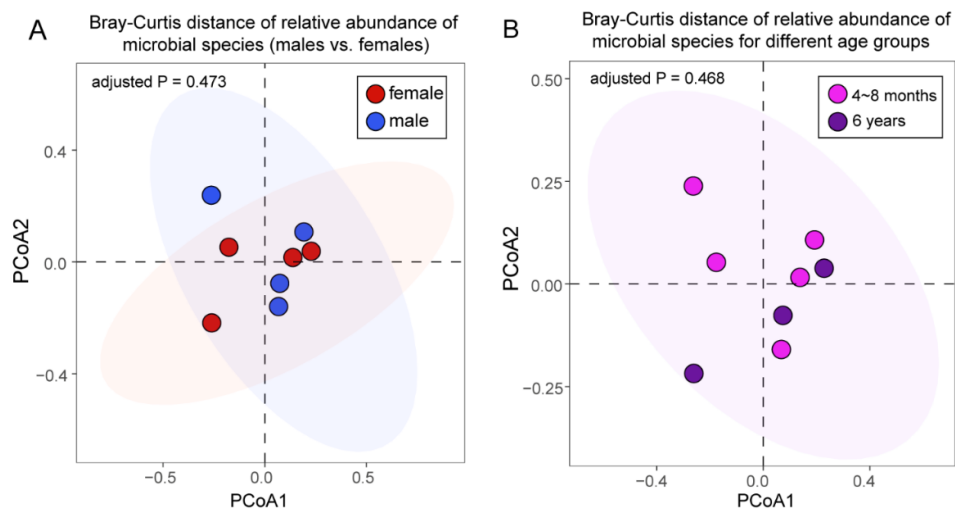


Figure 3.4 Principal Coordinates Analysis (PCoA) plots of beta diversity between rectum microbiota of cats of different sex or age using Bray-Curtis distance. (A) The Principal Coordinates Analysis (PCoA) plot of Bray-Curtis distance of relative abundance of microbial species between male cats and female cats. Statistical significance was assessed using permutational multivariate analysis of variance (PERMANOVA). (B) The Principal Coordinates Analysis (PCoA) plot of Bray-Curtis distance of relative abundance of microbial species between cats at 4 months to 8 months and cats at 6 years. Statistical significance was assessed using permutational multivariate analysis of variance (PERMANOVA).

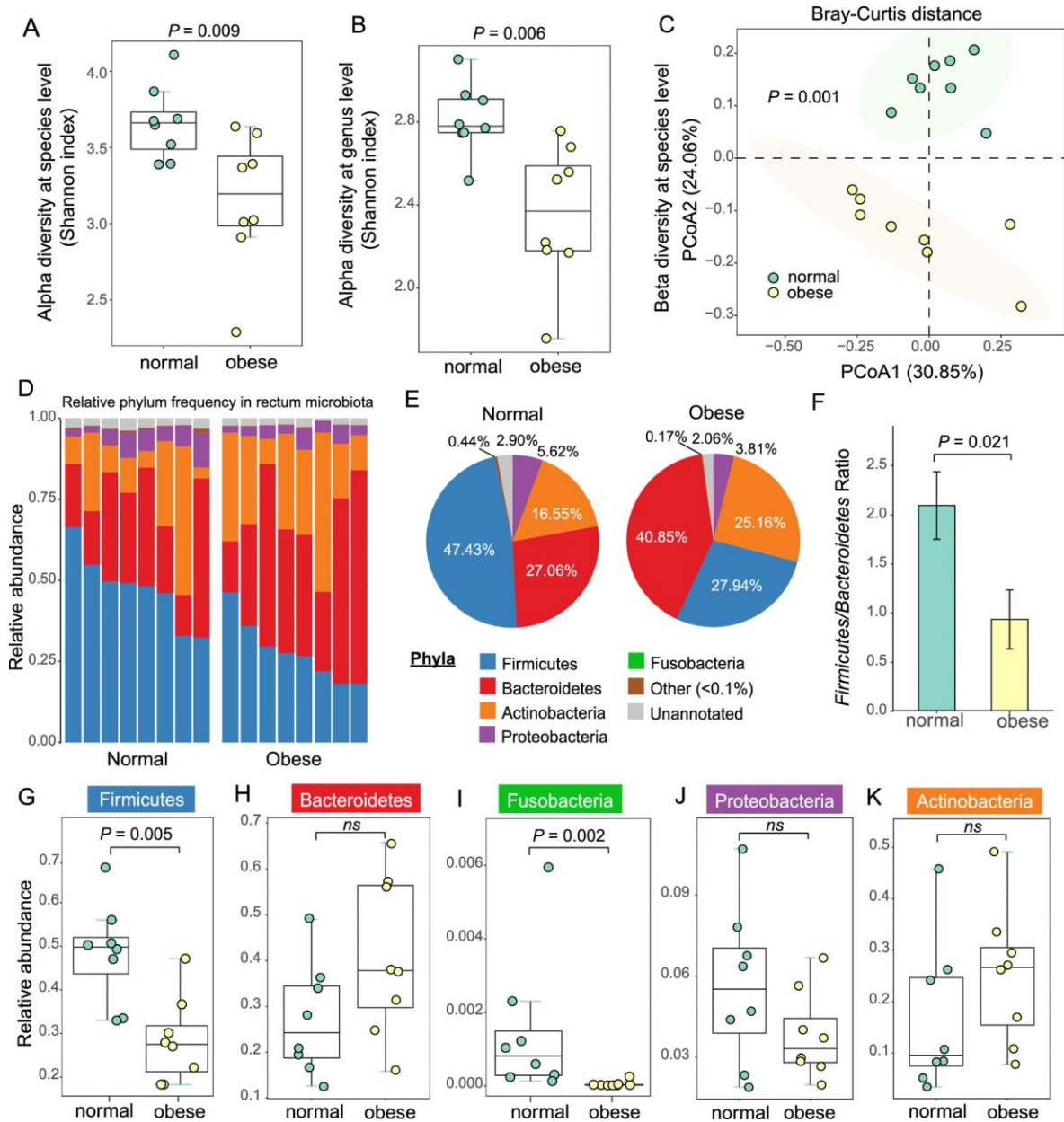


Figure 3.5 Significant changes of microbial diversity and phylum-level composition in cat gut microbiota. (A to B) Box plots of alpha diversity in normal (green) and obese (yellow) cat microbiota at the species (A) level and genus (B) level, measured using the Shannon index. (C) The PCoA plots of beta diversity between normal and obese rectum microbiota using Bray-Curtis distance. Statistical significance was assessed using permutational multivariate analysis of variance (PERMANOVA). (D) Bar plot of phylum-level relative frequency in normal and obese cat microbiota. (E) Pie charts of the phylum-level composition in normal and obese cat gut microbiota. (F) Bar plot of the Firmicutes-to-Bacteroidetes ratios in normal and obese cat gut microbiota. (G to K) Box plots of frequency for the five most abundant phyla: Firmicutes (G), Bacteroidetes (H), Fusobacteria (I), Proteobacteria (J), and Actinobacteria (K). Statistical significance was determined by the Mann-Whitney U test.

3.3.4 Significant reduction in microbial diversity in obese cat gut microbiota

A total of 92.6% of the cat gut microbial contigs were taxonomically classified at the superkingdom level, among which bacteria account for 99.5%, with the remaining 0.5% from archaea and viruses. At lower taxonomy levels, 61.7% and 54.7% of the reference contigs were assigned to genus and species, respectively. Alpha diversity measured by the Shannon index showed a significant reduction in obese cat microbiome compared to normal cats, at the species level (Figure 3.5A; $P = 0.009$, Mann-Whitney U test) and genus level (Figure 3.5B, $P = 0.006$, Mann-Whitney U test). This result indicated a substantial reduction in gut microbiome complexity in obese cats compared to normal cats, suggesting dysbiosis in the obese microbiota. Principal Coordinates Analysis (PCoA) plot of beta diversity between normal and obese cat gut microbiomes using Bray-Curtis distance showed significant separation between these two groups at the species level (Figure 3.5C; $P = 0.001$, PERMANOVA test). The diversity analyses identified distinct patterns of gut microbiota in obese cats and normal cats.

3.3.5 Phylum-level characterization of feline gut microbiota revealed a significantly lower Firmicutes-to-Bacteroidetes ratio in obese cats

Among the assembled microbial contigs, 87.2% were taxonomically classified at the phylum level. Almost 98% of the microbes belong to the top 5 phyla, including Firmicutes, Bacteroidetes, Actinobacteria, Proteobacteria, and Fusobacteria (Figure 3.5D). The most dominant phylum in normal cat gut microbiota was Firmicutes (47.4%), and the second was Bacteroidetes (27.1%), which was consistent with previously reported in 16S rDNA metagenomic studies [364] (63.3% Firmicutes and 27.6% Bacteroidetes; Figure 3.6A). In obese cats, the most abundant phylum was Bacteroidetes (40.9%), followed by Firmicutes (27.9%) (Figure 3.5E). This dramatic shift from Firmicutes to Bacteroidetes resulted in a significantly

lower Firmicutes-to-Bacteroidetes ratio (2.10 to 0.94) in obese cat microbiota (Figure 3.5F-H; $P = 0.021$, Mann-Whitney U test). Another phylum, Fusobacteria, which accounted for 0.3% of the normal gut microbiome, was also depleted in obese cats (Figure 3.5I; $P\text{-adj} = 0.002$, Mann-Whitney U test). No significant changes were detected at the phylum level for Proteobacteria or Actinobacteria (Figure 3.5J-K; $P\text{-adj} > 0.05$, Mann-Whitney U test).

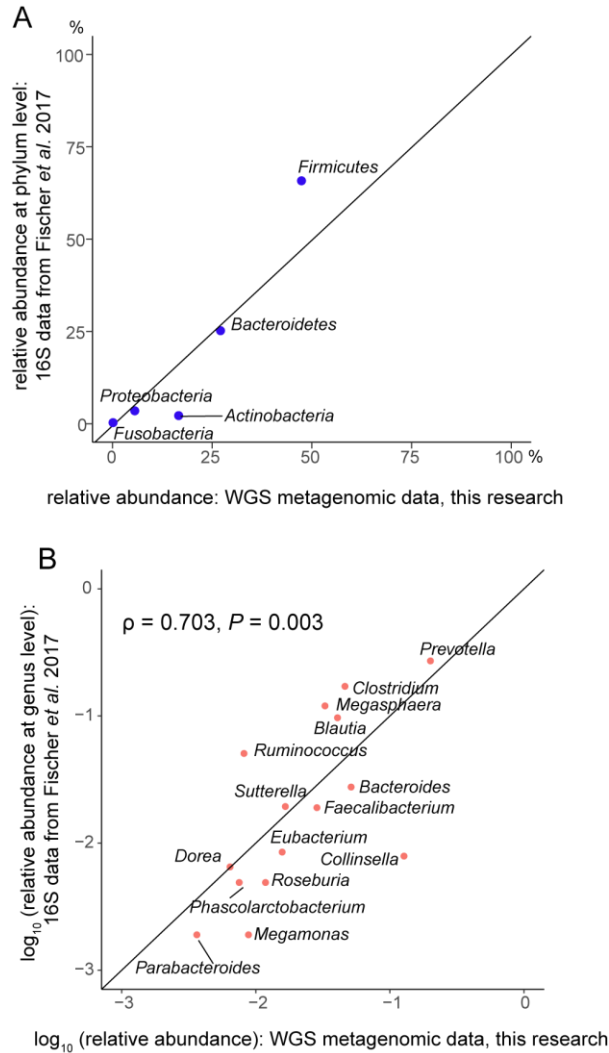


Figure 3.6 Bacterial relative abundance correlations between between WGS metagenomic data in this research and 16S rDNA ampliconic sequencing data in Fisher *et al.* 2017 at phylum and genus levels. (A) Scatterplot of relative frequency of the top 5 most abundant phyla from cat intestinal WGS metagenomic data in this research and the 16S ampliconic sequencing data in Fisher *et al.* 2017. (B) Scatterplot of relative frequency at \log_{10} scale of the 15 most abundant genera from normal cat intestinal WGS metagenomic data in this research and lean cat 16S ampliconic sequencing data in Fisher *et al.* 2017.

3.3.6 The top 20 most abundant bacterial genera distinguish the normal and obese cat gut microbiota.

The top 20 genera accounted for approximately 70% of total abundance (Table 3.3). The eight normal and eight obese cat microbiomes formed two distinct groups when unsupervised clustering was performed using the relative abundance of the top 20 genera (Figure 3.7A), indicating microbial composition differences occurred at the most abundant genera level.

Prevotella was the most abundant genus (24.3%; Figure 3.7A-B and Table 3.3-3.4), and the relative proportions of the top 20 genera were highly correlated with the previous 16S rDNA sequencing studies (Figure 3.6B; Spearman's $\rho = 0.703$, $P = 0.003$, Spearman's Rank Correlation test). Of the top five genera, *Bacteroides* increased in the obese cat gut microbiota with a marginal statistical significance (Figure 3.7C; P -adj = 0.059, Mann-Whitney U test). Two Firmicutes genera were significantly altered in the obese cat gut microbiome: *Lactimicrobium* and *Phascolarctobacterium* accounted for 0.87% and 0.75% respectively in normal cats, but were not found (<0.0005%) in obese cats (P -adj = 0.006; Figure 3.7C and Table 3.5). This result was consistent with the decreased abundance in Firmicutes in the obese microbiome at the phylum level (Figure 3.5E). The *Prevotella*-to-*Bacteroides* ratio, which was reported to predict body weight and fat loss potential in humans [383], showed no significant change in obese and normal cat gut microbiota (Figure 3.7D; $P > 0.05$, Mann-Whitney U test).

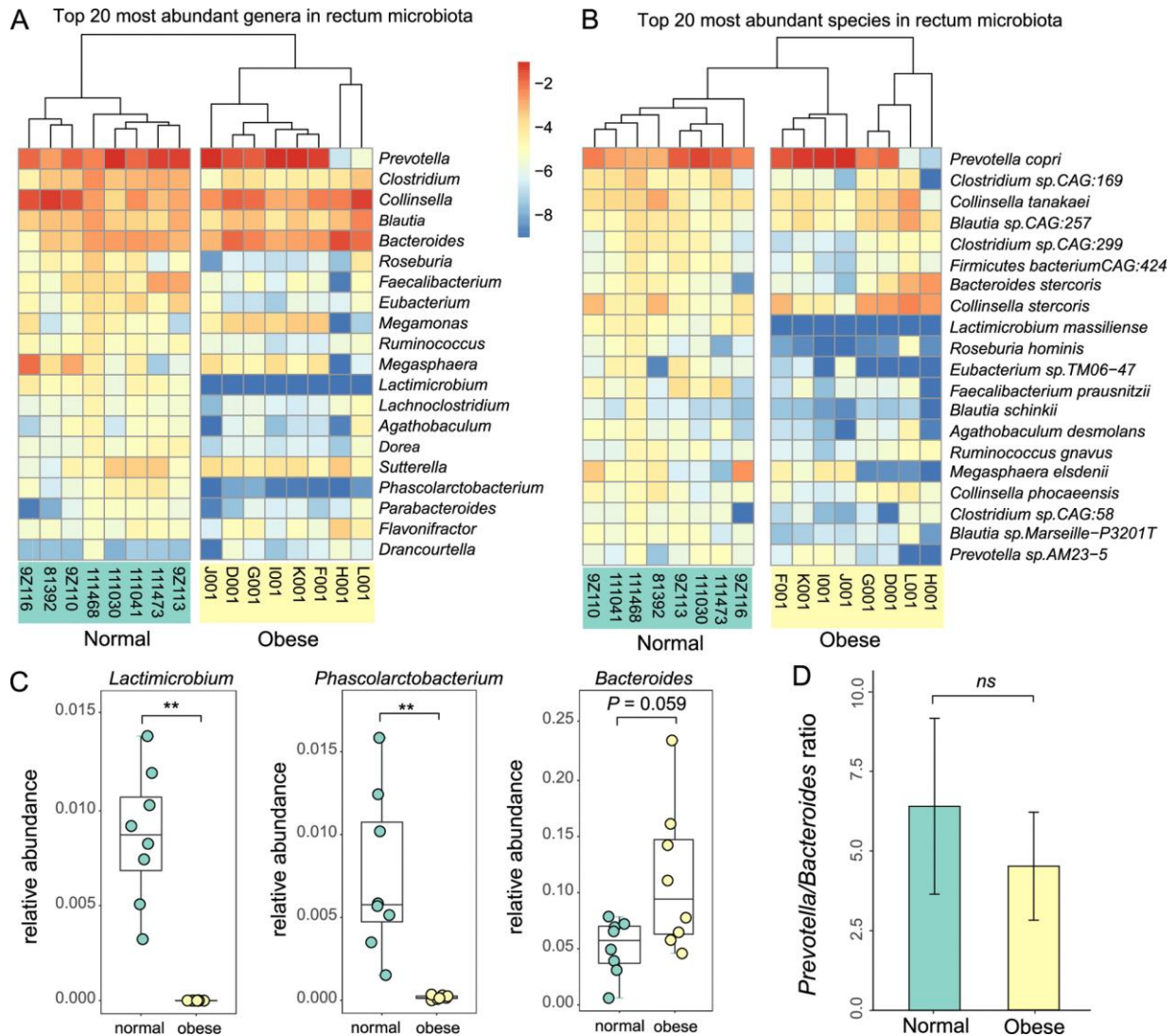


Figure 3.7 Top 20 abundant bacterial genera and species in cat gut microbiota, and their relationship to cat obesity. (A, B) Heatmap of relative frequency for the top 20 most abundant bacteria genera (A) and species (B). The taxa were rank-ordered with the most abundant taxon on the top. (C). Box plots of relative frequency for three top 20 genera that exhibit significant abundance differences between normal and obese cat gut microbiota: *Lactimicrobium*, *Phascolarctobacterium*, and *Bacteroides*. (D). Bar plot of *Prevotella*-to-*Bacteroides* ratios in normal and obese cat gut microbiota.

3.3.7 Linear discriminant analysis revealed the most featured bacterial families, genera, and species in normal vs. obese cat gut microbiota.

To identify the featured taxa associated with obesity, we performed linear discriminant analysis (LDA) on microbial abundance profiles at the family, genus, and species levels. At the family

level, *Bifidobacteriaceae* was the only featured family in obese cat gut microbiota (LDA > 3.0), whereas ten families were featured in the normal microbiome, including *Lachnospiraceae*, *Clostridiaceae*, *Acidaminococcaceae*, *Eubacteriaceae*, *Erysipelotrichaceae*, *Helicobacteraceae*, *Peptostreptococcaceae*, *Lactobacillaceae*, *Oscillospiraceae*, and *Enterobacteriaceae* (Figure 3.8A). At the genus level, *Bifidobacterium* and *Dialister* were the most featured obese genera to distinguish from normal cat microbiota (Figure 3.8B). The normal cat microbiome featured 15 genera, 14 of which belonged to the most featured families except *Succinatimonas*, in the family of *Succinivibrionaceae* (Figure 3.8A-B). The significance was driven by *Succinatimonas CAG:777*, which was the second most featured species (Figure 3.8C). We identified 11 featured bacteria species in the obese microbiome (LDA score > 3; Figure 3.8C), including 7 Actinobacteria in the genera of *Olsenella*, *Bifidobacterium*, *Collinsella*, two Bacteroidetes (*Phocaeicola*), a Firmicutes species *Dialister sp. CAG486*, and a Proteobacteria *Campylobacter upsaliensis*. In contrast, 11 Firmicutes and 3 Proteobacteria species were featured in the normal gut microbiome (Figure 3.8C), including the species in the top-20 genera we identified in Figure 3.7A. Our results further confirmed that the normal and obese cat gut microbiota have distinct taxonomical signatures.

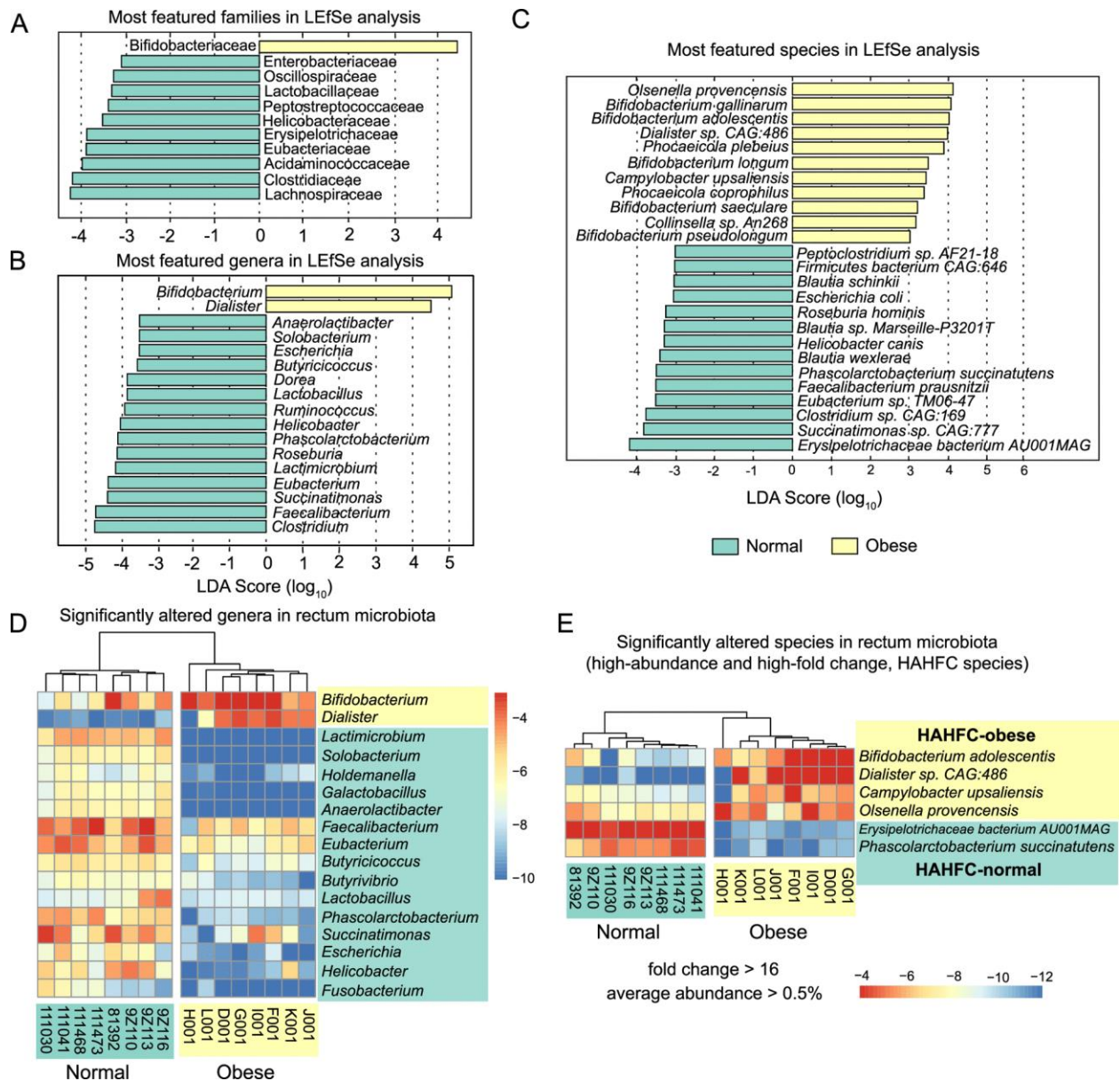


Figure 3.8 Significant differences in taxonomic abundance that discriminate normal and obese cat gut microbiome at the family, genus, and species levels. (A to C) Linear discriminant analysis (LDA) scores of top featured microbial families (A), genera (B), and species (C) in normal (green) and obese (yellow) cat gut microbiota. Taxa with an LDA score greater than 3.0 were included in these plots. (D) Heatmaps of the relative frequency for significantly (FDR < 0.10) altered genera in normal (green) and obese (yellow) cat gut microbiota. Genera with an average frequency of at least 0.1% and a minimum absolute value of log₂ fold change (log₂FC) of 2 were included in the plot. (E) High abundant bacterial species (relative abundance > 0.5%) with high-fold change (>16) between normal (green) and obese (yellow) cat gut microbiota. Four species enriched in obese microbiota (HAHFC-obese) and two species enriched in normal gut microbiota (HAHFC-normal) were shown in the heatmap.

To determine the degree of abundance changes in the obese microbiome, we performed pairwise nonparametric tests to identify significantly altered taxa based on relative abundance (see Materials and Methods). At an FDR (False Discovery Rate) of 10% and relative abundance of 0.5% or higher, 17 genera have a \log_2 fold change greater than 2 (Figure 3.8D). 14/17 significant featured genera with LDA score > 3 (Figure 3.8B) were also found in this list, and they were the most important genera that discriminate normal and obese cat gut microbiomes. High-abundance, high-fold change (HAHFC) marker species were filtered according to the criteria of 16-fold change and average abundance of 0.5% or higher. Six bacterial species were selected for further analysis and validation (Figure 3.8E).

3.3.8 Metagenomic-assembled genome (MAG) of the most featured species in LDA analysis - a previously uncharacterized Erysipelotrichaceae bacterium AU001MAG

The most featured species in the normal gut microbiome (LDA score > 4 ; Figure 3.8C) was initially annotated as *Lactimicrobium massiliense* (Figure 3.7B), and its reference genome sequenced strain was discovered in human breast milk from a healthy lactating mother [384]. However, when the metagenomic reads were aligned to its reference assembly (GCA_900343155), the mapping rate was poor with only 82% average nucleotide identity, suggesting that this OTU in the cat gut microbiome was a different uncharacterized species in the same family of Erysipelotrichaceae [385]. The metagenomic reads from this novel species were also misannotated as another closely related Erysipelotrichaceae species *Bulleidia sp. zg-1006* (78% sequence identity). Using the metagenomic assembly approach, we assembled a MAG genome of 1,798,709 bp in length, consistent with a single species (123 contigs with N50 = 25,047 bp and 1,657 protein-coding genes annotated). The checkM genome completeness was

96.2% (Figure 5A), which was comparable to the two related species *Lactimicrobium massiliense* (99.1%) and *Bulleidia sp. zg-1006* (86.7%). We concluded that the MAG assembly of this species was nearly complete and named it *Erysipelotrichaceae bacterium AU001MAG*. This species was also the most enriched species in the normal gut microbiome ($\log_2FC=10.8$, FDR = 0.01, Mann-Whitney U test, same below; Figure 3.8C, 3.10A, and Table 3.6), with an average depth of >200 across the entire genome in the normal microbiome but zero coverage in the obese microbiome (Figure 3.9B). *Erysipelotrichaceae bacterium AU001MAG* was the second most abundant bacterial species in the cat gut microbiome (3.1% in the normal microbiome), just trailing the most abundant species *Prevotella copri* (12.9%; Table 3.4). Gene annotation-based syntenic analysis revealed that *Erysipelotrichaceae bacterium AU001MAG* contigs could be anchored to ~2/3 of the *Lactimicrobium massiliense* genome, and most of the gene orders were conserved (Figure 3.9C), suggesting that *Lactimicrobium massiliense* was the closest genome-sequenced species in the NCBI database. In contrast, *Bulleidia sp. zg-1006* had fewer syntenic regions and more genome rearrangement events (Figure 3.9C).

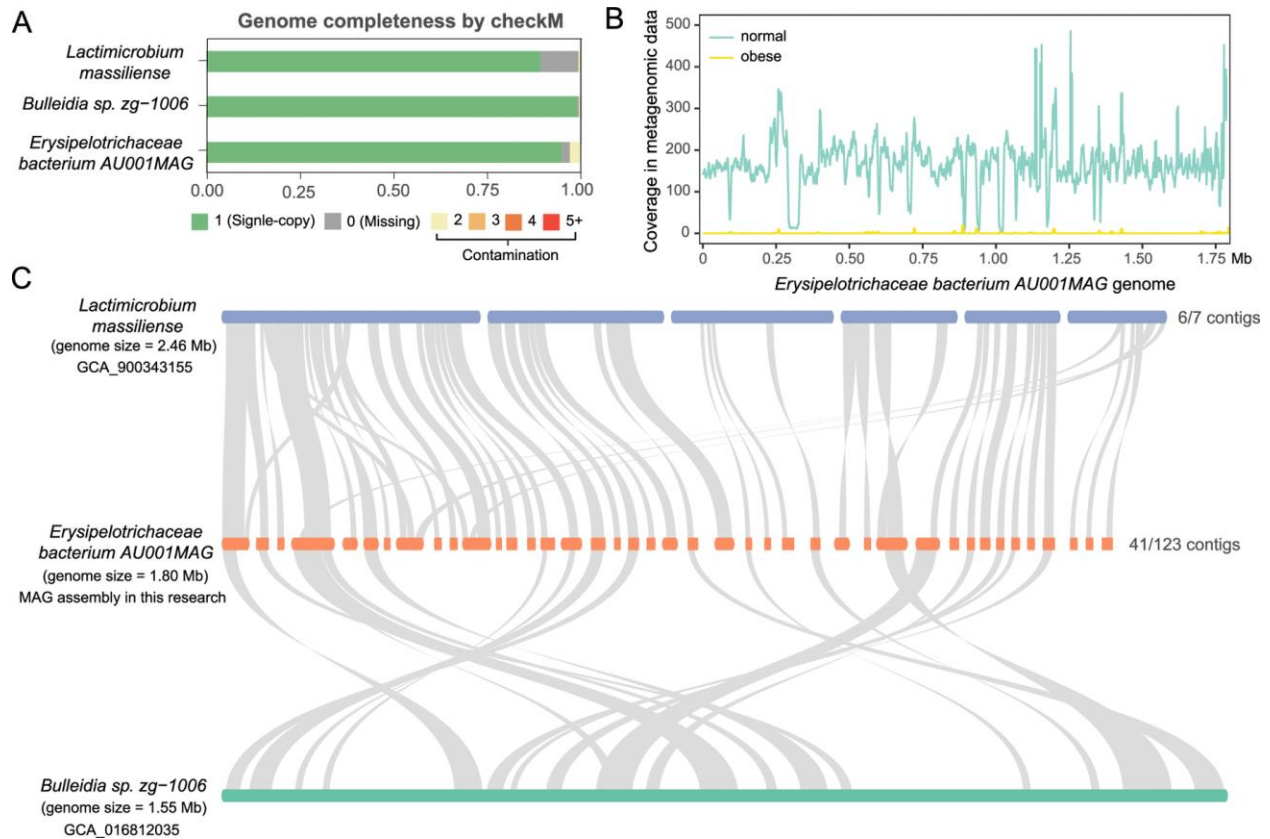


Figure 3.9 MAG genome quality assessment, normal and obese microbiota coverage, and syntenic analysis of the most featured species in obese cat gut microbiome, *Erysipelotrichaceae bacterium AU001MAG*. (A) Genome completeness of *Lactimicrobium massiliense*, *Bulleidia sp. Zg-1006*, and *Erysipelotrichaceae bacterium AU001MAG* assessed by checkM, showing the fraction of single-copy, missing, and contaminated genes. (B) Sliding window plot of the average coverage depth of *Erysipelotrichaceae bacterium AU001MAG* in normal (green) and obese (yellow) metagenomic data. (C) Syntenic region plot of *Erysipelotrichaceae bacterium AU001MAG* with its two most related species, *Lactimicrobium massiliense* and *Bulleidia sp. Zg-1006*.

3.3.9 Hallmark of the obese cat gut microbiome - dramatic increases in abundance of *Bifidobacterium sp.*, *Dialister sp.*, *Olsenella provencensis*, and *Campylobacter upsaliensis*

A total of 400 bacteria species were significantly enriched in the obese cat gut microbiome, at an FDR of 10% and \log_2 fold change of 2 or more. Of these, many had an extremely low relative abundance in both groups, which were unlikely to be relevant to the disease. Eighteen obese-

enriched species had a relative abundance of 0.05% or higher in the obese microbiome (Table 3.7), including 9 Actinobacteria, 4 Bacteroidetes, 4 Firmicutes, and 1 Proteobacteria. Among them, four species had high abundance in the obese cat gut microbiome (>0.5%) with extremely high fold increase (fold change >16), which were defined as HAHFC-obese species (Figure 3.8E). As a species in one of the two most featured genera in the obese microbiome (Figure 3.8B), *Dialister sp. CAG:483* accounted for less than 0.001% in the normal microbiome and 1.935% in the obese microbiome, with an over 1500-fold increase (FDR = 0.04; Table 3.7). *Dialister* is a Firmicutes genus in the class of Negativicutes. Although we observed an overall reduction of Firmicutes in obese cat gut microbiota (Figure 3.5E), the proportion of Negativicutes in Firmicutes increased from 14% to 20%, as shown in the Krona plot (Figure 3.10A), which was partly driven by a dramatic increase of the *Dialister* genus from 0.003% to 7% in Firmicutes in the obese cat gut microbiome (Figure 3.10A).

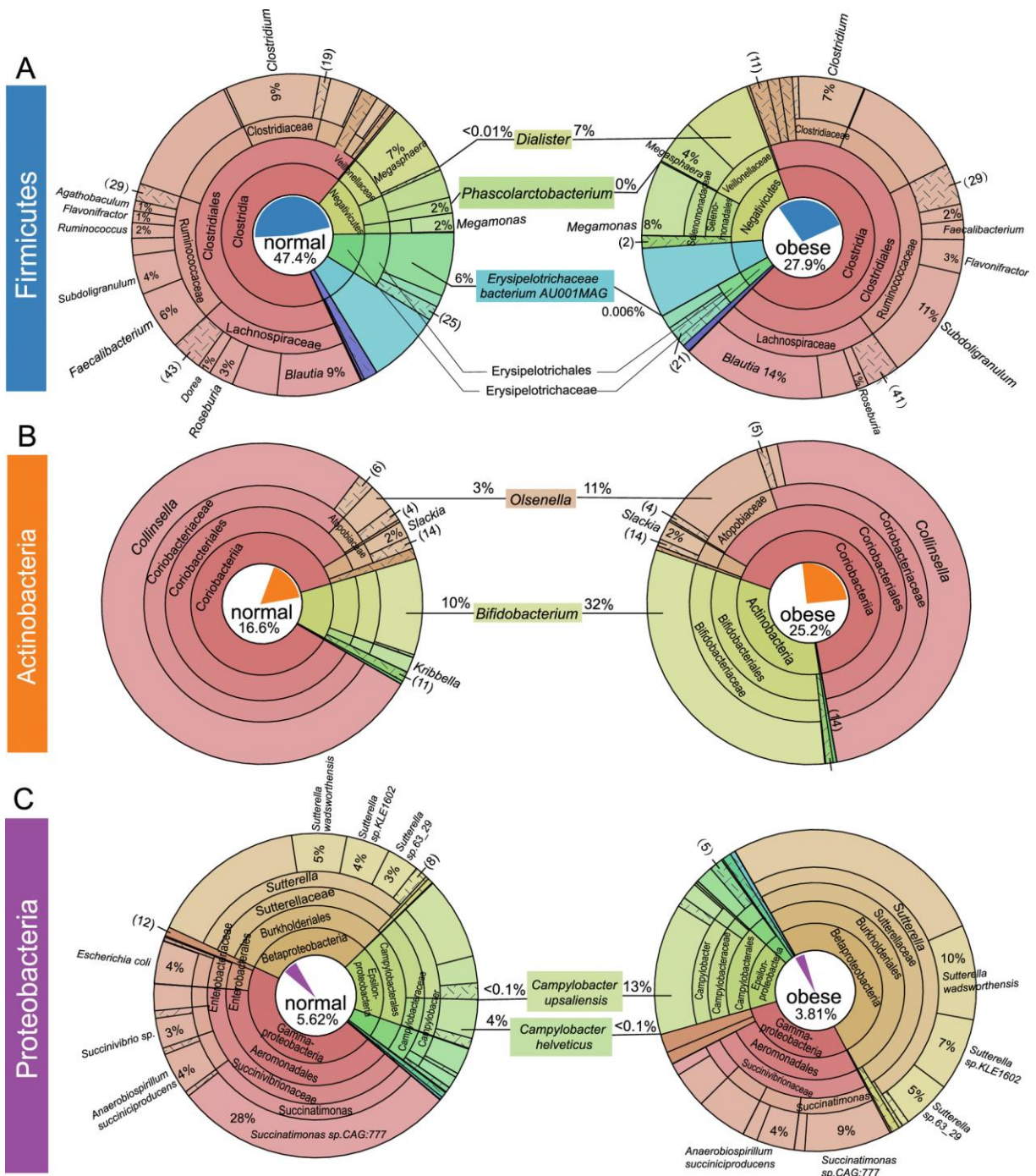


Figure 3.10 Krona plots reflecting the phylogenetic relationship and composition changes in Firmicutes, Actinobacteria, and Proteobacteria. Annotated taxonomy units within the phyla of Firmicutes (A), Actinobacteria (B), and Proteobacteria (C) were visualized in terms of relative abundance and taxonomic hierarchy for normal (left) and obese (right) cat gut microbiome. Different taxonomic terms are color-coded, and the composition percentages are labeled at the genus level (A, B) or the species level (C). The area in the chart is proportional to the relative abundance. The proportions of each phylum in the normal and obese microbiome were represented in a pie chart in the center of the circle.

The number of Actinobacteria species dominated the obese cat gut microbiome enriched species. *Bifidobacterium adolescentis* is the second most enriched species (FDR = 0.02, LDA score > 4; Figure 3.8C, E) with a fold change of over 50, accounting for 2.11% of the obese cat gut microbiome (Table 3.7). *Bifidobacterium* was the other featured genus in the obese cat gut microbiome, and six species were significantly overrepresented ($\log_2\text{FC} > 1.5$, FDR < 0.10), including *B. adolescentis*, *B. longum*, *B. pseudolongum*, *B. pullorum*, *B. pullorum subsp. Gallinarum*, and *B. pullorum subsp. Saeculare* (Figure 3.11). Collectively, these species caused an increase of the *Bifidobacterium* genus and the Bifidobacteriaceae family from 10% to 32% in Actinobacteria (Figure 3.10B), serving as a major signature of the obese cat gut microbiome (Figure 3.8A-B). The other two HAHFC-obese species were *Olsenella provencensis* (Actinobacteria) and *Campylobacter upsaliensis* (Proteobacteria). *Olsenella provencensis* was the most featured species (Figure 3.8C, E), with a 20-fold increase in the obese microbiome from 0.11% to 2.27% (Table 3.7 and Figure 3.11). The *Olsenella* genus was also overrepresented in the obese cat gut microbiome (Figure 3.10B). *Campylobacter upsaliensis* is a human pathogen found globally, associated with self-limiting diarrhea in companion animals and humans [386, 387]. As a featured species in the obese microbiome (Figure 3.8C), the abundance of *C. upsaliensis* is extremely low in the normal microbiome (0.020%), but a 25-fold increase was observed in the obese microbiome (Figure 3.8E, 3.10C, and Table 3.7).

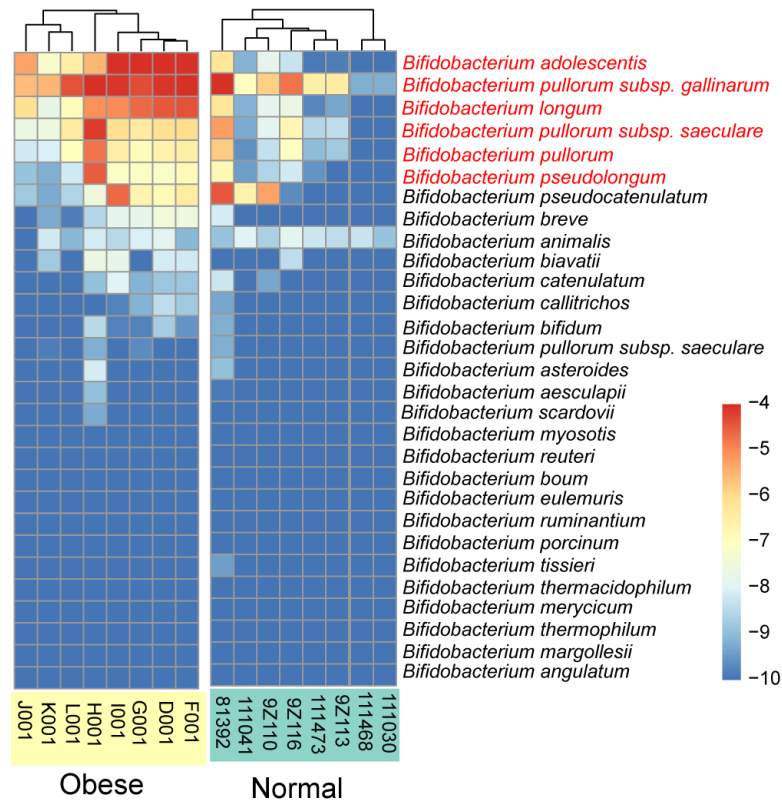


Figure 3.11 Heatmap of species abundance from the *Bifidobacterium* genus in normal vs. obese cat rectum microbiome. Heatmap of relative frequency at log₂ scale for all *Bifidobacterium* species detected in the cat rectum microbiome. Six significantly overrepresented species in the obese gut microbiome (log₂FC > 1.5, q < 0.10), including *B. adolescentis*, *B. longum*, *B. pseudolongum*, *B. pullorum*, *B. pullorum subsp. Gallinarum*, and *B. pullorum subsp. Saeculare*, were denoted in red.

3.3.10 Hallmark of the obese cat gut microbiome – depletion of two highly abundant species in the normal gut microbiome, *Erysipelotrichaceae* bacterium AU001MAG and *Phascolarctobacterium succinatutens*

The two top-20 genera that displayed significant differential abundance in normal vs. obese microbiome (Figure 3.7A, C) were driven by two HAHFC-normal species, *Erysipelotrichaceae* bacterium AU001MAG (initially annotated as *Lactimicrobium massiliense*) and *Phascolarctobacterium succinatutens* (Figure 3.8E). They were also featured in the linear discriminant analysis at species (Figure 3.8C), genus (Figure 3.8B), and family levels

(Erysipelotrichaceae and Acidaminococcaceae, respectively; Figure 3.8A). *Erysipelotrichaceae* bacterium AU001MAG accounted for 3.1% in the normal gut microbiome, with over one-thousand-fold reduction in the obese microbiome ($\log_2\text{FC} = 10.79$, FDR = 0.01; Figure 3.10A and Table 3.6). *P. succinatutens*, another highly abundant Firmicutes in the normal microbiome (0.62%), had a ~400-fold decrease in the obese microbiome ($\log_2\text{FC} = 8.57$, FDR = 0.01; Figure 3.10A and Table 3.6). The depletion of these two species is a hallmark of microbiome alterations in the obese cat gut microbiome.

3.3.11 Distinct metabolic pathways and CAZy families in normal and obese cat gut microbiota

At the microbial metabolic pathway level, we identified 10 pathways significantly enriched in abundance in the obese cat gut microbiome ($\log_2\text{FC} > 1.5$, FDR < 0.1), while 11 pathways were significantly depleted ($\log_2\text{FC} < -1.5$, FDR < 0.1). Among the obese microbiome enriched pathways, 8/10 were biosynthesis pathways. In sharp contrast, 9 of the 11 obese microbiome depleted pathways were involved in degradation and fermentation (Figure 3.12A).

Overrepresented pathways in the obese microbiome included the biosynthesis of fatty acids (stearate, palmitoleate, oleate, and oxononanoate), the biosynthesis of biotin, acyl-carrier protein, and nucleotide sugar CMP-legionaminate, as well as the saturated fatty acid elongation pathways. These pathways were mainly related to lipid biosynthesis. On the contrary, the normal microbiome was enriched for three degradation and two fermentation terms (Figure 3.12A). Methylcitrate cycle I and II, as well as the biosynthesis of glutamine and arginine amino acids were also enriched compared to the obese cat gut microbiome (Figure 3.12A).

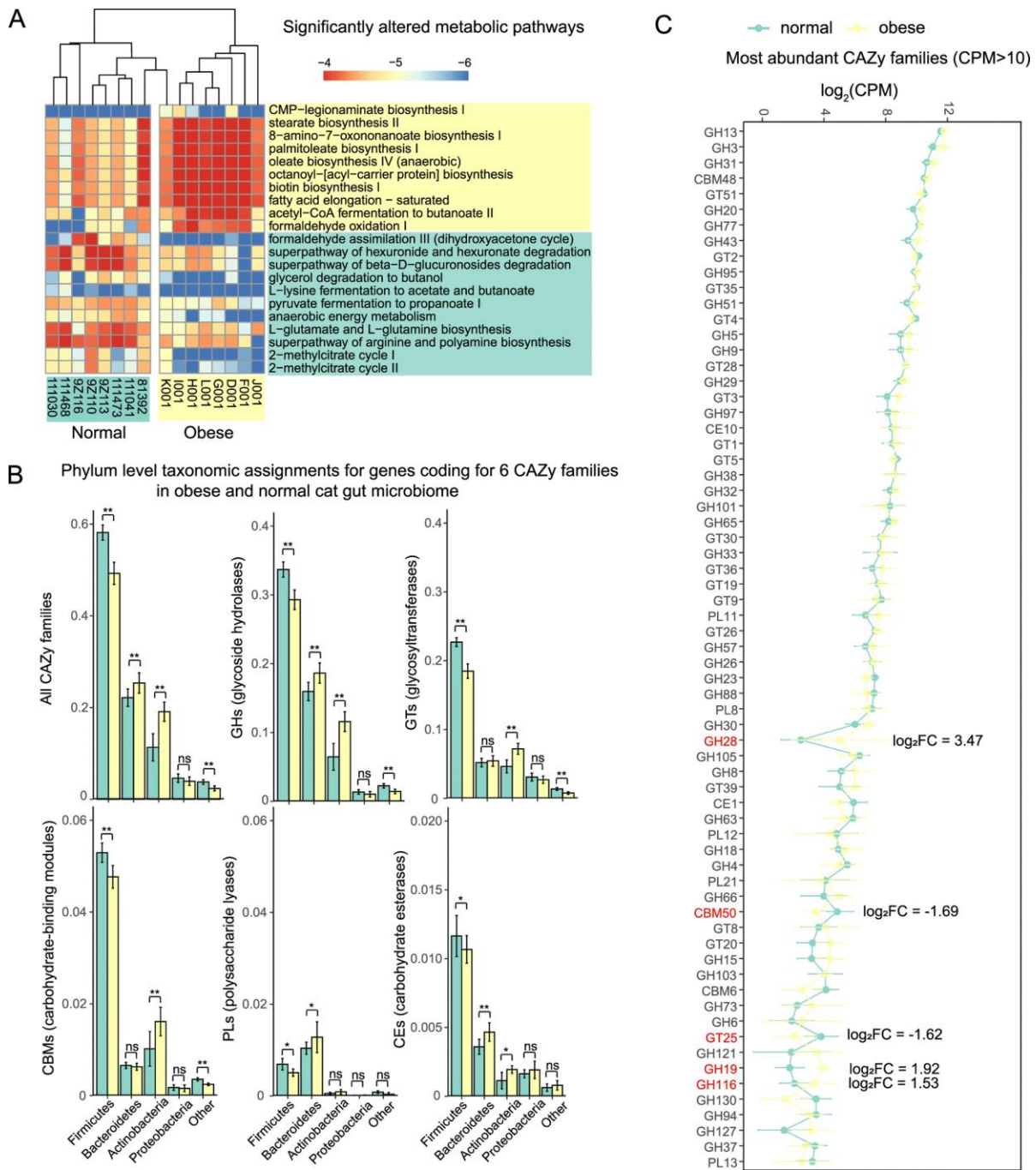


Figure 3.12 Significantly altered metabolic pathways and CAZy families in obese and normal cat gut microbiota. (A) Heatmap of the relative frequencies for significantly (FDR < 0.10) altered microbial metabolic pathways in normal (green) and obese (yellow) cat gut microbiota. Pathways with a minimum absolute value of \log_2 fold change (\log_2 FC) of 1.5 were included in the plot. (B) Bar plots of percentages for phyla to which CAZyme genes from different CAZy families in normal (green) and obese (yellow) cat gut microbiota belong. (C) Line plot of CPM (mapped reads) at \log_2 scale for most abundant CAZy families (CPM > 10) in normal (green) and obese (yellow) cat gut microbiota. CAZy families with a minimum absolute value of \log_2 FC of 1.5 were denoted in red.

As an important aspect of microbiome function, CAZymes are responsible for the synthesis and breakdown of complex carbohydrates in the cat gut microbiome. Based on the protein sequence homology to the CAZy database, we detected 105 CAZy families, which were assigned to 51 GHs (glycoside hydrolases), 38 GTs (glycosyltransferases), 7 CBMs (carbohydrate-binding modules), 6 PLs (polysaccharide lyases), 2 CEs (carbohydrate esterases) and 1 AA (auxiliary activities). Overall, a larger number of CAZyme encoding genes were characterized in the normal gut microbiome compared to the obese microbiome, but the proportion of CAZymes in all annotated genes was higher in the obese microbiome. A total of 1.26% of the annotated genes in the obese cat gut microbiome were CAZyme encoding genes, which was significantly higher ($P = 0.01$, Mann-Whitney U test) than the proportion of CAZymes in the normal microbiome (1.19%; Figure 3.13A). When taxonomy abundances of CAZymes were measured by CPM (Counts Per Million mapped reads), Firmicutes and Bacteroidetes were most abundant in CAZymes, accounting for 77.5% of all CAZyme abundance (Figure 3.12B). In the obese cat gut microbiome, a significant increase of CAZyme abundance originated from Bacteroidetes was observed, whereas Firmicutes CAZymes were significantly decreased ($P < 0.01$; Figure 3.12B), which was consistent with the microbial composition changes at the phylum level (Figure 3.5E). The top six CAZyme-encoding genera accounted for 32.2% of all CAZyme encoding genes, including *Bacteroides* (8.15%), *Clostridium* (5.83%), *Prevotella* (5.04%), *Blautia* (5.01%), *Collinsella* (4.46%), and *Bifidobacterium* (3.67%; Figure 3.13B).

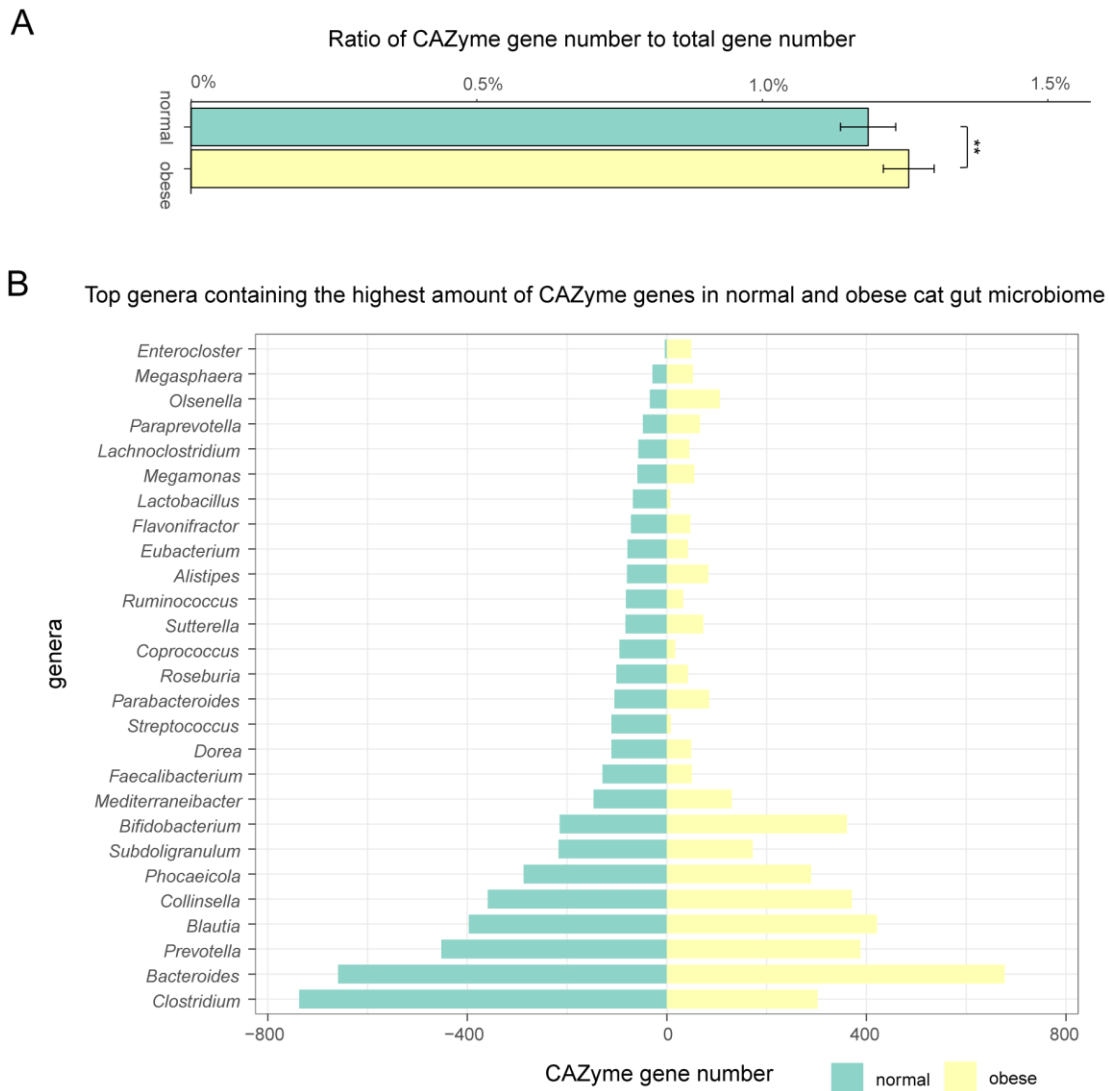


Figure 3.13 Numbers of CAZyme (Carbohydrate-Active Enzymes) genes identified in normal and obese cat gut microbiomes. **(A)** Percentage of CAZyme genes identified in normal (*green*) and obese (*yellow*) cat gut microbiomes. **(B)** Barplot of numbers of CAZyme encoding genes in top 20 most abundant genera in normal (*green*) and obese (*yellow*) cat gut microbiomes.

By comparing the relative abundance of CAZyme families between normal and obese microbiomes, we discovered that in the obese cat gut microbiome, Firmicutes were significantly less in GHs, GTs, CBMs, PLs, and CEs, whereas Bacteroidetes were significantly enriched for GHs, PLs, and CEs (Figure 3.12B). Actinobacteria were also higher in GHs, GTs, CBMs, and

CEs in the obese microbiome (Figure 3.12B), suggesting a potential contribution of the carbohydrate metabolism primarily in the obese microbiome. Among the 63 highly abundant CAZy families (CPM > 500), five enzymes had a \log_2 fold change of 1.5 or higher. GT25 ($\log_2FC = -1.62$) and CBM50 ($\log_2FC = -1.69$) were significantly decreased in obese cat gut microbiome (FDR < 0.05). Three glycoside hydrolases, GH28 ($\log_2FC = 3.47$), GH19 ($\log_2FC = 1.92$), and GH116 ($\log_2FC = 1.53$), were upregulated in the obese cat gut microbiome with marginal significance.

3.4 Discussion and conclusion

Discussion

Feline gut microbiota composition – similarity to canine and human microbiome and consistency between WGS and 16S rDNA data

To our best knowledge, we report here the first metagenomic assembly of the feline gut microbiome using whole-genome shotgun (WGS) metagenomic approaches. In normal lean cat gut microbiomes, Firmicutes, Bacteroidetes, Actinobacteria, Proteobacteria, and Fusobacteria were the top five most abundant phyla, which were also the top five phyla of the human and dog gut microbiome in the same order [388-390]. Compared to a previous 16S rDNA study of cat gut microbiome in 2017 [364], the taxonomy abundance quantified in this study has a high correlation when the top five phyla and the top 20 most abundant genera were examined, suggesting that the composition of the feline gut microbiome was stable in different cat populations under similar but slightly different standard diet (Mars Petcare diet with 39.8% protein, 12.5% fat, 38.3% carbohydrate, and 2.3% crude fiber was used in Fischer 2017). This

also serves as a proof of principle of our WGS metagenomic study.

The first cat gut microbiome contigs assembly and microbial gene catalog provided sequence references and information of sufficient samples size for future studies

In this study, we assembled 234 Gbp of high-quality microbial reads from a total of 16 metagenomes and generated a *de novo* assembly of the feline gut microbiome. The non-redundant contigs length was 961 Mbp in total, with 1.14 million predicted microbial genes. Rarefaction analyses found that both the number of bacterial species and microbial genes were >90% saturated when $n > 5$ samples were included, indicating that a sample size of $n = 6$ is sufficient in future WGS metagenomic analysis of cat gut microbiomes. A sample size larger than $n = 6$ would only have marginal benefit in identifying additional taxa. The result suggested that the sample size in this study ($n = 6$ for each group) is sufficient and the reference assembly with 16 metagenomes has excellent completeness. On average, 83% of the metagenomic reads were aligned to our reference assembly, which is comparable to the human gut microbiome reference genome [391]. Compared to the canine gut microbiome with 1.25 million predicted microbial genes [392], there were 9% fewer non-redundant genes in the cat gut microbiome. A total of 95.9% microbial genes in cat gut catalog had a phylum-level annotation, and genus/species level annotations were available for 68.9% and 62.7% of genes. The feline gut microbial gene catalog served as a comprehensive annotation set for functional studies of the microbiome.

Potential confounding factors in comparing normal vs. obese cat microbiomes

In humans and mice, sex, age, and diet can significantly affect the gut microbiome compositions.

The gut microbiota associations with feline obesity had been studied in the context of age, diet, neutering, and diabetic status [349, 360, 364, 365]. In all four independent studies, obese status was discovered to influence the cat gut microbiome, but no significant effects of age, sex, diet, or neutering status were detected in previous feline 16S rDNA studies by multiple research groups. In a 2016 study using 16S rDNA PCR analysis of fecal samples from shelter cats, no significant associations were identified between bacterial groups and sex or neutering status [349]. The cats were on various diets and of diverse age groups (16 cats between 10-week and 1-year, 41 between 1-year and 5-year, and 20 of unknown age). Another study in 2019 contrasting the microbiomes of diabetic and control cats found no effect of breed, sex, or age on the gut microbial communities [365]. In a 2020 study comparing lean and overweight cats, no significant differences were discovered in fecal microbiomes due to sex or age or different diet groups [360]. Another study published in 2017 also found no significant effects of sex or age on cat gut microbiome in adult cats [364]. In this study, the obese group consists of eight 6-year-old male cats. For the normal body weight group, we enrolled three 6-year-old cats to match the obese group; two 4-month-old cats and three 8-month-old cats were also included to make it a balanced comparison. No significant differences due to age or sex were detected according to permutational multivariate analysis of variance, which was consistent with all previous 16S rDNA studies [349, 360, 364, 365]. The normal and obese cats were on two different brands of standard adult cat food with similar nutritional compositions. There could be subtle gut microbiome changes due to the slight differences in the diet, but none of the minor variations between the diet are sufficient to explain the dramatic microbiome composition shifts observed between normal and obese groups. Consistent with this interpretation, the previous 16S rDNA studies confirmed that diets with similar nutrient ingredients did not affect the cat gut microbiota

[349, 360], and cross-comparison between our normal cat group and the Fischer 2017 16S rDNA study revealed highly correlated microbial genera composition (Figure 3.6B), despite the differences in diets. Therefore, it is extremely unlikely standard diets with similar nutrients will cause hundred-fold changes in bacterial composition observed in our study, but it is still a potential limitation of this research and might decrease the statistical power. Future studies that evaluate the feline microbiome using metagenomics sequencing should consider diet as a potential variable when interpreting their findings.

Signatures of obese cat gut microbiota – what did we learn at the microbial diversity level?

Since the gut microbiota composition is directly relevant to the host's digestion and energy metabolism, thorough identification of gut microbiome signatures is critical to define the medical condition of feline obesity in terms of microbiota dysbiosis. Significant differences in the gut microbiome have been reported in obese compared to lean cats using PCA analysis [349], but the qPCR approach cannot determine the microbial diversity. Another 16S rDNA metagenomic study of lean neutered/intact and obese cats identified a lower alpha diversity in lean neutered cats, and no significant grouping was detected when beta diversity was analyzed [364]. In this study, we discovered a significant reduction in alpha diversity at both the genus and species levels in the obese microbiome, suggesting dramatically reduced microbial complexity, which often reflects a state of dysbiosis in the gut microbiome. The beta-diversity analysis also revealed a distinct separation of the normal and obese cat microbiomes. In addition to the taxonomy level, the reduced diversity was also observed at the gene level, in which the number of microbial genes predicted in the obese microbiome (598,349) was significantly fewer than the normal cat microbiome (912,251). Another study of the gut microbiome of diabetic cats discovered

decreased gene mark richness in DM (diabetes mellitus) cats (FDR = 0.04) [365]. The obese cats in this study also demonstrated significant insulin resistance, and the reduction in gene richness was in the same direction as the 2019 study [365].

Shift from Firmicutes to Bacteroidetes in obese cat gut microbiota is in the opposite direction compared to human and mouse gut microbiomes

Phylum-level abundance changes are directly relevant to obesity. Previous studies in humans and rodents found that the ratio of the two most dominant phyla, the gram-positive Firmicutes over the gram-negative Bacteroidetes, was elevated in obese individuals and may be a hallmark of obesity [346, 393-395]. The validity of this potential marker was questioned subsequently by contradictory results [396-400], but this metric was still worth investigating. Interestingly, we observed an inverse pattern compared to what was reported in humans and rodents, with a significantly decreased Firmicutes-to-Bacteroidetes ratio in the obese cat gut microbiome. Bacteroidetes replaced Firmicutes as the most dominant phylum in obese cat gut microbiota. A similar pattern was also reported in a cat 16S rDNA study, in which lean neutered cats had a greater abundance of Firmicutes and a lower abundance of Bacteroidetes compared to obese neutered cats [364]. Based on the current knowledge, this dramatic shift in the F/B ratio is likely to be unique in cats, and may serve as an indicator of microbiome health in obese and overweight cats.

Signatures of obese cat gut microbiota – what did we learn at the microbial species level?

Previous 16S rDNA studies of the link between the gut microbiome and feline obesity were extremely informative at the phylum and genus levels, but failed to identify any individual

bacteria species associated with obesity. Thanks to the resolution enabled by the WGS metagenomic sequencing, we identified hundreds of bacterial species with a significantly altered abundance between normal and obese gut microbiomes. Since many of these significant species may not be biologically relevant due to low abundances, we focused on high abundance (>0.5%) microbial species with high fold change (>16) between obese and normal cat gut microbiomes (HAHFC species). Among the six HAHFC species, *Bifidobacterium adolescentis*, *Dialister sp. CAG:486*, *Olsenella provencensis*, and *Campylobacter upsaliensis* were significantly enriched in the obese cat gut microbiome, whereas *Erysipelotrichaceae bacterium AU001MAG* and *Phascolarctobacterium succinatutens* were depleted in the obese cat gut microbiome. The significant changes in these species were validated using qPCR experiments. At the genus level, *Bifidobacterium* and *Dialister* were identified to be increased in obese/overweight compared to lean cats (FDR = 0.04 for *Dialister* and FDR < 0.0001 for *Bifidobacterium*) in a 16S rDNA study of obese cat gut microbiota [365]. Our research has identified the driving microbial species in these two genera, which were the most featured genera in the obese cat gut microbiota discovered in this study. The family Erysipelotrichaceae was discovered to be significantly decreased (>5-fold) in obese women compared to healthy control individuals [401], which is the same direction as our results on the newly discovered species *Erysipelotrichaceae bacterium AU001MAG* in this family, suggesting it may play an important role in obesity. *Olsenella provencensis* and *Campylobacter upsaliensis* were not reported to be associated with obesity in any other species. Our findings of key bacterial community alterations at the species level will inform the development of probiotic treatment for weight loss therapy in cats.

Obesity etiology from cat to human – shared significant bacterial genera between human

and cat gut microbiota provide potential translational value

In a Mayo Clinic study published in 2017, 26 participants (18-65 years) were enrolled in the Mayo Clinic Obesity Treatment Research Program, and the body weight was measured at the beginning and after three months of this program. At least 5% weight loss after 3 months was defined as success [402]. Gut microbiome composition was compared between the success and failure groups. Two genera were identified with significant changes according to the LEfSe analysis (LDA score > 2), and the remaining ones were non-significant [402]. Increased *Phascolarctobacterium* abundance was associated with success ($P = 0.008$), and increased *Dialister* abundance was associated with failure of weight loss ($P = 0.030$) [402]. Strikingly, species in these two genera were among the six HAHFC species identified in this study:

Dialister sp. CAG486 was the most enriched bacterial species in the obese cat microbiome with 1500-fold increase; *Phascolarctobacterium succinatutens* was highly abundant in the normal cat gut microbiome, but almost missing in the obese cat gut microbiome with 400-fold reduction in abundance. Based on the human gut microbiome study on weight loss outcomes [402] and our results in obese cats, high levels of *Dialister* may prevent body weight loss, and *Phascolarctobacterium* was associated with lean microbiomes by promoting body weight loss.

***Bifidobacterium* in feline obesity – is *Bifidobacterium* a good choice for probiotic health supplement in cats?**

Bifidobacterium is believed to be among the first members of microbes colonizing the human gastrointestinal tract since the infant stage. They were known to positively impact the host gut health [403]. Therefore, *Bifidobacterium* are often used as probiotics to reduce gut problems such as diarrhea or constipation, and they were also shown to have impact on obesity. In rats, *B.*

adolescentis supplementation can reduce visceral fat accumulation [404]. In mouse models of high-fat diet-induced NAFLD (non-alcoholic fatty liver disease) [405] and colitis [406], *B. adolescentis* were shown to ameliorate the disease symptoms. Interestingly, *B. adolescentis* was identified as a HAHFC species in this study, with a 60-fold increase in the obese cat gut microbiome, which was in the opposite direction compared to previous rodent studies. In addition to *B. adolescentis*, we found that five other *Bifidobacterium* species/subspecies were also significantly increased in the obese cat microbiome. The effects on body weight were reported to be strain-dependent: *B. adolescentis* strains isolated from the feces of elderly human donors (Z25, 17_3, and 2016_7_2) decreased the body weight or weight gain in mice, while the strain isolated from the human newborn (N4_N3) increased the body weight in mice [407]. In a recent weight management and microbiome study, cats on a high-protein, low-carbohydrate diet had decreased *Bifidobacterium* level ($P = 0.002$) compared to animals on the control diet, suggesting a lower level of *Bifidobacterium* is beneficial to body weight loss [360]. Taken together, higher levels of *Bifidobacterium* were associated with obesity in cats, which was different from the human and rodent studies. We need to be cautious when designing probiotic formula for cat weight management.

***Erysipelotrichaceae* bacterium and *Phascolarctobacterium* – beneficial bacteria for feline weight loss?**

A previously uncharacterized genus *Erysipelotrichaceae* bacterium was largely depleted in obese cat gut microbiota (from 0.383% to <0.001%, FDR = 0.012), which was the most decreased species in the obese cat microbiome. Similarly, the abundance of *Phascolarctobacterium* dropped from 0.078% in normal cats to <0.001% in obese cats. We validated the dramatic

decreases in both *Erysipelotrichaceae* and *Phascolarctobacterium* by qPCR. Moreover, the increased abundance of *Phascolarctobacterium* was proved to be associated with successful weight loss in the Mayo Clinic study [402]. These two species deserve further consideration as potential probiotics for weight loss.

Microbiome signatures in feline obesity – obese cat microbiome index *C. ups/C. hel* and a qPCR panel to detect obesity-associated microbiomes

We detected 20 species in the genus of *Campylobacter* in the cat gut microbiome. A pathogenic species, *Campylobacter jejuni*, can colonize obese (*ob/ob*) mice with oral inoculation, and the *ob/ob* mice were extremely sensitive to *C. jejuni* infection [408]. However, *C. jejuni* had low abundance in this study, and there was no significant difference between normal and obese cats. Notably, *C. upsaliensis* and *C. helveticus*, which were not linked with obesity before, were discovered to have significant abundance changes in the obese cat gut microbiome in the opposite direction. As an HAHFC-obese species, *C. upsaliensis* was almost absent in the normal microbiome (0.02%) but accounted for 0.5% in the obese cat gut microbiome. In contrast, *C. helveticus*, was extremely low in abundance in the obese microbiome (0.02%), but with a 12-fold increase in the normal microbiome. This inverse pattern in the normal vs. obese microbiome was validated by qPCR, and the relative ratio of the two species had a much-improved discriminative power between obese and normal individuals. Therefore, we proposed to define the relative abundance of *C. upsaliensis* over *C. helveticus* as an obese cat microbiome index.

To investigate the microbiome features of feline obesity and define obesity-associated microbiomes, a total of eight microbial species were selected as an indicator panel for dysbiosis

in the obese cat gut microbiome. *Prevotella* is the most abundant genus in cat gut microbiome, according to 16S studies [364] and this WGS metagenomic study. At the microbial species level, we found that *Prevotella copri* is the most abundant species in the cat gut microbiome, accounting for 12.9% of the entire microbiota in normal cats. We also observed a potential trend of increasing abundance in the obese cat gut microbiome (19.6% abundance), but it was not statistically significant ($P = 0.44$ and $FDR = 0.67$). Interestingly, *Prevotella copri* has a significantly higher abundance in fat pigs, and was shown to promote host chronic inflammation, intestinal permeability, lipogenesis, and fat accumulation through the TLR4 and mTOR signaling pathways [409]. Our result showed a similar trend, but it did not reach statistical significance. *Prevotella copri* was selected as the control species for the indicator panel because of its high abundance. The panel also includes four highly enriched species in obese cat gut microbiota (*Bifidobacterium adolescentis*, *Olsenella provencensis*, *Dialister sp. CAG:486*, and *Campylobacter upsaliensis*), and three significantly depleted species in obese cat gut microbiota (*Phascolarcobacterium succinatutens*, *Erysipelotrichaceae bacterium AU001MAG*, and *Campylobacter helveticus*). This panel will serve as a cost-effective method to examine the microbiome correlates of feline obesity and can be applied in a much larger sample size.

Fatty acids biosynthesis pathways are enriched in obesity-associated microbiota

We discovered that fatty acid biosynthesis pathways were significantly overrepresented in the obese cat gut microbiome compared to normal cats, including biosynthesis and elongation of saturated fatty acids (SFAs). SFAs can add to the risk of cardiovascular disease by increasing the low-density lipoprotein (LDL) cholesterol levels in the serum. A study has found stearic acid-rich fat can raise the LDL/HDL (high-density lipoprotein) ratio [410]. These SFAs generated by

gut microbiota may contribute to lipid dyscrasia in obese and overweight cats [411]. One limitation of our results is that they were merely correlations, and we do not know whether the shifted metabolic pathways caused the obesity phenotype, or the obese environment drove the microbiome changes. Further studies are needed to disentangle the causal relationships.

Significant changes in carbohydrate metabolism on the obese cat gut microbiota

The metabolic pathway analyses suggested that increased carbohydrate metabolism in the gut microbiome may be associated with feline obesity. The carbohydrate biosynthesis pathway of certain sugar, including CMP-legionamate, was significantly overrepresented in the obese cat gut microbiome. A human study contrasting long-term healthy vs. unhealthy diet discovered that increased degradation (or reduced biosynthesis) of CMP-legionamate was associated with the healthy diet [412], which is consistent with the findings in this feline study. Compared to normal cats, the obese cat gut microbiome had a higher proportion of CAZymes. The elevated CAZymes were primarily driven by Bacteroidetes and Actinobacteria. When the individual CAZyme families were investigated, we discovered a significant decrease in the carbohydrate-binding module CBM50 and Glycosyltransferase GT25 in obese cat gut microbiota. GT25 belongs to GlycosylTransferase Family, usually acts as lipopolysaccharide β -1,4-galactosyltransferase, β -1,3-glucosyltransferase, and β -1,2-glucosyltransferase. CBM50s, also known as LysM domains, mainly bind to the N-acetylglucosamine residues in bacterial peptidoglycans and in chitin. Three glycoside hydrolases, GH28, GH19, and GH116, were enriched in the obese cat gut microbiota. These changes in different CAZyme categories may define the microbiome functional differences in carbohydrate metabolism.

Conclusions

Through comprehensive analyses of normal and obese cat gut microbiota using whole-genome shotgun metagenomic sequencing, we report the first reference contig assembly of the cat gut microbiome and its first microbial gene catalog. This contig assembly and gene catalog provide both the reference for cat metagenome study and the essential feline microbiome toolkit for comparative analysis across mammalian microbiomes. Obese cat gut microbiome has distinct patterns compared to cats with normal body weight, including significant reductions in microbial diversity and gene numbers, a dramatic shift in phylum-level composition from Firmicutes-dominant to Bacteroides-dominant microbiome, and a number of abundant bacterial species with extremely high-fold changes ($>0.5\%$ in composition with >16 -fold change). We identified the gut microbiome profiles associated with lean cat health, and a panel of marker species that indicate dysbiosis in obese cat microbiota, which may negatively impact feline health. The findings from this study will be critical to inform weight management strategies for obese cats, including evaluations of specific diet formulas that alter the microbiome composition, the development of prebiotics and probiotics that promote the increase of beneficial species and the depletion of obesity-associated species, as well as potential microbiome transplantation therapies. Bacteria identified in our study were also shown to affect the weight loss success in human patients, suggesting translational potential in human obesity.

CHAPTER 4

Metagenomic analysis reveals associations between memory performance and *Bifidobacterium pseudolongum* abundance in canine gut microbiome

4.1 Introduction

Working memory in non-human animals is defined as short-term memory for stimuli within a specific experimental trial or session [413, 414]. Animal working memory lasts from a couple of seconds to a few minutes, with dogs displaying an estimated memory performance half-life of 71 seconds [415]. A two-timepoint study of puppy (8-week) and adult dog (21-month) cognitive traits suggested that memory improved with age, but puppy memory performance did not predict the adult performance [416]. In addition, memory was less heritable ($h^2 = 0.17$) compared to other cognitive traits such as inhibitory control in dogs ($h^2 = 0.70$) [417]. Rearing environment, including diet and socialization, may affect canine memory development and performance. Training can improve odor memory in working dogs [418, 419]. Collectively, these reports suggest plasticity in canine memory performance, suggesting potential roles of nongenetic factors.

In mammals, behavior-related traits are heavily influenced by the gut microbiota [420, 421] through the microbiota–gut–brain axis [422]. Gut microbiota can produce neurotransmitters, impact the central nervous system and affect human cognition and behavior [423], especially in stress-related psychiatric diseases, including depression, anxiety, and even autism [420, 424, 425]. Recent metagenomic studies using 16S rDNA ampliconic sequencing in dogs showed correlation between aggression and microbiome composition in pit bull type rescue dogs [426]

and mixed breeds [427]. A recent study in pet dogs discovered that improved memory was associated with a lower abundance of Actinobacteria, whereas none of the lower taxonomy levels were significant [428]. The Kubinyi et al study provided some insights into the link between gut microbiome and memory. However, studies using client-owned dogs only detected phylum-level differences and suffer from confounding factors such as variable age, diet, breeds, housing, and body conditions, which substantially decreases the statistical power.

To address this, we enrolled four litters of dogs born, reared, and trained at the Auburn University College of Veterinary Medicine's Canine Performance Sciences Program (AUCVM-CPS) colony, a research and breeding program for purpose-bred detection dogs, to study the relationship between the gut microbiome and memory performance across three timepoints. To obtain the best resolution of the gut microbiome, we performed whole-genome shotgun (WGS) metagenomic sequencing from fecal samples collected near the three timepoints of memory test. Our study represents the most comprehensive and systematic assessment of the microbiome correlates of canine memory performance.

4.2 Materials and methods

4.2.1 Study subject and ethics statement

Dogs (11 females and 16 males) enrolled in this study were born, raised, and maintained at the Auburn University College of Veterinary Medicine Canine Performance Sciences program under the same diet, training, and medical care in a controlled environment (see Table 4.1). All experimental animal protocols were approved by the Auburn University Institutional Animal Care and Use Committee (approved protocol number PRN-2019-3564).

Table 4.1 Information of 27 dogs enrolled in this study.

Dog ID	Breed	Sex	Date of Birth	litter	Body condition score
2019041	Labrador Retriever	Male	3/14/2019	A	5
2019042	Labrador Retriever	Male	3/14/2019	A	5
2019044	Labrador Retriever	Female	3/14/2019	A	5
2019045	Labrador Retriever	Male	3/14/2019	A	5
2019046	Labrador Retriever	Female	3/14/2019	A	5
2019048	Labrador Retriever	Female	3/14/2019	A	5
2019049	Labrador Retriever	Male	3/27/2019	B	5
2019050	Labrador Retriever	Male	3/27/2019	B	5
2019051	Labrador Retriever	Female	3/27/2019	B	5
2019053	Labrador Retriever x German Wire Haired Pointer	Female	7/8/2019	C	5
2019054	Labrador Retriever x German Wire Haired Pointer	Female	7/8/2019	C	5
2019055	Labrador Retriever x German Wire Haired Pointer	Female	7/8/2019	C	5
2019056	Labrador Retriever x German Wire Haired Pointer	Female	7/8/2019	C	5
2019057	Labrador Retriever x German Wire Haired Pointer	Male	7/8/2019	C	5
2019059	Labrador Retriever x German Wire Haired Pointer	Male	7/8/2019	C	5
2019060	Labrador Retriever x German Wire Haired Pointer	Male	7/8/2019	C	5
2019061	Labrador Retriever x German Wire Haired Pointer	Male	7/8/2019	C	5
2019062	Labrador Retriever x German Wire Haired Pointer	Male	7/8/2019	C	5
2019063	Labrador Retriever x German Wire Haired Pointer	Male	7/8/2019	C	5
2019064	Labrador Retriever x German Wire Haired Pointer	Male	7/8/2019	C	5
2019065	Labrador Retriever	Male	7/24/2019	D	5
2019066	Labrador Retriever	Male	7/24/2019	D	5
2019067	Labrador Retriever	Male	7/24/2019	D	5
2019068	Labrador Retriever	Female	7/24/2019	D	5
2019069	Labrador Retriever	Female	7/24/2019	D	5
2019070	Labrador Retriever	Female	7/24/2019	D	5
2019071	Labrador Retriever	Male	7/24/2019	D	5

4.2.2 Phenotypic measurement and analysis

Working memory tests were performed three times for 27 dogs at the puppy stage (3.0–3.5 months), juvenile stage (5.2–6.2 months), and young adult stage (12.8–16.0 months; see Table 4.2).

Table 4.2 Short-term memory test scores for 27 dogs at the puppy stage (3.0~3.5 month), juvenile stage (5.2~6.2 month), and young adult stage (12.8~16.0 month).

Dog ID	DOB	Sex	Litter	Test Date	# correct in 3 trials, 10-s	# correct in 3 trials, 40-s	# correct in all 6 trials
2019041	3/14/2019	M	A	6/20/2019	1	1	2
2019042	3/14/2019	M	A	6/20/2019	1	0	1
2019044	3/14/2019	F	A	6/20/2019	1	2	3
2019045	3/14/2019	M	A	6/20/2019	2	0	2
2019046	3/14/2019	F	A	6/20/2019	0	2	2
2019048	3/14/2019	F	A	6/20/2019	2	2	4
2019049	3/27/2019	M	B	6/20/2019	3	3	6
2019050	3/27/2019	M	B	6/20/2019	2	2	4
2019051	3/27/2019	F	B	6/20/2019	0	2	2
2019053	7/8/2019	F	C	10/10/2019	2	1	3
2019054	7/8/2019	F	C	10/10/2019	2	3	5
2019055	7/8/2019	F	C	10/10/2019	2	1	3
2019056	7/8/2019	F	C	10/10/2019	1	2	3
2019057	7/8/2019	M	C	10/10/2019	3	2	5
2019059	7/8/2019	M	C	10/10/2019	2	1	3
2019060	7/8/2019	M	C	10/10/2019	3	2	5
2019061	7/8/2019	M	C	10/10/2019	3	1	4
2019062	7/8/2019	M	C	10/10/2019	2	2	4
2019063	7/8/2019	M	C	10/10/2019	2	1	3
2019064	7/8/2019	M	C	10/10/2019	2	3	5
2019065	7/24/2019	M	D	10/31/2019	2	1	3
2019066	7/24/2019	M	D	10/31/2019	3	2	5
2019067	7/24/2019	M	D	10/31/2019	2	2	4
2019068	7/24/2019	F	D	10/31/2019	1	2	3
2019069	7/24/2019	F	D	10/31/2019	3	3	6
2019070	7/24/2019	F	D	10/31/2019	2	2	4
2019071	7/24/2019	M	D	10/31/2019	3	2	5

Table 4.2 Continued.

Dog ID	DOB	Sex	Litter	Test Date	# correct in 3 trials, 10-s	# correct in 3 trials, 40-s	# correct in all 6 trials
2019041	3/14/2019	M	A	8/20/2019	3	2	5
2019042	3/14/2019	M	A	8/20/2019	2	2	4
2019044	3/14/2019	F	A	8/20/2019	1	1	2
2019045	3/14/2019	M	A	8/20/2019	3	1	4
2019046	3/14/2019	F	A	8/20/2019	1	2	3
2019048	3/14/2019	F	A	8/20/2019	1	2	3
2019049	3/27/2019	M	B	8/20/2019	3	2	5
2019050	3/27/2019	M	B	8/20/2019	3	1	4
2019051	3/27/2019	F	B	8/20/2019	3	2	5
2019053	7/8/2019	F	C	12/5/2019	2	3	5
2019054	7/8/2019	F	C	12/5/2019	2	1	3
2019055	7/8/2019	F	C	12/5/2019	1	1	2
2019056	7/8/2019	F	C	12/5/2019	2	2	4
2019057	7/8/2019	M	C	12/5/2019	3	1	4
2019059	7/8/2019	M	C	12/5/2019	1	1	2
2019060	7/8/2019	M	C	12/5/2019	3	1	4
2019061	7/8/2019	M	C	12/5/2019	1	3	4
2019062	7/8/2019	M	C	12/5/2019	1	2	3
2019063	7/8/2019	M	C	12/5/2019	2	2	4
2019064	7/8/2019	M	C	12/5/2019	2	1	3
2019065	7/24/2019	M	D	1/14/2020	1	2	3
2019066	7/24/2019	M	D	1/14/2020	3	1	4
2019067	7/24/2019	M	D	1/14/2020	2	2	4
2019068	7/24/2019	F	D	1/14/2020	1	2	3
2019069	7/24/2019	F	D	1/14/2020	3	3	6
2019070	7/24/2019	F	D	1/14/2020	1	3	4
2019071	7/24/2019	M	D	1/14/2020	3	2	5

Table 4.2 Continued.

Dog ID	DOB	Sex	Litter	Test Date	# correct in 3 trials, 10-s	# correct in 3 trials, 40-s	# correct in all 6 trials
2019041	3/14/2019	M	A	6/3/2020	3	2	5
2019042	3/14/2019	M	A	6/3/2020	2	2	4
2019044	3/14/2019	F	A	6/3/2020	3	3	6
2019045	3/14/2019	M	A	6/3/2020	2	2	4
2019046	3/14/2019	F	A	6/3/2020	2	1	3
2019048	3/14/2019	F	A	6/3/2020	1	0	1
2019049	3/27/2019	M	B	6/3/2020	3	3	6
2019050	3/27/2019	M	B	6/3/2020	3	3	6
2019051	3/27/2019	F	B	6/3/2020	2	3	5
2019053	7/8/2019	F	C	6/30/2020	2	1	3
2019054	7/8/2019	F	C	6/30/2020	2	3	5
2019055	7/8/2019	F	C	N/A	N/A	N/A	N/A
2019056	7/8/2019	F	C	6/30/2020	2	2	4
2019057	7/8/2019	M	C	6/30/2020	3	3	6
2019059	7/8/2019	M	C	6/30/2020	1	3	4
2019060	7/8/2019	M	C	6/30/2020	1	0	1
2019061	7/8/2019	M	C	6/30/2020	3	3	6
2019062	7/8/2019	M	C	6/30/2020	2	1	3
2019063	7/8/2019	M	C	6/30/2020	1	1	2
2019064	7/24/2019	M	C	6/30/2020	1	2	3
2019065	7/24/2019	M	D	8/4/2020	2	2	4
2019066	7/24/2019	M	D	8/4/2020	3	2	5
2019067	7/24/2019	M	D	8/4/2020	3	2	5
2019068	7/24/2019	F	D	8/4/2020	2	2	4
2019069	7/24/2019	F	D	8/4/2020	3	1	4
2019070	7/24/2019	F	D	8/4/2020	2	2	4
2019071	3/14/2019	M	D	8/4/2020	2	3	5

Dogs' ability to locate a visually displaced reward (a ball) after delays of 10 or 40 s was measured using methods similar to Bray et al. [429], with the exception that non-mnemonic cues were controlled during the delay[430]. On each trial, the handler brought the dog to the starting position. The experimenter stood 2 m away, facing the dog, in the center of two opaque plastic cups (12 × 12 × 14 cm) placed upside down, 2 m apart (Figure 4.1A).

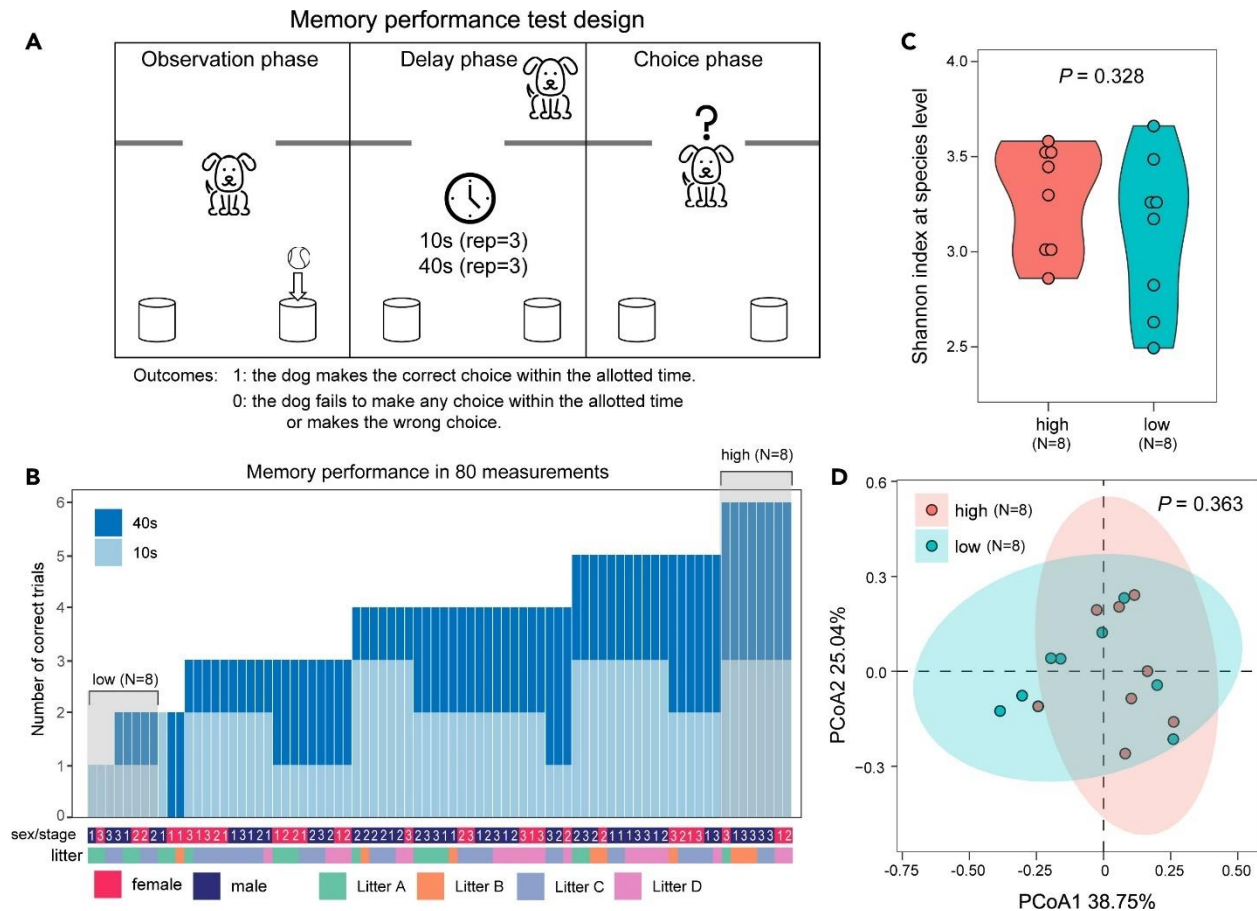


Figure 4.1 Memory performance in detection dogs at three developmental timepoints. (A) Schematic illustration of the working memory test. (B) Bar plots display the number of correct trials across 80 measurements. Dark blue bars represent correct trials after a 40-s delay interval, while light blue bars represent correct trials after a 10-s delay interval. Bars within gray-shaded boxes were selected for analysis among dogs that scored high and low on the memory test. (C) Violin plots illustrating microbial diversity (measured by Shannon index) for the high- and low-performance groups at the species level. P -value assessed by Mann-Whitney U test. (D) Principal Coordinates Analysis (PCoA) plots of beta diversity between the high and low memory performance groups are generated based on the Bray-Curtis distance. P -value assessed by PERMANOVA test (Permutational multivariate analysis of variance).

To begin the trial, the experimenter called the dog’s name, held up the reward, placed it underneath one of the two containers, and then stepped back and turned to face the back wall. Once the reward was hidden, the handler removed the dog from the room to the hallway for the duration of the delay. At the conclusion of the delay, the handler led the dog back to the starting position in the room and then released the dog, allowing 15 s to make a choice. Once the dog

chose a container (defined as the dog's snout coming within 5 cm of the container), the experimenter lifted the cup to reveal its contents. After either making a choice or 15 s lapsed, the handler led the dog back to the starting position to begin the next trial. Six trials were conducted, with a 10-s delay on trials 1–3, and a 40-s delay on trials 4–6. The number of correct trials was recorded as the overall memory score (OMS). The position of the reward (left or right) was counterbalanced throughout the session. If a dog scored more than 50% correct, an odor control test was conducted at the conclusion of the session to ensure that dogs were not locating the reward using odor cues. The odor control test was identical to the test trials, except that dogs did not witness the baiting of the container (i.e., the container was pre-baited when the dog was out of the room). A camera (GoPro Hero Session) positioned in the corner of the room recorded all trials and was used for post-session inter-reliability coding.

4.2.3 Statistical analysis

The effects of age, litter, sex, and breed on OMS were assessed using the Mann-Whitney U test [431] and the Kruskal-Wallis test [432] in the R software [433]. A *p*-value of 0.05 represents a statistically significant difference. Mean and standard deviation (SD) were plotted in Figure 4.2A. We simulated the distribution of OMS under a null assumption that each dog makes a random choice during the memory tests, and whether the observed OMS distribution in this experience deviates from the null (no memory) was assessed by the non-parametric Kolmogorov-Smirnov test [434] implemented in R.

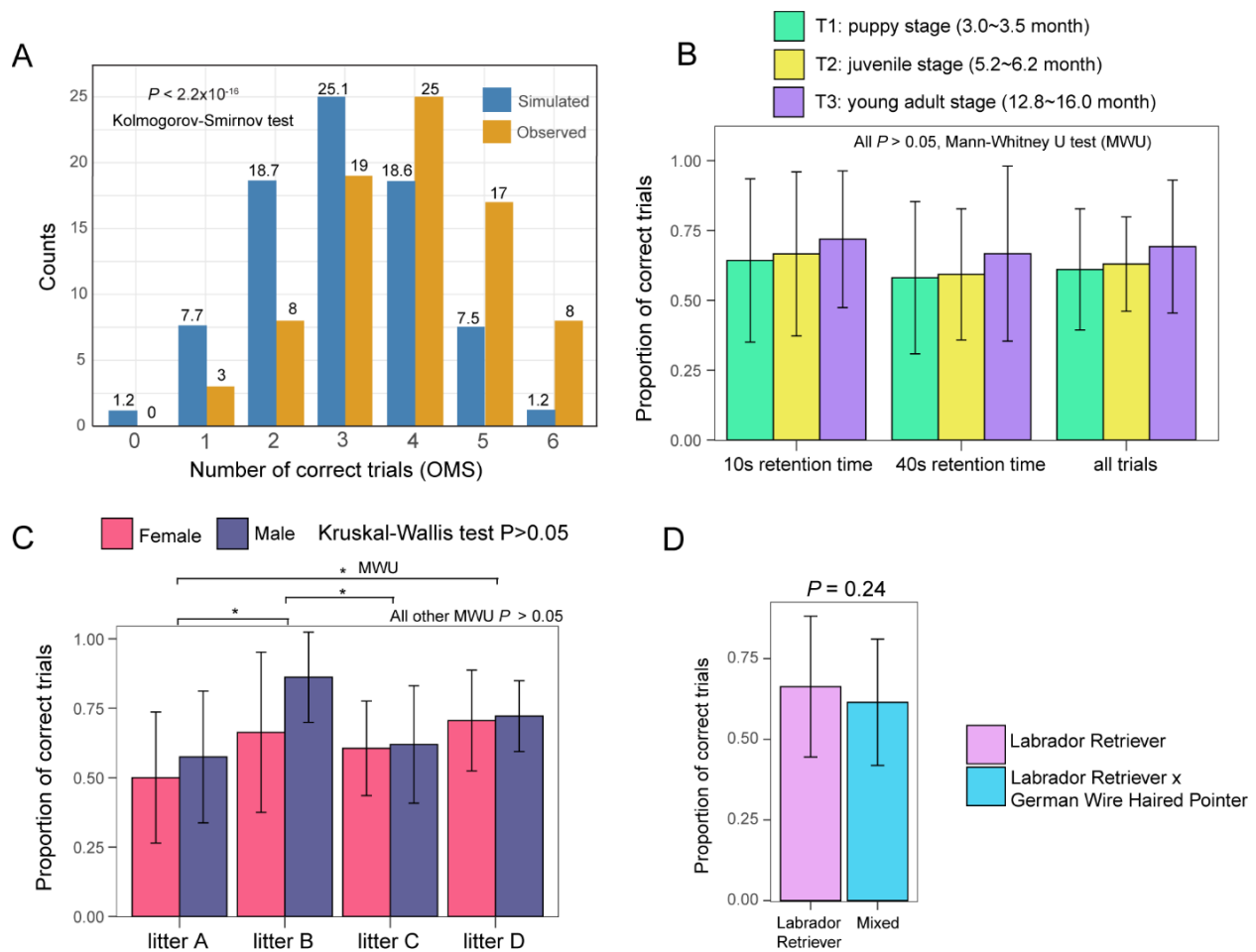


Figure 4.2 Distribution of overall memory score and effect of growth stage, sex, litter, and breed on the canine memory performance. (A) Barplot of the distribution of observed (*orange*) and simulated (*blue*) memory performance score measurements. The counts (y-axis) were plotted for each OMS category (x-axis). A simulation was performed in R, assuming a 50% chance of selecting the correct reward for each trial (N=1000 simulations). Non-parametric Kolmogorov-Smirnov test was performed to compare the two distributions. (B) Barplot of memory performance score measurements conducted at T1 (puppy stage; *Green*), T2 (juvenile stage; *Yellow*), and T3 (young adult stage; *Purple*). Statistical significance was determined by the Mann-Whitney U test. (C) Barplot of memory performance scores across four litters and the two sexes. Both the Kruskal-Wallis test and pairwise Mann-Whitney U tests were performed to determine the statistical significance. (D) Barplot of memory performance scores between the two breeds enrolled in this study: purebred Labrador Retrievers and Labrador Retrievers crossed with German Wire-Haired Pointer.

4.2.4 Fecal sample collection, microbial DNA extraction, and quality control

Fecal samples were collected on the memory test day or a few days apart (N = 10 days average), by putting a sterile P1000 pipettor tip (upside-down) into the feces immediately after the dogs

defecated. The fecal samples were placed in sterile 1.5mL Eppendorf tubes and stored immediately in -80°C freezer. For microbial DNA purification, ~ 200 mg fecal sample was homogenized by the PowerLyzer24 instrument (Qiagen, Germantown, MD, USA) in bead-containing tubes provided in the AllPrep PowerFecal DNA/RNA kit (Qiagen, Germantown, MD, USA), and DNA samples were extracted according to the manufacturer's protocol. DNA concentrations were measured on a Qubit Fluorometer (Invitrogen, Carlsbad, CA, USA), and A260/A280 absorption ratios were assessed using a NanoDrop One C Microvolume Spectrophotometer (Thermo Scientific, Waltham, MA, USA). The size distribution was checked on TapeStation 4200 using Genomic ScreenTape (Agilent Technologies, Santa Clara, CA, USA).

4.2.5 Whole-genome shotgun (WGS) metagenomic library preparation and sequencing

To construct the WGS metagenomic library, 500 ng of extracted microbial DNA was used as input for each sample. The DNA samples were first fragmented to a target size of 550 bp using the M220 Focused-ultrasonicator (Covaris, Woburn, MA, USA). Subsequently, the sequencing library constructions were performed using NEBNext Ultra II DNA Library Prep Kit for Illumina (New England Biolabs, Ipswich, MA, USA), along with adaptors and primers provided by NEBNext Multiplex Oligos for Illumina (Dual Index Primers Set 1 and Set 2). The final library concentrations were measured by Qubit 3.0 Fluorometer (Invitrogen, Carlsbad, CA, USA), and size distributions were checked using TapeStation 4200 System with the D1000 ScreenTape (Agilent Technologies, Santa Clara, CA, USA). Finally, the pooled library was sent for sequencing on an Illumina NovaSeq6000 machine at 150-bp paired-end mode at Novogene (Novogene Corporation Inc., Sacramento, CA, USA) to achieve an average yield of 64 million reads per sample.

4.2.6 Metagenome data processing, alignment, and taxonomy annotation

For the 27 dogs included in our study, we obtained a total of 1.8 billion, 1.8 billion, and 1.5 billion Illumina reads, respectively, at the puppy stage, the juvenile stage, and the young adult stage (Table 4.3). The adapter reads and low-quality bases were trimmed by Trimmomatic version 0.36 [435]. The host-contaminated sequences were removed by mapping the trimmed reads to the dog reference genome (CanFam3.1) using Burrows-Wheeler Aligner (BWA) version 0.7.17-r1188 [436]. The viral reads and rRNA sequences were deleted in the same way. The filtered reads were then aligned to the canine gut microbiome reference contigs (accession number JARCCX000000000), which were fully annotated using Kaiju version 1.7.3 [437] against the NCBI-NR database. The read counts were extracted using SAMtools version 1.6 [438] and BEDTools version 2.30.0 [248]. Taxonomic abundances were normalized in a relative abundance format on a scale of 0 to 1 for subsequent metagenomic analysis.

Table 4.3 Whole-genome shotgun metagenomic sequencing yield and mapping percentages to the canine microbiome contigs.

Dog ID	Time point	number of mapped reads after host removal	% mapped reads	Dog ID	Time point	number of mapped reads after host removal	% mapped reads
2019041	TP1	23,047,140	98.18%	2019057	TP2	45,885,206	99.30%
2019042	TP1	108,270,774	98.76%	2019059	TP2	52,039,920	98.29%
2019044	TP1	54,615,022	98.97%	2019060	TP2	59,515,922	99.29%
2019045	TP1	76,179,112	98.88%	2019061	TP2	38,750,064	99.22%
2019046	TP1	90,406,470	98.92%	2019062	TP2	60,527,504	98.45%
2019048	TP1	74,005,086	99.28%	2019063	TP2	230,396,568	98.62%
2019049	TP1	64,300,056	98.63%	2019064	TP2	53,049,088	97.29%
2019050	TP1	44,443,476	97.42%	2019065	TP2	43,153,532	98.82%
2019051	TP1	55,041,914	99.17%	2019066	TP2	37,567,050	98.34%
2019053	TP1	103,611,990	95.99%	2019067	TP2	51,380,576	98.71%
2019054	TP1	89,483,864	99.43%	2019068	TP2	50,239,984	98.45%
2019055	TP1	90,826,474	99.21%	2019069	TP2	53,279,418	99.33%
2019056	TP1	42,965,670	99.03%	2019070	TP2	45,835,280	97.96%
2019057	TP1	55,546,368	99.39%	2019071	TP2	51,639,770	98.70%
2019059	TP1	45,240,666	99.03%	2019041	TP3	84,509,216	97.63%
2019060	TP1	35,049,778	99.25%	2019042	TP3	112,751,426	97.24%
2019061	TP1	60,240,496	99.30%	2019044	TP3	49,109,446	98.89%
2019062	TP1	60,329,292	98.45%	2019045	TP3	74,378,904	98.91%
2019063	TP1	108,480,792	99.18%	2019046	TP3	64,156,198	99.29%
2019064	TP1	49,544,058	97.52%	2019048	TP3	55,635,650	97.29%
2019065	TP1	89,767,900	98.81%	2019049	TP3	68,661,036	99.28%
2019066	TP1	53,032,176	98.25%	2019050	TP3	45,780,394	99.11%
2019067	TP1	46,596,340	98.92%	2019051	TP3	63,370,802	99.02%
2019068	TP1	59,119,436	98.67%	2019053	TP3	22,368,280	97.56%
2019069	TP1	67,894,468	98.64%	2019054	TP3	56,830,994	99.18%
2019070	TP1	61,070,672	98.08%	2019056	TP3	55,812,734	98.52%
2019071	TP1	50,215,666	97.23%	2019057	TP3	66,104,436	99.38%
2019041	TP2	110,261,654	97.54%	2019059	TP3	34,170,730	99.11%
2019042	TP2	160,375,302	97.68%	2019060	TP3	51,526,808	99.07%
2019044	TP2	46,318,488	99.18%	2019061	TP3	31,240,048	99.10%
2019045	TP2	82,646,004	98.96%	2019062	TP3	51,181,700	98.09%
2019046	TP2	91,791,700	99.16%	2019063	TP3	50,632,280	97.74%
2019048	TP2	52,812,438	97.91%	2019064	TP3	57,738,412	97.16%
2019049	TP2	56,585,706	99.29%	2019065	TP3	50,630,464	98.41%
2019050	TP2	44,950,924	99.44%	2019066	TP3	43,250,144	97.67%
2019051	TP2	42,287,624	99.21%	2019067	TP3	56,167,696	99.03%
2019053	TP2	52,169,008	98.08%	2019068	TP3	59,033,762	98.10%
2019054	TP2	38,860,196	95.06%	2019069	TP3	57,198,994	97.45%
2019055	TP2	38,046,158	99.41%	2019070	TP3	50,792,036	97.92%
2019056	TP2	67,026,560	98.05%	2019071	TP3	53,701,688	98.82%

4.2.7 Microbial diversity analysis

R package vegan version 2.5.7 [250] was deployed to calculate the alpha- and beta-diversities of taxonomy profiles at the species level. Alpha-diversity of the microbial community was measured by Shannon index [251], while beta-diversity was assessed based on the Bray-Curtis dissimilarity [252]. Mann-Whitney U tests [431] were utilized to compare the alpha diversities of gut microbiomes from dogs of different litters, ages, sexes, and breeds. The cutoff for the null hypotheses was also set at 0.05. The beta diversities among gut microbiomes from different litter, age, sex, and breed groups were calculated using the Bray-Curtis distances. The beta diversity was analyzed by Principal Coordinate Analysis (PCoA) using Permutational multivariate analysis of variance (PERMANOVA) test [309], which is a permutation-based non-parametric statistical test that tests the null hypothesis that there is no difference in distribution among groups of multiple variables. Function adonis2 from the R package vegan was used to perform the PERMANOVA tests.

4.2.8 Identification of the most featured bacterial taxa between high and low memory performance groups

LEfSe (Linear discriminant analysis Effect Size) version 1.1.2 was utilized to discover the most featured orders, families, genera, and species between the high and low memory performance groups. The analysis was conducted via Galaxy web application (<http://huttenhower.org/galaxy>) using default options (alpha = 0.05). Moreover, Mann-Whitney U tests [431] were performed on the taxonomy profiles of the high and low memory performance groups, to identify the species that exhibited significant differences in relative abundance. These biomarkers were displayed in

heatmap plots, which were generated with R package *heatmap* version 1.0.12.

4.2.9 Correlation between bacterial taxa and overall memory score

To estimate the correlation between the bacterial taxa and memory performance, we performed Spearman's correlation test on the OMS and the abundance levels of the taxa across all 80 measurements using the R software.

4.2.10 Random forest regression analysis

Random forest model [439] was used to predict the working memory score. The initial model included all microbiome composition, age, litter, sex, and breed as features. The importance score, which quantifies the impact of each feature on the accuracy of the model, was calculated. The most critical features with high importance scores were included in the final predictive model. R package *Ranger version 0.15.1* was used to fit the random forest regression model, and *ggplot2 version 3.4.2* was used to display the feature importance. The SHAP values [440] were then computed to interpret the predictive model. R package *shapper*, *DALEX2*, *shapviz*, and *treeshap* were used to compute and visualize the SHAP values of each feature. Positive SHAP value indicates a positive impact on the memory score while negative SHAP indicates a negative impact. The magnitude of SHAP represents the degree of impact of each feature on the model output, with a larger magnitude indicating a greater impact on the model output.

4.2.11 Reconstruction of MAGs and qPCR validation of abundance differences for

Bifidobacterium pseudolongum

To confirm the species identity of our findings and obtain bacterial genome sequences for validation, metaBAT2 version 2.15-2 [441] was used to bin metagenome-assembled genomes (MAGs) from the canine gut microbiome reference microbial contigs (accession number JARCCX000000000). The genome completeness and contamination were assessed using checkM version 1.2.2 [375]. To confirm the association between *B. pseudolongum* abundance and memory performance, we designed qPCR assay targeting the *nusA* gene, which is one of the universal single-copy gene families [442]. *Prevotella copri*, the most abundant species in the canine gut microbiome, was chosen as the control species because its abundance is the most stable across 80 metagenomes. The qPCR primers were synthesized by Eurofins (Eurofins Genomics Inc., Huntsville, AL, USA) after being designed in Oligo 7 software [377]. The forward primer sequence for *P. copri* is GCAACACGCTGAGTACATGA, and the reverse primer sequence is CCGTGAGGTAGACGAGAATG. The forward primer sequence for *B. pseudolongum* is AGCTTGGCCGCCAGACG, and the reverse primer sequence is TGATCGGACCTGGTGGTTCG. PCR product lengths are 200 bp and 244 bp, respectively, and they were confirmed by regular PCR, electrophoresis, and visualization on 2% agarose gel. For each qPCR reaction, 2 ng fecal DNA sample was mixed with PerfeCTa SYBR Green FastMix, Low ROX (Quantabio, Beverly, MA, USA), and nuclease-free water in a 96-well plate. The qPCR was carried out using a Bio-Rad C1000 Touch Thermal Cycler equipped with CFX96 Real-Time PCR Detection Systems (Bio-Rad Laboratories, Hercules, CA, USA). To quantify the expression level of *B. pseudolongum* in each sample, the Ct value difference between *B. pseudolongum* and *P. copri* was computed for relative quantification. Non-parametric Wilcoxon Rank Sum test and Spearman's correlation test were performed on the log₂ scale of the relative abundance to verify the WGS results.

4.2.12 Data and code availability

The whole-genome shotgun metagenomic sequencing data are available at NCBI SRA (Short Read Archive) under accession number PRJNA936782. All code used in this study is available in GitHub (https://github.com/XuWangLab/2023_memory_and_canine_microbiome) or can be found on websites of corresponding software packages.

4.3 Results

4.3.1 Substantial variability was identified in canine memory performance at puppy, juvenile, and young adult stages

Memory tests were conducted with 27 dogs born and raised in the AUCVM-CPS colony at three timepoints (Table 4.1). The number of correct trials was recorded as the overall memory score (OMS, ranging from 0 to 6; see Methods). The distribution of OMS significantly deviated from random guessing ($p < 2.2 \times 10^{-16}$, Kolmogorov-Smirnov test), confirming the presence of working memory (Figure 4.1A). The average OMS at the young adult stage (OMS mean \pm SD = 4.15 ± 1.26 and age mean \pm SD = 13.23 ± 1.50 months) was higher than that at juvenile stage (OMS mean \pm SD = 3.78 ± 0.82 and age mean \pm SD = 5.26 ± 0.35 months) and puppy stages (OMS mean \pm SD = 3.67 ± 0.83 and age mean \pm SD = 3.17 ± 0.43 months). The results showed an improvement in memory performance with age. However, the difference was not statistically significant when pairwise non-parametric tests were conducted ($p > 0.05$ for all comparisons, Mann-Whitney U tests), or when or the non-parametric group was performed ($p = 0.08$, Kruskal-Wallis test; Figure 4.1B; Table 4.2). As expected, there was a slightly lower average number of correct trials (61.3%) associated with a longer (40 s) delay interval compared to the shorter (10 s) interval (67.5%), but the difference was not statistically significant ($p > 0.05$, Mann-Whitney U

test and $p = 0.16$, Kruskal–Wallis test; Figure 4.1B). Memory scores did not differ significantly between sexes (Figure 4.1C) or breeds (Figure 4.1D). The Kruskal-Wallis test did not identify any significant differences among the litters ($p > 0.05$). When pairwise tests were performed between litters, litter B showed differences compared to litters A and C (nominal $p < 0.05$, Mann-Whitney U test; Figure 4.1C), but the significance did not withstand multiple testing corrections (adjusted $p > 0.05$ based on Bonferroni adjustment). All four litters were produced by genetically related breeders from the same extended pedigree, which partially controlled the genetic background. Therefore, substantial variations in memory scores cannot be explained by litter, sex, breed, or environmental effects.

4.3.2 Microbial diversity in canine gut microbiome was not affected by sex or litter, and was only slightly lower in 3-month puppies

To determine the influence of gut microbiome on canine memory performance, we performed WGS metagenomic sequencing in fecal samples collected at each memory test timepoint for all 27 dogs (see Table 4.3 and Methods). The five most abundant bacterial phyla are Firmicutes, Bacteroidetes, Actinobacteria, Proteobacteria, and Fusobacteria (Figure 4.3A), which is consistent with a previous report [392]. No between-sex differences in microbial alpha-diversity (Figure 4.3B; $P=0.895$, Mann-Whitney U test) or beta-diversity (Figure 4.3C; $P=0.781$, PERMANOVA test) were observed, suggesting lack of sexual dimorphism in the gut microbiome.

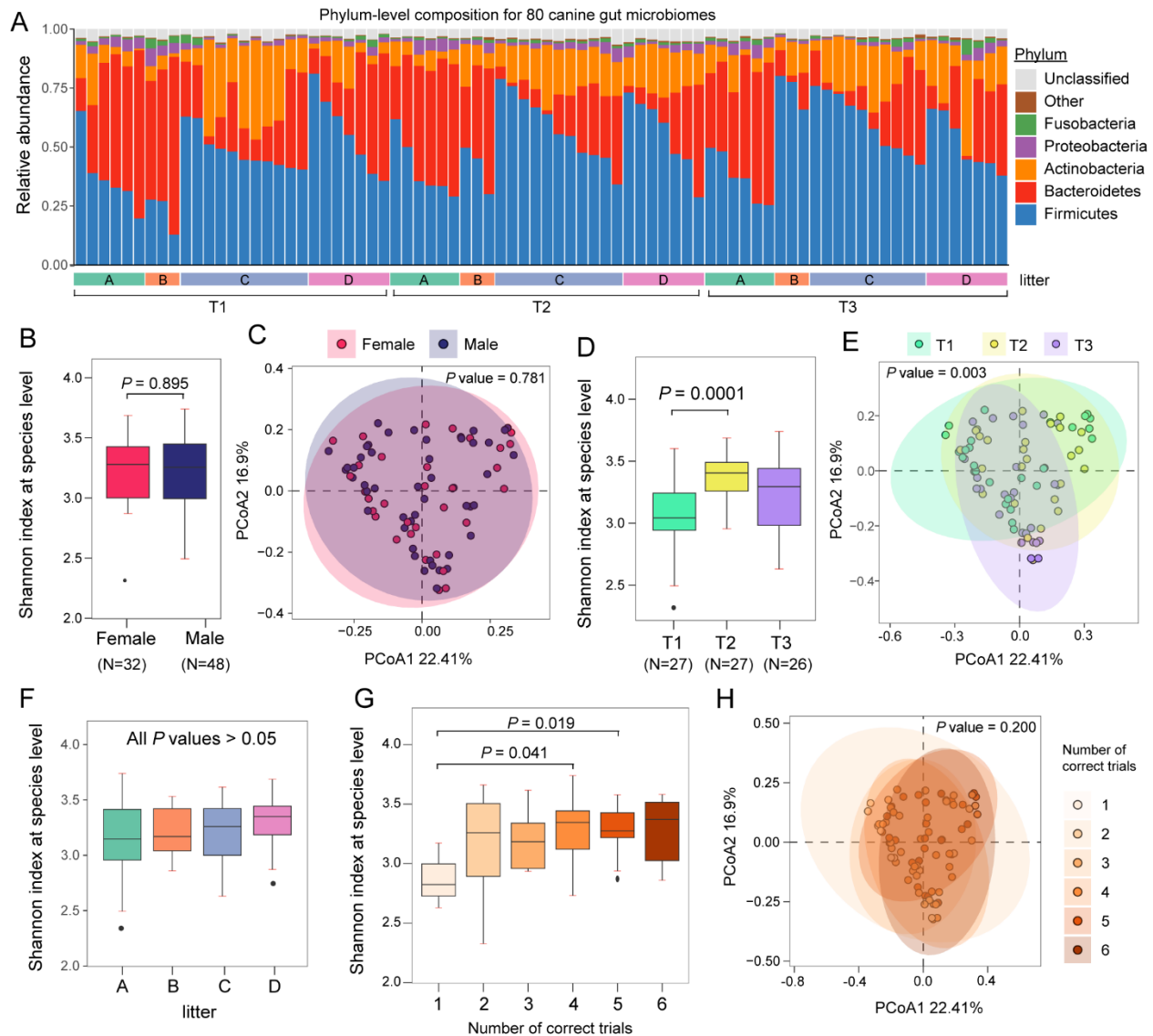


Figure 4.3 Effect of developmental stage, sex, litter, and breed on the canine gut microbiomes. (A) Barplots for phylum-level bacterial composition of 80 canine gut microbiomes ordered by timepoints (T1, puppy; T2, juvenile; T3, young adult stage) and litter identity (A, B, C, and D litters). (B) Boxplots for Shannon index of female and male microbiomes at the species level. (C) PCoA plot displaying the Bray-Curtis distances between the gut microbiomes of female and male canines at the species level. (D) Boxplots for Shannon index for the three stages at the species level. (E) PCoA plot showing the Bray-Curtis distances among gut microbiomes at three stages at the species level. (F) Boxplots for Shannon index for four litters at the species level. (G) Boxplots for Shannon index of gut microbiomes for six OMS (overall memory scores) groups measured by number of correct trials. (H) PCoA plot showing the Bray-Curtis distances among the canine gut microbiomes with different number of correct trials at the species level.

When microbial diversity was compared among the three stages, 3-month puppies had an 8.6% lower alpha-diversity compared to the juvenile stage (Figure 4.3D; $P < 0.001$, Mann-Whitney U test) and difference in the beta diversity was significant among the stages ($P = 0.003$, PERMANOVA test), but there was no separation on the Principal Coordinates Analysis (PCoA) plot with overlapped 95% confidence intervals (Figure 4.3E). The microbial alpha-diversity measured by Shannon index was not significantly different among four litters either (Figure 4.3F; $P > 0.05$, Mann-Whitney U test).

4.3.3 Linear discriminant analysis revealed a single most featured bacterial species, *Bifidobacterium pseudolongum*, is associated with memory performance

We investigated microbial diversity for measurement groups with the same overall memory scores. The only significant deviation we found was a slightly lower alpha-diversity in OMS1 group (Figure 4.3G; $P < 0.05$, Mann-Whitney U test), which could be due to a small number of measurements in this group ($N = 3$; Figure 4.1B). Beta diversity analysis confirmed no separation based on OMS (Figure 4.3H; $P = 0.200$, PERMANOVA test). To improve the power to detect microbiome differences, we defined a discovery set of eight dogs that had a high-OMS (OMS=6, high-OMS group) and eight dogs that has a low-OMS (OMS \leq 2, low-OMS group; Figure 4.1B). As expected, no significant differences were found in alpha diversity ($P = 0.328$, Mann-Whitney U test; Figure 4.1C) or beta diversity ($P = 0.363$, PERMANOVA test; Figure 4.1D). Collectively, these results suggest lack of any dysbiosis in the gut microbiome, as they are healthy dogs without any medical issues. With species-level resolution from the WGS metagenomic data, we performed linear discriminant analyses (LDA) between high-OMS and low-OMS groups on all bacterial taxonomical levels. At an LDA score cutoff of 3, the only significant species was

Bifidobacterium pseudolongum featured in high-OMS group, which drove the significance of its genus, family, and order (Figure 4.4A). When a less stringent LDA cutoff (LDA score<2) was used, *B. criceti* was also associated with high memory performance (Figure 4.4A), whereas *Collinsella ihuae* and the genus *Holdemanella* were negatively associated with memory performance (Figure 4.4A).

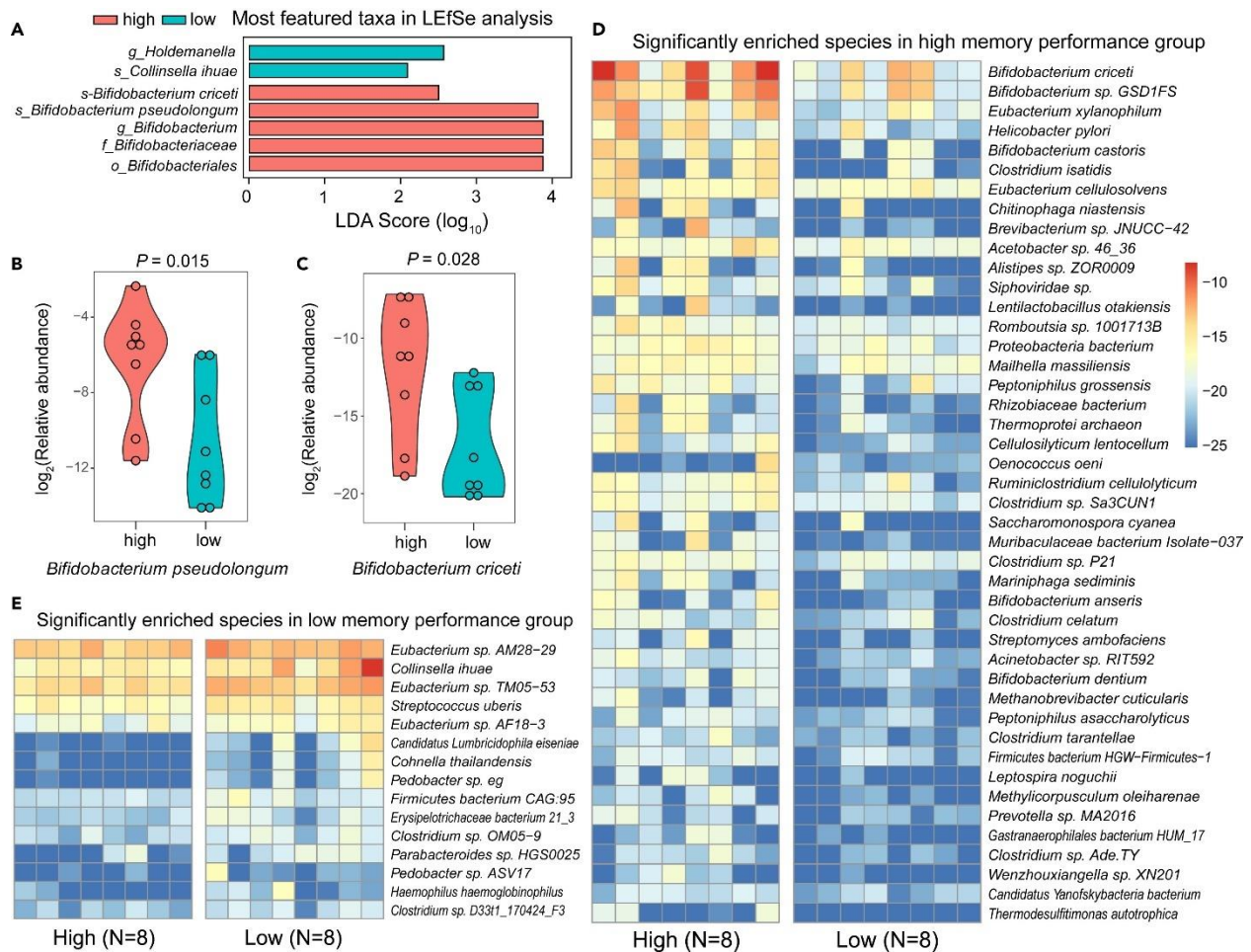


Figure 4.4 Microbial composition differences in the canine gut microbiome between the high and low memory performance groups. (A) Linear Discriminant Analysis (LDA) plots show the most featured taxa in dogs that scored high and low on the memory test at the order (*o_*), family (*f_*), genus (*g_*), and species (*s_*) levels. (B and C) Violin plots illustrating the relative abundance of *Bifidobacterium pseudolongum* (B) and *Bifidobacterium criceti* (C) in dogs that scored high and low on the memory test. P-value assessed by Mann-Whitney U test. (D and E) Heatmaps illustrating the abundance of bacterial species enriched in dogs that scored high (D) and low (E) on the working memory test.

4.3.4 Other bacterial taxa differ in abundance between high-OMS and low-OMS groups in addition to *B. pseudolongum*

To identify bacterial taxa with differential abundance between high-OMS and low-OMS groups, we performed non-parametric tests of relative abundance between groups. Among the significant taxa, *B. pseudolongum* had the highest abundance, accounting for 4.14% in high-OMS microbiome and 0.44% in low-OMS gut microbiome on average (Figure 4.4B; $P=0.015$, Mann-Whitney U test). *B. criceti*, another bacterium positively associated with high memory performance in the LDA analysis (Figure 4.4A), was also significantly more abundant in the high-OMS group (Figure 4.4C; $P=0.028$, Mann-Whitney U test). A total of 45 species were significantly enriched in the high-OMS group (Figure 4.4B and 4.4D), and another 15 bacterial species were enriched in the low-OMS group (Figure 4.4C and 4.4E).

4.3.5 Confirmation of memory performance associated microbial taxa using the 80 metagenomes as a validation set

For bacterial taxa showing abundance differences between high-OMS and low-OMS groups (Table 4.4), we quantified their relative abundance in the 80 metagenomes and correlated with OMS to determine significant correlations in the entire dataset. A total of 32 bacterial taxa were positively correlated with memory performance (false discovery rate $FDR < 0.1$), and 8 taxa were negatively correlated (Figure 4.5A and Table 4.5).

Table 4.4 Bacterial taxa with significant abundance differences between high performers and low performers in short-term memory tests.

Rank	Name	RA (OMS=6)	RA (OMS<=2)	P-value	Log2 FC
Order	<i>Bifidobacteriales</i>	5.3321%	1.0359%	0.0499	2.364
Order	<i>Chloroflexales</i>	0.0013%	0.0002%	0.0070	2.462
Order	<i>Pirellulales</i>	0.0005%	0.0011%	0.0499	-1.315
Family	<i>Bifidobacteriaceae</i>	5.3320%	1.0359%	0.0499	2.364
Genus	<i>Bifidobacterium</i>	5.3217%	1.0314%	0.0499	2.367
Genus	<i>Terrisporobacter</i>	0.0253%	0.0126%	0.0148	1.002
Genus	<i>Vagococcus</i>	0.0037%	0.0015%	0.0207	1.261
Genus	<i>Acetobacter</i>	0.0029%	0.0010%	0.0499	1.596
Genus	<i>Terribacillus</i>	0.0029%	0.0003%	0.0148	3.161
Genus	<i>Globicatella</i>	0.0012%	0.0005%	0.0379	1.398
Genus	<i>CandidatusLumbricidophila</i>	0.0000%	0.0012%	0.0159	-9.603
Genus	<i>Mailhella</i>	0.0012%	0.0006%	0.0499	1.042
Species	<i>Eubacterium cellulosolvens</i>	0.0034%	0.0009%	0.0379	1.885
Species	<i>Acetobacter sp. 46_36</i>	0.0022%	0.0006%	0.0499	1.857
Species	<i>Acinetobacter sp. RIT592</i>	0.0003%	0.0000%	0.0030	2.865
Species	<i>Alistipes sp. ZOR0009</i>	0.0021%	0.0001%	0.0405	3.917
Species	<i>Bifidobacterium anseris</i>	0.0005%	0.0000%	0.0165	5.488
Species	<i>Bifidobacterium castoris</i>	0.0038%	0.0002%	0.0173	4.284
Species	<i>Bifidobacterium criceti</i>	0.1898%	0.0057%	0.0281	5.063
Species	<i>Bifidobacterium dentium</i>	0.0002%	0.0000%	0.0400	3.010
Species	<i>Bifidobacterium pseudolongum</i>	4.1446%	0.4368%	0.0148	3.246
Species	<i>Bifidobacterium sp. GSDIFS</i>	0.0409%	0.0042%	0.0281	3.270
Species	<i>Brevibacterium sp. JNUCC-42</i>	0.0029%	0.0000%	0.0486	8.107
Species	<i>Gastranaerophilales bacterium HUM_17</i>	0.0001%	0.0000%	0.0496	5.080
Species	<i>Candidatus Lumbricidophila eiseniae</i>	0.0000%	0.0012%	0.0159	-9.603
Species	<i>Candidatus Yanofskybacteria bacterium</i>	0.0001%	0.0000%	0.0207	1.359
Species	<i>Cellulosilyticum lentocellum</i>	0.0010%	0.0000%	0.0047	4.514
Species	<i>Chitinophaga niastensis</i>	0.0029%	0.0003%	0.0380	3.515
Species	<i>Clostridium celatum</i>	0.0003%	0.0001%	0.0379	1.538
Species	<i>Clostridium isatidis</i>	0.0035%	0.0001%	0.0310	4.589
Species	<i>Clostridium sp. Ade.TY</i>	0.0001%	0.0000%	0.0129	3.262
Species	<i>Clostridium sp. D33t1_170424_F3</i>	0.0000%	0.0001%	0.0499	-1.315
Species	<i>Clostridium sp. OM05-9</i>	0.0001%	0.0002%	0.0281	-1.439
Species	<i>Clostridium sp. P21</i>	0.0006%	0.0002%	0.0281	1.387
Species	<i>Clostridium sp. Sa3CUN1</i>	0.0009%	0.0002%	0.0104	2.473
Species	<i>Clostridium tarantellae</i>	0.0002%	0.0000%	0.0281	3.077
Species	<i>Cohnella thailandensis</i>	0.0000%	0.0004%	0.0215	-7.424
Species	<i>Collinsella ihuae</i>	0.0023%	0.0519%	0.0499	-4.475
Species	<i>Erysipelotrichaceae bacterium 21_3</i>	0.0000%	0.0002%	0.0499	-2.051
Species	<i>Eubacterium sp. AF18-3</i>	0.0006%	0.0013%	0.0499	-1.204

Table 4.4 Continued.

Rank	Name	RA (OMS=6)	RA (OMS<=2)	P-value	Log2 FC
Species	<i>Eubacterium sp. AM28-29</i>	0.0123%	0.0258%	0.0379	-1.067
Species	<i>Eubacterium sp. TM05-53</i>	0.0071%	0.0191%	0.0070	-1.419
Species	<i>Eubacterium xylanophilum</i>	0.0117%	0.0006%	0.0281	4.271
Species	<i>Firmicutes bacterium CAG:95</i>	0.0001%	0.0003%	0.0281	-1.974
Species	<i>Firmicutes bacterium HGW-Firmicutes-1</i>	0.0001%	0.0001%	0.0499	1.285
Species	<i>Haemophilus haemoglobinophilus</i>	0.0000%	0.0002%	0.0310	-4.478
Species	<i>Helicobacter pylori</i>	0.0065%	0.0007%	0.0499	3.148
Species	<i>Lentilactobacillus otakiensis</i>	0.0014%	0.0000%	0.0246	8.614
Species	<i>Leptospira noguchii</i>	0.0001%	0.0000%	0.0240	5.033
Species	<i>Mailhella massiliensis</i>	0.0012%	0.0006%	0.0499	1.042
Species	<i>Mariniphaga sediminis</i>	0.0006%	0.0001%	0.0308	3.438
Species	<i>Methanobrevibacter cuticularis</i>	0.0002%	0.0000%	0.0131	4.939
Species	<i>Methylicorpusculum oleiharenae</i>	0.0001%	0.0000%	0.0355	4.263
Species	<i>Muribaculaceae bacterium Isolate-037</i>	0.0007%	0.0000%	0.0400	6.528
Species	<i>Oenococcus oeni</i>	0.0010%	0.0000%	0.0400	5.314
Species	<i>Parabacteroides sp. HGS0025</i>	0.0001%	0.0002%	0.0486	-1.671
Species	<i>Pedobacter sp. ASV17</i>	0.0000%	0.0002%	0.0496	-5.609
Species	<i>Pedobacter sp. eg</i>	0.0000%	0.0003%	0.0070	-7.787
Species	<i>Peptoniphilus asaccharolyticus</i>	0.0002%	0.0000%	0.0281	2.372
Species	<i>Peptoniphilus grossensis</i>	0.0012%	0.0005%	0.0207	1.268
Species	<i>Prevotella sp. MA2016</i>	0.0001%	0.0000%	0.0400	2.687
Species	<i>Proteobacteria bacterium</i>	0.0013%	0.0004%	0.0070	1.781
Species	<i>Rhizobiaceae bacterium</i>	0.0011%	0.0000%	0.0404	4.841
Species	<i>Romboutsia sp. 1001713B</i>	0.0013%	0.0002%	0.0011	2.784
Species	<i>Ruminiclostridium cellulolyticum</i>	0.0009%	0.0004%	0.0207	1.426
Species	<i>Saccharomonospora cyanea</i>	0.0008%	0.0001%	0.0496	3.037
Species	<i>Siphoviridae sp.</i>	0.0017%	0.0003%	0.0379	2.656
Species	<i>Streptococcus uberis</i>	0.0015%	0.0033%	0.0499	-1.155
Species	<i>Streptomyces ambofaciens</i>	0.0003%	0.0000%	0.0097	4.316
Species	<i>Thermodesulfatimonas autotrophica</i>	0.0001%	0.0000%	0.0325	Inf
Species	<i>Thermoprotei archaeon</i>	0.0011%	0.0001%	0.0308	3.697
Species	<i>Wenzhouxiangella sp. XN201</i>	0.0001%	0.0000%	0.0298	5.999

Table 4.5 Bacterial taxa with significant positive or negative correlation between relative abundance and memory performance.

Rank	Name	rho	P-value	FDR	RA
Order	<i>Bifidobacteriales</i>	0.2978	0.0073	0.0282	3.8114%
Order	<i>Chloroflexales*</i>	0.3512	0.0014	0.0253	0.0007%
Family	<i>Bifidobacteriaceae</i>	0.2978	0.0073	0.0282	3.8114%
Genus	<i>Bifidobacterium</i>	0.2986	0.0071	0.0282	3.7999%
Genus	<i>Candidatus Lumbricidophila</i>	-0.3094	0.0052	0.0282	0.0002%
Genus	<i>Globicatella*</i>	0.2911	0.0088	0.0295	0.0010%
Genus	<i>Vagococcus*</i>	0.2952	0.0078	0.0282	0.0031%
Species	<i>Acinetobacter sp. RIT592*</i>	0.2241	0.0457	0.0823	0.0001%
Species	<i>Bifidobacterium anseris*</i>	0.2346	0.0362	0.0686	0.0006%
Species	<i>Bifidobacterium castoris*</i>	0.3316	0.0027	0.0282	0.0019%
Species	<i>Bifidobacterium criceti*</i>	0.2228	0.0470	0.0825	0.1130%
Species	<i>Bifidobacterium dentium*</i>	0.3065	0.0057	0.0282	0.0001%
Species	<i>Bifidobacterium pseudolongum*</i>	0.3525	0.0013	0.0253	2.6134%
Species	<i>Bifidobacterium sp. GSD1FS*</i>	0.3021	0.0065	0.0282	0.0478%
Species	<i>Brevibacterium sp. JNUCC-42*</i>	0.3011	0.0066	0.0282	0.0005%
Species	<i>Gastranaerophilales bacterium HUM_17*</i>	0.2849	0.0104	0.0302	0.0000%
Species	<i>Candidatus Lumbricidophila eiseniae*</i>	-0.3094	0.0052	0.0282	0.0002%
Species	<i>Cellulosilyticum lentocellum*</i>	0.2329	0.0376	0.0695	0.0007%
Species	<i>Clostridium isatidis*</i>	0.2525	0.0239	0.0491	0.0017%
Species	<i>Clostridium sp. D33t1_170424_F3*</i>	-0.2887	0.0094	0.0295	0.0001%
Species	<i>Clostridium sp. P21*</i>	0.3069	0.0056	0.0282	0.0007%
Species	<i>Clostridium sp. Sa3CUNI*</i>	0.3363	0.0023	0.0282	0.0008%
Species	<i>Cohnella thailandensis*</i>	-0.2634	0.0182	0.0398	0.0001%
Species	<i>Eubacterium cellulosolvens*</i>	0.2899	0.0091	0.0295	0.0023%
Species	<i>Eubacterium xylanophilum*</i>	0.3204	0.0038	0.0282	0.0057%
Species	<i>Firmicutes bacterium HGW-Firmicutes-1*</i>	0.2805	0.0117	0.0302	0.0001%
Species	<i>Haemophilus haemoglobinophilus*</i>	-0.2688	0.0159	0.0382	0.0001%
Species	<i>Lentilactobacillus otakiensis*</i>	0.3023	0.0064	0.0282	0.0002%
Species	<i>Leptospira noguchii*</i>	0.2654	0.0173	0.0398	0.0000%
Species	<i>Mariniphaga sediminis*</i>	0.2512	0.0246	0.0492	0.0003%
Species	<i>Methanobrevibacter cuticularis*</i>	0.2840	0.0107	0.0302	0.0001%
Species	<i>Muribaculaceae bacterium Isolate-037 (Harlan) *</i>	0.2742	0.0138	0.0343	0.0006%
Species	<i>Pedobacter sp. ASV17*</i>	-0.2966	0.0075	0.0282	0.0000%
Species	<i>Pedobacter sp. eg*</i>	-0.3080	0.0054	0.0282	0.0001%
Species	<i>Peptoniphilus grossensis*</i>	0.2645	0.0178	0.0398	0.0012%
Species	<i>Ruminiclostridium cellulolyticum*</i>	0.2816	0.0114	0.0302	0.0006%
Species	<i>Siphoviridae sp.*</i>	0.2808	0.0116	0.0302	0.0009%
Species	<i>Streptococcus uberis*</i>	-0.2387	0.0330	0.0642	0.0021%
Species	<i>Streptomyces ambofaciens*</i>	0.4091	0.0002	0.0119	0.0001%
Species	<i>Thermoprotei archaeon*</i>	0.2600	0.0199	0.0420	0.0003%

Among the 32 taxa associated with improved memory performance, nine were related to *Bifidobacterium*, including six species (*B. pseudolongum*, *B. criceti*, *B. anseris*, *B. castoris*, *B. dentium*, and *B. sp. GSD1FS*), *Bifidobacterium* genus, Bifidobacteriaceae family, and Bifidobacteriales order (Figure 4.5A). *B. pseudolongum* was the most abundant species in its genus, and it drove the significant at genus, family, and order levels (Figure 4.5B). In contrast, the second most abundant *Bifidobacterium* species, *B. animalis*, did not show significant differences between high-OMS and low-OMS groups (Figure 4.5B). The Spearman's correlation coefficient (ρ) between *B. pseudolongum* and OMS was 0.352 ($P=0.001$; Figure 4.5C), which was the second highest among all significant taxa (Figure 4.5A). There were fewer taxa negatively correlated with OMS, including *Pedobacter sp. ASV17* (Figure 4.5D and Figure 4.6).

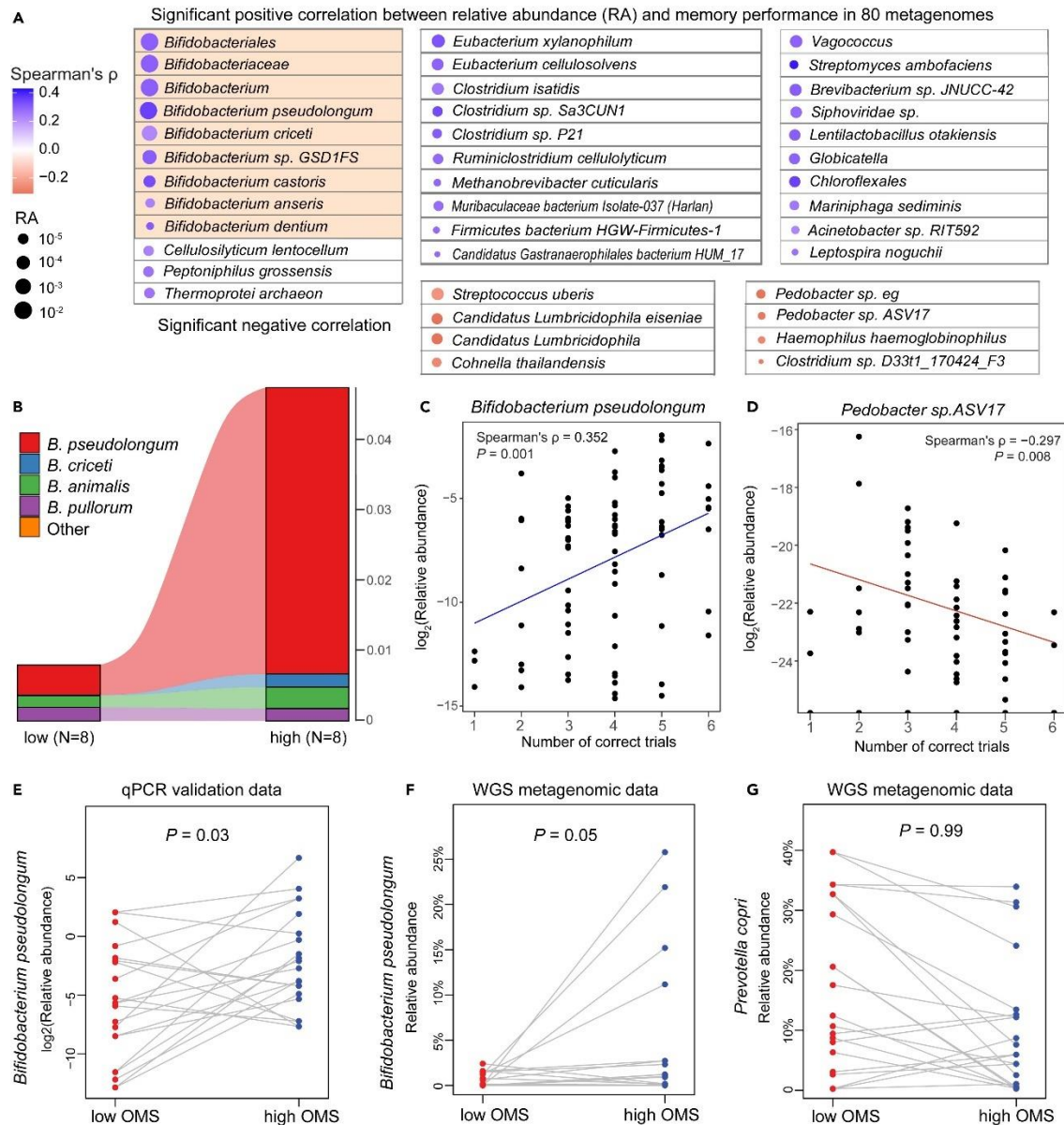


Figure 4.5 Correlation between memory performance and bacterial taxa abundance in 80 metagenomes. (A) Significant positive and negative correlations were found between the overall memory score (OMS) and taxa abundance ($p < 0.05$, FDR < 0.10 , Spearman's rank correlation test). The color of the dots represents the value of the Spearman correlation coefficient, and the dot is proportional to the relative abundance. (B) Alluvial plots demonstrate a significant increase in *Bifidobacterium pseudolongum* and *Bifidobacterium criceti* in the high-OMS group. No significant differences were observed among the other *Bifidobacterium* species. (C and D) Scatterplots between OMS and the relative abundance of *B. pseudolongum* (C) and *Pedobacter sp. ASV17* (D). (E–G) Plots of relative bacterial abundance at 21 high-OMS and low-OMS pairs of time points in the same dog for qPCR (E) and whole-genome sequencing (WGS) metagenomic quantification (F) of *B. pseudolongum* and WGS metagenomic quantification of the control species *Prevotella copri* (G). P -value assessed by Wilcoxon signed rank test.

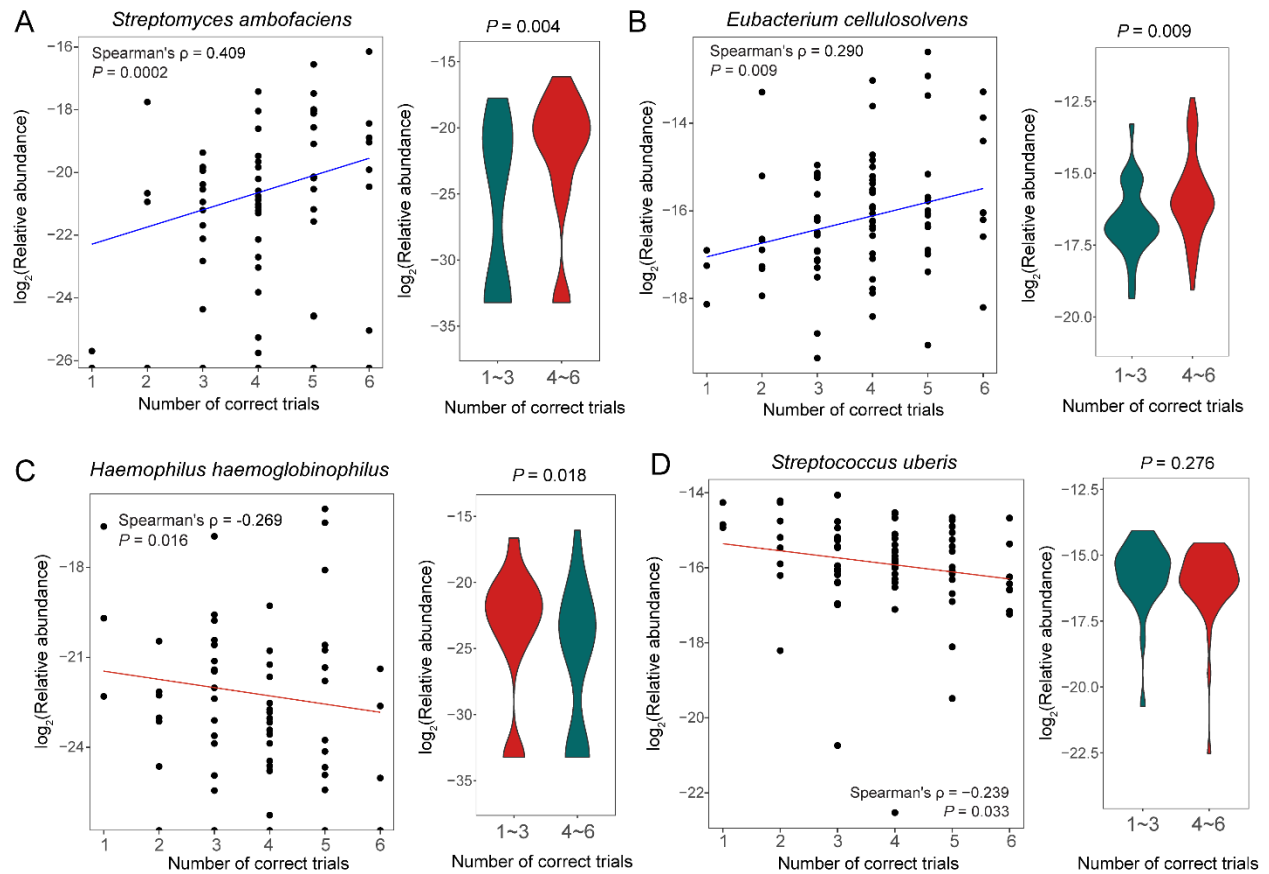


Figure 4.6 Correlation between memory performance and bacterial species abundance in the canine gut microbiome. Correlation plots and violin plots displaying the relationship between bacterial relative abundance (\log_2 scale) and the memory performance scores for *Streptomyces ambofaciens* (A), *Vagococcus* (B), *Pedobacter sp. ASV17* (C), and *Haemophilus haemoglobinophilus* (D).

4.3.6 Quantitative polymerase chain reaction validation confirmed that changes in *Bifidobacterium pseudolongum* abundance is associated with differences in working memory performance in the same dogs

B. pseudolongum was associated with improved canine memory function in LDA analysis, differential abundance analysis, and correlation analysis. It is also abundant in the canine microbiome. To validate the intriguing finding using an independent technique, we performed

qPCR quantification of the *nusA* gene in *B. pseudolongum*, using *Prevotella copri* as a positive control, whose abundance is stable across all samples (see Methods).

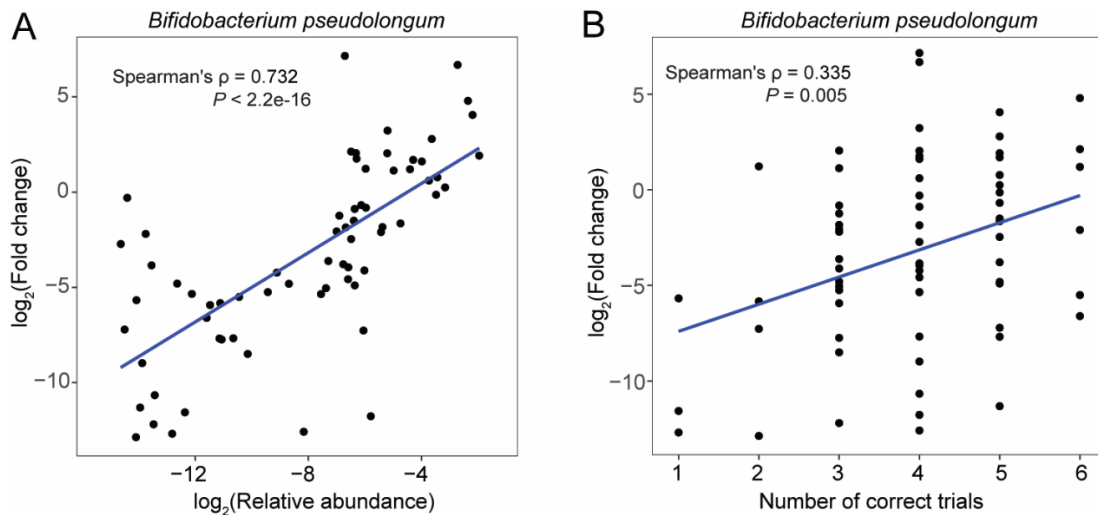


Figure 4.7 Quantitative PCR validation of *Bifidobacterium pseudolongum* across all 80 microbiome samples. **(A)** Scatterplot of \log_2 relative abundances of *Bifidobacterium pseudolongum* from WGS metagenomic data and its \log_2 fold changes compared to control species *Prevotella copri* through quantitative PCR (qPCR). A fitted line based on linear regression model is shown in blue. (Spearman’s correlation coefficient $\rho=0.732$, $P<0.0001$). **(B)** Scatterplot of overall memory test scores (OMS) measured by number of correct trials and the *Bifidobacterium pseudolongum* relative expression volume from qPCR results. A fitted line based on linear regression model is shown in blue. (Spearman’s correlation coefficient $\rho=0.335$, $P=0.0050$).

We observed high concordance between the qPCR measurements and the WGS metagenomic sequencing results ($\rho=0.73$, $P<0.0001$; Figure 4.7A), confirming high reproducibility and the significant positive correlation between *B. pseudolongum* and OMS ($\rho=0.34$, $P=0.005$; Figure 4.7B). If the presence of *B. pseudolongum* were causal to the improved OMS, for the same dog with variable OMS, we expect to observe significant changes in *B. pseudolongum* abundance across different timepoints. A total of 21 discordant pairs (OMS>3 and OMS<=3) were identified, and the *B. pseudolongum* abundance was significantly higher at the high OMS timepoint (mean=4.12%) than the low OMS timepoint (mean=0.55%; $P<0.05$, Wilcoxon signed

rank test), which implied a potential causal relationship between *B. pseudolongum* and working memory performance (Figure 4.5E-G).

4.3.7 Predictability of microbiome composition for working memory performance using random forest regression

A predictive model has been developed to predict the working memory performance with microbiome composition serving as features in a random forest regression model. The initial model includes 36 bacterial taxa showing significant correlation with memory scores (Table 4.5), as well as additional variables such as age, sex, litter, and breed. A total of 17 taxa had high discriminatory power (important value greater than 3; Figure 4.8A), and they were included in the final predictive model. Age, litter, sex, and breed were found to have negligible discriminatory capability and, therefore, not incorporated into the model (Figure 4.8A). The predicted memory score was significantly correlated with the observed memory score ($\rho=0.472$, $P<0.0001$; Figure 4.8B). SHAP values (SHapley Additive exPlanations) were then employed to interpret the predictive model (Figure 4.8C). Among the final list of predictive taxa, higher OMS were associated with increased abundance of *Bifidobacterium pseudolongum* (Figure 4.8D) and decreased abundance of *Pedobacter sp. ASV17* (Figure 4.8E).

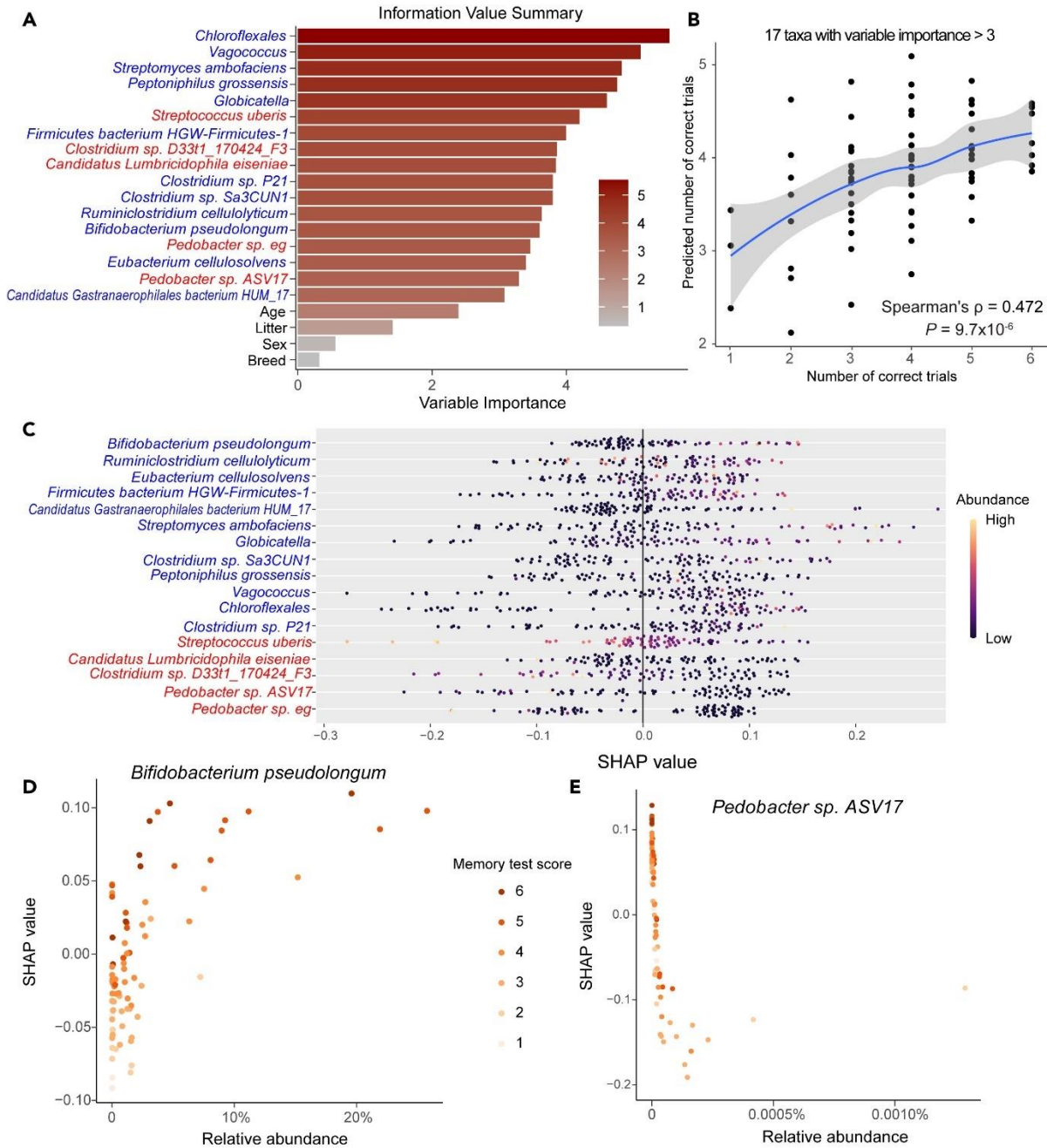


Figure 4.8 Variable importance and predictability modeled by random forest regression using 31 bacterial taxa with significant correlation with memory performance. (A) Feature importance scores computed using random forest. (B) Scatterplot of the observed memory score (x-axis) and predicted memory scores (y axis) using 17 taxa in the random forest regression. The fitted line is plotted in blue, with the confidence interval in gray. P -value assessed by Spearman's rank correlation test. (C) The impact of bacterial taxa (importance value >3) on the overall memory score is summarized by SHAP values. Color represents the relative abundance of bacterial taxa. (D and E) Scatterplot of SHAP values and the relative abundance of *B. pseudolongum* (D) and *Pedobacter sp. ASV17* (E). The dots were color-coded based on the overall memory score.

4.4 Discussion and conclusion

Domestic dogs share common social and environmental evolutionary history with humans and possess social and cognitive skills that are functional analogous to humans, making them an ideal model for translational and comparative research in cognitive neuroscience and behavioral genetics [443, 444]. In addition, these skills are particularly important for purpose-bred working dogs (e.g., detection dogs) to be successful in their work [445, 446]. However, cognitive and behavioral studies are challenging because these traits are heavily affected by the environment, experimenter, and other confounding factors. To address this, we measured working memory performance in 27 candidate detection dogs reared and maintained in controlled research setting and discovered significant variability in memory performance, even in the same dog across different timepoints. We concluded that the majority of phenotypic variation in canine memory capability cannot be explained by age, sex, or developmental stage, reflecting truly functional plasticity.

Animal gut microbiome is known to modulate the brain function and cognitive abilities through the microbiota–gut–brain axis [422]. However, gut microbiome composition is affected by diet, age, household environment, and host genetics. Many previous studies suffered from insufficient resolution to identify microbial species differences. Using fecal samples collected from age matched detection dog candidates in the same extended pedigree under the same diet, we performed WGS metagenomic sequencing to quantify the microbial abundance and maximized the statistical power to detect microbiome correlates of canine memory performance.

The phylum of Actinobacteria was shown to be negatively associated with canine memory

performance using dogs (N=29) with a large age range (3~13 years old, mean age 9.7) from diverse households and diverse breed backgrounds [428]. Since no specific bacterial species were significant in Kubnyi et al., it was unclear which microbes were driving the difference, and if the findings in phylum abundance variation were due to differences in age, sex, diet, breed, or other confounding factors. In our study, we focused on young dogs, and we did not find any significant correlation between memory performance and microbial diversity or phylum level composition. This lack of significant shifts in overall diversity and phylum abundance indicates that memory performance plasticity in young dogs is not caused by dysbiosis in the gut microbiome. This is expected because all enrolled animals in this study are healthy dogs. Thanks to the species resolution of WGS metagenomic sequencing and the experimental design that controls confounding factors, we were able to identify 41 microbial taxa that are significantly correlated with canine memory performance, revealing the microbiome influence of canine cognition at microbial species level for the first time.

In specialized settings, such as military working dog (MWD) populations, there are inherent challenges in controlling confounding factors, such as sex, age, body condition scores (BCS), breeds, and GI issues. A larger sample size is required to achieve meaningful microbiome discovery. A recent study conducted by Craddock et al. [447], which involved 134 MWDs spanning five different breeds, successfully revealed correlations between microbiome composition and behavioral attributes, including aggression, motivation, obedience, sociability, and BCS. Notably, these statistical associations were predominantly identified at the genus level or within species groups that were linked to specific metabolic pathways. Enhancing the metagenomic sequencing yield (~10 million reads per sample in the study by Craddock et al.) or

increasing the sample size could potentially enhance the ability to identify precise microbiome correlations at the species level.

Among the microbiome correlates of memory performance that we discovered, the single most striking findings is *Bifidobacterium pseudolongum*. This particular species stands out as the only significant taxon identified through the linear discriminant analysis, which couples statistical significance with effect relevance. The positive correlation between the relative abundance of *B. pseudolongum* and improved memory score was subsequently validated using qPCR assays. As a well-known genus of probiotics, *Bifidobacterium* produces lactic and acetic acids through fermentation, providing benefit to host gut health [403]. *B. pseudolongum* is the immediate outgroup of the *B. animalis* clade [448, 449]. *B. animalis* did not show abundance differences between high-OMS and low-OMS groups. This implies a species-specific phenomenon, rather than an overarching genus effect. Intriguingly, in a previous study, *Bifidobacterium longum* 1714, a remotely related *Bifidobacterium* species, was linked to reduced stress and enhanced memory in human subjects [450]. Further investigations suggest that the reduction of social stress is achieved by neural modulation[451], paving the way for the potential application of psychobiotics in enhancing human memory and ameliorating stress[452]. Nevertheless, in the canine microbiome, *B. longum* manifested a considerably lower mean abundance (0.02%) than *B. pseudolongum* (2.14%) and was not associated with working memory ($p = 0.17$) in our study. This distinction is not unexpected, given that the physiology is different between humans and canines. Therefore, findings centered on humans may not be directly to the canine microbiome.

Since dogs were domesticated ~15,000 years ago, they have become valuable partners working with humans in hunting, guarding, herding, guiding, and odor detection. Beyond their working capabilities, dogs provide humans with loyal companionship. Improving memory abilities in puppies will help them learn better and quicker, which can significantly enhance dog socialization and training [445, 453]. In senior dogs, memory loss is commonly observed as part of the canine cognitive dysfunction (CCD) syndrome, which is a progressive neurological and behavioral disease associated with aging [454, 455]. Improving memory function will help both puppy development and longevity in dogs. Our results will inform the development of probiotics and fecal microbiota transplantation (FMT) techniques to improve canine memory and cognition during puppy development. Whether our findings will apply in older dogs remain unclear and future studies are needed to explore it.

CHAPTER 5

Overall Conclusion and Future Direction

This dissertation provides a comprehensive examination of the gut microbiota in obese cats and its potential connections to memory performance in dogs, utilizing advanced metagenomic sequencing techniques. The results reveal key insights into the gut microbiome characteristics of obese cats, highlighting a significant reduction in microbial diversity and identifying specific microbial species that can be used as potential indicators of obesity. In addition, the study establishes a novel link between gut microbiota composition and memory performance in dogs, suggesting that specific bacterial taxa may play a role in memory performance.

To optimize the current fecal sampling methods for cats, we evaluated the impact of mineral oil lubrication during stool sample collection and compared the efficacy of two primary collection methods: using a fecal loop versus a litter box. We found that using mineral oil as a lubricant during fecal sample collection from cats does not affect the quality of the samples for gut microbiome analysis. We compared samples collected with and without lubrication and found no significant differences in microbial DNA yield, metagenomic sequencing yield, host contamination, or microbial diversity. This suggests that mineral oil can be used to improve animal welfare by reducing discomfort during sample collection without compromising the quality of the samples. We also found that while the fecal loop method resulted in a lower yield of microbial DNA, there were no significant differences in host contamination, virus contamination, microbial diversity, or relative taxonomy abundance between the two methods. Both methods were deemed reliable for microbiome research. The litter box method being less

invasive and more suitable for large-scale studies, while the fecal loop method provides a precise and sanitary collection technique, minimizing the risk of cross-contamination and exposure of anaerobes to oxygen. Optimizing fecal sampling methods for cats is important for advancing veterinary microbiome research, as it enhances the accuracy and reproducibility of microbiome data. It is critical for drawing reliable conclusions about feline health. These studies provide a foundation for standardized protocols, allowing researchers to better investigate the gut microbiota's role in feline disease, health, and overall physiology. Improved sampling methods contribute to a more consistent microbiome profile. It is essential for the development of microbiome-based health strategies in veterinary medicine.

To better characterize the gut microbiome of obese cats, we performed metagenomic analyses to assess microbial diversity, composition, and functional potential. The study concluded that obese cats have significantly decreased microbial diversity in their gut microbiota, indicating potential dysbiosis. A panel of seven significantly altered, highly abundant bacterial species was identified, which can serve as microbiome indicators of obesity. These findings provide new insights into the composition, abundance, and functional capacities of the obese cat microbiome, laying the groundwork for targeted microbiome interventions. This research could inform the development of innovative weight management and health strategies tailored for obese cats, potentially improving their quality of life and addressing obesity-related health issues more effectively.

To establish a link between memory performance and the canine gut microbiome, we conducted a metagenomic analysis focusing on identifying specific microbial species associated with

memory performance in dogs. The study concluded that there is a significant correlation between the abundance of *Bifidobacterium pseudolongum* in the canine gut microbiome and enhanced memory performance in dogs. This research highlights the critical role of non-genetic factors, particularly the gut microbiome, in influencing memory. These findings open promising avenues for the development of psychobiotics designed to improve memory and learning in dogs, which may have broader implications for understanding and enhancing cognitive health through microbiota-targeted therapies.

There are several avenues for future research to understand the role of the gut microbiome in feline obesity and canine cognitive function. One possible direction is to explore the mechanisms by which specific bacterial species affect obesity in cats and memory ability in dogs. Developing microbiome modulation strategies, such as probiotics, aimed at weight loss and cognitive enhancement could be a potential focus. Additionally, studying the effects of dietary interventions or prebiotics/probiotics on the gut microbiome and related health outcomes would provide valuable insights. Longitudinal studies can assess the long-term effects of microbiome alterations on obesity management in cats and memory and learning in dogs. Furthermore, given the similarities in microbiome changes observed across species, these studies highlight the potential to translate these findings to other animal species and even to humans.

Reference

1. Chivers, D.J. and P. Langer, *The digestive system in mammals: food form and function*. 1994: Cambridge University Press.
2. Chivers, D.J., *Functional anatomy of the gastrointestinal tract*. Colobine monkeys: their ecology, behaviour and evolution, 1994. **205**: p. 227.
3. Horstmann, L., *Anatomy and physiology of the gastrointestinal system*, in *The Bowhead Whale*. 2021, Elsevier. p. 165-183.
4. Squier, C.A. and M.J. Kremer, *Biology of oral mucosa and esophagus*. JNCI Monographs, 2001. **2001**(29): p. 7-15.
5. Chibly, A.M., et al., *Salivary gland function, development, and regeneration*. Physiological reviews, 2022. **102**(3): p. 1495-1552.
6. Tucker, A. *Salivary gland development*. in *Seminars in cell & developmental biology*. 2007. Elsevier.
7. Gyawali, C., et al., *Evaluation of esophageal motor function in clinical practice*. Neurogastroenterology & Motility, 2013. **25**(2): p. 99-133.
8. Morris, I.R., *Functional anatomy of the upper airway*. Emergency medicine clinics of North America, 1988. **6**(4): p. 639-669.
9. Gavaghan, M., *Anatomy and physiology of the esophagus*. AORN journal, 1999. **69**(2): p. 370-386.
10. Ellis, H., *Anatomy of the stomach*. Surgery (Oxford), 2011. **29**(11): p. 541-543.
11. Soybel, D.I., *Anatomy and physiology of the stomach*. Surgical Clinics, 2005. **85**(5): p. 875-894.
12. Mahadevan, V., *Anatomy of the stomach*. Surgery (Oxford), 2017. **35**(11): p. 608-611.
13. Volk, N. and B. Lacy, *Anatomy and physiology of the small bowel*. Gastrointestinal endoscopy clinics, 2017. **27**(1): p. 1-13.
14. Johansson, M.E., H. Sjövall, and G.C. Hansson, *The gastrointestinal mucus system in health and disease*. Nature reviews Gastroenterology & hepatology, 2013. **10**(6): p. 352-361.
15. Lantz, G.C., et al., *Small intestinal submucosa as a vascular graft: a review*. Journal of investigative surgery, 1993. **6**(3): p. 297-310.
16. Mikkelsen, H., *Macrophages in the external muscle layers of mammalian intestines*. Histology and histopathology, 1995. **10**(3): p. 719-736.
17. Freeman, D.E., *Surgery of the small intestine*. Veterinary Clinics of North America: Equine Practice, 1997. **13**(2): p. 261-301.
18. Mowat, A.M. and W.W. Agace, *Regional specialization within the intestinal immune system*. Nature Reviews Immunology, 2014. **14**(10): p. 667-685.
19. Gustafsson, J.K. and M.E. Johansson, *The role of goblet cells and mucus in intestinal homeostasis*. Nature reviews Gastroenterology & hepatology, 2022. **19**(12): p. 785-803.
20. Bernier-Latmani, J. and T.V. Petrova, *Intestinal lymphatic vasculature: structure, mechanisms and functions*. Nature reviews Gastroenterology & hepatology, 2017. **14**(9): p. 510-526.

21. Rüegg, J. and G. Pfitzer, *Modulation of calcium sensitivity in guinea pig taenia coli: skinned fiber studies*. *Experientia*, 1985. **41**(8): p. 997-1001.
22. Alamri, Z.Z., *The role of liver in metabolism: an updated review with physiological emphasis*. *Int J Basic Clin Pharmacol*, 2018. **7**(11): p. 2271-2276.
23. Ishibashi, H., et al. *Liver architecture, cell function, and disease*. in *Seminars in immunopathology*. 2009. Springer.
24. Leung, P.S. and P.S. Leung, *Physiology of the pancreas*. The renin-angiotensin system: current research progress in the pancreas: the RAS in the pancreas, 2010: p. 13-27.
25. Cade, J.E. and J. Hanison, *The pancreas*. *Anaesthesia & Intensive Care Medicine*, 2017. **18**(10): p. 527-531.
26. Mehta, V., et al., *Development of the human pancreas and its exocrine function*. *Frontiers in pediatrics*, 2022. **10**: p. 909648.
27. Turumin, J.L., V.A. Shanturov, and H.E. Turumina, *The role of the gallbladder in humans*. *Revista de gastroenterologia de Mexico*, 2013. **78**(3): p. 177-187.
28. Sekirov, I., et al., *Gut microbiota in health and disease*. *Physiological reviews*, 2010.
29. Lema, N.K., M.T. Gameda, and A.A. Woldesemayat, *Recent Advances in Metagenomic Approaches, Applications, and Challenges*. *Current Microbiology*, 2023. **80**(11): p. 347.
30. Walker, R.W., et al., *The prenatal gut microbiome: are we colonized with bacteria in utero?* *Pediatric obesity*, 2017. **12**: p. 3-17.
31. Gil, A., et al., *Is there evidence for bacterial transfer via the placenta and any role in the colonization of the infant gut?—a systematic review*. *Critical Reviews in Microbiology*, 2020. **46**(5): p. 493-507.
32. Ardisson, A.N., et al., *Meconium microbiome analysis identifies bacteria correlated with premature birth*. *PloS one*, 2014. **9**(3): p. e90784.
33. DiGiulio, D.B. *Diversity of microbes in amniotic fluid*. in *Seminars in fetal and neonatal medicine*. 2012. Elsevier.
34. Romero, R., et al., *Correction: the composition and stability of the vaginal microbiota of normal pregnant women is different from that of non-pregnant women*. *Microbiome*. 2014; **2** (1): 10. 2014.
35. MacIntyre, D.A., et al., *The vaginal microbiome during pregnancy and the postpartum period in a European population*. *Scientific reports*, 2015. **5**(1): p. 8988.
36. Contreras, D.-B.M.C.E., *Delivery mode shapes the acquisition and structure of the initial microbiota across multiple body habitats in newborns*. *Proc Natl Acad Sci USA*, 2010. **107**: p. 11971-5.
37. Fallani, M., et al., *Intestinal microbiota of 6-week-old infants across Europe: geographic influence beyond delivery mode, breast-feeding, and antibiotics*. *Journal of pediatric gastroenterology and nutrition*, 2010. **51**(1): p. 77-84.
38. Azad, M.B., et al., *Gut microbiota of healthy Canadian infants: profiles by mode of delivery and infant diet at 4 months*. *Cmaj*, 2013. **185**(5): p. 385-394.
39. Jakobsson, H.E., et al., *Decreased gut microbiota diversity, delayed Bacteroidetes colonisation and reduced Th1 responses in infants delivered by caesarean section*. *Gut*, 2014. **63**(4): p. 559-566.

40. Penders, J., et al., *Factors influencing the composition of the intestinal microbiota in early infancy*. Pediatrics, 2006. **118**(2): p. 511-521.
41. Salminen, S., et al., *Influence of mode of delivery on gut microbiota composition in seven year old children*. Gut, 2004. **53**(9): p. 1388-1389.
42. Ye, J., et al., *Searching for the optimal rate of medically necessary cesarean delivery*. Birth, 2014. **41**(3): p. 237-244.
43. Robson, M., L. Hartigan, and M. Murphy, *Methods of achieving and maintaining an appropriate caesarean section rate*. Best practice & research Clinical obstetrics & gynaecology, 2013. **27**(2): p. 297-308.
44. Kuhle, S., O. Tong, and C. Woolcott, *Association between caesarean section and childhood obesity: a systematic review and meta-analysis*. Obesity reviews, 2015. **16**(4): p. 295-303.
45. Huang, L., et al., *Is elective cesarean section associated with a higher risk of asthma? A meta-analysis*. Journal of Asthma, 2015. **52**(1): p. 16-25.
46. Penders, J., et al., *New insights into the hygiene hypothesis in allergic diseases: mediation of sibling and birth mode effects by the gut microbiota*. Gut microbes, 2014. **5**(2): p. 239-244.
47. Kalliomäki, M., et al., *Early differences in fecal microbiota composition in children may predict overweight*. The American journal of clinical nutrition, 2008. **87**(3): p. 534-538.
48. Zivkovic, A.M., et al., *Human milk glycobioime and its impact on the infant gastrointestinal microbiota*. Proceedings of the National Academy of Sciences, 2011. **108**(supplement_1): p. 4653-4658.
49. Pacheco, A.R., et al., *The impact of the milk glycobioime on the neonate gut microbiota*. Annu. Rev. Anim. Biosci., 2015. **3**(1): p. 419-445.
50. Rogier, E.W., et al., *Secretory antibodies in breast milk promote long-term intestinal homeostasis by regulating the gut microbiota and host gene expression*. Proceedings of the National Academy of Sciences, 2014. **111**(8): p. 3074-3079.
51. Ly, N.P., et al., *Gut microbiota, probiotics, and vitamin D: interrelated exposures influencing allergy, asthma, and obesity?* Journal of Allergy and Clinical Immunology, 2011. **127**(5): p. 1087-1094.
52. Griffin, M.D., N. Xing, and R. Kumar, *Vitamin D and its analogs as regulators of immune activation and antigen presentation*. Annual review of nutrition, 2003. **23**(1): p. 117-145.
53. Mai, V., et al., *Associations between dietary habits and body mass index with gut microbiota composition and fecal water genotoxicity: an observational study in African American and Caucasian American volunteers*. Nutrition journal, 2009. **8**: p. 1-10.
54. Lax, S., et al., *Longitudinal analysis of microbial interaction between humans and the indoor environment*. Science, 2014. **345**(6200): p. 1048-1052.
55. Penders, J., et al., *Establishment of the intestinal microbiota and its role for atopic dermatitis in early childhood*. Journal of Allergy and Clinical Immunology, 2013. **132**(3): p. 601-607. e8.

56. Laursen, M.F., et al., *Having older siblings is associated with gut microbiota development during early childhood*. BMC microbiology, 2015. **15**: p. 1-9.
57. Konya, T., et al., *Associations between bacterial communities of house dust and infant gut*. Environmental research, 2014. **131**: p. 25-30.
58. Azad, M., et al., *Investigators, CS (2013). Infant gut microbiota and the hygiene hypothesis of allergic disease: Impact of household pets and siblings on microbiota composition and diversity*. Allergy, Asthma & Clinical Immunology. **9**: p. 15.
59. Van de Merwe, J., J. Stegeman, and M. Hazenberg, *The resident faecal flora is determined by genetic characteristics of the host. Implications for Crohn's disease?* Antonie Van Leeuwenhoek, 1983. **49**: p. 119-124.
60. Zoetendal, E.G., et al., *The host genotype affects the bacterial community in the human gastrointestinal tract*. Microbial ecology in health and disease, 2001. **13**(3): p. 129-134.
61. Stewart, J.A., V.S. Chadwick, and A. Murray, *Investigations into the influence of host genetics on the predominant eubacteria in the faecal microflora of children*. Journal of medical microbiology, 2005. **54**(12): p. 1239-1242.
62. Murphy, K., et al., *The gut microbiota composition in dichorionic triplet sets suggests a role for host genetic factors*. PloS one, 2015. **10**(4): p. e0122561.
63. Goodrich, J.K., et al., *Human genetics shape the gut microbiome*. Cell, 2014. **159**(4): p. 789-799.
64. Rausch, P., et al., *Colonic mucosa-associated microbiota is influenced by an interaction of Crohn disease and FUT2 (Secretor) genotype*. Proceedings of the National Academy of Sciences, 2011. **108**(47): p. 19030-19035.
65. McGovern, D.P., et al., *Fucosyltransferase 2 (FUT2) non-secretor status is associated with Crohn's disease*. Human molecular genetics, 2010. **19**(17): p. 3468-3476.
66. Campi, C., et al., *Expression of the gene encoding secretor type galactoside 2 α fucosyltransferase (FUT2) and ABH antigens in patients with oral lesions*. Medicina oral, patologia oral y cirugia bucal, 2012. **17**(1): p. e63.
67. Marionneau, S., et al., *ABH and Lewis histo-blood group antigens, a model for the meaning of oligosaccharide diversity in the face of a changing world*. Biochimie, 2001. **83**(7): p. 565-573.
68. Lewis, Z., et al., *Maternal fucosyltransferase 2 status affects the gut bifidobacterial communities of breastfed infants*, Microbiome 3 (1)(2015) 13. 2015.
69. Petnicki-Ocwieja, T., et al., *Nod2 is required for the regulation of commensal microbiota in the intestine*. Proceedings of the National Academy of Sciences, 2009. **106**(37): p. 15813-15818.
70. Frank, D.N., et al., *Disease phenotype and genotype are associated with shifts in intestinal-associated microbiota in inflammatory bowel diseases*. Inflammatory bowel diseases, 2011. **17**(1): p. 179-184.
71. Khachatryan, Z.A., et al., *Predominant role of host genetics in controlling the composition of gut microbiota*. PloS one, 2008. **3**(8): p. e3064.
72. Wopereis, H., et al., *The first thousand days–intestinal microbiology of early life: establishing a symbiosis*. Pediatric Allergy and Immunology, 2014. **25**(5): p. 428-438.

73. Belkaid, Y. and T.W. Hand, *Role of the microbiota in immunity and inflammation*. Cell, 2014. **157**(1): p. 121-141.
74. Koleva, P.T., et al., *Microbial programming of health and disease starts during fetal life*. Birth Defects Research Part C: Embryo Today: Reviews, 2015. **105**(4): p. 265-277.
75. Dogra, S., et al., *Rate of establishing the gut microbiota in infancy has consequences for future health*. Gut microbes, 2015. **6**(5): p. 321-325.
76. Korpela, K. and W.M. de Vos, *Antibiotic use in childhood alters the gut microbiota and predisposes to overweight*. Microbial Cell, 2016. **3**(7): p. 296.
77. Avershina, E., et al., *Major faecal microbiota shifts in composition and diversity with age in a geographically restricted cohort of mothers and their children*. FEMS microbiology ecology, 2014. **87**(1): p. 280-290.
78. Backhed, F., et al., *Dynamics 684 and Stabilization of the Human Gut Microbiome during the First Year of Life*. Cell Host. **685**.
79. Koenig, J.E., et al., *Succession of microbial consortia in the developing infant gut microbiome*. Proceedings of the National Academy of Sciences, 2011. **108**(supplement_1): p. 4578-4585.
80. Yatsunenko, T., et al., *Human gut microbiome viewed across age and geography*. nature, 2012. **486**(7402): p. 222-227.
81. Stark, P.L. and A. Lee, *The microbial ecology of the large bowel of breastfed and formula-fed infants during the first year of life*. Journal of medical microbiology, 1982. **15**(2): p. 189-203.
82. Heikkila, M., *Inhibition of Staphylococcus aureus by the commensal bacteria of human milk,(Huovinen 2001), 471–478*. 2003.
83. Cabrera-Rubio, R., et al., *The human milk microbiome changes over lactation and is shaped by maternal weight and mode of delivery*. The American journal of clinical nutrition, 2012. **96**(3): p. 544-551.
84. Fernández, L., et al., *The human milk microbiota: origin and potential roles in health and disease*. Pharmacological research, 2013. **69**(1): p. 1-10.
85. Jost, T., et al., *Vertical mother–neonate transfer of maternal gut bacteria via breastfeeding*. Environmental microbiology, 2014. **16**(9): p. 2891-2904.
86. Bergström, A., et al., *Establishment of intestinal microbiota during early life: a longitudinal, explorative study of a large cohort of Danish infants*. Applied and environmental microbiology, 2014. **80**(9): p. 2889-2900.
87. Faith, J.J., et al., *The long-term stability of the human gut microbiota*. Science, 2013. **341**(6141): p. 1237439.
88. Rajilić-Stojanović, M., et al., *Long-term monitoring of the human intestinal microbiota composition*. Environmental microbiology, 2013. **15**(4): p. 1146-1159.
89. Palleja, A., et al., *Recovery of gut microbiota of healthy adults following antibiotic exposure*. Nature microbiology, 2018. **3**(11): p. 1255-1265.
90. David, L.A., et al., *Diet rapidly and reproducibly alters the human gut microbiome*. Nature, 2014. **505**(7484): p. 559-563.
91. Sender, R., S. Fuchs, and R. Milo, *Revised estimates for the number of human and bacteria cells in the body*. PLoS biology, 2016. **14**(8): p. e1002533.

92. Zhu, B., X. Wang, and L. Li, *Human gut microbiome: the second genome of human body*. Protein Cell, 2010. **1**(8): p. 718-25.
93. Fujisaka, S., Y. Watanabe, and K. Tobe, *The gut microbiome: A core regulator of metabolism*. Journal of Endocrinology, 2023. **256**(3).
94. Pryde, S.E., et al., *The microbiology of butyrate formation in the human colon*. FEMS microbiology letters, 2002. **217**(2): p. 133-139.
95. Gibson, S., et al., *Significance of microflora in proteolysis in the colon*. Applied and environmental microbiology, 1989. **55**(3): p. 679-683.
96. Macfarlane, S. and G.T. Macfarlane, *Composition and metabolic activities of bacterial biofilms colonizing food residues in the human gut*. Applied and environmental microbiology, 2006. **72**(9): p. 6204-6211.
97. Fava, F., et al., *The gut microbiota and lipid metabolism: implications for human health and coronary heart disease*. Current medicinal chemistry, 2006. **13**(25): p. 3005-3021.
98. Gustafsson, B.E., et al., *Effects of vitamin K-active compounds and intestinal microorganisms in vitamin K-deficient germfree rats*. Journal of Nutrition, 1962. **78**: p. 461-468.
99. LeBlanc, J.G., et al., *Bacteria as vitamin suppliers to their host: a gut microbiota perspective*. Current opinion in biotechnology, 2013. **24**(2): p. 160-168.
100. Karczewski, J., et al., *Regulation of human epithelial tight junction proteins by Lactobacillus plantarum in vivo and protective effects on the epithelial barrier*. American Journal of Physiology-Gastrointestinal and Liver Physiology, 2010. **298**(6): p. G851-G859.
101. Akritidou, T., et al., *Gut microbiota of the small intestine as an antimicrobial barrier against foodborne pathogens: Impact of diet on the survival of S. Typhimurium and L. monocytogenes during in vitro digestion*. Food Research International, 2023. **173**: p. 113292.
102. Sugrue, I., R.P. Ross, and C. Hill, *Bacteriocin diversity, function, discovery and application as antimicrobials*. Nature Reviews Microbiology, 2024: p. 1-16.
103. Gubatan, J., et al., *Antimicrobial peptides and the gut microbiome in inflammatory bowel disease*. World Journal of Gastroenterology, 2021. **27**(43): p. 7402.
104. Markowiak-Kopeć, P. and K. Śliżewska, *The effect of probiotics on the production of short-chain fatty acids by human intestinal microbiome*. Nutrients, 2020. **12**(4): p. 1107.
105. Pessione, E., *Lactic acid bacteria contribution to gut microbiota complexity: lights and shadows*. Frontiers in cellular and infection microbiology, 2012. **2**: p. 86.
106. Aldunate, M., et al., *Antimicrobial and immune modulatory effects of lactic acid and short chain fatty acids produced by vaginal microbiota associated with eubiosis and bacterial vaginosis*. Frontiers in physiology, 2015. **6**: p. 138618.
107. Lee, C.-G., et al., *Exploring probiotic effector molecules and their mode of action in gut-immune interactions*. FEMS Microbiology Reviews, 2023. **47**(4): p. fuad046.
108. Morais, L.H., H.L. Schreiber IV, and S.K. Mazmanian, *The gut microbiota-brain axis in behaviour and brain disorders*. Nature Reviews Microbiology, 2021. **19**(4): p. 241-255.

109. Mayer, E.A., K. Nance, and S. Chen, *The gut–brain axis*. Annual review of medicine, 2022. **73**: p. 439-453.
110. Clapp, M., et al., *Gut microbiota’s effect on mental health: The gut-brain axis*. Clinics and practice, 2017. **7**(4): p. 987.
111. Skonieczna-Żydecka, K., et al., *Microbiome—the missing link in the gut-brain axis: focus on its role in gastrointestinal and mental health*. Journal of clinical medicine, 2018. **7**(12): p. 521.
112. Dinan, T.G. and J.F. Cryan, *Brain-gut-microbiota axis and mental health*. Psychosomatic medicine, 2017. **79**(8): p. 920-926.
113. Mörkl, S., et al., *The role of nutrition and the gut-brain axis in psychiatry: a review of the literature*. Neuropsychobiology, 2020. **79**(1): p. 80-88.
114. Kennedy, P.J., et al., *Irritable bowel syndrome: a microbiome-gut-brain axis disorder?* World journal of gastroenterology: WJG, 2014. **20**(39): p. 14105.
115. Ancona, A., et al., *The gut–brain axis in irritable bowel syndrome and inflammatory bowel disease*. Digestive and Liver Disease, 2021. **53**(3): p. 298-305.
116. Gravina, A.G., et al., *Targeting the gut-brain axis for therapeutic adherence in patients with inflammatory bowel disease: a review on the role of psychotherapy*. Brain-Apparatus Communication: A Journal of Bacomics, 2023. **2**(1): p. 2181101.
117. Günther, C., et al., *The gut-brain axis in inflammatory bowel disease—current and future perspectives*. International Journal of Molecular Sciences, 2021. **22**(16): p. 8870.
118. Chen, Z., et al., *The role of intestinal bacteria and gut–brain Axis in hepatic encephalopathy*. Frontiers in Cellular and Infection Microbiology, 2021. **10**: p. 595759.
119. Zhu, R., et al., *The pathogenesis of gut microbiota in hepatic encephalopathy by the gut–liver–brain axis*. Bioscience Reports, 2023. **43**(6): p. BSR20222524.
120. Parodi, B. and N. Kerlero de Rosbo, *The gut-brain axis in multiple sclerosis. Is its dysfunction a pathological trigger or a consequence of the disease?* Frontiers in Immunology, 2021. **12**: p. 718220.
121. Doifode, T., et al., *The impact of the microbiota-gut-brain axis on Alzheimer’s disease pathophysiology*. Pharmacological Research, 2021. **164**: p. 105314.
122. Srikantha, P. and M.H. Mohajeri, *The possible role of the microbiota-gut-brain-axis in autism spectrum disorder*. International journal of molecular sciences, 2019. **20**(9): p. 2115.
123. Peirce, J.M. and K. Alviña, *The role of inflammation and the gut microbiome in depression and anxiety*. Journal of neuroscience research, 2019. **97**(10): p. 1223-1241.
124. Kumar, A., et al., *Gut microbiota in anxiety and depression: unveiling the relationships and management options*. Pharmaceuticals, 2023. **16**(4): p. 565.
125. Tilg, H. and A. Kaser, *Gut microbiome, obesity, and metabolic dysfunction*. The Journal of clinical investigation, 2011. **121**(6): p. 2126-2132.
126. Barlow, G.M., A. Yu, and R. Mathur, *Role of the gut microbiome in obesity and diabetes mellitus*. Nutrition in clinical practice, 2015. **30**(6): p. 787-797.

127. Trøseid, M., et al., *The gut microbiome in coronary artery disease and heart failure: Current knowledge and future directions*. EBioMedicine, 2020. **52**.
128. Avery, E.G., et al., *The gut microbiome in hypertension: recent advances and future perspectives*. Circulation research, 2021. **128**(7): p. 934-950.
129. Davani-Davari, D., et al., *Prebiotics: definition, types, sources, mechanisms, and clinical applications*. Foods, 2019. **8**(3): p. 92.
130. Gibson, G.R. and M.B. Roberfroid, *Dietary modulation of the human colonic microbiota: introducing the concept of prebiotics*. The Journal of nutrition, 1995. **125**(6): p. 1401-1412.
131. Howlett, J., et al., *The definition of dietary fiber—discussions at the Ninth Vahouny Fiber Symposium: building scientific agreement*. Food & nutrition research, 2010. **54**(1): p. 5750.
132. Slavin, J., *Fiber and prebiotics: mechanisms and health benefits*. Nutrients, 2013. **5**(4): p. 1417-1435.
133. Varzakas, T., et al., *Innovative and fortified food: Probiotics, prebiotics, GMOs, and superfood*, in *Preparation and processing of religious and cultural foods*. 2018, Elsevier. p. 67-129.
134. Al-Sheraji, S.H., et al., *Prebiotics as functional foods: A review*. Journal of Functional Foods, 2013. **5**(4): p. 1542-1553.
135. Ashaolu, T.J., J.O. Ashaolu, and S.A.O. Adeyeye, *Fermentation of prebiotics by human colonic microbiota in vitro and short-chain fatty acids production: a critical review*. Journal of Applied Microbiology, 2021. **130**(3): p. 677-687.
136. Fehlbaum, S., et al., *In Vitro Fermentation of Selected Prebiotics and Their Effects on the Composition and Activity of the Adult Gut Microbiota*. International Journal of Molecular Sciences, 2018. **19**(10): p. 3097.
137. Martin-Gallausiaux, C., et al., *SCFA: mechanisms and functional importance in the gut*. Proceedings of the Nutrition Society, 2021. **80**(1): p. 37-49.
138. Parada Venegas, D., et al., *Short Chain Fatty Acids (SCFAs)-Mediated Gut Epithelial and Immune Regulation and Its Relevance for Inflammatory Bowel Diseases*. Frontiers in Immunology, 2019. **10**.
139. Davani-Davari, D., et al., *Prebiotics: Definition, Types, Sources, Mechanisms, and Clinical Applications*. Foods, 2019. **8**(3): p. 92.
140. Tan, J., et al., *Chapter Three - The Role of Short-Chain Fatty Acids in Health and Disease*, in *Advances in Immunology*, F.W. Alt, Editor. 2014, Academic Press. p. 91-119.
141. Spiller, R., *Review article: probiotics and prebiotics in irritable bowel syndrome*. Alimentary Pharmacology & Therapeutics, 2008. **28**(4): p. 385-396.
142. Scaldaferri, F., et al., *Gut Microbial Flora, Prebiotics, and Probiotics in IBD: Their Current Usage and Utility*. BioMed Research International, 2013. **2013**(1): p. 435268.
143. Paiva, I.H.R., E. Duarte-Silva, and C.A. Peixoto, *The role of prebiotics in cognition, anxiety, and depression*. European Neuropsychopharmacology, 2020. **34**: p. 1-18.
144. Salminen, S., et al., *Probiotics: how should they be defined?* Trends in Food Science & Technology, 1999. **10**(3): p. 107-110.

145. Ng, S.C., et al., *Mechanisms of Action of Probiotics: Recent Advances*. Inflammatory Bowel Diseases, 2008. **15**(2): p. 300-310.
146. Wang, H., et al., *Effect of Probiotics on Central Nervous System Functions in Animals and Humans: A Systematic Review*. J Neurogastroenterol Motil, 2016. **22**(4): p. 589-605.
147. Walker, W.A., *Mechanisms of Action of Probiotics*. Clinical Infectious Diseases, 2008. **46**(Supplement_2): p. S87-S91.
148. Plaza-Diaz, J., et al., *Mechanisms of Action of Probiotics*. Advances in Nutrition, 2019. **10**: p. S49-S66.
149. Preidis, G.A., et al., *Probiotics, Enteric and Diarrheal Diseases, and Global Health*. Gastroenterology, 2011. **140**(1): p. 8-14.e9.
150. Fontana, L., et al., *Sources, isolation, characterisation and evaluation of probiotics*. British Journal of Nutrition, 2013. **109**(S2): p. S35-S50.
151. Wang, J.-W., et al., *Fecal microbiota transplantation: Review and update*. Journal of the Formosan Medical Association, 2019. **118**: p. S23-S31.
152. Zhang, F., et al., *Should We Standardize the 1,700-Year-Old Fecal Microbiota Transplantation?* Official journal of the American College of Gastroenterology | ACG, 2012. **107**(11).
153. Nood, E.v., et al., *Duodenal Infusion of Donor Feces for Recurrent *Clostridium difficile**. New England Journal of Medicine, 2013. **368**(5): p. 407-415.
154. Borody, T.J., et al., *Bowel-flora alteration: a potential cure for inflammatory bowel disease and irritable bowel syndrome?* Medical Journal of Australia, 1989. **150**(10): p. 604-604.
155. Borody, T.J., et al., *Treatment of Ulcerative Colitis Using Fecal Bacteriotherapy*. Journal of Clinical Gastroenterology, 2003. **37**(1).
156. Kao, D., et al., *Fecal Microbiota Transplantation Inducing Remission in Crohn's Colitis and the Associated Changes in Fecal Microbial Profile*. Journal of Clinical Gastroenterology, 2014. **48**(7).
157. Paramsothy, S., et al., *Multidonor intensive faecal microbiota transplantation for active ulcerative colitis: a randomised placebo-controlled trial*. The Lancet, 2017. **389**(10075): p. 1218-1228.
158. Cammarota, G., et al., *European consensus conference on faecal microbiota transplantation in clinical practice*. Gut, 2017. **66**(4): p. 569-580.
159. Smits, L.P., et al., *Therapeutic Potential of Fecal Microbiota Transplantation*. Gastroenterology, 2013. **145**(5): p. 946-953.
160. Bakken, J.S., et al., *Treating Clostridium difficile Infection With Fecal Microbiota Transplantation*. Clinical Gastroenterology and Hepatology, 2011. **9**(12): p. 1044-1049.
161. Vindigni, S.M. and C.M. Surawicz, *Fecal Microbiota Transplantation*. Gastroenterology Clinics, 2017. **46**(1): p. 171-185.
162. Tang, G., W. Yin, and W. Liu, *Is frozen fecal microbiota transplantation as effective as fresh fecal microbiota transplantation in patients with recurrent or refractory Clostridium difficile infection: A meta-analysis?* Diagnostic Microbiology and Infectious Disease, 2017. **88**(4): p. 322-329.

163. Evrensel, A. and M.E. Ceylan, *Fecal Microbiota Transplantation and Its Usage in Neuropsychiatric Disorders*. Clin Psychopharmacol Neurosci, 2016. **14**(3): p. 231-7.
164. Goldenberg, S.D., et al., *Comparison of Different Strategies for Providing Fecal Microbiota Transplantation to Treat Patients with Recurrent Clostridium difficile Infection in Two English Hospitals: A Review*. Infectious Diseases and Therapy, 2018. **7**(1): p. 71-86.
165. Kao, D., et al., *Effect of Oral Capsule- vs Colonoscopy-Delivered Fecal Microbiota Transplantation on Recurrent Clostridium difficile Infection: A Randomized Clinical Trial*. JAMA, 2017. **318**(20): p. 1985-1993.
166. Lee, C.H., et al., *Frozen vs Fresh Fecal Microbiota Transplantation and Clinical Resolution of Diarrhea in Patients With Recurrent Clostridium difficile Infection: A Randomized Clinical Trial*. JAMA, 2016. **315**(2): p. 142-149.
167. Tsai, H.-C., et al., *Current strategies employed in the manipulation of gene expression for clinical purposes*. Journal of Translational Medicine, 2022. **20**(1): p. 535.
168. Chen, Z., et al., *Decoding the microbiome: advances in genetic manipulation for gut bacteria*. Trends in Microbiology, 2023. **31**(11): p. 1143-1161.
169. Pickar-Oliver, A. and C.A. Gersbach, *The next generation of CRISPR-Cas technologies and applications*. Nature Reviews Molecular Cell Biology, 2019. **20**(8): p. 490-507.
170. Hayes, F., *Transposon-Based Strategies for Microbial Functional Genomics and Proteomics*. Annual Review of Genetics, 2003. **37**(Volume 37, 2003): p. 3-29.
171. McNERNEY, M.P., et al., *Theranostic cells: emerging clinical applications of synthetic biology*. Nature Reviews Genetics, 2021. **22**(11): p. 730-746.
172. Chien, T., et al., *Enhancing the tropism of bacteria via genetically programmed biosensors*. Nature Biomedical Engineering, 2022. **6**(1): p. 94-104.
173. Zheng, L., et al., *CRISPR/Cas-Based Genome Editing for Human Gut Commensal Bacteroides Species*. ACS Synthetic Biology, 2022. **11**(1): p. 464-472.
174. Mimee, M., et al., *Programming a Human Commensal Bacterium, *Bacteroides thetaiotaomicron*, to Sense and Respond to Stimuli in the Murine Gut Microbiota*. Cell Systems, 2015. **1**(1): p. 62-71.
175. Russell, B.J., et al., *Intestinal transgene delivery with native *E. coli* chassis allows persistent physiological changes*. Cell, 2022. **185**(17): p. 3263-3277.e15.
176. Lercher, M.J., E.J.B. Williams, and L.D. Hurst, *Local Similarity in Evolutionary Rates Extends over Whole Chromosomes in Human-Rodent and Mouse-Rat Comparisons: Implications for Understanding the Mechanistic Basis of the Male Mutation Bias*. Molecular Biology and Evolution, 2001. **18**(11): p. 2032-2039.
177. Vandamme, T.F., *Rodent models for human diseases*. European Journal of Pharmacology, 2015. **759**: p. 84-89.
178. Ogioldo, L., et al., *Intestinal dimensions of mice divergently selected for body weight*. The Anatomical Record, 1998. **250**(3): p. 292-299.
179. LANGER, P., *The digestive tract and life history of small mammals*. Mammal Review, 2002. **32**(2): p. 107-131.

180. Hammer, C., et al., *Organs from Animals for Man*. International Archives of Allergy and Immunology, 2009. **116**(1): p. 5-21.
181. Murphy, M.O., D.M. Cohn, and A.S. Loria, *Developmental origins of cardiovascular disease: Impact of early life stress in humans and rodents*. Neuroscience & Biobehavioral Reviews, 2017. **74**: p. 453-465.
182. Chen, D. and M.-W. Wang, *Development and application of rodent models for type 2 diabetes*. Diabetes, Obesity and Metabolism, 2005. **7**(4): p. 307-317.
183. Briese, T., M. Hornig, and W.I. Lipkin, *Bornavirus immunopathogenesis in rodents: models for human neurological diseases*. Journal of Neurovirology, 1999. **5**(6): p. 604-612.
184. Grover, M. and P.C. Kashyap, *Germ-free mice as a model to study effect of gut microbiota on host physiology*. Neurogastroenterology & Motility, 2014. **26**(6): p. 745-748.
185. Arvidsson, C., A. Hallén, and F. Bäckhed, *Generating and Analyzing Germ-Free Mice*. Current Protocols in Mouse Biology, 2012. **2**(4): p. 307-316.
186. Bhattarai, Y. and P.C. Kashyap, *Germ-Free Mice Model for Studying Host–Microbial Interactions*, in *Mouse Models for Drug Discovery: Methods and Protocols*, G. Proetzel and M.V. Wiles, Editors. 2016, Springer New York: New York, NY. p. 123-135.
187. Moretti, C.H., et al., *Germ-free mice are not protected against diet-induced obesity and metabolic dysfunction*. Acta Physiologica, 2021. **231**(3): p. e13581.
188. Nagao-Kitamoto, H., et al., *Functional Characterization of Inflammatory Bowel Disease–Associated Gut Dysbiosis in Gnotobiotic Mice*. Cellular and Molecular Gastroenterology and Hepatology, 2016. **2**(4): p. 468-481.
189. Forsberg, H., *Microbiome programming of brain development: implications for neurodevelopmental disorders*. Developmental Medicine & Child Neurology, 2019. **61**(7): p. 744-749.
190. Gandolfi, B. and H. Alhaddad, *Investigation of inherited diseases in cats: Genetic and genomic strategies over three decades*. Journal of Feline Medicine and Surgery, 2015. **17**(5): p. 405-415.
191. Adegá, F., A. Borges, and R. Chaves, *Cat Mammary Tumors: Genetic Models for the Human Counterpart*. Veterinary Sciences, 2016. **3**(3): p. 17.
192. Kim, S., et al., *Comparison of carnivore, omnivore, and herbivore mammalian genomes with a new leopard assembly*. Genome Biology, 2016. **17**(1): p. 211.
193. Verbrugghe, A. and M. Hesta, *Cats and Carbohydrates: The Carnivore Fantasy?* Veterinary Sciences, 2017. **4**(4): p. 55.
194. Sturgess, C.P., et al., *A Gross and Microscopical Morphometric Evaluation of Feline Large Intestinal Anatomy*. Journal of Comparative Pathology, 2001. **124**(4): p. 255-264.
195. He, W., E.D. Connolly, and G. Wu, *Characteristics of the Digestive Tract of Dogs and Cats*, in *Nutrition and Metabolism of Dogs and Cats*, G. Wu, Editor. 2024, Springer Nature Switzerland: Cham. p. 15-38.
196. Kienzle, E., *Carbohydrate metabolism of the cat 1. Activity of amylase in the gastrointestinal tract of the cat*. Journal of Animal Physiology and Animal Nutrition, 1993. **69**(1-5): p. 92-101.

197. Kieler, I., et al., *Overweight and the feline gut microbiome—a pilot study*. Journal of animal physiology and animal nutrition, 2016. **100**(3): p. 478-484.
198. Tun, H.M., et al., *Gene-centric metagenomics analysis of feline intestinal microbiome using 454 junior pyrosequencing*. Journal of microbiological methods, 2012. **88**(3): p. 369-376.
199. Hooda, S., et al., *The gut microbiome of kittens is affected by dietary protein: carbohydrate ratio and associated with blood metabolite and hormone concentrations*. British Journal of Nutrition, 2013. **109**(9): p. 1637-1646.
200. Barry, K.A., et al., *Effects of dietary fiber on the feline gastrointestinal metagenome*. Journal of proteome research, 2012. **11**(12): p. 5924-5933.
201. Deusch, O., et al., *Deep Illumina-based shotgun sequencing reveals dietary effects on the structure and function of the fecal microbiome of growing kittens*. PloS one, 2014. **9**(7): p. e101021.
202. Suchodolski, J.S., et al., *The fecal microbiome in cats with diarrhea*. PloS one, 2015. **10**(5): p. e0127378.
203. Šlapeta, J., et al., *Differences in the faecal microbiome of non-diarrhoeic clinically healthy dogs and cats associated with Giardia duodenalis infection: impact of hookworms and coccidia*. International Journal for Parasitology, 2015. **45**(9-10): p. 585-594.
204. Vester, B.M., et al., *Faecal microbial populations of growing kittens fed high-or moderate-protein diets*. Archives of Animal Nutrition, 2009. **63**(3): p. 254-265.
205. Kerr, K., S. Dowd, and K. Swanson, *Faecal microbiota of domestic cats fed raw whole chicks v. an extruded chicken-based diet*. Journal of nutritional science, 2014. **3**: p. e22.
206. Butowski, C.F., et al., *Addition of plant dietary fibre to a raw red meat high protein, high fat diet, alters the faecal bacteriome and organic acid profiles of the domestic cat (Felis catus)*. PloS one, 2019. **14**(5): p. e0216072.
207. Young, W., et al., *Pre-and post-weaning diet alters the faecal metagenome in the cat with differences in vitamin and carbohydrate metabolism gene abundances*. Scientific Reports, 2016. **6**(1): p. 34668.
208. Wernimont, S., et al., *Specialized dietary fibers alter microbiome composition & promote fermentative metabolism in the lower gastrointestinal tract of healthy adult cats (P20-045-19)*. Current Developments in Nutrition, 2019. **3**(Supplement_1): p. nzz040. P20-045-19.
209. Bermingham, E.N., et al., *Dietary format alters fecal bacterial populations in the domestic cat (Felis catus)*. Microbiologyopen, 2013. **2**(1): p. 173-181.
210. Bermingham, E.N., et al., *The fecal microbiota in the domestic cat (Felis catus) is influenced by interactions between age and diet; a five year longitudinal study*. Frontiers in microbiology, 2018. **9**: p. 1231.
211. Garcia-Mazcorro, J.F., et al., *Effect of a multi-species synbiotic formulation on fecal bacterial microbiota of healthy cats and dogs as evaluated by pyrosequencing*. FEMS microbiology ecology, 2011. **78**(3): p. 542-554.

212. Deb-Choudhury, S., et al., *The effects of a wool hydrolysate on short-chain fatty acid production and fecal microbial composition in the domestic cat (Felis catus)*. Food & function, 2018. **9**(8): p. 4107-4121.
213. Li, Q. and Y. Pan, *Differential responses to dietary protein and carbohydrate ratio on gut microbiome in obese vs. lean cats*. Frontiers in Microbiology, 2020. **11**: p. 591462.
214. Whittemore, J.C., et al., *Effects of a synbiotic on the fecal microbiome and metabolomic profiles of healthy research cats administered clindamycin: a randomized, controlled trial*. Gut Microbes, 2019. **10**(4): p. 521-539.
215. Summers, S.C., et al., *The fecal microbiome and serum concentrations of indoxyl sulfate and p-cresol sulfate in cats with chronic kidney disease*. Journal of veterinary internal medicine, 2019. **33**(2): p. 662-669.
216. Paul, A. and J. Stayt, *The intestinal microbiome in dogs and cats with diarrhoea as detected by a faecal polymerase chain reaction -based panel in Perth, Western Australia*. Australian veterinary journal, 2019. **97**(10): p. 418-421.
217. Marsilio, S., et al., *Characterization of the fecal microbiome in cats with inflammatory bowel disease or alimentary small cell lymphoma*. Scientific reports, 2019. **9**(1): p. 19208.
218. Fischer, M.M., et al., *Effects of obesity, energy restriction and neutering on the faecal microbiota of cats*. British Journal of Nutrition, 2017. **118**(7): p. 513-524.
219. Kieler, I.N., et al., *Diabetic cats have decreased gut microbial diversity and a lack of butyrate producing bacteria*. Scientific reports, 2019. **9**(1): p. 4822.
220. Jia, J., et al., *Investigation of the faecal microbiota of kittens: monitoring bacterial succession and effect of diet*. FEMS microbiology ecology, 2011. **78**(2): p. 395-404.
221. Leroy, G., et al., *Genetic diversity of dog breeds: within-breed diversity comparing genealogical and molecular data*. Animal Genetics, 2009. **40**(3): p. 323-332.
222. Kararli, T.T., *Comparison of the gastrointestinal anatomy, physiology, and biochemistry of humans and commonly used laboratory animals*. Biopharmaceutics & Drug Disposition, 1995. **16**(5): p. 351-380.
223. Bradshaw, J.W.S., *The Evolutionary Basis for the Feeding Behavior of Domestic Dogs (Canis familiaris) and Cats (Felis catus)*^{1, 2, 3}. The Journal of Nutrition, 2006. **136**(7): p. 1927S-1931S.
224. Bosch, G., E.A. Hagen-Plantinga, and W.H. Hendriks, *Dietary nutrient profiles of wild wolves: insights for optimal dog nutrition?* British Journal of Nutrition, 2015. **113**(S1): p. S40-S54.
225. Hernot, D.C., et al., *Relationship between total transit time and faecal quality in adult dogs differing in body size*. Journal of Animal Physiology and Animal Nutrition, 2005. **89**(3-6): p. 189-193.
226. Tolbert, M.K., et al., *Gastrointestinal transit time is faster in Beagle dogs compared to cats*. Journal of the American Veterinary Medical Association, 2022. **260**(S3): p. S8-S14.
227. Paczynska, P., A. Grzemski, and M. Szydlowski, *Distribution of miRNA genes in the pig genome*. BMC Genetics, 2015. **16**(1): p. 6.

228. Diamond, L.E., et al., *A HUMAN CD46 TRANSGENIC PIG MODEL SYSTEM FOR THE STUDY OF DISCORDANT XENOTRANSPLANTATION*. *Transplantation*, 2001. **71**(1).
229. Ekser, B., et al., *Xenotransplantation of solid organs in the pig-to-primate model*. *Transplant Immunology*, 2009. **21**(2): p. 87-92.
230. Thomson, J.R. and R.M. Friendship, *Digestive System*, in *Diseases of Swine*. 2019. p. 234-263.
231. Kobayashi, R., et al., *Comparison of the fecal microbiota of two monogastric herbivorous and five omnivorous mammals*. *Animal Science Journal*, 2020. **91**(1): p. e13366.
232. Ueda, K., et al., *Comparative evaluation of gastrointestinal transit and immune response between laparoscopic and open gastrectomy in a porcine model*. *Journal of Gastrointestinal Surgery*, 2006. **10**(1): p. 39-45.
233. Kim, H.B. and R.E. Isaacson, *The pig gut microbial diversity: Understanding the pig gut microbial ecology through the next generation high throughput sequencing*. *Veterinary Microbiology*, 2015. **177**(3): p. 242-251.
234. Douglas, A.E., *Simple animal models for microbiome research*. *Nature Reviews Microbiology*, 2019. **17**(12): p. 764-775.
235. Scher, J.U. and S.B. Abramson, *The microbiome and rheumatoid arthritis*. *Nature Reviews Rheumatology*, 2011. **7**(10): p. 569-578.
236. Ahn, J., et al., *Human gut microbiome and risk for colorectal cancer*. *Journal of the National Cancer Institute*, 2013. **105**(24): p. 1907-1911.
237. Zackular, J.P., et al., *The human gut microbiome as a screening tool for colorectal cancer*. *Cancer prevention research*, 2014. **7**(11): p. 1112-1121.
238. Peng, J., et al., *Interaction between gut microbiome and cardiovascular disease*. *Life Sciences*, 2018. **214**: p. 153-157.
239. Halfvarson, J., et al., *Dynamics of the human gut microbiome in inflammatory bowel disease*. *Nature microbiology*, 2017. **2**(5): p. 1-7.
240. Bernstein, C.N. and J.D. Forbes, *Gut microbiome in inflammatory bowel disease and other chronic immune-mediated inflammatory diseases*. *Inflammatory intestinal diseases*, 2017. **2**(2): p. 116-123.
241. Lloyd, J.K.F., *Minimising Stress for Patients in the Veterinary Hospital: Why It Is Important and What Can Be Done about It*. *Vet Sci*, 2017. **4**(2).
242. Rodan, I., et al., *AAFP and ISFM feline-friendly handling guidelines*. *J Feline Med Surg*, 2011. **13**(5): p. 364-75.
243. Ma, X., et al., *Whole-genome shotgun metagenomic sequencing reveals distinct gut microbiome signatures of obese cats*. *Microbiology spectrum*, 2022. **10**(3): p. e00837-22.
244. Bolger, A.M., M. Lohse, and B. Usadel, *Trimmomatic: a flexible trimmer for Illumina sequence data*. *Bioinformatics*, 2014. **30**(15): p. 2114-2120.
245. Buckley, R.M., et al., *A new domestic cat genome assembly based on long sequence reads empowers feline genomic medicine and identifies a novel gene for dwarfism*. *PLoS Genet*, 2020. **16**(10): p. e1008926.
246. Li, H. and R. Durbin, *Fast and accurate short read alignment with Burrows–Wheeler transform*. *bioinformatics*, 2009. **25**(14): p. 1754-1760.

247. Li, H., et al., *The sequence alignment/map format and SAMtools*. Bioinformatics, 2009. **25**(16): p. 2078-2079.
248. Quinlan, A.R. and I.M. Hall, *BEDTools: a flexible suite of utilities for comparing genomic features*. Bioinformatics, 2010. **26**(6): p. 841-842.
249. Ma, X., et al., *Whole-Genome Shotgun Metagenomic Sequencing Reveals Distinct Gut Microbiome Signatures of Obese Cats*. Microbiol Spectr, 2022: p. e0083722.
250. Oksanen, J., et al., *Community ecology package*. R package version, 2013. **2**(0).
251. Shannon, C.E., *The mathematical theory of communication*. 1963. MD computing: computers in medical practice, 1997. **14**(4): p. 306-317.
252. Bray, J.R. and J.T. Curtis, *An Ordination of the Upland Forest Communities of Southern Wisconsin*. Ecological Monographs, 1957. **27**(4): p. 326-349.
253. Team, R.C., *R: A language and environment for statistical computing*. 2013.
254. Bauer, D.F., *Constructing confidence sets using rank statistics*. Journal of the American Statistical Association, 1972. **67**(339): p. 687-690.
255. Hollander, M., D.A. Wolfe, and E. Chicken, *Nonparametric statistical methods*. Vol. 751. 2013: John Wiley & Sons.
256. Anderson, M.J., *A new method for non-parametric multivariate analysis of variance*. Austral ecology, 2001. **26**(1): p. 32-46.
257. Excoffier, L., P.E. Smouse, and J. Quattro, *Analysis of molecular variance inferred from metric distances among DNA haplotypes: application to human mitochondrial DNA restriction data*. Genetics, 1992. **131**(2): p. 479-491.
258. Legendre, P. and M.J. Anderson, *Distance-based redundancy analysis: testing multispecies responses in multifactorial ecological experiments*. Ecological monographs, 1999. **69**(1): p. 1-24.
259. McArdle, B.H. and M.J. Anderson, *Fitting multivariate models to community data: a comment on distance-based redundancy analysis*. Ecology, 2001. **82**(1): p. 290-297.
260. Warton, D.I., S.T. Wright, and Y. Wang, *Distance-based multivariate analyses confound location and dispersion effects*. Methods in Ecology and Evolution, 2012.
261. Day, M.J., *Cats are not small dogs: is there an immunological explanation for why cats are less affected by arthropod-borne disease than dogs?* Parasites & vectors, 2016. **9**: p. 1-9.
262. Suchodolski, J.S., *Diagnosis and interpretation of intestinal dysbiosis in dogs and cats*. The Veterinary Journal, 2016. **215**: p. 30-37.
263. Overgaauw, P.A., et al., *A one health perspective on the human-companion animal relationship with emphasis on zoonotic aspects*. International journal of environmental research and public health, 2020. **17**(11): p. 3789.
264. Bhat, A.H., *Bacterial zoonoses transmitted by household pets and as reservoirs of antimicrobial resistant bacteria*. Microbial pathogenesis, 2021. **155**: p. 104891.
265. Wang, Z., et al., *Comparison of fecal collection methods for microbiome and metabolomics studies*. Frontiers in cellular and infection microbiology, 2018. **8**: p. 301.

266. Watson, E.-J., et al., *Human faecal collection methods demonstrate a bias in microbiome composition by cell wall structure*. Scientific reports, 2019. **9**(1): p. 16831.
267. Tang, Q., et al., *Current sampling methods for gut microbiota: a call for more precise devices*. Frontiers in cellular and infection microbiology, 2020. **10**: p. 151.
268. Jones, J., et al., *Fecal sample collection methods and time of day impact microbiome composition and short chain fatty acid concentrations*. Scientific Reports, 2021. **11**(1): p. 13964.
269. Hale, V.L., et al., *Effects of field conditions on fecal microbiota*. Journal of Microbiological Methods, 2016. **130**: p. 180-188.
270. Tal, M., et al., *The effect of storage at ambient temperature on the feline fecal microbiota*. BMC Veterinary Research, 2017. **13**: p. 1-8.
271. Tap, J., et al., *Effects of the long-term storage of human fecal microbiota samples collected in RNAlater*. Scientific reports, 2019. **9**(1): p. 601.
272. Sherding, R.G. and S.E. Johnson, *Diseases of the intestines*. Saunders manual of small animal practice, 2009: p. 702.
273. Fukuda, S. and H. Ohno. *Gut microbiome and metabolic diseases*. in *Seminars in immunopathology*. 2014. Springer.
274. Parekh, P.J., L.A. Balart, and D.A. Johnson, *The influence of the gut microbiome on obesity, metabolic syndrome and gastrointestinal disease*. Clinical and translational gastroenterology, 2015. **6**(6): p. e91.
275. Sanz, Y., et al., *Understanding the role of gut microbiome in metabolic disease risk*. Pediatric research, 2015. **77**(1): p. 236-244.
276. Quigley, E.M., *Gut microbiome as a clinical tool in gastrointestinal disease management: are we there yet?* Nature Reviews Gastroenterology & Hepatology, 2017. **14**(5): p. 315-320.
277. Gopalakrishnan, V., et al., *The influence of the gut microbiome on cancer, immunity, and cancer immunotherapy*. Cancer cell, 2018. **33**(4): p. 570-580.
278. Gorkiewicz, G. and A. Moschen, *Gut microbiome: a new player in gastrointestinal disease*. Virchows Archiv, 2018. **472**(1): p. 159-172.
279. Dabke, K., G. Hendrick, and S. Devkota, *The gut microbiome and metabolic syndrome*. The Journal of clinical investigation, 2019. **129**(10): p. 4050-4057.
280. Li, W., et al., *Gut microbiome and cancer immunotherapy*. Cancer letters, 2019. **447**: p. 41-47.
281. Akbar, N., et al., *The role of gut microbiome in cancer genesis and cancer prevention*. Health Sciences Review, 2022. **2**: p. 100010.
282. Claassen-Weitz, S., et al., *Optimizing 16S rRNA gene profile analysis from low biomass nasopharyngeal and induced sputum specimens*. BMC microbiology, 2020. **20**: p. 1-26.
283. Villette, R., et al., *Refinement of 16S rRNA gene analysis for low biomass biospecimens*. Scientific Reports, 2021. **11**(1): p. 10741.
284. Kennedy, K.M., et al., *Questioning the fetal microbiome illustrates pitfalls of low-biomass microbial studies*. Nature, 2023. **613**(7945): p. 639-649.

285. Howell, J., M.S. Coyne, and P. Cornelius, *Effect of sediment particle size and temperature on fecal bacteria mortality rates and the fecal coliform/fecal streptococci ratio*. 1996, Wiley Online Library.
286. Amir, A., et al., *Correcting for microbial blooms in fecal samples during room-temperature shipping*. *Msystems*, 2017. **2**(2): p. 10.1128/msystems.00199-16.
287. De Bustamante, M., et al., *Impact of Ambient Temperature Sample Storage on the Equine Fecal Microbiota*. *Animals* 2021, **11**, 819.
288. Van der Waaij, L., et al., *Direct flow cytometry of anaerobic bacteria in human feces*. *Cytometry: The Journal of the International Society for Analytical Cytology*, 1994. **16**(3): p. 270-279.
289. Dominianni, C., et al., *Comparison of methods for fecal microbiome biospecimen collection*. *BMC microbiology*, 2014. **14**: p. 1-6.
290. Doukhanine, E., et al., *OMNIgene®• GUT enables reliable collection of high quality fecal samples for gut microbiome studies*. DNA Genotek, 2014. **2015**(2).
291. Flores, R., et al., *Collection media and delayed freezing effects on microbial composition of human stool*. *Microbiome*, 2015. **3**: p. 1-11.
292. Loftfield, E., et al., *Comparison of collection methods for fecal samples for discovery metabolomics in epidemiologic studies*. *Cancer Epidemiology, Biomarkers & Prevention*, 2016. **25**(11): p. 1483-1490.
293. Song, S., et al., *Preservation methods differ in fecal microbiome stability, affecting suitability for field studies*. *Msystems* **1**: e00021–e00016. 2016.
294. Vogtmann, E., et al., *Comparison of collection methods for fecal samples in microbiome studies*. *American journal of epidemiology*, 2017. **185**(2): p. 115-123.
295. Wong, W.S., et al., *Collection of non-meconium stool on fecal occult blood cards is an effective method for fecal microbiota studies in infants*. *Microbiome*, 2017. **5**: p. 1-11.
296. Burz, S.D., et al., *A guide for ex vivo handling and storage of stool samples intended for fecal microbiota transplantation*. *Scientific reports*, 2019. **9**(1): p. 8897.
297. Conrads, G. and M.M. Abdelbary, *Challenges of next-generation sequencing targeting anaerobes*. *Anaerobe*, 2019. **58**: p. 47-52.
298. Papanicolas, L.E., et al., *Bacterial viability in faecal transplants: which bacteria survive?* *EBioMedicine*, 2019. **41**: p. 509-516.
299. Wu, W.-K., et al., *Optimization of fecal sample processing for microbiome study—The journey from bathroom to bench*. *Journal of the Formosan Medical Association*, 2019. **118**(2): p. 545-555.
300. Liang, Y., et al., *Systematic analysis of impact of sampling regions and storage methods on fecal gut microbiome and metabolome profiles*. *mSphere* **5**, e00763–19. 2020.
301. Shalaby, A.G., et al., *Evaluating Flinders Technology Associates card for transporting bacterial isolates and retrieval of bacterial DNA after various storage conditions*. *Veterinary World*, 2020. **13**(10): p. 2243.
302. Ma, X., et al., *Whole-Genome Shotgun Metagenomic Sequencing Reveals Distinct Gut Microbiome Signatures of Obese Cats*. *Microbiology Spectrum*, 2022. **10**(3): p. e00837-22.

303. Buckley, R.M., et al., *A new domestic cat genome assembly based on long sequence reads empowers feline genomic medicine and identifies a novel gene for dwarfism*. PLOS Genetics, 2020. **16**(10): p. e1008926.
304. Li, H., et al., *The sequence alignment/map format and SAMtools*. bioinformatics, 2009. **25**(16): p. 2078-2079.
305. Menzel, P., K. Ng, and A. Krogh, *Fast and sensitive taxonomic classification for metagenomics with Kaiju*. Nat Commun 7: 11257. 2016.
306. Oksanen, J., et al., *Package 'vegan'. Community ecology package, version 2*. The comprehensive R network (CRAN).[Google Scholar], 2013.
307. Shannon, C.E., *The mathematical theory of communication*. 1963. Md Comput, 1997. **14**: p. 306.
308. Bray, J.R. and J. Curtis, *T.(1957). An ordination of the upland forest communities of southern Wisconsin*. Ecol. Monogr, 1957. **27**: p. 325-349.
309. Anderson, M.J., *Permutational multivariate analysis of variance (PERMANOVA)*. Wiley statsref: statistics reference online, 2014: p. 1-15.
310. Zhu, W., A. Lomsadze, and M. Borodovsky, *Ab initio gene identification in metagenomic sequences*. Nucleic acids research, 2010. **38**(12): p. e132-e132.
311. Li, W. and A. Godzik, *Cd-hit: a fast program for clustering and comparing large sets of protein or nucleotide sequences*. Bioinformatics, 2006. **22**(13): p. 1658-1659.
312. Fu, L., et al., *CD-HIT: accelerated for clustering the next-generation sequencing data*. Bioinformatics, 2012. **28**(23): p. 3150-3152.
313. Hollander, M., D.A. Wolfe, and E. Chicken, *Nonparametric statistical methods*. 2013: John Wiley & Sons.
314. Team, R.C., *R: A language and environment for statistical computing*. Foundation for Statistical Computing, Vienna, Austria, 2013.
315. Dabney, A., J.D. Storey, and G. Warnes, *qvalue: Q-value estimation for false discovery rate control*. R package version, 2010. **1**(0).
316. Lin, H. and S.D. Peddada, *Analysis of compositions of microbiomes with bias correction*. Nature communications, 2020. **11**(1): p. 3514.
317. Brown, M.B. and A.B. Forsythe, *Robust tests for the equality of variances*. Journal of the American statistical association, 1974. **69**(346): p. 364-367.
318. Carroll, R.J. and H. Schneider, *A note on Levene's tests for equality of variances*. Statistics & probability letters, 1985. **3**(4): p. 191-194.
319. Iachine, I., H.C. Petersen, and K.O. Kyvik, *Robust tests for the equality of variances for clustered data*. Journal of Statistical Computation and Simulation, 2010. **80**(4): p. 365-377.
320. Verocai, G.G., U.N. Chaudhry, and M. Lejeune, *Diagnostic methods for detecting internal parasites of livestock*. Veterinary Clinics: Food Animal Practice, 2020. **36**(1): p. 125-143.
321. Marks, S., et al., *Enteropathogenic bacteria in dogs and cats: diagnosis, epidemiology, treatment, and control*. Journal of veterinary internal medicine, 2011. **25**(6): p. 1195-1208.
322. Sykes, J.E., *Canine parvovirus infections and other viral enteritides*. Canine and feline infectious diseases, 2013: p. 141.

323. Vandeputte, D., et al., *Stool consistency is strongly associated with gut microbiota richness and composition, enterotypes and bacterial growth rates*. Gut, 2016. **65**(1): p. 57-62.
324. Ohlund, M., M. Palmgren, and B.S. Holst, *Overweight in adult cats: a cross-sectional study*. Acta Vet Scand, 2018. **60**(1): p. 5.
325. Sandoe, P., et al., *Canine and feline obesity: a One Health perspective*. Vet Rec, 2014. **175**(24): p. 610-6.
326. Chiang, C.-F., et al., *Prevalence, risk factors, and disease associations of overweight and obesity in cats that visited the Veterinary Medical Teaching Hospital at the University of California, Davis from January 2006 to December 2015*. Topics in Companion Animal Medicine, 2021: p. 100620.
327. Rowe, E.C., et al., *Early-life risk factors identified for owner-reported feline overweight and obesity at around two years of age*. Prev Vet Med, 2017. **143**: p. 39-48.
328. Hoenig, M., et al., *Effects of obesity on lipid profiles in neutered male and female cats*. Am J Vet Res, 2003. **64**(3): p. 299-303.
329. Strage, E.M., et al., *Homeostasis model assessment, serum insulin and their relation to body fat in cats*. BMC Vet Res, 2021. **17**(1): p. 34.
330. German, A.J., *The growing problem of obesity in dogs and cats*. J Nutr, 2006. **136**(7 Suppl): p. 1940S-1946S.
331. O'Connell, E.M., et al., *Factors associated with overweight cats successfully completing a diet-based weight loss programme: an observational study*. BMC Vet Res, 2018. **14**(1): p. 397.
332. Sender, R., S. Fuchs, and R. Milo, *Revised Estimates for the Number of Human and Bacteria Cells in the Body*. PLoS Biol, 2016. **14**(8): p. e1002533.
333. Cani, P.D. and N.M. Delzenne, *Interplay between obesity and associated metabolic disorders: new insights into the gut microbiota*. Current opinion in pharmacology, 2009. **9**(6): p. 737-743.
334. Baothman, O.A., et al., *The role of Gut Microbiota in the development of obesity and Diabetes*. Lipids in health and disease, 2016. **15**(1): p. 108.
335. Cani, P.D., et al., *Changes in gut microbiota control metabolic endotoxemia-induced inflammation in high-fat diet-induced obesity and diabetes in mice*. Diabetes, 2008. **57**(6): p. 1470-1481.
336. Liu, K.H., et al., *Microbial metabolite delta-valerobetaine is a diet-dependent obesogen*. Nat Metab, 2021. **3**(12): p. 1694-1705.
337. Hata, T., et al., *The gut microbiome derived from anorexia nervosa patients impairs weight gain and behavioral performance in female mice*. Endocrinology, 2019. **160**(10): p. 2441-2452.
338. Bahr, S.M., et al., *Risperidone-induced weight gain is mediated through shifts in the gut microbiome and suppression of energy expenditure*. EBioMedicine, 2015. **2**(11): p. 1725-1734.
339. Lai, Z.-L., et al., *Fecal microbiota transplantation confers beneficial metabolic effects of diet and exercise on diet-induced obese mice*. Scientific reports, 2018. **8**(1): p. 1-11.

340. de Clercq, N.C., et al., *Weight gain after fecal microbiota transplantation in a patient with recurrent underweight following clinical recovery from anorexia nervosa*. *Psychotherapy and psychosomatics*, 2019. **88**(1): p. 58-60.
341. Alang, N. and C.R. Kelly. *Weight gain after fecal microbiota transplantation*. in *Open forum infectious diseases*. 2015. Oxford University Press.
342. Angelakis, E., et al., *The relationship between gut microbiota and weight gain in humans*. *Future microbiology*, 2012. **7**(1): p. 91-109.
343. Chen, Y.-T., et al., *A combination of Lactobacillus mali APS1 and dieting improved the efficacy of obesity treatment via manipulating gut microbiome in mice*. *Scientific reports*, 2018. **8**(1): p. 1-14.
344. Ley, R.E., et al., *Human gut microbes associated with obesity*. *nature*, 2006. **444**(7122): p. 1022-1023.
345. Le Chatelier, E., et al., *Richness of human gut microbiome correlates with metabolic markers*. *Nature*, 2013. **500**(7464): p. 541-546.
346. Turnbaugh, P.J., et al., *A core gut microbiome in obese and lean twins*. *nature*, 2009. **457**(7228): p. 480-484.
347. Harris, K., et al., *Is the gut microbiota a new factor contributing to obesity and its metabolic disorders?* *Journal of obesity*, 2012. **2012**.
348. Ley, R.E., et al., *Obesity alters gut microbial ecology*. *Proceedings of the national academy of sciences*, 2005. **102**(31): p. 11070-11075.
349. Kieler, I.N., et al., *Overweight and the feline gut microbiome—a pilot study*. *Journal of animal physiology and animal nutrition*, 2016. **100**(3): p. 478-484.
350. Deusch, O., et al., *Deep Illumina-based shotgun sequencing reveals dietary effects on the structure and function of the fecal microbiome of growing kittens*. *PLoS One*, 2014. **9**(7): p. e101021.
351. Slapeta, J., et al., *Differences in the faecal microbiome of non-diarrhoeic clinically healthy dogs and cats associated with Giardia duodenalis infection: impact of hookworms and coccidia*. *Int J Parasitol*, 2015. **45**(9-10): p. 585-94.
352. Vester, B.M., et al., *Faecal microbial populations of growing kittens fed high- or moderate-protein diets*. *Archives of Animal Nutrition*, 2009. **63**(3): p. 254-265.
353. Kerr, K.R., S.E. Dowd, and K.S. Swanson, *Faecal microbiota of domestic cats fed raw whole chicks v. an extruded chicken-based diet*. *J Nutr Sci*, 2014. **3**: p. e22.
354. Young, W., et al., *Pre- and post-weaning diet alters the faecal metagenome in the cat with differences in vitamin and carbohydrate metabolism gene abundances*. *Sci Rep*, 2016. **6**: p. 34668.
355. Wernimont, S., et al., *Specialized Dietary Fibers Alter Microbiome Composition & Promote Fermentative Metabolism in the Lower Gastrointestinal Tract of Healthy Adult Cats (P20-045-19)*. *Current Developments in Nutrition*, 2019. **3**(Suppl 1): p. nzz040.P20-045-19.
356. Bermingham, E.N., et al., *Dietary format alters fecal bacterial populations in the domestic cat (Felis catus)*. *MicrobiologyOpen*, 2013. **2**(1): p. 173-181.
357. Bermingham, E.N., et al., *The Fecal Microbiota in the Domestic Cat (Felis catus) Is Influenced by Interactions Between Age and Diet; A Five Year Longitudinal Study*. *Front Microbiol*, 2018. **9**: p. 1231.

358. Garcia-Mazcorro, J.F., et al., *Effect of a multi-species synbiotic formulation on fecal bacterial microbiota of healthy cats and dogs as evaluated by pyrosequencing*. FEMS Microbiol Ecol, 2011. **78**(3): p. 542-54.
359. Deb-Choudhury, S., et al., *The effects of a wool hydrolysate on short-chain fatty acid production and fecal microbial composition in the domestic cat (Felis catus)*. Food Funct, 2018. **9**(8): p. 4107-4121.
360. Li, Q. and Y. Pan, *Differential Responses to Dietary Protein and Carbohydrate Ratio on Gut Microbiome in Obese vs. Lean Cats*. Front Microbiol, 2020. **11**: p. 591462.
361. Summers, S.C., et al., *The fecal microbiome and serum concentrations of indoxyl sulfate and p-cresol sulfate in cats with chronic kidney disease*. J Vet Intern Med, 2019. **33**(2): p. 662-669.
362. Paul, A. and J. Stayt, *The intestinal microbiome in dogs and cats with diarrhoea as detected by a faecal polymerase chain reaction-based panel in Perth, Western Australia*. Aust Vet J, 2019. **97**(10): p. 418-421.
363. Marsilio, S., et al., *Characterization of the fecal microbiome in cats with inflammatory bowel disease or alimentary small cell lymphoma*. Sci Rep, 2019. **9**(1): p. 19208.
364. Fischer, M.M., et al., *Effects of obesity, energy restriction and neutering on the faecal microbiota of cats*. Br J Nutr, 2017. **118**(7): p. 513-524.
365. Kieler, I.N., et al., *Diabetic cats have decreased gut microbial diversity and a lack of butyrate producing bacteria*. Sci Rep, 2019. **9**(1): p. 4822.
366. Ranjan, R., et al., *Analysis of the microbiome: Advantages of whole genome shotgun versus 16S amplicon sequencing*. Biochemical and biophysical research communications, 2016. **469**(4): p. 967-977.
367. Bjornvad, C.R., et al., *Evaluation of a nine-point body condition scoring system in physically inactive pet cats*. Am J Vet Res, 2011. **72**(4): p. 433-7.
368. Laflamme, D., *Development and validation of a body condition score system for cats: a clinical tool*. Feline practice., 1997. **25**(5/6): p. 13-18.
369. Strage, E.M., et al., *Validation of an enzyme-linked immunosorbent assay for measurement of feline serum insulin*. Veterinary Clinical Pathology, 2012. **41**(4): p. 518-528.
370. Zhang, J., et al., *PEAR: a fast and accurate Illumina Paired-End reAd mergeR*. Bioinformatics, 2014. **30**(5): p. 614-620.
371. Wheeler, D.L., et al., *Database resources of the national center for biotechnology information*. Nucleic acids research, 2000. **28**(1): p. 10-14.
372. Li, D., et al., *MEGAHIT: an ultra-fast single-node solution for large and complex metagenomics assembly via succinct de Bruijn graph*. Bioinformatics, 2015. **31**(10): p. 1674-1676.
373. Menzel, P., K.L. Ng, and A. Krogh, *Fast and sensitive taxonomic classification for metagenomics with Kaiju*. Nature communications, 2016. **7**(1): p. 1-9.
374. Storey, J.D., *The positive false discovery rate: a Bayesian interpretation and the q -value*. The Annals of Statistics, 2003. **31**(6): p. 2013-2035, 23.

375. Parks, D.H., et al., *CheckM: assessing the quality of microbial genomes recovered from isolates, single cells, and metagenomes*. *Genome research*, 2015. **25**(7): p. 1043-1055.
376. Wang, Y., et al., *MCScaN: a toolkit for detection and evolutionary analysis of gene synteny and collinearity*. *Nucleic acids research*, 2012. **40**(7): p. e49-e49.
377. Rychlik, W., *OLIGO 7 primer analysis software*. *PCR primer design*, 2007: p. 35-59.
378. Beghini, F., et al., *Integrating taxonomic, functional, and strain-level profiling of diverse microbial communities with bioBakery 3*. *Elife*, 2021. **10**: p. e65088.
379. Karp, P.D., et al., *The metacyc database*. *Nucleic acids research*, 2002. **30**(1): p. 59-61.
380. Huerta-Cepas, J., et al., *Fast genome-wide functional annotation through orthology assignment by eggNOG-mapper*. *Molecular biology and evolution*, 2017. **34**(8): p. 2115-2122.
381. Huerta-Cepas, J., et al., *eggNOG 5.0: a hierarchical, functionally and phylogenetically annotated orthology resource based on 5090 organisms and 2502 viruses*. *Nucleic acids research*, 2019. **47**(D1): p. D309-D314.
382. Yin, Y., et al., *dbCAN: a web resource for automated carbohydrate-active enzyme annotation*. *Nucleic Acids Res*, 2012. **40**(Web Server issue): p. W445-51.
383. Hjorth, M.F., et al., *Prevotella-to-Bacteroides ratio predicts body weight and fat loss success on 24-week diets varying in macronutrient composition and dietary fiber: results from a post-hoc analysis*. *International Journal of Obesity*, 2019. **43**(1): p. 149-157.
384. Togo, A.H., et al., *Lactimicrobium massiliense gen. nov., sp. nov.; Anaerolactibacter massiliensis gen. nov., sp. nov.; Galactobacillus timonensis gen. nov., sp. nov. and Acidipropionibacterium timonense sp. nov. isolated from breast milk from healthy breastfeeding African women*. *New Microbes New Infect*, 2019. **29**: p. 100537.
385. Chan, J.Z., et al., *Defining bacterial species in the genomic era: insights from the genus Acinetobacter*. *BMC Microbiol*, 2012. **12**: p. 302.
386. Bourke, B., V.L. Chan, and P. Sherman, *Campylobacter upsaliensis: waiting in the wings*. *Clin Microbiol Rev*, 1998. **11**(3): p. 440-9.
387. Goossens, H., et al., *Campylobacter upsaliensis enteritis associated with canine infections*. *Lancet*, 1991. **337**(8755): p. 1486-7.
388. Arumugam, M., et al., *Enterotypes of the human gut microbiome*. *nature*, 2011. **473**(7346): p. 174-180.
389. Suchodolski, J.S., J. Camacho, and J.M. Steiner, *Analysis of bacterial diversity in the canine duodenum, jejunum, ileum, and colon by comparative 16S rRNA gene analysis*. *FEMS microbiology ecology*, 2008. **66**(3): p. 567-578.
390. Honneffer, J.B., et al., *Variation of the microbiota and metabolome along the canine gastrointestinal tract*. *Metabolomics*, 2017. **13**(3): p. 26.
391. Vogtmann, E., et al., *Colorectal cancer and the human gut microbiome: reproducibility with whole-genome shotgun sequencing*. *PloS one*, 2016. **11**(5): p. e0155362.
392. Coelho, L.P., et al., *Similarity of the dog and human gut microbiomes in gene content and response to diet*. *Microbiome*, 2018. **6**(1): p. 72.

393. Turnbaugh, P.J., et al., *An obesity-associated gut microbiome with increased capacity for energy harvest*. *nature*, 2006. **444**(7122): p. 1027-1031.
394. Koliada, A., et al., *Association between body mass index and Firmicutes/Bacteroidetes ratio in an adult Ukrainian population*. *BMC microbiology*, 2017. **17**(1): p. 120.
395. Armougom, F., et al., *Monitoring bacterial community of human gut microbiota reveals an increase in Lactobacillus in obese patients and Methanogens in anorexic patients*. *PloS one*, 2009. **4**(9): p. e7125.
396. Jumpertz, R., et al., *Energy-balance studies reveal associations between gut microbes, caloric load, and nutrient absorption in humans*. *The American journal of clinical nutrition*, 2011. **94**(1): p. 58-65.
397. Zhang, H., et al., *Human gut microbiota in obesity and after gastric bypass*. *Proceedings of the National Academy of Sciences*, 2009. **106**(7): p. 2365-2370.
398. Duncan, S.H., et al., *Human colonic microbiota associated with diet, obesity and weight loss*. *International journal of obesity*, 2008. **32**(11): p. 1720-1724.
399. Schwartz, A., et al., *Microbiota and SCFA in lean and overweight healthy subjects*. *Obesity*, 2010. **18**(1): p. 190-195.
400. Tims, S., et al., *Microbiota conservation and BMI signatures in adult monozygotic twins*. *The ISME journal*, 2013. **7**(4): p. 707-717.
401. Chávez-Carbajal, A., et al., *Gut microbiota and predicted metabolic pathways in a sample of Mexican women affected by obesity and obesity plus metabolic syndrome*. *International journal of molecular sciences*, 2019. **20**(2): p. 438.
402. Pedogo, D.A.M., et al. *Gut microbial carbohydrate metabolism hinders weight loss in overweight adults undergoing lifestyle intervention with a volumetric diet*. in *Mayo Clinic Proceedings*. 2018. Elsevier.
403. O'Callaghan, A. and D. van Sinderen, *Bifidobacteria and Their Role as Members of the Human Gut Microbiota*. *Front Microbiol*, 2016. **7**: p. 925.
404. Chen, J., et al., *Bifidobacterium adolescentis supplementation ameliorates visceral fat accumulation and insulin sensitivity in an experimental model of the metabolic syndrome*. *Br J Nutr*, 2012. **107**(10): p. 1429-34.
405. Wang, G., et al., *Bifidobacterium adolescentis and Lactobacillus rhamnosus alleviate non-alcoholic fatty liver disease induced by a high-fat, high-cholesterol diet through modulation of different gut microbiota-dependent pathways*. *Food Funct*, 2020. **11**(7): p. 6115-6127.
406. Lim, S.M. and D.H. Kim, *Bifidobacterium adolescentis IM38 ameliorates high-fat diet-induced colitis in mice by inhibiting NF-kappaB activation and lipopolysaccharide production by gut microbiota*. *Nutr Res*, 2017. **41**: p. 86-96.
407. Wang, B., et al., *Bifidobacterium adolescentis Isolated from Different Hosts Modifies the Intestinal Microbiota and Displays Differential Metabolic and Immunomodulatory Properties in Mice Fed a High-Fat Diet*. *Nutrients*, 2021. **13**(3).
408. Bereswill, S., et al., *What you eat is what you get: Novel Campylobacter models in the quadrangle relationship between nutrition, obesity, microbiota and susceptibility to infection*. *Eur J Microbiol Immunol (Bp)*, 2011. **1**(3): p. 237-48.

409. Chen, C., et al., *Prevotella copri* increases fat accumulation in pigs fed with formula diets. *Microbiome*, 2021. **9**(1): p. 1-21.
410. Sundram, K., T. Karupaiah, and K. Hayes, *Stearic acid-rich interesterified fat and trans-rich fat raise the LDL/HDL ratio and plasma glucose relative to palm olein in humans*. *Nutrition & metabolism*, 2007. **4**(1): p. 1-12.
411. Jordan, E., et al., *Dyslipidemia in obese cats*. *Domest Anim Endocrinol*, 2008. **35**(3): p. 290-9.
412. Yu, D., et al., *Long-term Diet Quality and Gut Microbiome Functionality: A Prospective, Shotgun Metagenomic Study among Urban Chinese Adults*. *Current developments in nutrition*, 2021. **5**(4): p. nzab026.
413. Olton, D.S. and R.J. Samuelson, *Remembrance of places passed: Spatial memory in rats*. *Journal of Experimental Psychology: Animal Behavior Processes*, 1976. **2**: p. 97-116.
414. Honig, W.K., *Studies of working memory in the pigeon*. *Cognitive processes in animal behavior*, 2018: p. 211-248.
415. Lind, J., M. Enquist, and S. Ghirlanda, *Animal memory: A review of delayed matching-to-sample data*. *Behav Processes*, 2015. **117**: p. 52-8.
416. Bray, E.E., et al., *Dog cognitive development: a longitudinal study across the first 2 years of life*. *Anim Cogn*, 2021. **24**(2): p. 311-328.
417. Gnanadesikan, G.E., et al., *Estimating the heritability of cognitive traits across dog breeds reveals highly heritable inhibitory control and communication factors*. *Anim Cogn*, 2020. **23**(5): p. 953-964.
418. Krichbaum, S., et al., *Dissociating the effects of delay and interference on dog (*Canis familiaris*) working memory*. *Anim Cogn*, 2021. **24**(6): p. 1259-1265.
419. Krichbaum, S., et al., *Odor span task in dogs (*Canis familiaris*)*. *Anim Cogn*, 2020. **23**(3): p. 571-580.
420. Luna, R.A. and J.A. Foster, *Gut brain axis: diet microbiota interactions and implications for modulation of anxiety and depression*. *Curr Opin Biotechnol*, 2015. **32**: p. 35-41.
421. Carabotti, M., et al., *The gut-brain axis: interactions between enteric microbiota, central and enteric nervous systems*. *Ann Gastroenterol*, 2015. **28**(2): p. 203-209.
422. Dinan, T.G. and J.F. Cryan, *Gut-brain axis in 2016: Brain-gut-microbiota axis - mood, metabolism and behaviour*. *Nat Rev Gastroenterol Hepatol*, 2017. **14**(2): p. 69-70.
423. Tremlett, H., et al., *The gut microbiome in human neurological disease: A review*. *Ann Neurol*, 2017. **81**(3): p. 369-382.
424. Foster, J.A. and K.A. McVey Neufeld, *Gut-brain axis: how the microbiome influences anxiety and depression*. *Trends Neurosci*, 2013. **36**(5): p. 305-12.
425. Yu, Y. and F. Zhao, *Microbiota-gut-brain axis in autism spectrum disorder*. *J Genet Genomics*, 2021. **48**(9): p. 755-762.
426. Kirchoff, N.S., M.A.R. Udell, and T.J. Sharpton, *The gut microbiome correlates with conspecific aggression in a small population of rescued dogs (*Canis familiaris*)*. *PeerJ*, 2019. **7**: p. e6103.
427. Mondo, E., et al., *Gut microbiome structure and adrenocortical activity in dogs with aggressive and phobic behavioral disorders*. *Heliyon*, 2020. **6**(1): p. e03311.

428. Kubinyi, E., et al., *Gut Microbiome Composition is Associated with Age and Memory Performance in Pet Dogs*. *Animals (Basel)*, 2020. **10**(9).
429. Bray, E.E., et al., *Dog cognitive development: a longitudinal study across the first 2 years of life*. *Animal Cognition*, 2021. **24**(2): p. 311-328.
430. Krichbaum, S., et al., *Dissociating the effects of delay and interference on dog (*Canis familiaris*) working memory*. *Animal Cognition*, 2021. **24**(6): p. 1259-1265.
431. McKnight, P.E. and J. Najab, *Mann -Whitney U Test*. *The Corsini encyclopedia of psychology*, 2010: p. 1-1.
432. Kruskal, W.H. and W.A. Wallis, *Use of ranks in one-criterion variance analysis*. *Journal of the American statistical Association*, 1952. **47**(260): p. 583-621.
433. R Core Team, R., *R Core Team R: a language and environment for statistical computing*. Foundation for Statistical Computing, 2020.
434. Massey, F.J., *Distribution table for the deviation between two sample cumulatives*. *The annals of mathematical statistics*, 1952. **23**(3): p. 435-441.
435. Bolger, A.M., M. Lohse, and B. Usadel, *Trimmomatic: a flexible trimmer for Illumina sequence data*. *Bioinformatics*, 2014. **30**(15): p. 2114-20.
436. Li, H. and R. Durbin, *Fast and accurate short read alignment with Burrows-Wheeler transform*. *Bioinformatics*, 2009. **25**(14): p. 1754-60.
437. Menzel, P., K.L. Ng, and A. Krogh, *Fast and sensitive taxonomic classification for metagenomics with Kaiju*. *Nature Communications*, 2016. **7**(1): p. 11257.
438. Danecek, P., et al., *Twelve years of SAMtools and BCFtools*. *GigaScience*, 2021. **10**(2).
439. Breiman, L., *Random Forests*. *Machine Learning*, 2001. **45**(1): p. 5-32.
440. Lundberg, S.M. and S.-I. Lee, *A unified approach to interpreting model predictions*, in *Proceedings of the 31st International Conference on Neural Information Processing Systems*. 2017, Curran Associates Inc.: Long Beach, California, USA. p. 4768-4777.
441. Kang, D.D., et al., *MetaBAT 2: an adaptive binning algorithm for robust and efficient genome reconstruction from metagenome assemblies*. *PeerJ*, 2019. **7**: p. e7359.
442. Nayfach, S. and K.S. Pollard, *Average genome size estimation improves comparative metagenomics and sheds light on the functional ecology of the human microbiome*. *Genome Biol*, 2015. **16**(1): p. 51.
443. Bunford, N., et al., *Canis familiaris As a Model for Non-Invasive Comparative Neuroscience*. *Trends Neurosci*, 2017. **40**(7): p. 438-452.
444. Topal, J., V. Roman, and B. Turcsan, *The dog (*Canis familiaris*) as a translational model of autism: It is high time we move from promise to reality*. *Wiley Interdiscip Rev Cogn Sci*, 2019. **10**(4): p. e1495.
445. MacLean, E.L. and B. Hare, *Enhanced Selection of Assistance and Explosive Detection Dogs Using Cognitive Measures*. *Front Vet Sci*, 2018. **5**: p. 236.
446. Lazarowski, L., et al., *Comparing pet and detection dogs (*Canis familiaris*) on two aspects of social cognition*. *Learn Behav*, 2020. **48**(4): p. 432-443.
447. Craddock, H.A., et al., *Phenotypic correlates of the working dog microbiome*. *npj Biofilms and Microbiomes*, 2022. **8**(1): p. 66.

448. Xiao, Y., et al., *Colonized Niche, Evolution and Function Signatures of Bifidobacterium pseudolongum within Bifidobacterial Genus*. *Foods*, 2021. **10**(10).
449. Rodriguez, C.I. and J.B.H. Martiny, *Evolutionary relationships among bifidobacteria and their hosts and environments*. *BMC Genomics*, 2020. **21**(1): p. 26.
450. Allen, A.P., et al., *Bifidobacterium longum 1714 as a translational psychobiotic: modulation of stress, electrophysiology and neurocognition in healthy volunteers*. *Transl Psychiatry*, 2016. **6**(11): p. e939.
451. Wang, H., et al., *Bifidobacterium longum 1714™ strain modulates brain activity of healthy volunteers during social stress*. *Official journal of the American College of Gastroenterology| ACG*, 2019. **114**(7): p. 1152-1162.
452. Wissel, E., L. Leon, and L. Tipton, *Opportunities for growth in the growing field of psychobiotics*. *Beneficial Microbes*, 2022. **13**(6): p. 445-452.
453. Bray, E.E., et al., *Cognitive characteristics of 8- to 10-week-old assistance dog puppies*. *Anim Behav*, 2020. **166**: p. 193-206.
454. Dewey, C.W., et al., *Canine Cognitive Dysfunction: Pathophysiology, Diagnosis, and Treatment*. *Vet Clin North Am Small Anim Pract*, 2019. **49**(3): p. 477-499.
455. Landsberg, G.M., J. Nichol, and J.A. Araujo, *Cognitive dysfunction syndrome: a disease of canine and feline brain aging*. *Vet Clin North Am Small Anim Pract*, 2012. **42**(4): p. 749-68, vii.